INVESTIGATION OF THE ANTI-INFLAMMATORY PROPERTIES OF 17β-ESTRADIOL THROUGH THE DEVELOPMENT OF NANOMATERIALS FOR CARDIOVASCULAR DRUG DELIVERY AND DIAGNOSTIC APPLICATIONS.

Kristen Bowey, M.Sc.

Biomedical Engineering Department

McGill University

Montréal, Canada

Submitted July 2014

A thesis submitted to McGill University in partial fulfillment of the requirements of the degree of Ph.D. in Biomedical Engineering.

For my Mom.

Thank you.

Abstract

Atherosclerosis is a chronic disease characterized by lipid plaque accumulation in arterial blood vessels, which leads to luminal reduction. Over time, this condition can restrict vital blood flow causing chronic conditions, such as angina, as well as acute coronary events, such as myocardial infarction. Although therapies aimed at treating conditions of atherosclerosis, such as hyperlipidemia and hypertension, can successfully mitigate clinical symptoms, preventing atheroma development early on is critical to long-term success. Accordingly, recent research demonstrating the critical role of the inflammatory response during initiation of the disease has spurred the development of treatments and techniques aimed to identify and treat areas of inflammation, with the ultimate goal of attenuating atherogenesis.

17β-Estradiol (E2) is a sex steroid that has been shown to have such anti-inflammatory effects on the vascular system. However, conventional pharmaceutical treatments of hydrophobic active agents, such as E2, typically cannot be administered locally due to insufficient uptake at sites of delivery. Therefore, the main objective of this thesis was to develop a nanoliposome delivery system for E2 with the aim of treating atherosclerotic inflammation. To this end, a liposomal delivery system composed of 1,2-dioleoyl-*sn*-glycero-3-phosphocholine (DOPC), cholesterol, and a cationic charging agent, dimethyldioctadecyl-ammonium (DDAB), was developed. The optimized vector was capable of an E2 encapsulation efficiency of 51.2 ± 3.6% and loading capacity of 7.3 ± 0.5 μg/mg, while cellular uptake in human coronary artery endothelial (HCAE) cells was demonstrated using florescence

spectroscopy and confocal microscopy. E2-loaded liposomes were shown to reduce the expression of vascular cell adhesion molecule-1 (VCAM-1), an inflammatory cell biomarker, in response to the proinflammatory agent, C-reactive protein (CRP) in HCAE cells. Similarly, pretreatment with E2-loaded liposomes reduced the secretion of interleukin-8 (IL-8) and tumor necrosis factor alpha (TNF-α) by 60% and 68%, respectively, demonstrating the potential for this therapy to be used to address atherosclerotic-based inflammation.

Within the framework of treating cardiovascular inflammation, the localization and detection of early stages of atherosclerotic plaque formation is crucial to successful diagnosis and, consequently, the appropriate application of therapeutic drug delivery vehicles. Accordingly, the second major objective of this work was to develop a surface-enhanced Raman scattering (SERS) nanoprobe for the detection of vascular inflammation *in vitro*. The SERS nanoprobe was fabricated by microwave technology and composed of a gold core, coated with the Raman reporter 4-mercaptobenzoic acid (4-MBA), and poly(allylamine hydrochloride) (PAH). To detect the upregulation of VCAM-1 in HCAE cells, the nanoprobe was biofunctionalized with the target antibody (anti-VCAM-1). Results demonstrated that SERS nanoprobes could successfully be used to detect and localize VCAM-1 expression *in vitro* via confocal Raman microscopy. Overall, this dissertation serves as an important step towards both delivering E2-loaded liposomes with the aim of attenuating the inflammatory response during the initiation of atherosclerosis, in tandem with a novel approach to detect and visualize areas of inflammation *in vitro*.

Résumé

L'athérosclérose est une maladie chronique caractérisée par l'accumulation d'une plaque lipidique dans les vaisseaux sanguins artériels résultant une réduction luminal. Au cours des années, cette condition peut restreindre le flux vital de sang et provoque des maladies chroniques, comme l'angine, ou bien des évènements coronariens sérieux, tels que l'infarctus du myocarde. Même si les thérapies pour traiter certaines conditions d'athérosclérose, comme l'hyperlipidémie et l'hypertension, peuvent atténuer les symptômes cliniques, la prévention du développement de l'athérome est essentielle au succès à long terme de ces thérapies. Par conséquent, des recherches récentes démontrant le rôle critique de la réponse inflammatoire lors de l'initiation de l'athérosclérose ont conduit à développer des traitements qui peuvent réduire l'inflammation, et de ce fait, l'athérogenèse.

17β-Estradiol (E2) est un stéroïde qui a des effets anti-inflammatoires sur le système vasculaire. Cependant, étant an agent hydrophobe, E2 ne peut généralement pas être administré localement en raison d'une mauvaise absorption des sites de livraison. C'est dans ce contexte que cette thèse vise à développer tout d'abord un véhicule d'un agent anti-inflammatoire (E2) dans le but de traiter une inflammation athéroscléreuse. Ce système était composé de 1,2-dioléoyl-sn-glycéro-3-phosphocholine (DOPC), cholestérol et d'un agent cationique, diméthyldioctadécyl-ammonium (DDAB) pour former des nanoliposomes. Une fois optimisés, les nanoliposomes étaient en mesure d'encapsuler 51,2 ± 3,6 % de l'E2, avec une capacité de 7,3 ± 0,5 μg/mg. L'internalisation cellulaire a été évaluée en utilisant des

cellules de l'artère coronarienne humaine via la spectroscopie de fluorescence et microscopie confocale. Les liposomes encapsulant E2 ont réduit l'expression du molécule adhésion de cellulaire vasculaire-1 (VCAM-1), un biomarqueur de cellules inflammatoires, en réponse à l'agent pro-inflammatoire, protéine C-réactive (CRP) dans les cellules de l'artère coronarienne humaine. De plus, prétraitement avec les liposomes-E2 a réduit la sécrétion de l'interleukine-8 (IL-8) et facteur de nécrose tumorale alpha (TNF-α) de 60% et 68%, respectivement, ce qui démontre le potentiel de cette thérapie pour traiter l'inflammation à base d'athérosclérose.

Afin de diagnostiquer et utiliser des agents thérapeutiques, il est également nécessaire de localiser et détecter les plaques athérosclérotiques. C'est ainsi que le deuxième objectif majeur de cette thèse s'inscrit dans le cadre de développement des nanoprobes pour détecter l'inflammation vasculaire *in vitro* à l'aide de la spectroscopie Raman exaltée par effet de surface (SERS). Ces nanoprobes, fabriquées par la technologie de microonde, sont composées d'un noyau d'or, enrobées du rapporteur Raman 4-mercaptobenzoïque acide (4-MBA), et poly(allylamine hydrochloride) (PAH). Pour détecter l'expression des molécules de l'adhésion des cellules vasculaires (VCAM-1) dans les cellules de l'artère coronarienne humaine, les nanoprobes ont été biofonctionnalisées avec l'anticorps de VCAM-1 (anti-VCAM-1). Les résultats ont démontré que les nanoprobes peuvent être utilisées pour détecter et localiser l'expression de VCAM-1 *in vitro* par la spectroscopie Raman et la microscopie confocale. Les résultats de cette thèse constituent donc un pas important vers le développement d'un véhicule d'agents anti-

inflammatoires afin d'adresser la réponse inflammatoire impliquée dans l'initiation de l'athérosclérose. Ceci accompagné de la méthode d'imagerie proposée offrirait un outil robuste pour la détection des zones inflammatoires *in vitro*.

Acknowledgements

First and foremost I would like to thank my supervisor, Dr. Maryam Tabrizian, for her enduring support, unwavering patience, and guidance throughout this process. Her stalwart mentorship has been invaluable to my development as a researcher, and I aspire to carry on the work ethic and principles she has demonstrated in her career into my own. I distinctly remember during a difficult period a few years ago, she offered the following words of wisdom – *the strongest steel is forged in the hottest fire*. I will never forget this sentiment and carry it with me always. Thank you.

I would like to gratefully acknowledge and thank Dr. Jean-François Tanguay for his supervisory role and encouragement throughout these past 4 (or so!) years. Despite his demanding clinical duties, Dr. Tanguay was always available to me for an email, phone call, or meeting. His enthusiasm for the project and pioneering work in the field of atherosclerosis and estrogen therapy proved instrumental in shaping this thesis. It was a privilege to work for him. Thanks as well to the great team he assembled at the Montréal Heart Institute – Isabelle Cloutier, Kim Tardif, Sandra Gilligan, and Julie Lebel, for their kindness and assistance.

My deepest thanks to Dr. Marinella Sandros who introduced me to the - quite literally – bright world of inorganic chemistry. She believed in this work and in me from the very start and I am thankful to have been able to work for her and be a part of her group. I would also like to acknowledge the members of this team - *Team Sandros* - Stephen Vance, Effat Zeidan, and Jacob Smith – who straight away

welcomed me into their group and let me access the clandestine SPR/cell culture room! It was a pleasure to work with all three of you.

I am equally grateful to the faculty, staff, and other students at the Joint School of Nanoscience and Nanoengineering at the University of Greensboro in North Carolina for allowing me to work in their facility. Particular thanks to Dean James Ryan and Dr. Daniel Herr for supporting my stay at JSNN.

To all the members of the Biomat'X lab past and present – Amir, Andrew, Christina, Jamal, Mina, Lamees, Khalil, Kaushar, Ryan, and Steve – for putting up with my inane questions, controversial political views, and broken Farsi. Working with you all was a great honor. Thanks for making our hours in the lab pass as minutes. Thanks in particular to Samira Taherkhani for her fastidious work on all things liposome and her willingness to discuss the finer points of their use for hours on end. As well to Dr. Tohid Fatanat Didar for collaboration on the micro-contact printing project – his enthusiasm for research was and continues to be a great inspiration to me. *Merci*. I would also like to thank Ms. Line Mongeon, Ms. Jeannie Mui, and Dr. Kelly Sears for their time and technical expertise towards the microscopy studies in this thesis. Sincerest thanks to Mr. Timothy Jones and to Dr. Hana Anatonicka without whom the Western blot aspects of this project would simply not have been possible.

Thanks to all the members of my Ph.D. advisory committee, Dr. Robert Funnell, Dr. Marta Cerruti, and Dr. Yahye Merhi for their time, advice and support

of this project over the years. I would also like to gratefully acknowledge NSERC and FQRNT for funding my research.

I would again like to extend my gratitude to Dr. Ronald Neufeld, my master's supervisor. The experience of working for him no doubt shaped my future as a research scientist. I hope this work makes him proud.

To my extended family - my friends - who supported me always on this journey and stuck by me despite bouts (years?) of hibernation – especially Caitlin, Amanda, Supriya, Erin A. and F., Aenida, Rebecca, Sarah, Tina, Lauren, and Vanessa.

To Anthony, for his endless support, epic trail runs and adventures that kept my mind clear.

To my grandmother, Silvia, whose zest for life, travel, politics, and science continues to be an inspiration to me. Also, thank you for being the only person outside of academia to actually read my papers.

To my Dad and stepmother, Mary, for your constant support and patience over the past few years. Sunday night dinners and time at home were immensely restorative; thank you for the insightful discussions, encouragement, and faithful kindness during the ups and downs of this journey.

To my 'little' brother, Mike, and in the words of Ray Lewis*, in any war, you put your back to mine; I put my back to yours, and let's do what we gotta do*. Thanks for always having my back, bro.

This thesis is dedicated to my Mom: my role model, cheerleader, and dearest friend. Despite your continual praise of my writing skills, I am at a loss for the words that can adequately express my thoughts and thanks. So let's keep it simple…

Thank you. For everything.

Table of Contents

List of Figures

List of Tables

Glossary

Akt = Protein kinase B
ATP = Adenosine triphosphate
AVE = Artificial viral envelope
BGNP = Bioactive glass nanoparticle
BP = Bisphosphonate
CAM = Cellular adhesion molecule
cAMP= Cyclic adenosine monophosphate
CaP = Calcium phosphate
CRP = C-reactive protein
CS = Chitosan
CT = Computed tomography
CVD = Cardiovascular disease
DDAB = Dimethyldioctadecyl-ammonium
DPPG = 1,2 Dipalmitoyl-snglycero-3-phosphoglycerol
DMPC = 1,2-dimyristoyl-sn-glycero-3-phosphocholine
DOTAP = 1,2-Dioleoyl-3-trimethylammonium-propane
DPPC= 1,2-dipalmitoyl-sn-glycero-3-phosphocholine
DMPG = 1,2-Ditetradecanoyl-*sn*-glycero-3-phospho-(1'rac-glycerol)
DSPE = 1,2-Diastearoyl-sn-glycero-3-phosphoethanolamine
DSPG = Distearoyl phosphatidyl glycerol
E1 = Estrone
E2 = 17β-Estradiol
E3 = Estriol
ER α = Estrogen receptor alpha
ER β = Estrogen receptor beta
EE = Encapsulation efficiency
EDTA = Ethylenediaminetetraacetic acid
ELIP = Echogenic immunoliposome
ELISA = Enzyme linked immunoassay
ECs = Endothelial cells
ELAM-1= Endothelial-leukocyte adhesion molecule-1
EPC = Endothelial progenitor cell
EPhC = Egg phosphatidylcholine
ERK = Extracellular signal-regulated kinase
eNOS = Endothelial nitric oxide synthase
FACS = Fluorescence-activated cell sorting
FBS = Fetal bovine serum
HPLC = High performance liquid chromatography
HVJ = Hemagglutinating virus of Japan
HCAE cells = Human coronary artery endothelial cells
HRT = Hormone replacement therapy
ICAM-1 = Intercellular adhesion molecule-1
IgG = Immunoglobin G

IL = Interleukin
iNOS = Inducible nitric oxide synthase
IFNϒ = Interferon gamma
LC = Loading capacity
LDL = Low density lipoprotein
MAPK = Mitogen-activated protein kinases
mAb = Monoclonal antibody.
4-MBA = 4-Mercaptobenzoic acid
MR = Magnetic resonance
MTT = 3-(4,5-Dimethylthiazol-2-yl)-2,5-diphenyltetrazolium bromide
NIR = Near-infrared
N-dod-PE = 1,2-Dioleoyl-sn-glycero-3-phosphoethanolamine-N-dodecanoyl
NO = Nitric oxide
NP = Nanoparticle
PAH = Poly(allylamine)
PBS = Phosphate buffered saline
PC = Phosphatidylcholine
PCI = Percutaneous coronary intervention
PCL = Poly(ε-caprolactone)
PE= Phosphatidylethanolamine
PEG = Polyethylene glycol
PG = Phosphatidylglycerol
PI3K = Phosphatidylinositide 3-kinase
POPC = 1-Palmitoyl-2-oleoyl-sn-glycero-3-phosphotidylcholine
PVDF = Polyvinylidene fluoride
ROS = Reactive oxygen species
SDS-PAGE = Sodium dodecyl sulfate-polyacrylamide gel electrophoresis
SPR = Surface plasmon resonance
SERS = Surface-enhanced Raman scattering
TBS = Tris-buffered saline
TEM = Transmission electron microscopy
TF= Tissue factor
TFPI = Tissue factor pathway inhibitor
TFF = Tangential flow filtration
TGF-β = Transforming growth factor beta
TNF-α = Tumor necrosis factor alpha
TSPP = Tetrasodium pyrophosphate
VCAM-1 = Vascular cell adhesion molecule-1
VEGF = Vascular endothelial growth factor

Contribution of Authors

This thesis is presented as a collection of manuscripts written by the candidate with the collaboration and guidance of co-authors. Chapter 5 is an original article reviewing the application of liposomes to treat and diagnose cardiovascular disease. This was the first article to be published in the literature that features a comprehensive review of liposomal applications in drug and gene delivery, as well as cardiovascular imaging techniques. The manuscripts comprising Chapter 7, 8 and 9 are written and based on experiments that were originally designed and carried out by the candidate. The candidate developed both the liposomal delivery system for 17β-estradiol, as well as the surface-enhanced Raman scattering nanoprobe utilized in this thesis.

Dr. Marinella Sandros appears as co-author on one of the manuscripts in reflection of her role as a collaborator and her contribution to the fabrication and application of the surface-enhanced Raman scattering nanoprobe; as well as involvement in the corresponding manuscript's preparation.

Dr. Jean-François Tanguay appears as co-author on all papers to reflect his role as co-supervisor and contributor to the cardiovascular-based aspects of this thesis.

Dr. Maryam Tabrizian appears as co-author on all papers as a reflection of her role as primary supervisor throughout the execution of this work, as well as her involvement in the manuscript preparation.

Thesis Outline

In Chapter 1, a general introduction to this thesis is presented. Motivation for the project, specifically the need to treat and diagnose atherosclerosis prior to the onset of clinical symptoms, underpins the problem statement and objectives. The originality of this work and highlights of accomplishments are also presented in this chapter. Chapter 2 provides the rationality for the application of E2 to address atherosclerotic inflammation, the requirement for a liposome-based system to deliver E2, and the application of surface-enhanced Raman spectroscopy to diagnose inflammation *in vitro*. The research hypothesis and objectives are presented in Chapter 3.

Chapters 4, 5, and 6 present background information and a comprehensive literature review of the topics covered in this thesis. Chapter 4 describes the pathophysiology of atherosclerosis, contribution of the inflammatory system, as well as current therapeutics approaches to the disease. A primer on the role of estrogen in the cardiovascular system is also included in Chapter 4, with an emphasis on its role in vascular inflammation. Chapter 5 is comprised of a published review article that details the role of liposome-based systems to treat and diagnosis cardiovascular disease. A critique is additionally provided in this chapter on the future of liposome technology in the context of cardiovascular disease. Chapter 6 highlights various technologies used to assess inflammation *in vitro* and explores, in particular, the application of surface-enhanced Raman spectroscopy to achieve this goal.

Chapter 7 presents the development of a novel liposome vector for the delivery of 17β-estradiol (E2). The purpose was to optimize delivery system fabrication via thin film hydration and characterize in terms of E2 encapsulation efficiency, loading capacity, and release kinetics. The cytotoxicity and cellular uptake capabilities of the liposomes were assessed in human coronary artery endothelial cells. Results showed that liposomes could be used to deliver E2 with the aim of reducing vascular inflammation, which is a key to attenuating atherogenesis.

Chapter 8 reports the *in vitro* application of the liposome vehicle developed in Chapter 7 to address inflammation in a vascular cell model. E2-loaded liposomes were investigated for their ability to attenuate the inflammatory response initiated by C-reactive protein (CRP) in a vascular cell model. Results demonstrated that E2-loaded liposomes could successfully be applied to address and possibly treat the inflammatory components of atherosclerotic initiation.

Chapter 9 investigates the application of a surface-enhanced Raman spectroscopy nanoprobe fabricated via microwave irradiation to localize the expression of inflammatory biomarkers *in vitro*. Specifically, the fabrication of gold nanoparticles coated with 4-mercaptobezoic acid, layered with a protective polymer of poly(allylamine) hydrochloride, and functionalized with the antibody to VCAM-1 is introduced. Detection and localization of VCAM-1 expression using the assembled nanoprobes in human coronary artery endothelial cells is presented.

Finally, Chapter 10 provides a summary and discussion of this thesis project and submits an outline of the future work to move the application of the E2 delivery vehicle to *in vivo* studies and clinical translation. The combinatorial tactic that could be utilized to maximize the therapeutic and diagnostic potential of this work is explored.

Chapter 1: Introduction

Cardiovascular disease (CVD), which encompasses a collection of heart and vascular-based disorders, is the second leading cause of death amongst Canadians [1]. Despite recent reductions in the morbidity and mortality associated with CVD, it still accounts for roughly 30% of deaths in Canada and imposes a significant economic burden, with over $20 billion attributable to health care costs, lost wages, and decreased productivity. Atherosclerosis, which is characterized by the build-up of plaque in blood vessels, is the underlying condition of the majority of CVD complications and deaths, including myocardial infarction, stroke, and aneurism. However, the complex pathophysiology of atherosclerosis, characterized by a diverse accumulation and remodeling of plaque [2], can make it difficult to correctly diagnose and effectively treat [3]. Common therapeutic strategies include lipid-lowering [4, 5] and anti-hypertensive drugs [6, 7], though recent evidence highlighting the role of inflammation has engendered the application of strategies to attenuate the immune-mediated aspects of the disease [8-10]. Equally, the inflammatory initiation of atherosclerosis and associated endothelial dysfunction may serve as a practical target to localize and detect plaque prior to the onset of clinical symptoms.

The female sex hormone 17β-estradiol (E2) has been shown to decrease vascular inflammation [11-13], in addition to other cardioprotective effects [14, 15]. However, conventional pharmaceutical treatments of hydrophobic active agents, such

as E2, cannot be administered locally due to toxicity effects, poor retention, and cellular uptake at sites of delivery. Therefore, for the first part of this project, we propose to engineer and study the effects of a liposomal delivery vehicle for E2 with the aim of treating inflammatory-based atheroma initiation. In parallel, we recognize that early detection and localization of endothelial dysfunction is of particular importance to efficiently deliver nanoparticle-based delivery vectors to sites of atherosclerotic initiation. Consequently, for the second part of the project, we focused on the development and application of a surface-enhanced Raman scattering (SERS) nanoprobe to detect and localize areas of inflammation in an *in vitro* vascular cell model. The application of this technology in tandem with E2-liposome based-vectors could allow for precise localization of plaque formation, facilitate the delivery of therapeutic drugs to areas of endothelial activation, and ultimately attenuate the development of atherosclerotic plaque and reduce acute coronary events.

The originality of this project lies in two general areas: (i) the development of a cytocompatible liposome delivery vehicle for E2 with demonstrated cellular uptake and anti-inflammatory properties, and (ii) the engineering of a novel surface-enhanced Raman scattering (SERS) nanoprobe via microwave technology for the detection of inflammatory biomarkers *in vitro*. Although some researchers have investigated the delivery of E2 with various nanoparticles [16-18], and others have probed the application of liposomes with various estrogens [19, 20], this work is the

first to conduct a study on the encapsulation of E2 within various lipids and report effects on encapsulation efficiency and loading capacity. Furthermore, we are the first to demonstrate that liposome uptake in human coronary artery endothelial cells is increased significantly in liposomes composed of cationic lipids, compared to those made of neutral or anionic lipids. As well, we show for the first time that pre-treatment with E2-liposomes confers anti-inflammatory effects in human coronary artery endothelial cells by decreasing the expression of inflammatory cell adhesion markers and cytokines. With regards to the SERS imaging, there are no reports on the application of microwave technology to successfully synthesize SERS nanoprobes. We are the first to apply this technology to rapidly produce stable nanoprobes capable of straightforward bioconjugation and application to map the expression of inflammatory biomarkers *in vitro*.

Chapter 2: Thesis Rationale

2.1 Rationale for 17β-Estradiol to Treat Atherosclerotic Inflammation

Epidemiological data has shown that premenopausal woman experience significantly less incidents of adverse coronary events compared to men of the same age and postmenopausal women [21]. Though there are a variety of factors that may contribute to this finding, numerous studies have demonstrated convincing evidence for the role of estrogens, which are present in higher levels in premenopausal females [22]. Particularly, E2 has been shown to affect a variety of cardiovascular processes, conferring local effects on cardiac [23, 24] and endothelial cells [25, 26], reactive oxygen species [27], and inflammatory mechanisms [28]. In terms of attenuating the early development of atherosclerosis, the effects of E2 on inflammation are of particular interest. Indeed, it has been shown the blocking the attachment and entry of monocytes may prevent the development of atherosclerotic lesions in murine models [29] and that the modulating expression of endothelial cell ligands, such as ICAM-1 and VCAM-1, play an integral role in this process [30]. The early expression of VCAM-1 in the development of atheromas [2] is particularity relevant in the context of E2, since E2 has been shown to downregulate VCAM-1 expression in cells [13, 31]. As well, E2 has been shown to inhibit the secretion of cytokines, such as IL-1 and IL-6 [28], IL-8[32], and TNF-α [33], which are key modulators of inflammation. Considering this data, we propose to develop and characterize a

liposomal-E2 delivery system with the aim of attenuating the inflammatory response, and consequently the progression of atherosclerotic disease.

2.2 Rationale for Liposome-Based Delivery System

Conventional pharmaceutical treatments, such as E2, often require high dosages due to non-specific distribution, poor retention at sites of delivery, and short half-lives experienced *in vivo*. These levels can lead to adverse side effects and unsustainable drug levels. Encapsulation into liposomes, which are defined as artificial vesicles composed of an aqueous core surrounded by lipid bilayers, has been proposed as a means to remedy these obstacles by controlling therapeutic delivery over a desired timeline [34], shielding the body from toxicity [35], increasing residence time, and protecting therapeutic agents from degradation [36]. In addition, liposomes are advantageous since they are generally composed of naturally derived materials that are biocompatible. On account of their hydrophilic core and lipophilic outer layer, liposomes can encapsulate most active agents, irrespective of solubility and physical properties. This property makes them well suited to delivering a variety of drugs.

The application of liposomes to deliver E2 is therefore proposed to improve delivery efficacy over conventional methods. Oral delivery of E2 suffers from poor bioavailability (~10%) due to first pass metabolism, and can elicit negative changes in hepatic gene expression due to uptake by the liver [37]. Furthermore, a systemic delivery of free E2 cannot specifically migrate to areas of vascular inflammation in

the body, which could result in potentially unwanted side effects. On the other hand, a liposomal delivery of E2, specifically designed for uptake by endothelial cells, could serve to improve delivery to affected sites. Moreover, the capability of liposomes to carry highly specific targeting antibodies, could further improve accumulation, target cell uptake and, consequently, therapeutic efficacy. While water soluble E2, which is enclosed within a cyclodextrin matrix, can be purchased commercially and utilized for *in vitro* studies, it is not suitable for translation to *in vivo* studies due to potential toxicity issues [38] and lack of a control over delivery compared to nanoparticulate vehicles. It is for these reasons that we propose to develop a liposomal delivery system for E2, capable of assisting the cellular delivery of E2 with the ultimate goal of attenuating the development of atherosclerosis.

2.3 Rationale for Surface-Enhanced Raman Scattering to Detect Atherosclerotic Inflammation

Biochemical assays, such as Western blot and ELISAs, are routinely used to quantify the expression of cellular adhesion molecules, however these approaches do not furnish localization information. Raman micro-spectroscopy, on the other hand, enables simultaneous chemical identification and imaging. Raman micro-spectroscopy has recently been used in the pharmaceutical and biomaterial fields owing to advantages such as minimal sample processing, as well as the non-invasive and non-contact nature of the technique [39]. However, the primary challenge to

using Raman spectroscopy effectively, especially to study cellular systems, is weak signal intensities.

Of interest to diagnostic and drug delivery research is the application of surface enhanced Raman scattering (SERS), which can yield significant improvements in signal intensity when molecules are near or adsorbed to the surface of nanostructured materials [40]. Such nanomaterials, referred to as SERS substrates or probes, can be exploited to specifically identify target molecules, such as cellular adhesion molecules, when studded with Raman reporters and functionalized with bioactive ligands [41]. With these properties in mind, we aimed to develop a Raman scattering nanoprobe capable of detecting and localizing the expression of VCAM-1 expression in human coronary artery endothelial cells. The ultimate goal of this technology would be to use SERS diagnostic information as a basis for cell treatment with E2.

Commercially available 50 nm gold nanoparticles were selected based on their inert properties, cytocompatibility, long-term stability, and Raman signal intensifying properties [42]. The aromatic thiol, 4-MBA, was selected as Raman reporter due to its propensity to form surface adsorbed monolayers (SAMs) onto gold nanostructures that yield strong Raman scatting signals, with characteristic peaks at 1076 and 1586 cm^{-1} (attributed to aromatic ring vibrations) [42, 43]. The cationic polyelectrolyte, poly(allylamine hydrochloride) (PAH), was selected as the protective coating due to it's amine groups that serve as antibody functionalization anchors, as

well as previous research supporting successful application both *in vitro* and *in vivo* [44]. Finally, VCAM-1 was selected as the target biomarker for vascular inflammation since previous research had shown upregulation in HCAE cells upon activation with the proinflammatory agent, CRP [13].

Chapter 3: Thesis Hypothesis and Objectives

3.1 Hypothesis

Recent evidence citing the role of the inflammatory response in the development of atherosclerosis has incited the application of anti-inflammatory agents to reduce atherogenesis in the vasculature. Accordingly, we hypothesized that a liposomal delivery vehicle for E2 may aid delivery of the drug and attenuate the inflammatory response in human coronary artery endothelial cells, while surface-enhanced Raman scattering could be used as a means to detect and localize sites of inflammation in the same cell model.

3.2 Thesis Objectives

The main objective of this dissertation was, therefore, to develop a delivery system for E2 with the goal of treating inflammatory-mediated aspects of atherosclerosis. Given the role of accurate detection in the treatment and diagnosis of atherosclerosis, the secondary objective was to investigate a novel approach to detect and localize the upregulation of inflammatory biomarkers *in vitro* using confocal Raman microscopy.

The goals of this project can be broken into the following sub-objectives:

Objective #1: Develop and characterize a liposome based-delivery system for E2 (Chapter 7).

Objective #2: Study the *in vitro* uptake capacity of liposomal-E2 delivery device in human coronary artery endothelial cells (Chapter 7).

Objective #3: Investigate the ability of E2-loaded liposomes to attenuate the inflammatory response incited by C-reactive protein in human coronary artery endothelial cells (Chapter 8).

Objective #4: Develop and characterize a surface-enhanced Raman scattering nanoprobe with the goal of detecting inflammatory biomarkers *in vitro* (Chapter 9).

Objective #5: Utilize the probe developed for Objective #4 in combination with confocal Raman microscopy to localize and detect the inflammation biomarker VCAM-1 in human coronary artery endothelial cells (Chapter 9).

Literature Review and Background

The following three chapters provide the contextual knowledge and comprehensive literature review required for the completion of this thesis project. Chapter 4 presents the pathophysiology of atherosclerosis and features recent evidence demonstrating the role of the inflammatory response in the initiation of atherogenesis. Current approaches to the treatment of atherosclerosis, including therapies aimed at controlling serum lipid levels, reducing blood pressure and clots, as well as invasive interventions, are described. An analysis of the applications and advantages of anti-inflammatory treatments with the aim of attenuating atherogenesis are also presented in this chapter. The cardioprotective effects of estrogens in general and in the context of addressing atherosclerotic inflammation, are also included in Chapter 4.

Chapter 5 is comprised of a published review article written by the candidate and is focused on the application of liposome vectors to treat and diagnose cardiovascular-based diseases. An exhaustive review of liposomal targeting to the cardiovascular system, as well as various pharmacological and gene delivery applications using liposomes to treat cardiovascular diseases are included. Finally, the application of liposomes for cardiovascular imaging and diagnostic purposes is highlighted. This review paper, entitled "Liposome Technology for Cardiovascular Disease Treatment and Diagnosis", was accepted for publication in the journal *Expert Opinion on Drug Delivery* in February 2012.

Chapter 6 details current technological approaches to assessing inflammation *in vitro*. Western blot, enzyme-linked immunosorbant assay, fluorescence, and spectroscopy-based techniques are explored. A particular emphasis on the use and purported advantages of surface-enhanced Raman scattering for detection and localization of inflammation *in vitro* is included. The need for a multifaceted method, such as surface-enhanced Raman scattering, to both detect and localize inflammation in the vasculature is described.

The knowledge gained from these literature reviews aided to inform the problem statement and provide the candidate with the basic biological and technological background needed to design, characterize, and demonstrate the application of the nanoparticle-based vectors developed in this project.

Chapter 4: Atherosclerosis and Estradiol Delivery

4.1 Atherosclerosis

Atherosclerosis is a class of CVD, characterized by the build-up of fatty lesions or plaques in arteries [2]. Encompassing both genetic and lifestyle components, physiological progression of the disease begins early in life with clinical symptoms often only revealed in later years. Atherosclerosis can be manifested in both chronic and acute aspects, with the rupture of lesions leading to major adverse cardiovascular events, such as myocardial infarction and stroke [45]. Acute coronary syndrome can also result from atherosclerotic plaque formation, and may encompass chronic chest pain or angina pectoris.

Traditional concepts of the disease portrayed hyperlipidemia, the ensuing accumulation of lipoproteins in the vascular wall, and the proliferation of cells upon activation of the endothelium to be the basis of plaque development, however recent evidence has indicated that the immune system may play an equally significant role in the initiation and evolution of the disease [8, 30]. The next section will provide a brief introduction to the basics of vascular biology and outline the current understanding of the pathophysiology of atherosclerosis, which will serve as a backdrop for the summary and rationale for the various treatments approaches that follow.

4.1.1 Atherosclerosis Pathogenesis

Atherosclerosis occurs in the medium- and large sized artery walls. Arteries are composed of three distinct concentric layers of tissue: the intima, media, and adventitia (See Figure 4.1) [2]. The intima is composed of endothelial cells (ECs) that line the arterial wall and are the point of contact with blood in healthy individuals. Not simply a static barrier, ECs participate in a dynamic process of monitoring vascular permeability, inflammation, interactions with blood components, as well as in the construction of new blood vessels [2]. The endothelial layer resides on an internal elastic lamina, which is composed primarily of fibronectin, collagen, and proteoglycans. The medial layer affords structural support, and is comprised of smooth muscle cells (SMCs) interlaced with layers of extracellular matrix. The outermost adventitial layer is similarly composed of collagen, though less densely packed than the collagen of the intima, and houses nerve endings, as well as fibroblasts, and mast cells.

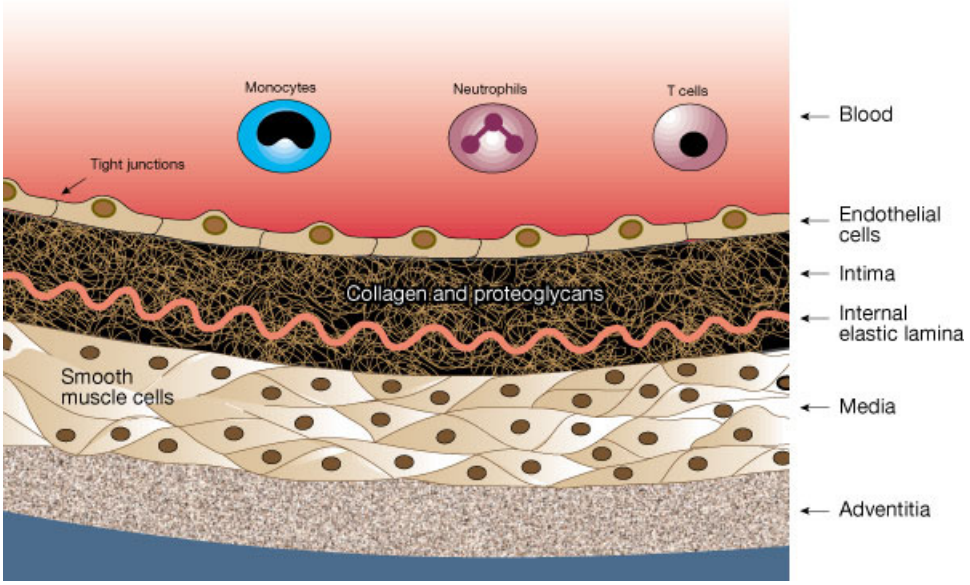

Figure 4.1 – Schematic depicting the basic structures of normal arteries. The intima is made up of endothelial cells, which are in direct contact with blood, and a fibrous matrix constituting the internal elastic lamina. The media is primarily smooth muscle cells that provide tone and structural support to the artery. The outermost layer, or adventitia, is made of loosely packed extracellular matrix proteins, fibroblasts, and mast cells. Reproduced from [46].

The initial stages of atheroma progression are understood to occur when small lipoproteins accumulate in the wall of the intima [2]. Overtime, these lipoproteins, specifically low-density lipoprotein (LDL), tend to form aggregates in the arterial wall and undergo various chemical changes, such as oxidation or glycation, which induces the activation of ECs (See Figure 4.2). Activated ECs then express inflammatory adhesion molecules, such as vascular cell adhesion molecule-1 (VCAM-1) and intercellular adhesion molecule-1 (ICAM-1), as well as secrete chemokines that recruit monocytes to the area. Monocytes that adhere to the endothelium then permeate the intima, where they can differentiate into macrophages

and endocytose oxidized-LDL (ox-LDL) to become fat-laden foam cells. These foam cells serve as the basis for the formation of 'foamy plaques' or 'fatty streaks' [46]. Though such lesions may not be clinically significant, they can undergo necrotic breakdown to transform into more threatening fibrous lesions that can occlude blood flow, erode, or rupture, resulting in unstable angina, myocardial infarction, and/or stroke [30].

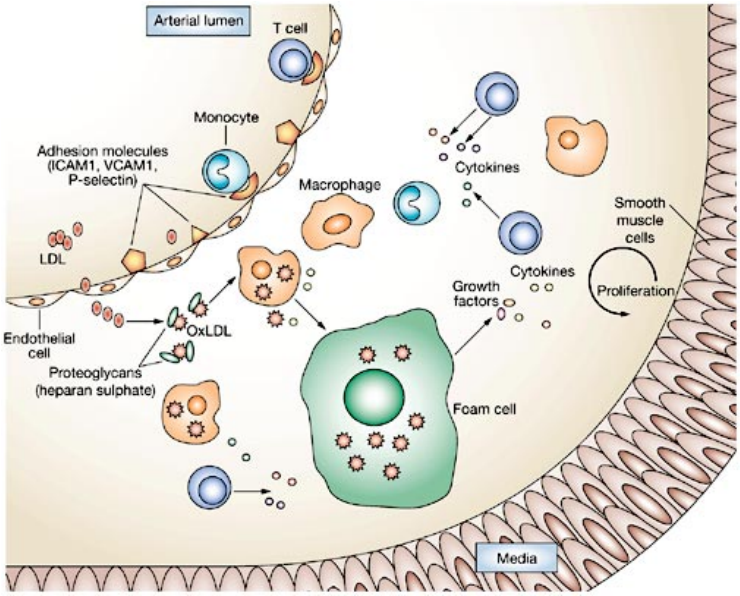

Figure 4.2 – Schematic of the evolution of atherosclerotic plaque. Low-density lipoprotein accumulates in the arterial wall, becoming oxidized. Oxidized low-density lipoprotein induces activation of endothelial cells, which express inflammatory adhesion molecules and secrete chemokines. Recruited monocytes migrate into the artery, differentiate into macrophages, and take up oxidized low-density lipoprotein to become foam cells. These foam cells, as well as T cells, release growth factors that promote proliferation of smooth muscle cells and extracellular matrix proteins creating a fibro-fatty lesion. Reproduced from [47].

The transition from fatty streak to fibrous lesion occurs upon accumulation of foam cells that secrete growth factors promoting the migration and proliferation of SMCs, as well as the secretion of extracellular matrix proteins (see Figure 4.2). Overtime, this process leads to significant plaque growth that can impede blood flow through the artery. T helper cells at the site may also promote further activation of the endothelium by secreting proinflammatory chemokines, such as interferon gamma (IFNϒ) and tumor necrosis factor-alpha (TNF-α) [47]. These can alter plaque composition and increase susceptibility to rupture. In later stages of the disease, SMCs that have penetrated the intima may undergo programmed cell death (apoptosis) triggered by inflammatory molecules present in the atheroma. The resulting plaque becomes a cesspool of dead or dying cells and associated debris that may become calcified. Eventually, the fibrous capsule encasing a lipid-rich core may severely restrict blood flow, resulting in chronic stable angina. Acute events, such as myocardial infarction or unstable angina, occur primarily from lesions that do not cause significant stenosis of the artery, though the mechanism of plaque development is similar [2]. A given plaque's susceptibility to rupture, initiate thrombosis, and thus, trigger acute cardiovascular events, may likewise be governed by inflammatory mechanisms. Specifically, macrophages at the site that express catabolic enzymes, such as matrix metalloproteinases and elastic cathepins, can break down collagen and extracellular matrix, weakening the structural integrity of the fibrous cap and leaving it prone to rupture [48].

Overall, it is evident that the initiation of a maladaptive inflammatory response plays a critical role in atherogenesis, as well as associated atheroma complications, and thrombosis. Figure 4.3 summarizes the role of inflammation and lipid metabolism on the accumulation of plaque. Specifically, the activation of ECs to express inflammatory adhesion molecules, such as ICAM-1 and VCAM-1, helps promote blood-borne monocyte attachment, and infiltration into local tissue. Furthermore, cells secrete proinflammatory mediators and oxidants that can exacerbate the response and promote plaque development. The proinflammatory response releases markers such as TNF-α, interleukin-6 (IL-6), and interleukin-8 (IL-8), which can engage hepatic receptors to release C-reactive protein (CRP). Accordingly, an increase in circulating inflammation markers, such as CRP, is predictive of cardiovascular events even in individuals with normal levels of traditional lipid biomarkers, such as LDL cholesterol [49]. In addition, CRP has been shown to mediate local inflammation, which may also contribute to cyclical feedback of inflammation and exacerbation of this chronic condition [50]. Thus, potential approaches to atherosclerosis management and treatment may well benefit from a focus on addressing the inflammatory components of the disease, in addition to the dyslipidemia that contributes plaque initiation and evolution.

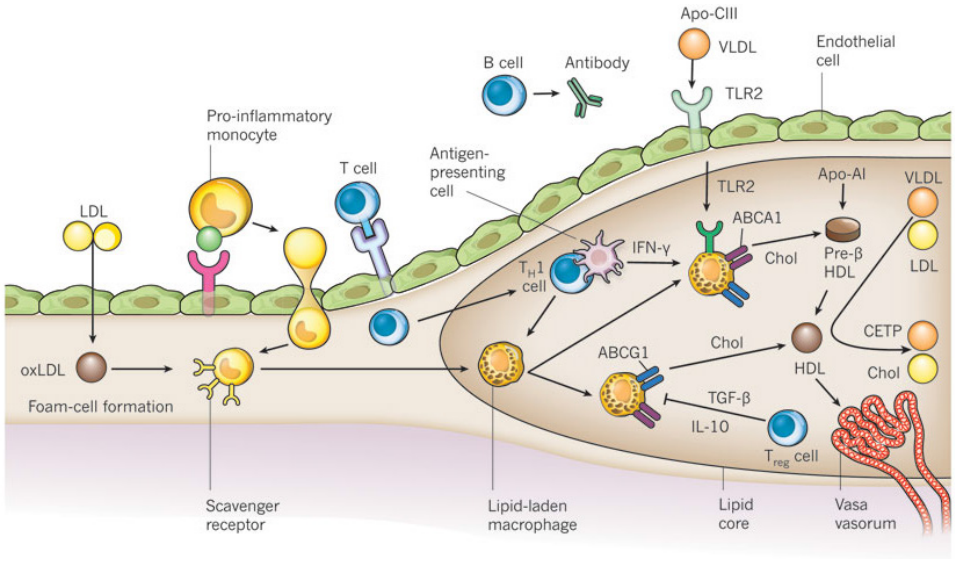

Figure 4.3 – Schematic diagram depicting the inflammation cascade and its effects on atherosclerotic plaque development.
Reproduced from [51].

4.1.2 Therapeutic Approaches for Atherosclerosis

Due to the multifaceted nature of atherosclerosis, current treatments can broadly be categorized based on their target actions. Specifically, these can be broken down into strategies aimed to: (i) control serum lipid levels, (ii) reduce blood pressure, and (iii) mediate or attenuate thombolytic complications [52]. In addition to modulating risk factors through diet and lifestyle, a significant portion of atherosclerosis prevention and treatment has focused on addressing dyslipidemia, which is highly predictive of CVD [48]. Pharmacological approaches have been designed to reduce lipid cholesterol levels and/or target certain enzymes and molecules involved in the atherogenic process [53]. For example, 3-hydroxy-3-methylglutaryl-CoA reductase inhibitors (statins) [5], ezetimibe [54], nicotinic acid

[55], and fibrates [56] have all been shown to have favorable effects on hypercholesterolemia. Reducing cholesterol levels via drug therapy has indeed been correlated to decreased atheroma size (evolution stage), with statins in particular, demonstrating the most promising changes in CVD morbidity and mortality [57].

In addition to lipid lowering treatments, alternative approaches include anti-hypertensives or vasodialators, such as β-blockers [58] and renin-angiotensin (ACE) inhibitors [59], that work to control blood pressure and reduce the risk of atherosclerotic complications [60]. However, this approach does not treat atheroma initiation or progression but rather reduces one of the risk factors (high blood pressure) associated with atherosclerotic complications. Other approaches include anti-thrombolytic agents or anti-platelet therapies, such as aspirin and/or clopidogrel [61], similarly are used to prevent acute atherosclerotic events. Invasive strategies, such as percutaneous coronary interventions and coronary by-pass surgery, are typically utilized upon clinical manifestation of symptoms and for the management of acute or chronic complications, for example thrombosis and myocardial infarction [2].

Owing to the prominent role of inflammation in the pathogenesis of atherosclerosis described in Section 4.1 [8], an alternative treatment strategy has recently been employed to target this component of the disease. Specifically, pharmacological immunomodulation agents and vaccination have been investigated as a means to delay atheroprogression [62]. Exploiting adaptive immunity via

vaccination has afforded limited success, with some groups demonstrating that immunization with oxLDL reduces atherosclerotic lesion formation and size [63, 64], with the induction of an oral tolerance [65, 66]. Anti-inflammatory pharmacological agents have also induced changes in plaque formation, size, and stability [67]. Mechanisms to explain these phenomena include: a down-regulation of inflammatory cell adhesion markers, a decrease in proinflammatory cytokine excretion, and overall reduction in inflammatory cell activity at the endothelium. For example, estrogen has been shown to decrease cell adhesion molecules ICAM-1 and VCAM-1 expression in ECs [13], and, accordingly, to decrease fatty lesion formation *in vivo* [68]. While TNF-α blockers, such as cilostazol, decreased atheroma formation in mice [69]. In addition to effects on lipid levels, statins have also been shown to influence the inflammatory process, which may account for their continued clinical application [70]. No doubt, the preferred course of disease management would focus on the formation of plaque prior to manifestation of clinical symptoms and, accordingly, it is likely that targeting the immune response right at the initiation of plaque formation may provide the key to combatting atherosclerosis in the future.

4.2 Estrogen and Cardiovascular Disease

Both anecdotal evidence and clinical studies have indicated that pre-menopausal women experience significantly lower rates of cardiac events compared to men of the same age and postmenopausal women [21, 71, 72]. Researchers speculated that this phenomenon could be associated with the relatively high

estrogen levels present in premenopausal women and their potentially cardioprotective effects [73, 74]. For example, Hamelin *et al.* (2003) reported a higher risk of cardiac episodes for premenopausal women during and immediately after menses, when estrogen concentrations are lowest [75]. Although controversies arose from large-scale hormone replacement therapy (HRT) control trials as to whether estrogen actually conferred positive effects on cardiovascular morbidity and mortality in postmenopausal women [76], significant experimental evidence has nevertheless demonstrated the multifaceted and potent role of estrogens on the cardiovascular system [15, 77-81]. Furthermore, recent analysis of HRT trials, specifically the largest Women's Health Initiative (WHI) and Heart Estrogen/progestin Replacement Study (HERS), revealed several shortcomings in study designs, including the type of hormone used (typically equine) and the intervention timing, which may account for such unexpected results [82].

The following section will provide an introduction to the physiological functions of estrogen and highlight research on its role in diverse physiological processes within the cardiovascular system. As well, the therapeutic potential of estrogen for the management of CVD will be discussed, with an emphasis on atherosclerosis related therapy.

4.2.1 Biological Functions of Estrogen

Estrogens are a group of steroids primarily involved in female sexual development, reproductive, and menstrual cycles. They are predominantly found in

high concentrations in women from adolescence to menopause, though they are also present at lower doses in men and postmenopausal women [83]. Three naturally occurring forms of estrogen are found in the body: estrone (E1), 17β-estradiol (E2) and estriol (E3) (see Figure 4.4). E2 is the most potent form of estrogen and found in the highest concentration in non-pregnant premenopausal women.

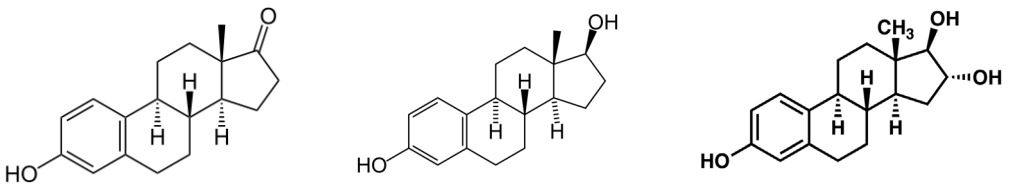

Figure 4.4 – Chemical structures of estrogen subtypes: estrone, 17β-estradiol, and estriol.

Estrogen acts via two ligand-activated transcription factors that regulate gene expression, estrogen receptor-alpha (ERα) and estrogen receptor-beta (ERβ). These receptors may be localized in the plasma membrane, cytoplasm, and/or nucleus of various cell types, including endothelial [84] and smooth muscle cells [85]. Genomic effects of estrogen are most likely mediated by intra-nuclear ERα and ERβ, which can form E2-ER complexes and initiate protein transcription [86]. Non-genomic effects are thought to occur when E2 binds to receptors located in the plasma membrane, which initiates a rapid response independent of transcriptional regulation [87]. Membrane associated ERα and ERβ receptors have been shown to activate or

inhibit signaling cascades including phosphatidylinositol-3 kinase (PI3K)/Akt [88], JNK, MAPK p44/p42, and MAPK p38 [78], all of which influence various processes within the cardiovascular system.

Recently, a third receptor, G protein-coupled receptor 30 (GPR30), localized in the plasma membrane and endoplasmic reticulum of both SMC and ECs, has been shown to play a role in mediating non-genomic estrogen functions [89, 90]. Particularly, evidence has demonstrated GPR30's role in the regulation of endothelial inflammation and vasoregulation [91], though its precise role in estrogen physiology is still under active research [92]. Figure 4.5 outlines the various receptors and pathways that mediate E2 action on cells.

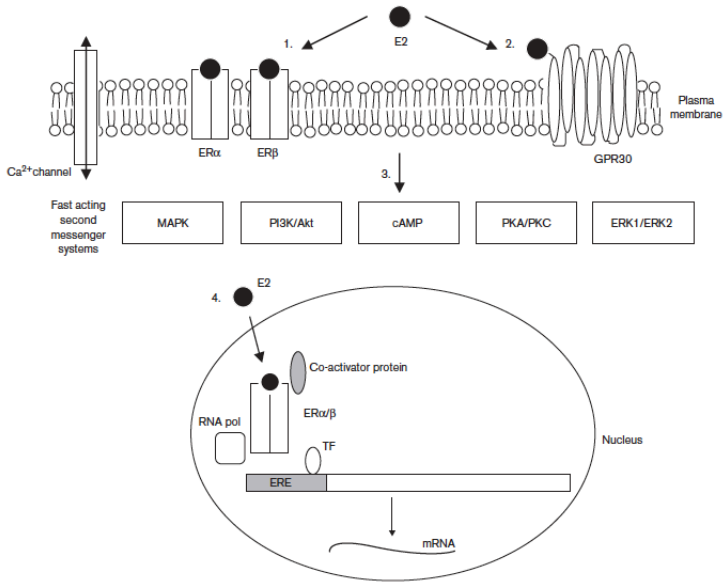

Figure 4.5 – Schematic summarizing the genomic and non-genomic actions of E2 via receptors present on the cell membrane and nucleus. Reproduced from [87].

4.2.2 Cardioprotective Effects of Estrogen

Numerous studies and clinical trials have demonstrated that estrogen plays a multifaceted and complex role in cardiovascular dynamics, with the majority of its effects proffering varying degrees of protection against CVD [73, 83, 93, 94]. For example, E2 has been shown to reduce restenosis after angioplasty [95], attenuate the development of atherosclerotic lesions [96], prevent the development of heart failure [14], and improve healing following myocardial infarction [97]. With regards to specific actions that might account for these observations, estrogens have been implicated in both indirect (systemic) and direct (local) processes [83, 93, 98, 99]. In terms of systemic effects, estrogen favorably affects blood lipid and lipoprotein levels [100, 101]. However, this effect is only thought to account for roughly 30% of the cardioprotection afforded by E2 [102], with local effects of E2, particularly on the vasculature [103] and cardiac tissue [22], likely contributing to the observed benefits in a greater capacity. Figure 4.6 graphically depicts the reported benefits of estrogen on the cardiovascular system, while Table 4.1 details a selection of studies demonstrating cardioprotective effects.

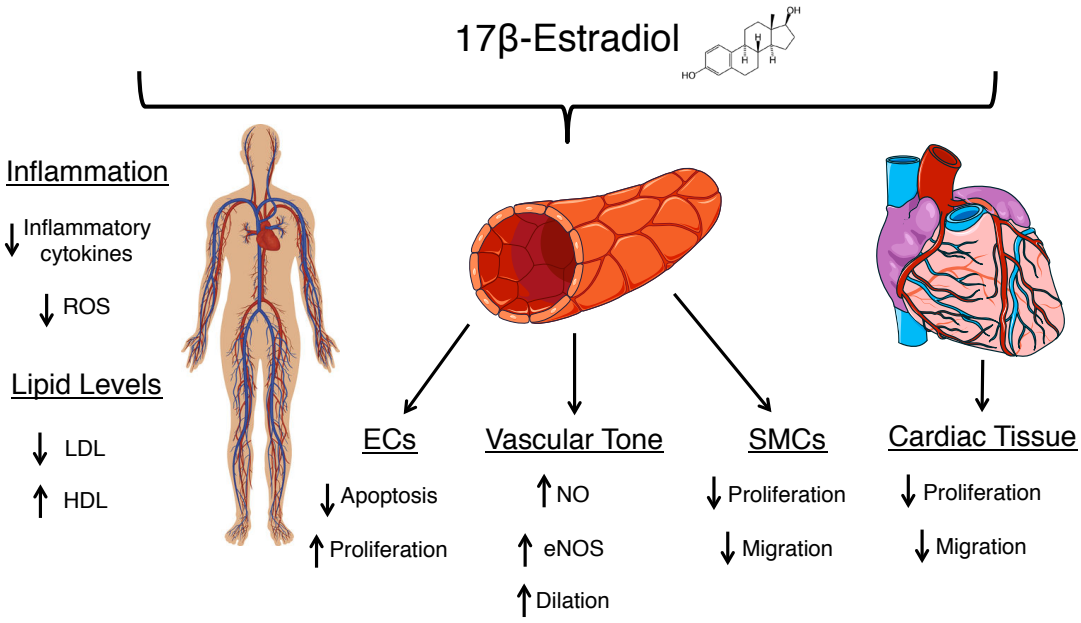

ROS = Reactive oxygen species; LDL = low density lipoprotein; HDL = high density lipoprotein; EC = endothelial cell; NO = nitric oxide; eNOS = endothelial nitric oxide synthase; SMC = smooth muscle cell

Figure 4.6 – Schematic of estrogen's effects on the cardiovascular system.

Table 4.1 – Cardioprotective effects of estrogen.

Target/ System	Mechanism of Estrogen Action	Potential Outcome(s)	Ref.
Serum lipids	Associated with smaller LDL	Decreased oxidation of LDL may reduce atherogenesis	[104]
Cardiac tissue	Activates PI3K/Akt pathway	Reduced cardiomyocyte apoptosis, improve prognosis after injury	[88]
	Stabilizes pH, Na^{+}, influx of Ca^{2+}	Improved recovery after reperfusion, reduce apoptosis	[105]
EPCs	Enhances EPC mobilization	Contributes to remodeling, improved vascular function	[106]
Endothelium	Reduces EC apoptosis, attenuated phosphorylation of MAPK p38, p44, p42	Decreased endothelial dysfunction associated with plaque initiation	[26]
	Increases NO, cAMP production	Vasorelaxation, lower blood pressure	[107]

Vasculature	Inhibits hyaluroic acid synthase 1	Decreased SMC proliferation and luminal thickening	[108]
	Increases basal NO production	Protects against platelet aggregation, endothelial dysfunction	[109]
	Phosphorylates MAPK p44, p42, p38 in ECs, reverse in SMCs	Improved vascular healing and reduces restenosis after injury	[110]
	Activates PI3K/Akt pathway	Increased eNOS and vasorelaxation	[110]
	Inhibits progression of fatty streak	Attenuates the progression of atherosclerosis	[111]
	Regulates expression of microRNAs, inhibiting SMC proliferation	Reduced restenosis after endothelial injury	[85]
	Downregulates matrix metaloproteinase-9 expressions via regulation of oxLDL	Decreased matrix metaloproteinase may attenuate plaque disruptions	[112]
	Activates MAPK signaling	Increased EC proliferation, decreased SMC proliferation	[25]

ROS	Activates PI3K/Akt pathway	Inhibited ROS formation	[113]
	Activates MAPK p44/p42 and NFκ B cascade	Increased antioxidant expression, inhibited ROS formation	[114]
Inflammation	Decreases CRP production and proinflammatory IL-8, VCAM-1, ICAM-1	Modulated inflammatory response and improve vascular repair	[13]
	Negatively modulates pro-inflammatory mediators, inhibits neutrophil infiltration	Modulated inflammatory response	[28]
	Decreases TNF-α and TNF-α receptors	Modulated inflammatory response, attenuated atherogenensis	[115]
	Decreases TNFα, IL-1β, and IL-6	Modulated inflammatory response, attenuated atherogenensis	[78]
	Increases anti-inflammatory cytokine TGF-β	Prevents vascular inflammation and stabilize atheromas	[116]

LDL = Low density lipoprotein; PI3K = phosphatidylinositide 3-kinase; Akt = protein kinase B; EPC = endothelial progenitor cell; EC = endothelial cell; NO = nitric oxide; cAMP= cyclic adenosine monophosphate; SMC = smooth muscle cell; oxLDL = oxidized LDL; MAPK = mitogen-activated protein kinases; ROS = reactive oxygen species; eNOS = endothelial nitric oxide synthase; CRP = C-reactive protein; VCAM-1 = vascular cell adhesion molecule-1, ICAM-1= intercellular adhesion molecule-1; IL = interleukin; TNF-α = tumor necrosis factor alpha; TGF-β = transforming growth factor beta

Based on the studies presented in Table 4.1, we can conclude that estrogen is a potent factor in the cardiovascular system affecting lipid levels, local processes such as vasodilation, endothelial repair, inflammation, and oxidation. The following sections will briefly expand on the discussion of the influence of estrogen in the vasculature and on the inflammatory response.

4.2.3 Estrogen and the Vasculature

The role of estrogens in the regulation of the vasculature has been an area of intense research over the past 30 years [86]. Estrogen has been shown to directly affect ECs [117] and vascular SMCs [118], as well as regulate vasodilatation [107] and reduce the expression of inflammatory cytokines [13], all of which may contribute to the therapeutic effects of estrogen observed after injury to the endothelium [119] or to the improvement in the prognosis of atherosclerosis [120].

A critical component of estrogen's cardiovascular benefit appears to be its influence over the generation and regulation of nitric oxide (NO) [121, 122]. NO, a free radical messenger, plays a multifaceted role in vascular biology and endothelial regulation [2]. In particular, NO affects the endothelium via its action on inflammatory cells and cytokine expression, platelet aggregation and adhesion [123], as well as SMC proliferation [124]. Indeed, a dysfunctional endothelium is associated with reduced levels of NO, which can exacerbate the pathogenesis of atherosclerosis and CVD [125]. Darblade *et al.* (2002) demonstrated that E2 increased the basal production of NO in murine models [109], which is mechanistically thought to occur through E2's non-genomic influence on endothelial nitric oxide synthase (eNOS) production [126]. Chambliss *et al.* (2000) showed that

estrogen causes NO-dependent vasodilation via ERα localized in the caveolae of ECs, and thus activation of eNOS [122]. In the same vein, E2 was shown to affect vasodilation by inhibiting the production of NOS inhibitors, such as asymmetric dimethylarginine [84].

Recent research has shown that E2 directly regulates vascular healing, which is likely mediated by its effects on endothelial progenitor cells (EPCs), as well as local action on SMCs [24, 97, 106, 127]. Lemieux *et al.* (2008) demonstrated that E2 affects the bone marrow stem cell niche and may according influence bone marrow derived-EPC activity [81]. While Ruifrok *et al.* (2009) showed that E2 dose-dependently mobilized EPCs from bone marrow and, furthermore, that these cells subsequently participated in neovascularization [127]. Taken together, these results demonstrate that E2 has an effect on EPCs and local responses to injury, which could be exploited to promote vascular healing.

4.2.4 Estrogen and Inflammation

In addition to direct effects of estrogen on the vascular system, a wide body of evidence has demonstrated that modulation of the inflammatory response may also account for the cardioprotective and anti-atherogenic effects of E2 observed in both experimental and clinical models (See Table 4.1). Specifically, antioxidant properties and the regulation of proinflammatory cytokines have been shown to contribute to the reduced inflammatory responses observed *in vitro* [13, 128], *ex vivo* [78], and *in vivo* [28]. In addition, the generation of NO by estrogen, as detailed in Section 4.2.3, may also partially contribute to its anti-inflammatory effects, as NO has been shown

to mediate inflammation [129] via decreased leukocyte recruitment and scavenging of ROS [11].

E2 itself may also function as an antioxidant [130], attributed to the phenolic group and hydrogen donations, which may enable it to function as a free radical scavenger [120]. ROS, such as superoxide ions (e.g. O_2^-), are known to contribute to oxidative stress, which is a potent factor in the pathogenesis of CVD, endothelial dysfunction, and oxidation of LDL, a critical step atherogenesis [131]. Indeed, Lee *et al.* (2008) demonstrated that E2 blocks the increase of ROS generated upon induction of hypoxia in chicken hepatocytes [132], while Kim *et al.* (2006) showed that E2 suppressed ROS generation and activated the survival enzyme, PI3K [113]. Further evidence showed estrogen's ability to upregulate superoxide dismutase and glutathione peroxidase [114], potent antioxidants that convert ROS into less hazardous hydrogen peroxide and, accordingly, attenuate oxidative stress responses [11].

Another hallmark of the development of atherosclerosis and cardiovascular inflammation is the upregulation of inflammatory cell adhesion molecules, such as VCAM-1 and ICAM-1, as well as inflammatory cytokines such as TNF-α, interleukin 6 (IL-6), and interleukin 8 (IL-8) [8]. Cossette *et al.* (2013) demonstrated that human coronary ECs pretreated with E2 demonstrated marked decreases in VCAM-1, ICAM-1, IL-6, and IL-8 after exposure to the proinflammatory agent CRP [13]. Similar results were report by Chakrabarti *et al.* (2012) in human umbilical vein ECs treated with TNF-α [91]. Wang *et al.* (2006) demonstrated that supplementation with E2 decreased the production of inflammatory cytokines TNF-α, IL-1β, and IL-6,

in male and ovarectomized female rats, which improved functional recovery after myocardial ischemia and reperfusion injury [78].

4.2.5 Estrogen and Atherosclerosis - Perspectives

The multifaceted actions of estrogen on the cardiovascular system, including functions in modulating inflammation, decreasing oxidative stress, and increasing vasorelaxation make it a particularly attractive treatment option for atherosclerosis. Specifically, high levels of LDL particles, oxidation of LDL, and the inflammatory response initiated by endothelial activation, as well as SMC proliferation, EC apoptosis, and atheroma-induced stenosis could be addressed by estrogen therapy. In fact, Villablanca *et al.* (2009) demonstrated that exogenous E2 significantly decreased lesion size and number in mice fed an atherogenic diet [133], with other studies supporting similar anti-atherogenic effects [128, 134, 135]. Overall, we can conclude that estrogens possess potent cardioprotective, anti-inflammatory, and anti-oxidant properties [119], which could be directed towards attenuating the progression of atherosclerotic disease or mitigating its symptoms. However, more research must be conducted on the means of delivery in order for estrogen to be a considered a viable treatment option. Thus, various E2 delivery routes and vectors will be explored in the following section.

4.2.6 17β-Estradiol Delivery

Typically, E2 and other derivatives of estrogen, such as ethinyl estradiol, for HRT are administered orally, however this route tends produces high hepatic levels since the steroid must undergo first pass metabolism and, moreover, may lead to

unwanted changes in heptatic gene expression. As well, specifically in regards to the treatment of atherosclerosis, active agents delivered orally will likely reach the diseased artery at subtherapeutic levels and cannot exert the intended actions to a significant extent. Alternatively, direct injection and transdermal delivery routes may be employed, however these typically also lead to non-specific tissue distribution with potentially toxic side effects. In fact, studies have indicated that both the delivery route and method strongly influence estrogen's activity [83], therefore, successful estrogen therapy for CVD treatment would likely require new approaches in delivery systems, with the capability to improve cellular uptake kinetics, control release of the agent, all while avoiding potentially toxic side effects.

Various E2 delivery vehicles have been developed for both cardiovascular and non-cardiovascular based applications. Examples include encapsulation into liposomes [19, 136], microparticles [137, 138], nanoparticles [139, 140], nanoemulsions [25], nanotubes [141], organogels [137], as well as delivery via coated stents [142]. Such tactics may allow for controlled and prolonged estrogen release, which is beneficial since high concentrations of E2 can be cytotoxic [143]. Liposomes, in particular, hold notable promise for the delivery of E2 to treat atherosclerosis. This is due to their ability to accommodate E2 within the lipid bilayer, as well as to their successful application as drug delivery vectors for CVD, which is discussed further in Chapter 5.

Chapter 5: Liposome Technology for Cardiovascular Disease Treatment and Diagnosis

The following article entitled "Liposome Technology for Cardiovascular Disease Treatment and Diagnosis" summarizes the applications of liposomes to treat and diagnose cardiovascular disease. The paper details their use as pharmacological and gene delivery vectors, in addition to functions as contrast agents for imaging applications. The article was published by the journal *Expert Opinion on Drug Delivery* in February 2012.

Article Highlights

- Targeting liposomes specifically to the cardiovascular system can improve the delivery efficiency of therapeutics. Homing mechanisms can include passive targeting, which can be achieved by adjusting liposomal charge and/or size, as well as active targeting, in which functional moieties specific to the vasculature are attached to the liposomes' surface.
- Drug delivery from liposomes has been shown to be an effective means of improving therapeutic outcomes in animal models of cardiovascular disease. Clinical trials are still forthcoming.
- Experimental evidence suggests that the incorporation of genetic material in liposomes may aid to improve gene therapy to treat cardiovascular diseases. Despite some promising studies, much work is required before any systems are viable for use in humans. Liposomes conjugated with hemagglutinating virus of Japan showed promising results in attempts to improve transfection efficiencies in the vasculature.

- Both computer tomography and magnetic resonance imaging of the cardiovascular system can benefit from the application of liposomes in conjunction with contrast agents. Such formulations can be used to improve signal intensity and contrast-to-noise ratios.
- Echogenic immunoliposomes, specifically designed to enhance ultrasound images, have been applied to aid in the diagnosis of cardiovascular diseases. Preliminary studies show promising applications for delineating regions of atherosclerotic plaque.

Liposome Technology for Cardiovascular Disease Treatment and Diagnosis

Kristen Bowey[1], Jean-François Tanguay[2], Maryam Tabrizian[1,3,*]

[1]Department of Biomedical Engineering, McGill University, Montréal, Quebec, Canada

[2]Montréal Heart Institute, Department of Medicine, Université de Montréal, Montréal, Québec, Canada

[3]Faculty of Dentistry, McGill University, Montréal, Québec, Canada

*Corresponding author: maryam.tabrizian@mcgill.ca

5.1 Abstract

Introduction: Over the past several decades, liposomes have been used in a variety of applications, from delivery vehicles to cell membrane models. In terms of pharmaceutical use, they can offer control over the release of active agents encapsulated into their lipid bilayer or aqueous core, while providing protection from degradation in the body. In addition, liposomes are versatile carriers since targeting moieties can be conjugated on the surface to enhance delivery efficiency. It is for these reasons that liposomes have been applied as carriers for a multitude of drugs, genetic material, and contrast agents, aimed to treat and diagnose cardiovascular diseases.

Areas covered: This review aims to detail advancements in liposome technology used in cardiovascular medicine. In particular, the application of liposomes to the field of cardiovascular disease treatment and diagnosis, with a focus on delivering drugs, genetic material, and improving cardiovascular imaging will be explored. Advances in targeting liposomes to the vasculature will also be detailed.

Expert opinion: Liposomes may provide the means to deliver drugs and other pharmaceutical agents for cardiovascular applications, however there is still a vast amount of research and clinical trials that must be performed before a formulation is brought to market. Advancements in targeting abilities within the body, as well as the introduction of theranostic liposomes, capable of both delivering treating and imaging cardiac diseases, may be expected in the future of this burgeoning field.

5.2 Introduction

Liposomes were first described by Bangham *et al.* (1965) and are defined as artificial vesicles between 20 nm and 10 μm in diameter, made of an aqueous core surrounded by lipid bilayers [144]. Structurally, liposomes are composed of naturally derived phospholipids or synthetic amphiphiles, and are almost always incorporated with sterols, such as cholesterol, to affect membrane permeability. Liposomes are frequently prepared by thin-film hydration, which involves dissolving lipid components in organic solvent, drying down by rotary evaporation, and rehydrating in aqueous solution, as well as by freeze-drying, reverse-phase evaporation, and ethanol injection [145]. Subsequent processing steps, such as membrane extrusion, sonication and/or freeze-thawing may be employed to control the size distribution.

Liposomes have been used in medicine as delivery vehicles for drugs [146], genetic material [147], and imaging agents [148]. Due to their hydrophilic (aqueous core) and lipophilic (lipid bilayer) domains, liposomes can be used to encapsulate most active agents, irrespective of solubility and physical properties [149]. Encapsulation into liposomes can protect or control the release of an active drug agent or genetic material and reduce systemic toxicity by minimizing dosage requirements. As well, owing to their unique structure, liposomes can help to overcome the tissue and cellular barriers necessary to deliver their payload and exert the desired pharmacological effect. Drawbacks include a surface chemistry that can

attract circulatory proteins and mark liposomes for rapid clearance from the circulatory system. Thus, researchers began stabilizing liposomes by coating with hydrophilic polymers, such as polyethylene glycol (PEG), or other polyelectrolytes specifically designed to increase circulation time and reduce clearance *in vivo* [150]. Compared to traditional nanoparticulate delivery vehicles, liposomes also offer the ability to co-currently load both hydrophilic and hydrophobic components within the same system.

Although a great deal of liposome-based research has been devoted to treating cancer [151], work has also been underway to develop liposomal drug and gene delivery devices and imaging agents for cardiovascular disease (CVD) applications. Unlike most tumors, many parts of the vasculature are highly accessible through intravenous injections, although direct administration of various active agents for CVD treatment and diagnosis can be prone to washout due to high shear stresses [152]. In contrast, some forms of CVD, such as atherosclerosis, can cause impaired blood flow and make it difficult to transport therapeutics or contrast materials to sites of interest. In either case, liposomes are particularly well-suited to overcoming these challenges since a number of factors, such as size [153], charge [154], as well as the inclusion of targeting moieties [155], can be adjusted to improve delivery efficiency.

In terms of overcoming blood flow blockages, Caride and Zaret (1977) were one of the first to suggest that positively charged liposomes preferentially accumulate in areas of myocardial infarction [154]. Subsequent studies showed that liposomes may exhibit an enhanced permeability and retention effect in certain areas of the vasculature [156], which could be exploited to influence the distribution of therapeutics in the cardiovascular system. Early studies also proposed that liposomes could serve as direct treatments, forming a 'plug' and sealing damaged endothelial membranes to prevent further damage [157]. Furthermore, liposomes are capable of accommodating a wide variety of cardio-specific adhesion molecules and polymers on their surface, which can aid in increasing adhesion to vascular tissues or cells.

This review will highlight the research conducted on the use of liposome technology to treat and diagnose CVD. Targeting liposomes with surface moieties to the vascular system will be explored, as well as their applications in delivering pharmacological agents and genetic material to treat CVD. Finally, the use of liposomes in aiding to image the cardiovascular system will be detailed. An expert opinion section provides a perspective and opinion on the current state and future directions in the field.

5.3 Targeting Liposomes to the Cardiovascular System

Liposomes are suitable for vascular drug delivery and imaging since they can be precisely tailored to preset conditions by varying the formulation and/or

processing steps. In addition, both passive and active targeting can be exploited to improve payload delivery and residence time within the body. Regarding the passive targeting of liposomes, size, charge, and polymeric surface coatings have all been shown to affect blood clearance, cellular uptake, and distribution throughout the cardiovascular system [158, 159]. Liposome size, for instance, can be altered to passively target a specific population of cells. It has been observed that larger liposomes are more likely to be phagocytosed by macrophages, while smaller liposomes are readily taken up by fibroblasts [160]. Since one of the main drawbacks of liposome use is rapid clearance by the liver and reticuloendothelial system [153], polymer coats, such as PEG, can also affect blood residence time, which is attributed to steric interactions and enhanced stability *in vivo* [161]. Indeed, so-called 'stealth liposomes' named for their ability to improve blood circulation time and avoid clearance, are characterized by the incorporation of PEG into the liposomal formulation by adsorption, conjugation, or covalent linkage [162]. It has been postulated that PEG can increase liposomal circulation times by reducing activation of the component system through steric interactions and enhancing stability. Although is should be noted that results are highly dependent on the molecular weight and grafting density of the polymer.

Targeting moieties can also be used to improve delivery efficiency by actively targeting a specific location, increasing local concentration, and cellular

internalization, which is an essential step to achieve the desired therapeutic effects of pharmaceutical agents and genetic material, in particular. Regarding vascular delivery, targeting ligands can help reduce washout by promoting adhesion to vessel walls or atherosclerotic lesions [155, 163]. Possible cardiac targeting moieties include lectins, proteins, and antibodies. Liposomes conjugated to antibodies, also known as immunoliposomes, are predominately used to target the cardiovascular system, and will be discussed in the following section.

5.3.1 Immunoliposomes

During the mid seventies, Gregoriadis *et al.* (1975) proposed the concept of homing liposomes to target cells by attaching antibodies to the surface [164]. Since then, immunoliposomes have been employed to treat variety of diseases, including cancer [165] and cardiovascular disease [166]. Undoubtedly, an important aspect of cardiovascular targeting research lies in acquiring an in-depth understanding of the cellular processes and underlying pathways that occur during each stage of disease evolution or healing. Particularly, information relating to the migration of certain cell types or the expression of receptors can help elucidate which antibodies should be selected to target the liposomal vectors to a desired location. For instance, in the early stages of atherosclerosis, adhesion molecules for leukocytes, such as VCAM-1, can be targeted since they are expressed on the surface of endothelial cells [2]. Whereas in later stages of the disease, receptors on proliferating smooth muscle cells

may be more widely expressed and targeted instead. Depending on the type of drug or imaging agent to be delivered, careful consideration of the target cell population or adhesion molecules and antibody selection will very likely affect carrier efficiency. Table 5.1 lists a selection of publications that feature immunoliposomes designed to target various vascular receptors and regions. As well, Figure 5.1A and B schematically depict an antibody-conjugated liposomes and a selection of inducible receptors on activated endothelium and platelets, common to diseased vascular tissue. In many cases, immunoliposomes targeting the cardiovascular system have been directed to glycoproteins on the activated endothelium or cardiac myosin, both of which will be described further in the following section.

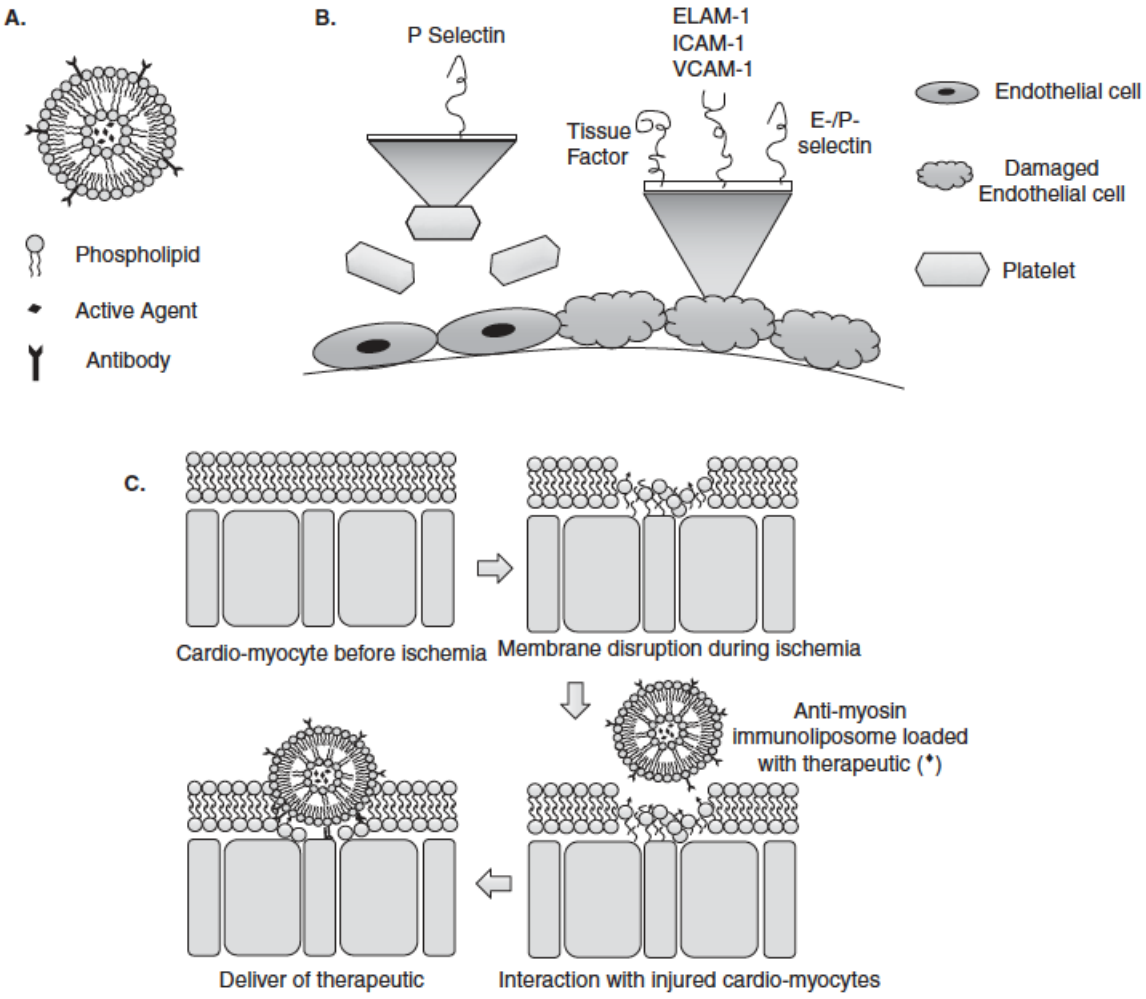

Figure 5.1 - Schematic representation of (A) immunoliposomes, (B) selected molecules to target damaged endothelium, (C) proposed 'plug and seal' mechanism of immunoliposomes to ischemic cardiac cells.
Adapted from Verma *et al.* (2006) [167].
VCAM-1 = vascular cell adhesion molecule-1; ICAM-1= intercellular adhesion molecule-1; ELAM-1= endothelial-leukocyte adhesion molecule-1.

Table 5.1 – Selected examples of immunoliposomes used to target specific sites/receptors in the vasculature.

Receptor/Target	Antibody	Lipid Formulation	Liposome Size (nm)	Ref.
VCAM-1	Anti-VCAM-1-Fab' mAb	DMPC, glutaryl-N-PE	~ 400	[168]
ICAM-1	Anti-ICAM-1 mAb	DPPC, DSPE-PEG(2000)-COOH, DSPE-PEG(2000)	132-149	[169]
ELAM-1	Anti-ELAM mAb	DOPC, DPPC, N-dod-PE	201 - 205	[170]
E-Selectin	mAb H18/7	DOPC, DPPC, N-dod-PE	201 - 205	[171]
P-Selectin	Anti-P-selectin	PC, DSPE-PEG2000, and DSPE-PEG-maleimide	~180	[166]
Tissue factor	Anti-TF mAb	PC, PG, PE	500-800	[172]
Fibrinogen	Anti-fibrinogen	PC, PG, maleimido-4(p-phenylbutyrate)-PE	60 - 100	[173]
Cardiac myosin	Cardiac myosin 2G4 mAb	PC, mPEG2000-DSPE, DOTAP	156 - 189	[167]

PC = phosphatidylcholine; **PE**= phosphatidylethanolamine; **PG** = phosphatidylglycerol; **DMPC** = 1,2-dimyristoyl-sn-glycero-3-phosphocholine; **DOPC** = 1,2-dioleoyl-sn-glycero-3-phosphocholine; **DPPC**= 1,2-dipalmitoyl-sn-glycero-3-phosphocholine; **DOTAP** = 1,2-dioleoyl-3-trimethylammonium-propane; **DSPE** = 1,2-diastearoyl-sn-glycero-3-phosphoethanolamine; **N-dod-PE** = 1,2-Dioleoyl-sn-glycero-3-phosphoethanolamine-N-dodecanoyl; **PEG** = polyethylene glycol; **VCAM**= vascular cell adhesion molecule; **ICAM**= intercellular adhesion molecule; **ELAM**= endothelial-leukocyte adhesion molecule; **TF**= tissue factor; **mAb**= monoclonal antibody.

The endothelium is the principal site of cellular infiltration and inflammation during the development of atherosclerotic lesions and injury. Thus, it follows that one of the prime targets for cardiovascular therapeutic delivery and imaging is the activated endothelial lining [174]. During activation, glycoproteins such as endothelial-leukocyte adhesion molecule-1 (ELAM-1), VCAM-1, and/or ICAM-1, can be upregulated and expressed on the surface of cells. Depending on the degree and type of disease or injury, these molecules may serve as potential targets for liposomes functionalized with the appropriate monoclonal antibodies. For example, using an *in vitro* model for activated endothelial cells, Lim *et al.* (2011) showed that liposomes, loaded with celecoxib and designed to target VCAM-1, successfully increased liposomal uptake in human umbilical vein endothelial cells compared to un-conjugated liposomes [168]. Homem de Bittencourt *et al.* (2007) detailed an *in vivo* study, in which atherosclerotic mice were subjected to a dose of anti-VCAM-1 immunoliposomes [175]. It was determined that the presence of anti-VCAM-1 antibodies improved distribution to the thoracic aorta, while reducing accumulation in the spleen and kidneys. These results demonstrate that antibodies directed towards inducible cell surface glycoproteins could aid in localizing liposomes to areas of vascular disease, thereby improving cellular uptake rates.

Another notable cardiac target is the myosin that is exposed if the membranes of endothelial cells are damaged. Torchilin *et al.* (1979) first described the covalent coupling of antibodies to liposomes in order to specifically target canine cardiac myosin [176]. Subsequent studies demonstrated that antimyosin immunoliposomes

improved the survival of H9C2 rat embryonic cardiomyocytes [177], and decreased mean infarct size in rabbit models of acute myocardial infarction, compared to bare liposomes and non-specific IgG-liposomes [178]. Cytoskeletal specific antibodies, such as anti-cardiac myosin 2G4, are favorable since they can uniquely target exposed myosin. It follows that liposomes are therefore less likely to enter healthy myocardial cells, which could again minimize exposure of potentially toxic materials to healthy cells, and improve the overall effective dosage to unhealthy cells. Owing to the phospholipid components, it has also been suggested that myosin-specific liposomes can work to 'plug and seal' damage suffered by cellular membranes on top of delivering active pharmacological agents, as seen in Figure 5.1C [177]. Given this theory, liposomes may offer a multifaceted treatment alternative to conventional single-component systems, and may accordingly improve clinical outcomes. In addition to the activated endothelium and myosin, other cardiac targets, outlined in Table 5.1, have been investigated. For example, Scott *et al.* (2009) chose the cell adhesion molecule P-selectin, which is expressed on platelets and endothelial cells in response to inflammation, to direct liposomes containing vascular endothelial growth factor (VEGF) to sites of myocardial infarction in rat models [166]. Results showed that cardiac functionality was significantly improved compared to unencapsulated VEGF and non-targeted liposomal controls.

Evidently, there are a multitude of target/antibody combinations that can be used to home liposomes to diseased areas of the cardiovascular system. In addition to selecting antibodies based on availability and specificity to a given target, it is important to keep in mind the following: (i) targets should be accessible by the vascular system; (ii) targets should preferably be selected based on cell surface glycoproteins or receptors that are not present or exposed in healthy cells; (iii) antibodies must be able to attach to the liposomal surface without undergoing any deleterious effects on targeting activity (iv); antibodies should elicit no immunogenic effect.

Based on the studies presented, it is clear that antibodies can provide a degree of active targeting that significantly improves liposomal retention in a given site and improves therapeutic outcomes in animal models of CVD. As a result, the required dosage can be reduced, and non-specific accumulation in healthy areas in the body may be avoided. Ultimately, immunoliposomes can be expected to continue to play a pivotal role in improving the efficiency of drug, gene and imaging agent delivery to treat and diagnose CVD, in conjunction with further advancements in the fields of ligand and cardiac biomarker discovery [179].

5.4 Liposomal Therapeutic Delivery to the Cardiovascular System

5.4.1 Pharmacological Agents

Conventional pharmaceutical treatments for CVD suffer from a variety of drawbacks related to their method of administration. Systemic delivery of active agents often requires high concentrations owing to non-specific distributions and short half-lives experienced *in vivo*. These levels can lead to adverse toxic side effects, unsustainable drug levels, and developed drug resistance. The application of liposome technology can offer an alternative form of delivery specifically designed to remedy these obstacles by providing the means to control therapeutic delivery over a desired timeline, as well as target specific tissues in the body. An ideal particulate-based drug formulation would specifically target diseased tissue, provide a sufficient dose to elicit the desired therapeutic response, and minimize adverse side effects. Liposomes may very well address these conditions, given their ability to protect the active agent from degradation, improve residence time *in vivo* [36], shield the body from toxicity [35], offer control over pharmacokinetics [34], and, as discussed, accommodate ligands that can target specific areas of the vasculature [166]. Although there are no liposomal drug formulations currently available on the market to treat CVD, liposomes have made considerable progress to alter the efficiency of cardiovascular drug delivery within the context of *in vivo* animal studies. Table 5.2 provides a selection of research that has incorporated pharmacological agents into

liposomes with the intention of treating CVD. Of these pharmacological agents, statins, adenosine triphosphate, and bisphosphonates will be discussed further in the following sections.

5.4.4.1 Statins

3-Hydroxy-3-methylglutaryl (HMG-CoA) reductase inhibitors, also known as statins, are a class of drugs that inhibit the action of HMG-CoA reductase, which is an enzyme that converts HMG-CoA to mevalonic acid for cholesterol synthesis [180]. In addition to decreasing lipid levels, statins have been shown to attenuate EPC senescence and, in some cases, effectively increase EPC proliferation [181]. Statins may also inhibit inflammation and trigger macrophage/monocyte apoptosis [146], which could contribute to the reduction in the rates of restenosis observed after percutaneous coronary interventions [182]. These pleiotropic effects likely explain the benefits of statin therapy in CVD, however, they can be difficult to deliver reproducibly owing to their low aqueous solubility. Thus, researchers have examined various methods to improve drug bioavailability and therapeutic efficacy.

In particular, liposomes have been proposed as a means to increase the efficiency of statin therapy [146, 183, 184]. For example, Afergan *et al.* (2010) encapsulated simvastatin in liposomes to investigate effects on monocyte/macrophage growth and neointimal formation after balloon injury in rat models [146]. Results showed that both simvastatin-liposomes and free simvastatin

administered systemically attenuated the monocyte response to injury and decreased neointimal formation compared to saline injections, although liposomes demonstrated significantly prolonged monocyte depletion *in vivo*.

Table 5.2 – Selected publications detailing the use of pharmacological agents encapsulated into liposomes to treat CVD.

Pharmacological Agent	Lipid Formulation	Liposome Size (nm)	Experimental Model	Experiment Outcomes	Ref.
Simvastatin	DSPC, DSPG	~ 164	Carotid-injured rat model	Inhibited neointimal growth	[146]
ATP	PC, PEG-DSPE, DOTAP	167 - 189	Rabbit model of myocardial infarction	Reduced damage to myocardium	[185]
Alendronate	DSPC, DSPG	176 - 183	Carotid-injured rat model	Suppressed intimal growth	[186]
Nitric oxide	DPPC, DOPC	NA	Rabbit model of atherogenesis	Neointimal hyperplasia was attenuated	[187]
Prostaglandin E1	NA	NA	Rat model of myocardial infarction	Reduced neointimal hyperplasia and lipid accumulation	[175]
Tissue-plasminogen activator	PC, DPPG, -(maleimidophenyl) butyrate-PE	NA	Rabbit aorta thrombus model	Improved recanalization of the abdominal aorta	[188]

VEGF	PC, DSPE-PEG2000, and DSPE-PEG-maleimide	~180	Rat model of myocardial infarction	Improved cardiac function	[166]
Streptokinase	PC	~330	Rabbit model of carotid artery thrombosis	Reduced reperfusion times and residual clot mass, improved arterial blood flow	[189]
Prednisolone	HSPC, 3,5-dipentadecyloxy benzamidine hydrochloride	~100	Rabbit model of atheroma	Reduced neointimal growth	[190]

PC = phosphatidylcholine; **DPPG =** 1,2 dipalmitoyl-snglycero-3-phosphoglycerol; **DOTAP** = 1,2-dioleoyl-3-trimethylammonium-propane; **DSPE** = 1,2-diastearoyl-sn-glycero-3-phosphoethanolamine; **DSPG =** distearoyl phosphatidyl glycerol; **PEG** = polyethylene glycol; **POPC** = 1-palmitoyl-2-oleoyl-sn-glycero-3-phosphotidylcholine; **ATP** = adenosine triphosphate; **VEGF** = vascular endothelial growth factor; **NA** = not available.

Another liposome-statin delivery system, formulated to target injured myocardium, was detailed by Aso *et al.* (2007) [181]. Liposomes were loaded with pravastatin and conjugated with a cardiomyocyte targeting lectin, N-acetylglucosamine. Since cells sparingly take it up, liposomes were proposed as a means to increase cellular internalization. Figure 5.2 shows electron micrographs of N-acetylglucosamine-liposome uptake by cardiomyocytes. It was determined that the targeting moiety significantly increased delivery efficiency, which may aid in improving delivery of statins, as well as other cardioprotective drugs, to the myocardium. These results indicate that liposomes may be used to promote statin delivery to diseased myocardium, however it remains to be seen whether these treatments can be translated to a clinical setting.

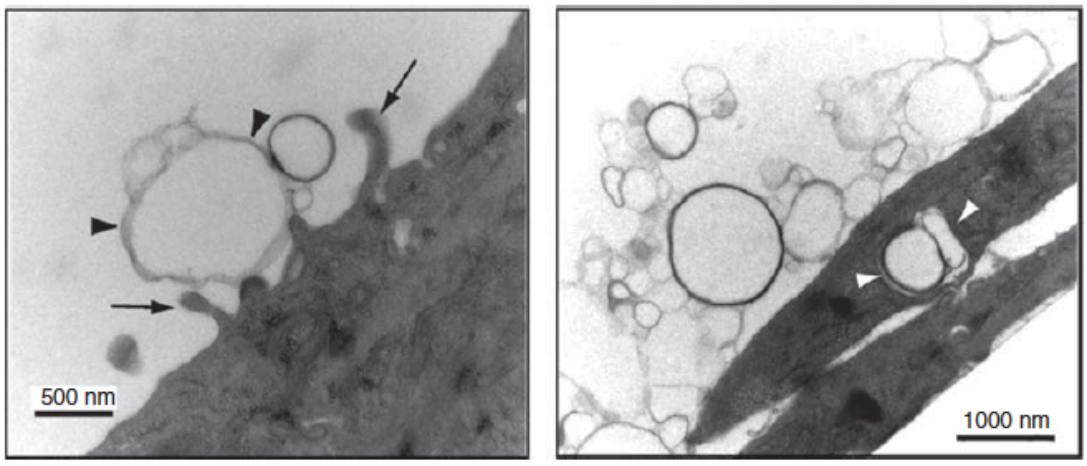

Figure 5.2 - Photomicrographs of the internalization process of liposomes conjugated with N-acetylglucosamine by cardiomyocytes. Black arrowheads indicate the microvilli of the cells; white arrowheads indicate liposomes internalized by cells.
Reprinted with permission from Aso *et al.* (2007) [181].

5.4.4.2 Adenosine triphosphate

During myocardial ischemia, levels of adenosine triphosphate (ATP) can quickly become depleted, owing to a restricted blood supply and associated loss of oxygen [191]. Low levels of ATP can affect contraction and functionality and thus, researchers have looked into methods of delivering exogenous ATP to sites of injury in an attempt to treat and prevent damage to cardiac myocytes [192]. Encapsulation into liposomes offers a convenient means to improve delivery efficiencies compared to free ATP, which exhibits a short half-life *in vivo* since it can be degraded by plasma endonucleotidases, and is poorly permeable through hydrophobic membranes [191].

An early study by Xu *et al.* (1990), determined that positively charged ATP-loaded liposomes accumulated at ischemic areas in an experimental canine model of myocardial infarction [193]. Since then, Vladimir Torchillin and his colleagues have published several papers detailing promising results of both PEGylated liposomes and immunoliposomes and their effects on myocardial ischemia [167, 185, 194, 195]. For instance, Verma *et al.* (2005) demonstrated that liposomal-ATP improved contractile function in a Langendorff isolated rat heart model of ischemia compared to free ATP, as well provided superior protection against enzymatic attack [195]. An *in vivo* rabbit study also concluded that liposomal-ATP diminished the proportion of irreversibly damaged tissue after myocardial infarction [185]. In a follow-up study,

Verma *et al.* (2006) determined that the inclusion of a cardiac myosin-specific antibody to ATP-loaded liposomes enhanced myocardial protection, compared to non-specific liposomes. A dual-mechanism of treatment was proposed, in which the immunoliposomes may 'plug and seal' the membranes of damaged myocytes while delivering exogenous ATP (See Figure 4.1C) [167]. Though research is still ongoing, it is clear that the pharmacological delivery of ATP by liposomes may offer cardio-protection during ischemia and reperfusion [192].

5.4.4.3 Bisphosphonates

Bisphosphonates (BPs) are a class of drugs typically used to treat osteoporosis and other bone diseases, since they decrease the resorptive capacity of osteoclasts and promote apoptosis [196]. BPs have also been shown to affect the activity of immune cells [197] and vascular SMCs [198], which may explain some of their beneficial effects in treating certain cardiovascular afflictions, such as restenosis [199]. However, due to a bulky bisphosphonate group and anionic charge, BPs are not easily internalized by cells. To increase delivery efficiency, BPs were encapsulated into liposomes, which could thereby mediate transfer through the cellular membrane.

Immune cell infiltration to sites of vascular injury may play a significant role in restenosis and, as a result, strategies aimed to reduce macrophage/monocyte activation and proliferation have been proposed [200]. The effects of free BP as well

as liposomal-BP on inflammatory cells and macrophages have been well documented [197, 201]. For instance, Ylitalo *et al.* (1998) studied the effects of liposomal clodronate, etidronate, and pamidronate on macrophages, macrophage-like RAW 264 cells and the formation of LDL-derived foam cells [202]. Results showed that clodronate and etidronate-encapsulated liposomes reduced the release of degradation agents from RAW 264 cells, which also inhibited the degradation of acetylated LDL. Since free BPs did not produce the same effects on the degradation of acetylated LDL, it could be concluded that liposomes increased their effectiveness *in vitro*.

Danenburg *et al.* (2002) proposed the application of clodronate-encapsulated liposomes to reduce restenosis *in vivo* [201]. Liposomes were formed by reverse-phase evaporation and injected intravenously into rabbits, which had undergone a standard balloon injury procedure. Morphometric analysis of carotid arteries showed that SMC proliferation, extracellular matrix formation, and luminal stenosis were significantly decreased in animals treated with liposomal-clodronate compared to free clodronate, and controls. It was found that liposomal-clodronate did not directly inhibit endothelial or smooth muscle cells, but rather attenuated the increase in circulating monocytes observed shortly after injury, affecting macrophage numbers and activity in the liver, spleen and injured arteries. Similarly, alendronate encapsulated into liposomes was shown to decrease circulating monocytes and attenuate neointimal formation after balloon injury and stent deployment in rabbits

[203]. Liposomes were again selected as a delivery vehicle since they are thought to increase BP delivery efficiency to macrophages, resulting in apoptosis once the liposomes are metabolized. Epstein *et al*. (2008) demonstrated the favorable effect of liposomal alendronate on restenosis in a rabbit carotid injury model [204], as seen in Figure 5.3.

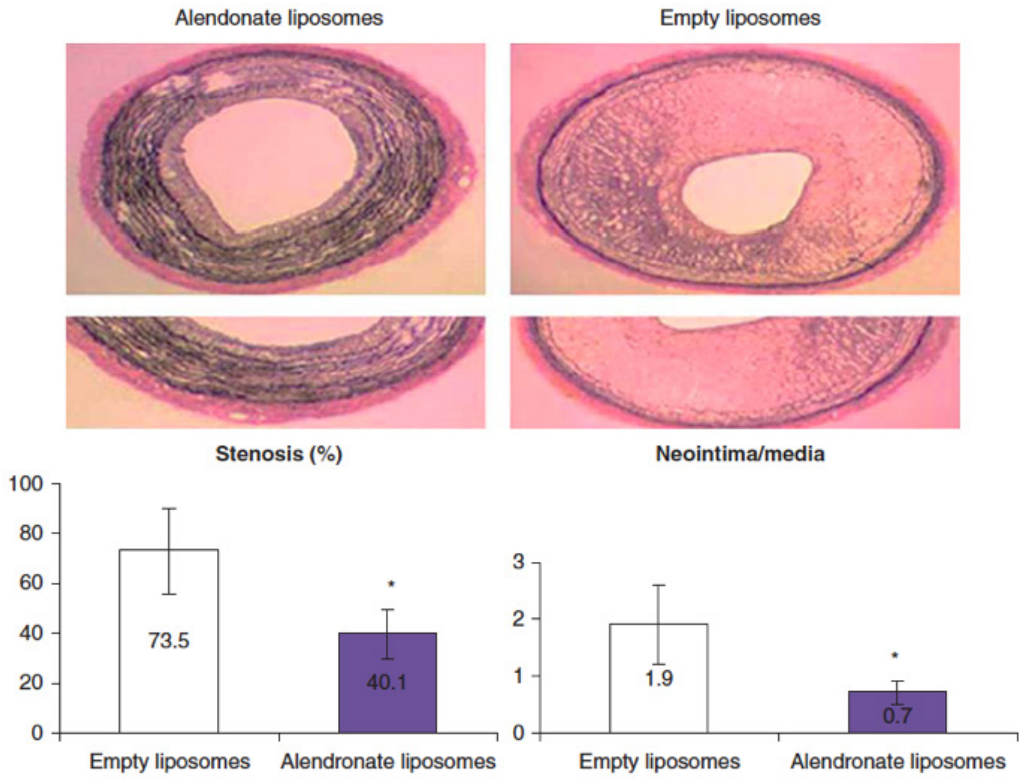

Figure 5.3 - Photomicrographs of alendronate liposome-treated and untreated tissue sections in a hypercholesterolemic rabbit model of carotid artery injury. Bar graphs depict the inhibition of stenosis and neointimal formation in liposomal alendronate treated rabbits.
Adapted from Epstein *et al.* (2008) [204].

As of February 2010, the Biorest Liposomal Alendronate with Stenting sTudy (BLAST) phase II clinical trial was underway to determine the effectiveness of liposomal alderonate to reduce restenosis in patients having undergone a PCI with a bare metal stent [205]. The estimated study completion date is not set until January 2015, but based on the experimental evidence detailed so far, liposomes may indeed be promising vehicles for the delivery of BPs to treat CVD.

5.4.2 Genetic Material

Gene therapy can offer a local, sustained production of molecules by incorporating exogenous DNA or oligonucleotides into the genome of target cells. Although direct gene transfer with naked DNA has been investigated, it is clear that genetic carriers can offer superior rates of transfection efficiency. Genetic material can benefit from encapsulation into liposomes by improving transfer across biological membranes, increasing residence time, and reducing degradation *in vivo*. Cationic liposomes, in particular, have commonly been used to promote gene transfer, since they can condense plasmid DNA to form stable complexes, called lipoplexes [206].

Gene therapy has been widely used to treat CVD [207]. The vast majority of gene carriers for CVD research and clinical trials are viral vectors [208], however a number of groups have also utilized liposomes, owing to their non-immunogenic and low-toxicity profiles in the body [207]. For example, Khuarana *et al.* (2004)

investigated the application of liposome-mediated VEGF gene transfer to collar-induced intimal thickening of the carotid artery in rabbits [209]. Results showed that VEGF expression exhibited cardioprotective effects, successfully attenuating thickening, as well as diminishing local macrophage infiltration. In another study, Abegunewardene *et al.* (2010) studied the expression of the inducible nitric oxide synthase transgene, which was delivered by liposomes to a porcine model of chronic myocardial ischemia [210]. Only moderate recovery in ischemic areas was reported compared to control procedures, which suggests the need for further study and optimization. Table 5.3 presents selected *in vivo* studies of liposomal gene therapy for CVD. A handful of clinical trials have also detailed liposome-mediated transfer of genes for treatment of restenosis and ischemia [211, 212], which produced some promising results but have yet to be translated to any viable product.

Based on recent evidence, liposomes are still vastly inferior to viral vectors in terms of transfection efficiency, and make up a minority of the gene carriers used in cardiovascular clinical trials [213]. With the aim of improving transfection capabilities, complexes formed between liposomes and viral components have been investigated. A hybrid vector commonly applied to treat cardiovascular symptoms is the hemagglutinating virus of Japan (HVJ) liposome.

Table 5.3 – Selection of publications detailing liposomal delivery of genetic material to treat models of vascular disease.

Gene Encoded	Experimental Model	Experimental Outcomes	Reference
iNOS	Porcine model of ischemia	Delivery by intramyocardial injection did not significantly affect cardiac functionality; showed moderate improvement in neovascularization	[210]
Human tissue inhibitor of metallo-proteinase-1	Rat model of vascular injury	Successful transfection and associated decrease in neointimal hyperplasia	[214]
Heat shock protein 90 cDNA	Rabbit model of chronic ischemia	Improved hindlimb perfusion by influencing nitric oxide	[215]
VEGF	Porcine occlusion model	In coronary and peripheral arteries, treatments resulted in angiogenesis/arteriogeneis	[216]

iNOS = inducible nitric oxide synthase; **VEGF** = vascular endothelial growth factor.

5.4.2.1 Hemagglutinating Virus of Japan Liposomes

The inactivated Sendai virus (hemagglutinating virus of Japan; HVJ) was complexed to liposomes pre-loaded with genetic material in an attempt to improve transfection efficiency and safety profile relative to bare liposomes and complete viral vectors [217]. The viral envelope of HVJ contains two glycoproteins, hemagglutinating neuroaminidase and fusion proteins, which promote cellular attachment and subsequent gene delivery directly into the cytoplasm. The genetic material is complexed with DNA-binding proteins to enhance expression and

incorporated into liposomes, which are subsequently fused with UV-inactivated HVJ [217]. This method can avoid endocytosis and the associated lysosomal degradation, which is widely believed to significantly impede transfection rates.

Early results demonstrated that HVJ-liposomes could improve DNA transfer in cultured cardiac myocytes compared to unconjugated liposomes [218]. In later studies, another version of HVJ-artificial viral envelope (AVE) liposome hybrid vectors were loaded with the tissue factor pathway inhibitor (TFPI) gene, in rabbits after balloon angioplasty [219]. Since tissue factor (TF) is a glycoprotein involved in coagulation, it was postulated that the gene encoding for TFPI might lessen TF expression in turn attenuating restenosis. Indeed, HVJ-AVE liposomes were shown to successfully mediate TFPI gene transfection since TFPI mRNA and protein were detected locally. Moreover, rabbits that received HVJ-AVE liposomes loaded with TFPI cDNA exhibited significantly reduced rates of stenosis, as shown in Figure 5.4. A follow-up study reported that a combination of TFPI genes delivered by HVJ-AVE liposomes and recombinant TFPI produced an even greater inhibitory effect on restenosis as compared to either method alone [220]. This positive effect of co-delivering genes and pharmacological agents could be further explored in future studies.

These studies seem to indicate that HVJ liposomes may be well suited to mediating gene delivery in the vasculature. However, one drawback associated with

HVJ-liposome preparations is that they are not specifically targeted to a given cardiac cell population, in contrast to the application of myocardial or smooth muscle cell-specific antibodies. Forthcoming studies may perhaps consider functionalizing HVJ-liposomes with targeting antibodies to determine whether transfection specificity in the vasculature could be further enhanced.

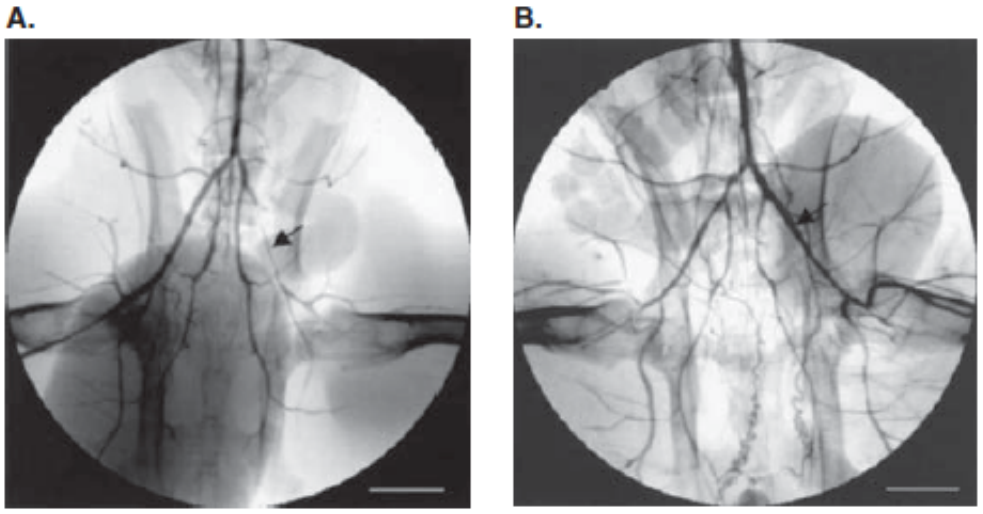

Figure 5.4 - Angiographs depicting the effects of liposomal tissue factor pathway inhibitor genes on neointimal formation and stenosis in rabbit models of angioplasty. (A) Angiogram of an animal that received the control plasmid, and (B) angiogram of an animal that received the tissue factor pathway inhibitor gene. Arrows indicate gene-transferred iliac arteries, bar = 1.05 cm. Reprinted with permission from Yin *et al.* (2002) [219].

As a final point, despite the widespread use of viral vectors and viral derivatives, they can pose serious toxicity and immunological issues [221]. Evidently, prior to treating cardiac diseases with genes loaded into liposomes or

hybrid liposomes, it is vital to rigorously test *in vivo* safety and immune reactions. However, it is likely that liposomal gene therapy will continue to pervade the area of CVD treatments.

5.5 Liposomes in Cardiovascular Imaging

While drugs and gene delivery can be used to treat CVD once symptoms have manifested, a more conservative approach, involving early diagnosis and intervention prior to reversible damage, may be favorable [222]. Thus, the importance of improving imaging technologies to detect early signs of atherosclerosis and heart disease cannot be understated. Currently, there exists a multitude of cardio-imaging techniques, including cardiac catheterization, computer tomography (CT), magnetic resonance (MR), echocardiography, and chest radiography. Of these, liposomes have been used as contrast agents to improve image resolution in CT [148], MR [223], and echocardiography [172]. Recent research in the area of liposomes and cardiac imaging will be detailed in the following sections.

5.5.1 Liposomal Contrast Agents

Atherosclerosis is characterized by a complex cascade of events that involve a number of molecular factors, chemokines, and various cells types [2]. Since coronary events, such as myocardial infarction and stroke, can occur from relatively small lesions, early and accurate diagnosis is necessary in order to begin appropriate

treatments and prevent acute complications [224]. Indeed, the key to reversing atherosclerosis may be locating sites of plaque formation before blood flow has even been affected [225]. Although X-ray coronary arteriography is currently the standard for diagnosing atherosclerosis, the procedure is invasive, can often fail to spot vulnerable atheromas due to negative remodeling of the vessel, and can introduce a risk of bleeding at the site of catheter insertion, vascular complications, and in severe cases, myocardial infarction [2]. Non-invasive imaging technologies, such as conventional ultrasound, CT, and MR, may offer lower-risk alternatives to facilitate the characterization of atherosclerotic plaque, though technical advancements are still needed before they may be widely employed.

One of the advancements in the field of MR angiography, is the use of contrast agents or tracers, which can improve image clarity, reduce artifacts, and decrease scan time [226]. Optimal contrast agents should be able to accumulate preferentially at sites of disease for a sufficient amount of time, so as to allow for enhanced image acquisition, while improving the signal-to-noise ratio [227]. Since MR signals are generated from protons, most contrast agents are used to improve the signal by accelerating proton relaxation [2, 222]. For example, gadolinium chelates are currently administered intravenously to image vessels in conjunction with MR, however owing to high throughput *in vivo*, it is often challenging to obtain good quality images. In addition, they can rapidly diffuse through vascular tissue, thus

diminishing the ability to visualize the border between lesions and healthy tissue [228]. To overcome this challenge, it is proposed to employ nanoparticulate delivery vehicles that could transport imaging agents and control their distribution. In the same way that nanoparticles can improve delivery efficiency of drugs and genes, they can also reduce the toxicity of tracers, as well as bear surface targeting ligands to improve residence time and target cell/tissue delivery specificity. Liposomes are of particular interest to this application, owing to their characteristic ability to improve residence time and stabilize contrast agents in the blood pool [229].

For example, Ayyagari *et al.* (2006) encapsulated gadodiamide in liposomes coated with PEG, in an attempt to improve MR angiography [228]. As shown in Figure 5.5A and B, results indicate that liposomes improved residence time in blood vessels with enhanced image contrast. In regards to further improving residence time and homing accuracy, it has been proposed that inflammatory cells, such as macrophages and monocytes, are ideal targets for imaging agents since they are capable of taking up nano-sized particulates and play an active role in the development of atherosclerotic plaque [222]. Maiseyeu *et al.* (2009) showed that liposomal-gadolinium enriched with exteriorized phosphatidylserine residues, known to promote macrophage recognition and apoptosis, enhanced the MR imaging signal of plaques in $ApoE^{-/-}$ mice compared to un-targeted liposomal-gadolinium (Figure 5.5C) [230]. Thus, formulating liposomes loaded with tracers that are specifically

engineered to be attracted to macrophages at atherosclerotic lesions could facilitate imaging, and enable better resolution for MR scanning. CT imaging can also benefit from targeted liposomal imaging agents. For example, Conyers *et al.* (2009) formulated ICAM-1 specific immunoliposomes loaded with iodinated contrast media [169]. Preliminary results *in vitro* showed that immunoliposomes selectively bound to inflamed endothelium, which may prove to enhance CT image resolution in future studies.

Advanced studies involving animal models will surely continue to probe the use of liposomal contrast agents in CT and MR cardiovascular imaging applications. Liposomes hold great promise and potential in improving image properties by increasing half-lives and imparting homing abilities to contrast agents that may otherwise be non-specifically taken up by the reticuloendothelial system. In addition, liposomes may make it possible to co-encapsulate materials that enable dual imaging by CT and MR [231], and/or synergistic targeting of two or more receptors [232], which could help to further elucidate CVD progression, improve diagnosis, and subsequent treatment.

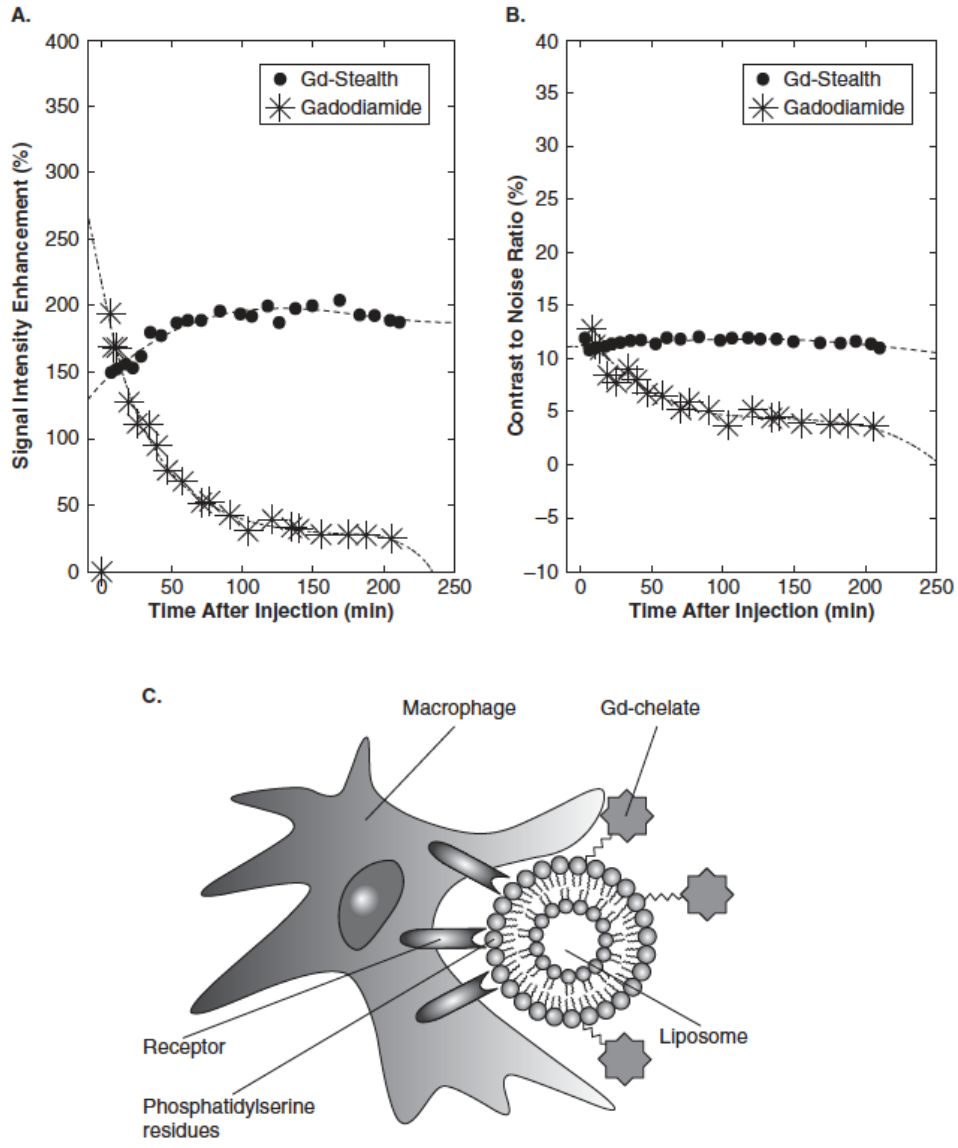

Figure 5.5 - Graphs depict the signal intensity (A) and contrast-to-noise (B) enhancements obtained from gadodiamide encapsulated in liposomes (Gd-stealth) as compared to gadodiamide controls in the magnetic resonance imaging of blood vessels. (C) Proposed interaction between gadolinium-liposomes studded with phosphatidylserine residues and macrophages. (A,B) Reproduced with permission from Ayyagari *et al.* (2006) [228]. (C) Reproduced with permission from Maiseyeu *et al.* 2009 [230].

5.5.2 Echogenic Liposomes

Ultrasound has widely been used for imaging and diagnostic purposes, since it can be directed to specific regions of interest, enables real time image acquisition, is widely available, and economical [222, 225]. Ultrasonic contract agents were introduced with the aim of improving image quality, sensitivity, and tissue characterization [233]. In addition, by improving the signal-to-noise ratio, contrast agents can decrease the amount of ultrasound energy directed to tissues, thus minimizing any peripheral damage. Unlike MR or CT contrast agents, ultrasonic contrast agents can simply be liposomes that contain gas within the core, which significantly improves the imaging contrast by altering backscatter intensity and ultrasound wave re-radiation [225, 234]. Alternative forms of acoustically sensitive liposomal contrast agents, devoid of gas, were also developed to overcome the inherent instability of the two-phased systems [235]. For these formulations, lipid compositions were varied to produce carriers that could still exhibit echogenicity and enhance image contrast.

In terms of cardiovascular applications, echogenic liposomes have been employed to improve the characterization of atherosclerotic plaque [236]. Echogenic liposomes that attach specifically to the plaque via conjugated antibodies, also called echogenic immunoliposomes (ELIPs), can be used to identify specific surface morphologies and delineate diseased regions *in vivo*. In addition, ELIPs can be

tailored to specific sizes (< 1μm), which are required to adequately perfuse vascular tissues while avoiding accumulation in pulmonary capillaries [236].

Demos *et al.* (1999) demonstrated that antifibrinogen ELIPs can be directed to thrombi and fibrin-rich areas of atheromas, while anti-ICAM-1 ELIPs attached to early plaque formations and retained acoustic sensitivity in porcine models [236]. Hamilton *et al.* (2004) showed that anti-VCAM-1 ELIPs could enhance echocardiography images of atheroma in the left carotid artery of swine [172]. In another study, Hagisawa *et al.* (2010) described the application of liposomal microbubbles coupled with Arg-Gly-Asp (RGD) peptides in an attempt to bind activated platelets. Results showed that these contrast agents, coupled to liposome delivery vehicles, could markedly enhance ultrasound imaging in rabbit models of acute thrombotic occlusion [237].

Molecular imaging of the cardiovascular system with liposomes will certainly help to enhance current imaging technologies. Indeed, the versatility of liposomes as carriers of imaging agents and gases, as well as their innately ultrasonic properties, renders them well suited for use in a variety cardiac imaging applications, and may indeed push the limits of CVD diagnosis in the future.

5.6 Conclusion

Currently, although there are no liposome-based drug, gene or imaging formulations clinically available to diagnose or treat CVD, this review presents a

wide range of ongoing research in the field. It highlights innovative approaches from actively targeting liposomes with antibodies to their use as inherently echogenic contrast agents. The majority of the research indicates that liposomes may indeed allow for therapeutic and diagnostic efficiencies not previously possible with conventional formulations, though it is clear that a great deal of work and advancements are still required.

5.7 Expert Opinion

The application of liposome-based technologies to diagnose and treat CVD has not been as widely investigated as compared to applications within oncology; nevertheless, it is evident that this field of research presents great possibilities. As detailed in this review, liposomes have facilitated the delivery of drugs and genetic material to a variety of CVD models, in addition to improving cardio-imaging for CT, MR and ultrasound technologies. In terms of drug delivery to the vascular system, it is clear that liposomes can enhance therapeutic outcomes in animal models of disease for a number of formulations. In particular, poorly soluble drugs, such as statins, and large bulky agents, such as bisphosphonates, can benefit from encapsulation to improve cellular permeability and therapeutic effectiveness. As well, actively targeting liposomes to sites of injury or disease can further the desired outcomes, within the context of CVD treatment and diagnosis.

However, despite this mostly positive progress, further steps must be made in order to improve effectiveness and translate these findings to clinical relevance. For instance, preliminary results have indicated that applying multiple targeting ligands to liposomes could further enhance homing and cellular uptake, compared to single-ligand systems [147, 232]. As demonstrated by Kluza *et al.* (2010), liposomes complexed with two antibodies specific to receptors present on activated endothelial cells, synergistically improved particulate uptake compared to either moiety alone [232]. In another study, it was determined that liposomes specific for CD34 antigens and ICAM-1 significantly improved the adherence and penetration of CD34+ adult bone marrow stem cells in aortic tissues [238]. Ma *et al.* (2011) also showed that liposomal gene delivery vectors could benefit from multi-ligand targeting, by combining cellular and nuclear homing molecules to improve transfection [147].

In terms of further improving the delivery success of liposomes, it has been suggested that exogenous triggers, such as temperature and ultrasound, may be able to provide better control over the release of active agents [239], enhance tissue perfusion [240], and cellular permeability [241]. Specifically, ultrasound has widely been used to modify the delivery profile of active agents from liposomes, by inducing thermal or mechanical effects [241, 242]. As well, ultrasound has been shown to improve the expression of transgenes delivered from echogenic liposomes, perhaps through cavitation effects [243]. Ultrasound frequency can also affect the

cellular uptake of liposomes by temporarily disrupting membranes or tight junctions [242]. In terms of delivery to the cardiovascular systems, these capabilities can lend to enhancing pharmacological effects in future formulations, though it will be vital to closely test and monitor ultrasound dosage to avoid peripheral tissue damage.

While liposome-encapsulated drug and gene delivery can be used in CVD treatment, and liposomal imaging agents can help elucidate and diagnose similar afflictions, the most important developments in the next few years can be expected to come in the form of theranostic agents, which combine both "therapy" and "diagnostic" components into a single system [152]. Indeed, theranostic agents could facilitate the drive towards personalized medicine and thereby improve the outcome of treatments. Liposomes are ideally suited for this form of research, since they are comprised of separate compartments that can house more than one substrate or active agent. The inherent echogenic properties of liposomes could also make it possible to, for example, simultaneously image thrombi by echocardiography and deliver thrombolytic agents. In a recent study, Laing *et al.* (2011) demonstrated the multifaceted capacities of echogenic liposomes by imaging the delivery of liposomal tissue plasminogen activator to thombi in rabbit aorta [188]. In the future, the ability to co-currently image diseased cardiovascular tissue and deliver cardiovascular drugs by the application of liposome vehicles may have a positive effect on the clinical outcomes for millions of patients suffering from CVD.

In addition to improving vascular targeting and control over therapeutic release timelines, it is imperative that the toxicological and inflammatory effects of liposomes be rigorously investigated. Indeed, one of the current limitations of liposome use *in vivo* is related to immunological reactions, which are characterized by activation of the complement system and inflammatory cells upon administration [244]. To address this issue, researchers have studied the effects of the liposome size, surface charge, and phospholipid components, all of which can alter the degree of immunological activation [244]. It has been proposed that surface coatings can also improve liposomal stabilization and reduce aggregation [245], which may consequently affect biocompatibility [246]. However, toxicity issues still remain one of the biggest barriers to the success of the liposomal delivery of therapeutic or diagnostic agents. Therefore, further research must be conducted with the aim of minimizing adverse reactions and undesirable side effects before significant advancements can be made towards developing clinically relevant formulations for CVD applications.

Considering the recent success and FDA-approval of several liposome-based formulations to treat various forms of cancer, it is likely that liposomes will continue to be probed as a medium for the delivery of active agents to the cardiovascular system [247]. Though additional research must be conducted, it is clear that various cardiovascular drugs, for example statins and bisphosphonates, and imaging agents,

such as gadolinium, can greatly benefit from encapsulation into liposomes. Based on the work detailed in this review, it is clear that liposomes present interesting therapeutic and diagnostic capabilities that will continue to be explored and developed in the future with the ultimate aim of improving CVD treatment and diagnosis.

Chapter 6: Assessing Inflammation In Vitro

Tangible progress in the field of CVD treatment is underpinned by our current methods to accurately detect undesirable changes in the vasculature prior to the onset of clinical symptoms. Specifically in regards to atherosclerosis, early detection and localization of plaque initiation could significantly improve prognosis when combined with effective therapy. In light of the inflammatory response's critical role in early atherogenesis, particularly the upregulation of cellular adhesion molecules, it follows that precise detection and localization of these molecules may provide a means to characterize the disorder and treat the affected area before irreversible damage can occur. Accordingly, the technologies used to visualize and analyze the expression of such molecules are of vital importance to achieve this goal. Ideally, these technologies would be highly sensitive, selective, non-invasive, non-destructive, and provide both specific target identification, as well as localization information. Furthermore, inflammation detection tools that are initially tested and assessed *in vitro* should be designed so that translation to an *in vivo* settings can be achieved.

The concept of inflammation encompasses a variety of processes within the body, typically involving interactions between immune cells and healthy tissue [248]. The ultimate aim of the inflammatory response is to protect the host against infection or injury, as well as to participate in tissue repair. In the context of atherosclerosis,

the innate immune response plays a significant role, with the recruitment and attachment of mononuclear phagocytes by leukocyte adhesion molecules (e.g. ICAM-1, VCAM-1) to be a hallmark of early atherogenesis [249]. It follows that attempts to diagnose and treat initial plaque formations may be facilitated by accurate detection and localization of such adhesion molecules. Immunochemical techniques that are commonly used to detect such proteins and molecules via specific antibodies, including Western blot, ELISA, fluorescence, will be explored in the following sections, followed by a more detailed summary of surface-enhanced Raman scattering (SERS)-based approaches.

6.1 Western Blot Technique

Western blot is a robust technique widely used to detect proteins from cells or whole tissue [250]. The assay uses gel electrophoresis to separate proteins by molecular weight from a given sample, which are subsequently transferred to a nitrocellulose or polyvinylidene difluoride (PVDF) membrane and stained with antibodies specific to the target analyte. In the final step, an enzyme-linked secondary antibody is typically applied, which produces a colourimetric or chemiluminescent signal that can be detected by x-ray film, CCD camera imaging devices, or phosphoimagers. Figure 6.1a schematically depicts the generalized steps of the Western blot method.

The technique is moderately sensitive, reproducible, and quantitative, with several groups demonstrating application of the technique to detect inflammatory adhesion molecules. Cossette *et al.* (2013) detected both ICAM-1 and VCAM-1 expression in human coronary artery endothelial (HCAE) cells [13], while Liang *et al.* (2006) also applied the Western technique for VCAM-1 expression in aortic endothelial cells [251]. However, the method necessitates cell lysis and, therefore, cannot be used to localize lesions or realistically translated to *in vivo* models. In addition, rigorous experimental methods, laboratory expertise, and reagents are required to successfully perform the assay.

6.2 Enzyme-Linked Immunosorbant Assays

Three variations of ELISAs can be used to robustly quantify the amount of protein present in a given sample: direct, indirect, and sandwich methods (see Figure 6.1b). All are based on the attachment of an enzyme-linked antibody, which reacts with a substrate solution producing a colourimetric reaction proportional to the amount of protein present in the sample. The direct ELISA utilizes a labeled primary antibody immobilized on the capture plate to detect the target antigen, whereas the indirect assay incorporates a secondary antibody. The sandwich approach utilizes an antibody-coated platform to capture the antigen followed by a secondary detection antibody.

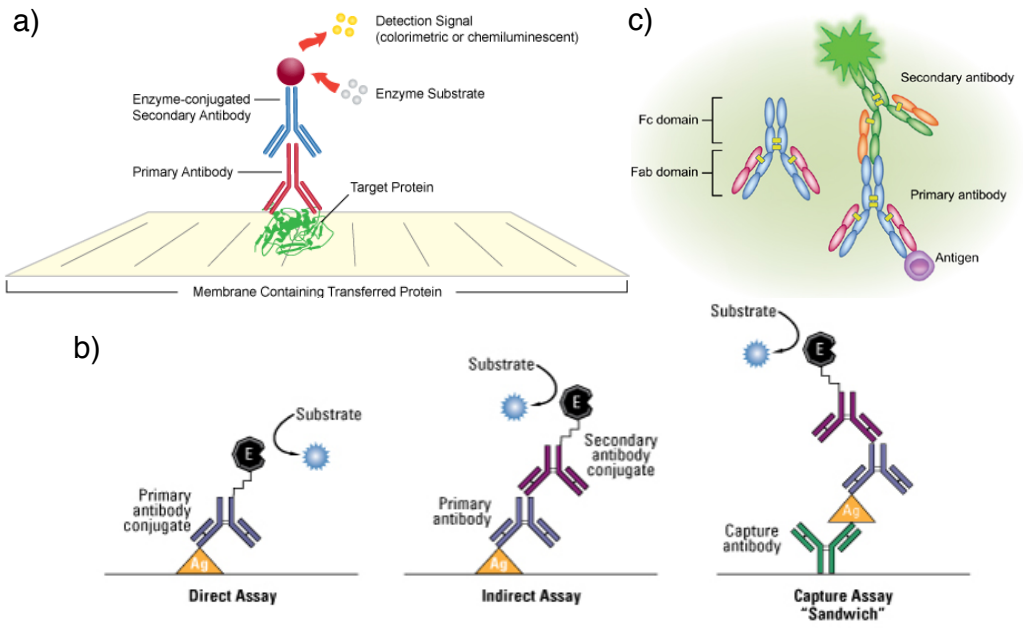

Figure 6.1 – Schematic diagrams showing the antigen-antibody interactions of immunochemical techniques for antigen/protein detection. (a) Protein detection via Western blot technique. (b) Three common ELISA formats for antigen detection. (c) IgG antibody (left) and target antigen bound to a primary- and fluorophore-conjugated secondary antibody, demonstrating the binding events and signal generation that occurs in fluorescence-based detection (right). Figure (a) is reproduced from [252], (b) from [253], and (c) from [254].

ELISAs are highly quantifiable and sensitive means of detection, and require relatively cheap equipment to perform. Indeed, Zhang *et al.* (2011) demonstrated that VCAM-1 and ICAM-1 expression increases in response to proinflammatory cytokines in murine heart endothelial cells using ELISAs [255]. However, the technique nevertheless suffers from drawbacks similar to Western blot, in particular the inability to localize protein expression in cells.

6.3 Fluorescence-Based Techniques

Immunofluorescence techniques are based on the interaction of target antigens with antibodies conjugated to fluorophores (see Figure 6.1c) [256] or quantum dots [257]. When combined with microscopy, the technique allows for localization of target immunoantigens *in vitro*, as well as quantitative analysis since the fluoresce signal intensity is generally regarded as proportional to the amount of antigen present in a given sample. However, due to broad bandwidths of fluorophores and quantum dots, the technique is limited in terms of multiplexing capabilities. As well, fluorescent dyes are sensitive to photobleaching, require expensive microscopy equipment, and often experience interference due to autofluorescing of cells and tissues. Fluorescence-activated cell sorting (FACS) can also be applied to quantify the fluorescent signal, as well as distinguish the proportion of cells expressing a given target antigen. The technique is similarly based on labeling antigens with flurorophores, however detached cells are flown through a specialized flow cytometer equipped with an excitation source and fluorescence detector. Disadvantages of this approach include costly equipment and the inability to localize expression of cells in their local environment.

6.4 Spectroscopy-Based Techniques

The expression of various inflammatory proteins and cytokines can also be assessed by spectroscopy-based approaches, which measure changes in optical

absorbance or reflective spectra. Examples include surface plasmon resonance (SPR) [258] and Raman spectroscopy [259]. Advantages of SPR include the ability to detect very low levels of proteins and biomarkers, however the technology is currently not adaptable to *in vitro* or *in vivo* environments. A more detailed review of Raman spectroscopy is presented in the following section.

6.5 Raman Spectroscopy

Raman spectroscopy is a useful tool in many research fields, since it can yield highly specific structural information, with very little sample preparation and minimal equipment. Historically, weak Raman signals precluded the application of Raman spectroscopy to study cells and biological tissues, however developments pioneered in the past few decades, such as surface-enhanced Raman scattering (SERS), have allowed for translation into this field due to improved signal intensities and detection capabilities. This section will review the principles of Raman spectroscopy and SERS, as well as detail recent progress in the field of SERS-based biomedical research.

6.5.1 Principles of Raman Spectroscopy

Raman spectroscopy is a light scattering technique used to detect, characterize, and elucidate the molecular structure of materials [260]. The principle is based on the interaction of a photon of light with a given sample, which results in

varying degrees of reflection, absorption, and scatter depending on vibrational modes of the molecules under investigation. Most of the scattered radiation is called Rayleigh or elastic scattering since the frequency is unchanged, however a small proportion is scattered at a different wavelength and is termed Raman or inelastic scattering (see Figure 6.2a). Raman scattering can further be differentiated into Stokes, where the photon is scattering at a lower energy, and anti-Stokes, where the molecules are scattered at a higher energy (see Figure 6.2b). The Stokes scattering is of particular interest to Raman spectroscopists since it is typically more intense than the anti-Stokes radiation, and thus, can be used to provide detailed insight into chemical structures, or more specifically, vibrational structures of a given sample.

Typical Raman spectroscopy measurements are conducted by illuminating a sample with a monochromatic light source, generally a laser in the visible, NIR or UV range. After excitation and generation of the Raman signal, a notch filter is used to absorb or reflect any Rayleigh scattering and transmits the Raman signal whereby a detector and spectrograph are used to image the Raman spectra (see Figure 6.2c). The addition of a confocal microscope to the set-up can be used to localize detection of Raman signals further, since it is designed to reject background noise. However, despite the advantages of Raman spectroscopy, the technique suffers from the key drawback of weak signal intensities that may be lost amongst background scatter and noise. Although multivariate analysis and data interpretation may be applied to

dissect spectral information [261, 262], complex statistical models and specific software are typically required, and, even so, may not be capable of analyte detection at low levels. Particularly in regards to the study of biological systems, where target molecules may be present in nanomolar or femtomolar concentrations, signal amplification is required to yield functional results.

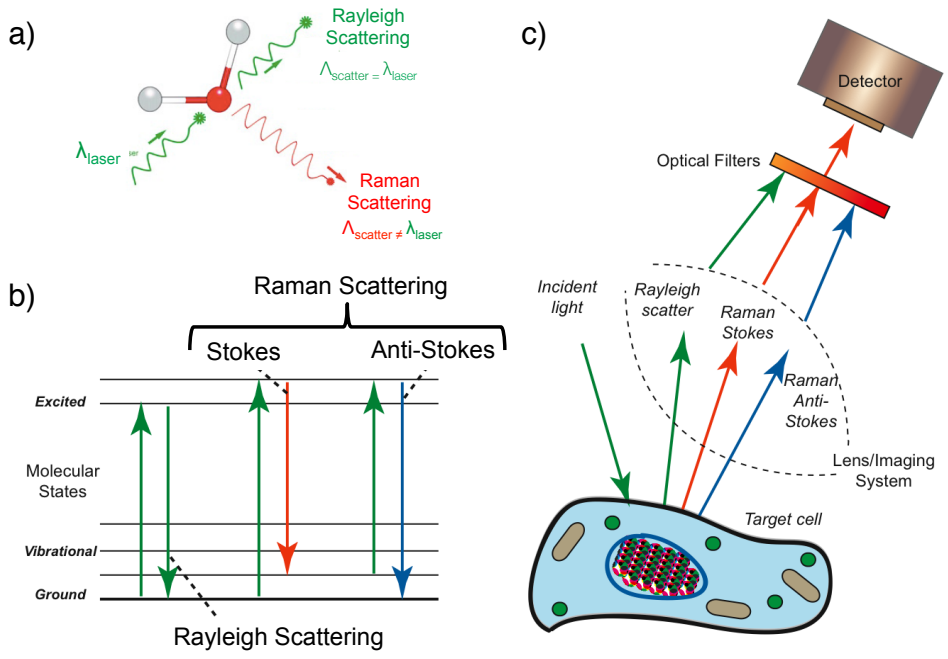

Figure 6.2 – Principles of Raman Spectroscopy. (a) Interaction of a molecule with a photon of light to produce scattered radiation. (b) Energy level diagram showing Rayleigh, Stokes and anti-Stokes Raman scattering modes. (c) Typical Raman spectroscopy set-up showing a target cell as sample. Adapted from [263] and [264].

6.6 Surface-Enhanced Raman Scattering

6.6.1 Principles of Surface-Enhanced Raman Scattering

The first reported observation of a surface-enhanced Raman signal was published by Fleischmann *et al.* (1974), who described the increase in Raman signal of pyridine observed on a roughened surface electrode [265]. Since that time, the technology has been employed in variety of fields including materials [266], analytical [267], and life science [268, 269] to detect and identify samples previously indiscernible by traditional Raman spectroscopy. Essentially, the SERS effect involves an amplification of Raman signal when molecules are adsorbed or are in close proximity (~10 nm) to metal surfaces, commonly referred to as *SERS substrates*. Indeed, Raman signal intensities have been frequently documented to increase 10^4-10^6 fold [270-272], and as much as 10^{10} given ideal conditions [273], with single molecule detection equally reported in the literature [274, 275]. Two factors are thought to contribute to the SERS effect and are categorized into (i) electromagnetic mechanisms and (ii) chemical mechanisms [276, 277]. Long-range electromagnetic field enhancement is based on the interaction between target molecule and the localized surface plasmon resonance (LSPR) induced by laser light on a metal surface [276]. While short-range chemical interactions are believed to contribute to signal enhancement by the charge transfer that occurs between the analyte and metal surface, subsequently enhancing vibrations [278].

As described, SERS substrates are typically metallic nanostructures characterized by their ability to enhance Raman scattering signal intensities. Typically, these substrates are subcategorized into two classes: (i) variations of colloidal nanoparticles and (ii) nanopatterned 'planar' substrates fabricated by nano-lithography or self-organization [279] The nanostructured component of these substrates allows for greater signal amplification compared to flat metallic surfaces, due to increased surface area. Coinage metals, gold, silver, and/or copper are most often employed as SERS substrates since they exhibit good plasmon resonances in the visible/near-infrared (NIR) region [40].

Among diverse applications, the SERS spectroscopic technique is particularly well suited to the study of biological systems due to the weak Raman scattering property of water, compatibility at NIR, minimal sample preparation, and low limits of analyte detection [280, 281]. Furthermore, narrow vibrational spectral bandwidths (~1 nm) compared to fluorescent and quantum dot probes, make SERS well suited to multiplexing applications [282, 283]. The selection of colloidal (3D) or planar (2D) nanosubstrates depends on the experimental set-up and ultimate application. However, for the purposes of this review, we will focus on the use of colloidal systems since they represent the majority of the current and future of SERS-based *in vitro* and *in vivo* research [284-286].

SERS colloidal nanostructures are employed in two main areas of biological-based research: label-free detection of analytes (direct sensing) and targeted detection with SERS labels (indirect sensing). Figure 6.3a depicts these two areas of research using nanoparticles (NPs) as SERS substrates.

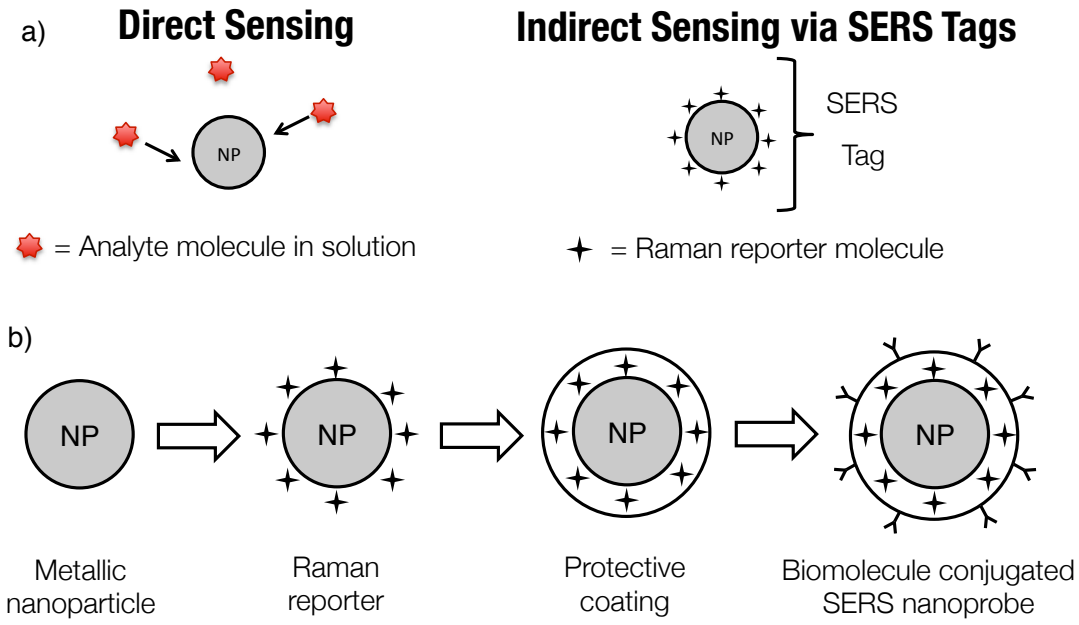

Figure 6.3 - (a) SERS applications of metallic NPs for direct and indirect sensing. (b) Step-by-step fabrication of antibody-functionalized SERS nanoprobes for target sensing applications. Adapted from [287] and [288].

For label-free detection, colloidal nanostructures introduced into a solution amplify the characteristic Raman signal of molecules when adsorbed or in close proximity to the surface of nanostructures [287]. The label-free approach has been applied to monitor cell viability [289] and measure apoptosis [290], however detection capability is limited by non-specific sample interactions and is therefore

typically not suitable for bioanalysis. Indirect sensing via SERS nanotags, on the other hand, provides the capability to directly sense target molecules when combined with Raman microscopy and functions similar to quantum dots and fluorophores [284]. Compared to these other optical probes, SERS tags offer greater sensitivity and capacity for multiplexing, enhanced photostability, and compatibility at NIR excitation [291]. As well, SERS nanotags merely require a single laser excitation wavelength for detection. The design and fabrication of the SERS probes is integral to successful application and bioanalytical detection. Accordingly, each element of the SERS tags will be described in more detail in Section 6.6.2.

6.6.2 Surface-Enhanced Raman Scattering Nanoparticle Probes

As described above, each step in the design and construction of SERS nanoprobes can affect the degree of Raman signal enhancement and ultimate analysis. In addition to significantly enhancing Raman signal intensities, SERS nanoprobes should be stable, and support biofunctionalization [285]. As depicted in Figure 6.3b, SERS nanotags are comprised of four main components, they are the: (i) metal nanosubstrate, (ii) Raman reporter molecule, (iii) protective surface coating (optional), and (iv) targeting molecule. Table 6.1 provides a general overview of each component along with relevant examples and references from the literature.

Table 6.1 – Components of SERS nanoprobes used for biomedical applications.

Component	Function	Type	Main Advantages	Main Disadvantages	Example	Ref.
SERS Substrate	Increases Raman signal intensity via LSPR	Gold	Stable, biocompatible, inert, LSPR in visible/NIR range	Inferior signal enhancement	Gold nanorods	[292]
		Silver	Substantial Raman signal enhancement, LSPR in visible/NIR range	Cytotoxic, poor long term stability	Silver nanoparticles	[293]
		Copper	LSPR in visible/ NIR range	Reactive to air	Copper nanoparticles	[294]
Raman Reporter	Imparts characteristic Raman Signal	Nitrogen-containing cationic dyes	Cheap	Weak affinity for metal, poor stability	Crystal violet	[295]
		Sulfur-containing dyes	Strong affinity for metal	Expensive, difficult to form SAM	Malachite green isothiocyanate	[296]

		Thio-small molecules	Cheap, few Raman peaks, strong affinity for metal, SAM formation	Can be unstable in solution	4-Mercaptobenzoic acid	[297]
Surface Coating	Improves stability, biocompatibility, surface for functionalization	Silica	Stable, good water solubility, non-specific binding	May require pretreatment to make probe vitrophilic	Silica	[298]
		Polymers	Large variety, biocompatible, biodegradable, water soluble	-	PEG	[299]
Surface Ligands	Biofunctionality, targeting capability	Aptamers	*Selection depends on application*		Vasopressin aptamer	[300]
		Antibodies			F-19 Monoclonal antibody	[301]

6.6.2.1 Metallic Nanoparticles

Typically coinage metals, such as gold, silver, copper, and/or a combination thereof, are employed as the structural scaffold and signal amplifier for SERS labels since they possess the necessary optical properties to enhance Raman scattering signals. Although silver often bests gold in signal enhancement, gold particles are typically favored for biological applications since they are less cytotoxic [284]. In addition to material selection, substrate size can affect optical properties and must thusly be tailored to the desired application [302]. Typically diameters between 30 - 100 nm are most suitable for SERS applications [303]. Finally, a variety of substrate shapes can be used to affect signal enhancement, including nanoparticles [304], nanorods [305], nanoflowers [306], and nanostars [307].

6.6.2.2 Raman Reporter

The next step in SERS probe construction is the selection and conjugation of the Raman scattering reporter molecule onto the nanosubstrate, which imparts the characteristic spectral signal. Main criteria for Raman reporters include strong Raman scattering properties with few characteristic peaks (for multiplexing) and suitable affinity for the metallic nanosubstrate to prevent desorption. Common types of Raman reporters are nitrogen- or sulfur- containing dyes, and thio-small molecules. Table 6.1 outlines the advantages and disadvantages of each reporter types along with common examples. Thiol-small molecules are of particular interest for highly sensitive SERS detection, since they can form self-assembled monolayers (SAMs) on the surface of nanosubstrates. Since the number of Raman reporter

molecules on the substrate surface directly influences Raman signal intensity [308], it follows that the maximal surface coverage afforded by SAM formation significantly improves detection capacities [287].

6.6.2.3 Protective Coating

Protective coatings, such as polymers and silica, are often employed in SERS probes design to enhance stability, reduce non-specific binding, and provide a surface for functionalization [284]. As well, the protective coating can serve to improve biocompatibility and decrease detachment of Raman reporter, which is particularly relevant when probes are introduced into biological systems. Examples of protective coatings are included in Table 6.1.

6.6.2.4 Targeting Molecules

In order to target SERS probes to specific analytes, biomolecules, such as aptamers or antibodies, must be conjugated to the probe surface. The type of biomolecule is dependent on resources available and on the ultimate target application. Various functionalization techniques can be applied, such as 1-ethyl-3-(3-dimethylaminopropyl) carbodiimide (EDC)/N-hydroxysuccinimides (NHS) chemistry [309] or via direct conjugation to the Raman reporter [310].

6.6.3 Surface-Enhanced Raman Scattering Nanoprobe Applications

The application of SERS nanoprobes for bioanalysis can broadly be divided into two categories: sandwich SERS-based immunoassays and SERS-based biosensing and bioimaging (see Figure 6.4), each of which will be detailed in the following sections.

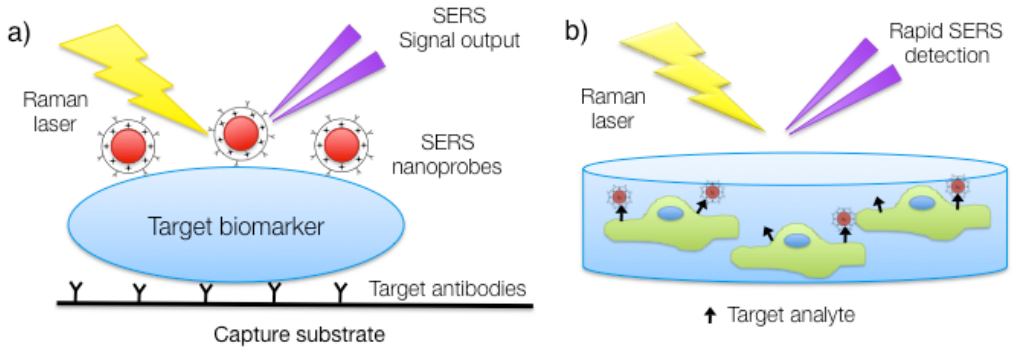

Figure 6.4 – Schematic diagram representing the components of a SERS-based (a) immunoassay platform and (b) cellular nanosensing application.

6.6.3.1 SERS-Based Immunoassays

Typically, SERS-based immunoassays are employed to detect protein biomarkers in complex biological samples to diagnosis various pathophysiological states. As depicted in Figure 6.4a, the scheme is based on three components: the capture substrate, biofunctionalized SERS nanoparticle, and Raman signal output [311]. The principle advantages of SERS-based immunoassays compared to

traditional methods of biomarker detection, such as Western blot, mass spectrometry, and ELISA, include lower limits of detection (down to zeptomolar [312, 313]) and the opportunity to scale to point-of-care (POC) devices thanks to recent innovations in portable Raman instrumentation [311]. A study by Li *et al.* (2013) detailed the fabrication of a SERS immunosensor for protein biomarker detection with the aim of detecting VEGF in the human plasma of patients with breast cancer [314]. The design was based on capture antibodies immobilized on a plasmonic substrate and gold nanostars fabricated with the Raman reporter malachite green isothiocyanate coated with silica. The lower limit for VEGF detection was determined to be 7 fg/mL in human serum, demonstrating the platform as a possible ultrasensitive biomarker detection technique. Based on these results, as well as a several other groups demonstrating promising outcomes [283, 315-317], the use of this SERS-based approach will no doubt endure and continue to make significant impacts in the field of diagnostics.

6.6.3.1 SERS-Based Biosensing and Bioimaging

SERS-based nanosensing can be applied to detect intra- [40, 318] or extracellular analytes [318] and, when combined with confocal microscopy, provides high resolution images [319, 320]. This dual advantage is unique among bioanalysis methods since conventional techniques, such as Western blot and ELISA, do not yield distribution information and typically require cell disruption or lysis. Similarly,

fluorescence-based single cell imaging and spectroscopy affords poor limits of detection, restricted multiplexing potential due to broad bandwidths, and cytotoxicity over prolonged incubation times [285]. Given the advantages of SERS-based detection, the technique has been applied to a variety of applications including intracellular monitoring of pH [321], differentiation over time [322], and drug delivery [323, 324]. When biofunctionalized SERS-nanoprobes are used, highly specific detection of molecules such as surface receptors and markers can be achieved [325-327]. Lee *et al.* (2014) demonstrated that SERS nanoprobes functionalized with antibodies specific for epidermal growth factor, ErbB2, and insulin-like growth factor could be used to distinguish cancer cell phenotype, quantify, and localize surface expression [318]. The article also highlights the tremendous potential for SERS-based analysis to be used in multiplex detection, which is increasingly becoming relevant to the field of personalized medicine [282, 328, 329]. Specifically in regards to assessing inflammation *in vitro*, McQueenie *et al.* (2012) reported that antibody functionalized SERS probes could be applied to detect ICAM-1 expression *in vitro* with superior sensitivity compared to fluorescence techniques [288]. Furthermore, ICAM-1 expression in atherosclerotic mice was demonstrated, which highlights the application of SERS-based detection *in vivo* [330].

Certainly, one of the main challenges associated with SERS-based bioanalysis lies in the development of stable and reproducible SERS nanosensors, with significant enhancement capacities. Presently, SERS probes are custom fabricated by, for the most part, complex and multi-step procedures that can take several days and are difficult to reproduce [331]. Other limitations of the technique include the cost and practicality of the current instrumental systems including the spectrophotometer, laser, and detector, as well as the confocal microscopy component that is crucial to much of the biological-based SERS studies. As far as translation to *in vivo* studies, Raman lasers have been shown to penetrate murine tissues approximately 1-2 cm for adequate SERS detection [41] and stability over a week in mouse models has been demonstrated [332]. Universal application of the technology will certainly be dependent on the ability to maintain significant signal intensities from SERS substrates over time and at suitable depths for diverse tissue analysis. In tandem with the continued development of more precise and portable Raman spectroscopy systems, applications of this technology in the field of medicine will no doubt continue into the future.

Chapter 7: 1,2-Dioleoyl-sn-Glycero-3-Phosphocholine–Based Liposomal Nanoparticles as an Effective Delivery Platform for 17β-Estradiol

In order to meet the first two objectives of this thesis, that is to design and characterize an E2 liposome-based delivery vehicle, an investigation into the components and formulation of such a system was undertaken. Briefly, three types of lipids were investigated for their ability to accommodate varying concentrations of E2 within the lipid bilayer. The encapsulation efficiency, loading capacity, and release kinetics of E2 from lipid bilayers were assessed by a high performance liquid chromatography (HPLC) method developed for E2 quantification (see Appendix B). 1,2-Dioleoyl-*sn*-glycero-3-phosphocholine (DOPC) was shown to accommodate the highest amount of E2 by weight, with a 5% initial E2 loading demonstrating the best encapsulation efficiency. Varying charging agents were subsequently included in the formulation composed of DOPC and 5% E2, with the formulation containing the cationic charging agent dimethyldioctadecyl-ammonium (DDAB) demonstrating the best cellular uptake in human coronary artery endothelial (HCAE) cells. No adverse cytotoxicity effects in HCAE cells were observed in any of the formulations tested.

The results of this study are presented in following manuscript entitled "1,2-Dioleoyl-*sn*-Glycero-3-Phosphocholine–Based Nanolipsomes as an Effective Delivery Platform for 17β-Estradiol", which was accepted for publication by the *European Journal of Pharmaceutics and Biopharmaceutics* in October 2013.

2-Dioleoyl-*sn*-Glycero-3-Phosphocholine–Based Nanolipsomes as an Effective Delivery Platform for 17β-Estradiol

Kristen Bowey[1], Jean-François Tanguay[2], Maryam Tabrizian[1,3,*]

[1]Department of Biomedical Engineering, McGill University, Montréal, Quebec, Canada

[2]Montréal Heart Institute, Department of Medicine, Université de Montréal, Montréal, Québec, Canada

[3]Faculty of Dentistry, McGill University, Montréal, Québec, Canada

*Corresponding author: maryam.tabrizian@mcgill.ca

7.1 Abstract

The high loading efficiency and efficient delivery of hydrophobic drugs is still an unmet goal in the development of drug delivery systems. In the present study, liposomes were developed to encapsulate 17β-estradiol (E2), which is a sex steroid shown to confer protective effects in the cardiovascular system. Egg phosphatidylcholine (EPhC), 2-dioleoyl-*sn*-glycero-3-phosphocholine (DOPC), or 1,2-dipalmitoyl-*sn*-glycero-3-phosphocholine (DPPC) were used to prepare liposomes by thin film hydration and tested for their ability to load E2 with a high efficiency. DOPC-based liposomes were found to improve E2 encapsulation efficiency and loading capacity compared to those composed of EPhC and DPPC. In addition, neutral liposomes, liposomes prepared with the cationic charging agent dimethyldioctadecyl-ammonium (DDAB), and liposomes prepared with the anionic charging agent 1,2-ditetradecanoyl-*sn*-glycero-3-phospho-(1'rac-glycerol) (DMPG), were characterized with regards to their E2 encapsulation efficiency, loading capacity, particle size, zeta potential, and *in vitro* drug release. A human coronary artery endothelial (HCAE) cell model was used to further evaluate effects on cytotoxicity and relative cellular uptake efficiency of each formulation. Results showed that DOPC liposomes composed of DDAB had the highest E2 improved cellular uptake compared to uncharged and DMPG-based liposomes, demonstrating the greatest potential to be used in future cardiovascular therapeutic applications.

7.2 Introduction

Despite extensive applications of small hydrophobic pharmaceutical agents, efficient delivery is often challenged by short biological half-lives and rapid clearance within the body, which translates to narrow pharmacological windows. Since high doses must be administered to compensate for this clearance, toxicity and undesirable side effects may be an obstacle to effective treatment regimes. An alternative to a bolus delivery of such active agents is incorporation into liposomes [333], which are small vectors, composed of phospholipid bilayers [334, 335]. Liposomes can alter drug solubility [336], cellular delivery [337], and distribution *in vivo* [338, 339], as well as control release of active agents [340], and decrease toxicity [341]. In addition, liposomes are biodegradable and generally non-toxic, making them ideal candidates for the delivery of active agents to the body. They have been employed in a variety of applications including chemotherapy [342, 343], enzyme [344, 345] and protein delivery [346, 347], gene therapy [348, 349], diagnostic imaging [350, 351], and vaccination [352, 353]. Liposomes are particularly well suited to delivering hydrophobic molecules, since they can be loaded into the lipophilic domain [354, 355].

One of the hydrophobic active agents of interest is the family of estrogens and their investigation, not only for the treatment of hormonal efficiency, but also in treating cardiovascular disease. Epidemiological data has shown that premenopausal

woman experience significantly less incidents of adverse coronary events compared to men of the same age, and postmenopausal women [21]. Though there are a variety of factors that may contribute to this finding, numerous studies have demonstrated convincing evidence for the role of estrogens, which are present in higher levels in premenopausal females [22, 356, 357]. Particularly, 17β-estradiol, abbreviated as E2, has been shown to affect a variety of cardiovascular processes, conferring both systemic [106], and local effects [23]. Recent research has also investigated the role of estrogens in inflammation [357], attenuating reactive oxygen species development [358], collagen synthesis [359], and cellular apoptosis [23], all of which are contributing factors to the development and progression of cardiovascular-based diseases. Conventional E2 treatments delivered via peroral or transdermal routes typically result in non-specific tissue distribution and may be subject to first pass-metabolism, requiring potentially toxic doses to achieve desired therapeutic effects [360]. Indeed, proposed links between estrogen replacement therapy and increased incidences of breast cancer emphasize this drawback [361]. Therefore, different iterations of carrier systems, for example E2 conjugated-phosphatidylethanolamine liposomes [362], 2-methoxyestradiol loaded phosphatidylcholine liposomes [19], and PEGylated estradiol liposomes [363], have been developed for various delivery applications.

The focus of our study was to engineer a liposome-based nanoparticulate carrier from the bottom up to deliver E2 for cardiovascular diseases, such as atherosclerosis. Indeed, a reduced burst effect, washout, and lower levels of drug required compared to conventional administration, all contribute to the advantages bestowed upon systems delivered via nanoparticulate vehicles [364]. For our purposes, an optimal E2 formulation would deliver the active agent in a controlled and reproducible manner over a 48-hour period, potentially improve residence time in the body, as well as cellular uptake and decrease overall dosage requirements. As such, the objective of this study was to design and characterize a delivery system specifically for the incorporation of E2 into the lipophilic bilayers of liposomes, which could be used for future applications to treat vascular disease *in vivo*. Neutral liposomes, cationic liposomes, and anionic liposomes were characterized with regards to their E2 entrapment efficiency, loading, and release profile. Due to the incidence of studies reporting the significance of E2 to vascular health and disease, the cytotoxic activity and cellular uptake against a model cell line of human coronary artery endothelial (HCAE) cells and were evaluated after short-term *in vitro* assays.

7.3 Materials and Methods

7.3.1 Materials

Cholesterol, 17β-estradiol (E2), methanol, chloroform, HPLC-grade acetonitrile and methanol were purchased from Sigma Aldrich (St. Louis, USA). 1,2-dipalmitoyl-*sn*-glycero-3-phosphocholine (DPPC) was purchased from CordenPharma (Colorado, USA). Egg phosphatidylcholine (EPhC), 1,2-dioleoyl-*sn*-glycero-3-phosphocholine (DOPC), 1,2-ditetradecanoyl-*sn*-glycero-3-phospho-(1'rac-glycerol) (DMPG) and dimethyldioctadecyl-ammonium (DDAB) were purchased from Avanti Polar Lipids (Alabaster, USA). Oregon Green ®, 1,2-dihexadecanoyl-*sn*-glycero-3-phosphoethanolamine, triethylammonium salt was purchased from Molecular Probes (Oregon, USA). Human coronary artery endothelial (HCAE) cells were purchased from Lonza (Basel, Switzerland), along with the EGM-2 BulletKit containing Endothelial Basal Medium-2, 10% FBS, and EGM-2 SingleQuots comprised of appropriate growth factors, cytokines and supplements to support cell growth. Ultra pure water (UPW) from a Millipore filtration system was used for all experiments. All other chemicals used were analytical grade.

7.3.2 Preparation of E2-Loaded Liposomes

Liposomes were prepared by the thin film hydration technique. Briefly, the main lipid, either EPhC, DOPC, or DPPC, cholesterol (30 mol %), DDAB (10 mol %), and E2 (varied between 1 and 10 mol %) were dissolved in a chloroform/methanol solvent mixture (4:1 vol/vol). Organic solvent was removed by rotary evaporation under reduced pressure until a lipid film was observed. The film was flushed with nitrogen to remove any traces of solvent. The thin film was hydrated with PBS for 30 min to form multilamellar vesicle dispersions. Liposomes were allowed to mature for 2 h at room temperature and then extruded successively through 0.4 and 0.2 μm polycarbonate membranes to reduce their size. Unencapsulated E2 was removed by a Labscale™ tangential flow filtration (TFF) system in conjunction with a Pelicon® XL polyethersulfone filter (100K) from Millipore (Billerica, USA). Fluorescent liposomes were prepared by incorporating either Oregon Green® 1,2-dihexadecanoyl-*sn*-glycero-3-phosphoethanolamine, triethylammonium salt (Molecular Probes, USA) for cellular uptake experiments or Texas Red ® 1,2-dihexadecanoyl-*sn*-glycero-3-phosphoethanolamine, triethylammonium salt for confocal visualization at 1 mol% into the original formulation and processed as described.

7.3.3 E2 Encapsulation Efficiency

After un-entrapped E2 was removed by TFF, the encapsulation efficiency (EE) and loading capacity (LC) of E2 in the liposomes was determined directly by drying 1 mL of liposomes overnight at 50ºC and then dissolving the liposomes methanol to solubilize the formulation. The solution was sonicated for 30 min to obtain a completely clear liquid, and filtered. The sample was then resuspended in the mobile phase and assayed by a high performance liquid chromatography (HPLC) system as described in Section 7.3.8. The drug EE was determined as the ratio between the amount of entrapped E2 in the liposomes and the initial drug added based on the total weight:

$$EE = \frac{\text{Experimental drug loading}}{\text{Theoretical drug loading}} \text{ x } 100\ \%$$

The LC of the liposomes was calculated as the ratio of the amount of entrapped drug in the liposomes to the total weight of the formulation:

$$LC = \frac{\text{Total Amount of E2 (μg)}}{\text{Total Dry Weight of Liposomes (mg)}}$$

The mass yield of the liposomes after extrusion and purification was calculated as the recovered mass of the formulation divided by the original weight of the formulation:

$$\text{Mass Yield} = \frac{\text{Recovered Weight of Liposomes (mg)}}{\text{Total Dry Weight of Liposomes (mg)}} \times 100$$

7.3.4 Particle Size and Zeta Potential

The particle size and polydispersity index were measured by photon correlation spectroscopy using the 90Plus/BI-MAS Multi Angle Particle Sizer (Brookhaven Instruments, USA). Zeta potential (ξ) was determined using a ZetaPlus analyzer by laser Doppler anemometry (Brookhaven Instruments, USA).

7.3.5 Preparation of Charged E2-Loaded Liposomes

Anionic, cationic and neutral liposomes were prepared to investigate the effects of charge on the physiochemical, E2 release and *in vitro* properties. Liposomes were fabricated as described in Section 7.3.2 with DOPC as main lipid constituent, with DDAB (10 mol %) included to prepare cationic liposomes or DMPG to prepare anionic liposomes. Neutral liposomes were prepared in the absence of both DDAB and DMPG.

7.3.6 E2 Release Study

In vitro release from liposomes was assayed by dialysis method. Known quantities of the liposome formulation were placed into a Float-A-Lyzer® G2 device

(Spectra/Por, molecular weight cutoff of 3.5-5 kDa, Spectrum Laboratories Inc. USA) and release was measured over a predetermined time of 48 h. Since E2 is lipophilic, it is necessary to include a wet agent to assure sink conditions within the release medium [365]. Thus, formulations were dialyzed against 40% ethanol added to PBS (pH = 7.4). All release studies were conducted at 37°C under gentle agitation. At appropriate time intervals, aliquots were removed and E2 content was assayed by HPLC. The profiles of *in vitro* E2 cumulative release (CR%) from liposomes were expressed as:

$$CR\% = \frac{C_{0-t}}{C_0} \text{ x } 100$$

Where C_{0-t} is the amount of drug released from liposomes at time t and C_0 is the total amount of drug in the liposome suspension.

7.3.7 Shape and Surface Morphology

The shape and surface structure of liposomes were visualized by cryogenic transmission electron microscopy (cryo-TEM). Briefly, 5 µL of liposome suspension was dropped onto a copper grid. The sample was then blotted with filer paper to remove excess and rapidly plunged into liquid ethane. Imaging was performed with a FEI Tecnai G^2 F20 microscope operating an accelerating voltage of 120 kV.

7.3.8 Chromatographic Conditions

The amount of E2 in liposomal formulations and in release medium was assessed by reverse-phase High Pressure Liquid Chromatography (HPLC) using a Flexar LC Perkin Elmer HPLC system equipped with a photodiode array detector (Waltham, USA). A Brownlee Spheri-5 column was used (220 x 4.6 mm, 5 μm, Perkin Elmer) was used at ambient temperature for E2 detection at 205 nm. The mobile phase was an aqueous solution of acetonitrile and water (70:30, v/v). The flow rate was 1 mL/min and the sample injection volume 50 μL. The chromatographic control system, data acquisition and analysis were performed using Chromera software (Version 3.3, Perkin Elmer). The retention time for E2 was 4.4 min and linearity was assessed to be 0.9979.

7.3.9 Cell Culture Experiment

Human coronary artery endothelial (HCAE) cells used in cell culture experiments were grown in tissue culture flasks, maintained in 5% CO_2 at 37°C. The culture medium was prepared according to the manufacturer's instructions using an EGM-2 BulletKit. Cells used for experimentation were released with 0.25% trypsin/0.1% EDTA (Gibco, Invitrogen).

7.3.10 Cytotoxicity Assay

The effect of the E2-liposomes on the cellular viability of HCAE cells was examined by 3-(4,5-Dimethylthiazol-2-yl)-2,5-diphenyltetrazolium bromide (MTT) assay, according to the manufacturer's protocol (Vybrant® MTT Cell Proliferation Assay Kit, Invitrogen). HCAE cells were seeded into a 96-well plate at a density of $2x10^4$ cells/cm and allowed to mature for 24 h. The culture medium was removed and washed twice with PBS, wherein the cells were then exposed to 150 µL of E2-liposomes. After 48 h, cells were washed twice with PBS and 100 µL of fresh medium was added to the wells. Next, 10 µL of 12 mM MTT stock was added to each well. After incubating for 4 h at 37ºC, absorbance values were measured using a microplate reader (µQuant, BioTek, Winooski, USA) at a wavelength of 540 nm. Cell viability was calculated using the formula, where blank control cells receiving no sample served as the absorbance control:

$$\text{Cell Viability\%} = \frac{\text{Absorbance Sample}}{\text{Absorbance Control}} \text{x} 100$$

7.3.11 Cellular Uptake Experiments

Cellular uptake was studied using fluorescent liposomes, adapted from protocols developed by Muthu *et al.* (2011) [366] and Murata *et al.* (2012) [337]. Briefly, HCAE cells, harvested as described in section 7.3.10, were plated at a density of $1x10^5$ cells/cm^2 onto 96 well plates and allowed to mature for 24 h prior to

experimentation. Next, the cells were incubated with fluorescent liposomes, which were prepared with Oregon Green® 1,2-dihexadecanoyl-*sn*-glycero-3-phosphoethanolamine, triethylammonium salt, as described in section 7.3.2. Fluorescent liposomes were incubated either for 2 h or 24 h. Following incubation, cells were washed 3X with ice cold PBS (pH 7.4) and lysed with 0.2 mL of 1 N NaOH. The relative quantity of fluorescent dye was measured using a fluorescence spectrophotometer at an excitation wavelength of 501 nm and an emission wavelength of 526 nm (FLx-800, BioTek, Winooski, USA).

Cellular localization of liposomes was investigated by confocal microscopy. After 24 h incubation with fluorescent liposomes labeled with Texas Red ® 1,2-dihexadecanoyl-*sn*-glycero-3-phosphoethanolamine cells were washed with PBS and fixed with 4% paraformaldehyde solution. Next, cells were stained with phalloidin for 30 min, followed by a nucleus stain (DAPI) in PBS, which was applied for 15 min. Cells were observed using an inverted fluorescence microscope (Nikon TE 2000-E). Images were captured using a CCD camera (Photometrics CoolSNAP HQ2) and analyzed by MBF_ImageJ (MacBiophotonics, McMaster University). Non-fluorescent liposomes were also investigated as a control.

7.3.12 Statistical Analysis

Data is expressed as mean ± standard deviation (S.D.) of n replicates per group. Statistical analysis was performed using Student's t-test and multiple

comparisons were done using one-way ANOVA with *post hoc* Tukey's test. Differences were considered significant at $p<0.05$.

7.4 Results and Discussion

7.4.1 Preparation and Physicochemical Characterization of Liposomes

The formulation and composition of the liposomal core was first investigated in an attempt to maximize the loading capacity of E2 within the lipid bilayers. In particular, three phospholipids EPhC, DOPC, and DPPC, were studied for their ability to accommodate E2 within their formulation. Since estradiol has previously been shown to interact with both the phospholipid head and lipophilic core of the bilayers [367], and particularly with the acyl chains of the lipid membrane, it is reasonable to assume that the phospholipid composition likely affects E2 incorporation. The initial E2 included into the liposome formulation was also considered with the aim of determining the maximal loading capacity of E2 within the liposomes. Preliminary work established that the upper limit of E2 loading was 10 mol % of the main lipid, since any surplus would precipitate out of solution and clog extrusion filters. Thus, to determine the effects of initial drug loading, a range from 1 to 10 mol % was investigated. Table 7.1 outlines the experimental formulations along with the resulting characterization data, demonstrating the effects of lipid selection and E2 drug loading on the encapsulation efficiency and loading

capacity. No significant differences were observed in regards to the size and zeta potential.

Results presented in Table 7.1 show that E2 encapsulation efficiency varied between 8.2 and 68.8%, and was dependent on both the main lipid and initial E2. EE increased significantly when the initial E2 loading was decreased from 10 to 1% mol/mol for all of lipid compositions tested ($p<0.05$). Furthermore, EE was significantly higher in formulations composed of DOPC, compared to both EPhC and DPPC for all initial E2 loadings ($p<0.05$).

E2 loading capacity for all formulations varied between 1.9 to 8.8 μg/mg, depending on the main lipid employed. E2 was incorporated into liposomes composed of phospholipids in the order of DOPC>EPhC>DPPC for equal levels of E2 loading. The lowest loading capacity was observed in liposomes made of DPPC. This may be due to the saturated nature of DPPC that tends to form a more rigid membrane structure compared to DOPC and EPhC, which are primarily composed of unsaturated phospholipids. The chain length may also be a determining factor in the extent of incorporation. As shown in Table 7.1, E2 was loaded to a higher degree in DOPC, which is composed of the longest proportion of fatty acid tails compared to both EPhC and DPPC. However, the loading capacity was not necessarily influenced by the initial E2 loading. For example, liposomes composed of DOPC and EPhC demonstrated statistically insignificant differences in loading capacity at initial E2

loadings of 5 and 10 % mol/mol ($p>0.05$). Whereas loading capacity decreased significantly at an initial E2 loading of 1 % mol/mol. These findings are consistent with the theory that lipid bilayers posses an inherent loading capacity for hydrophobic molecules and that any excess will precipitate out in solution. As a result, liposomes composed of EPhC, DOPC, and DPPC reached maximal-loading capacities of 5.5 ± 0.2, 7.3 ± 0.5, and 2.2 ± 0.1 μg/mg, respectively.

Table 7.1 - Effects of main lipid and initial E2 loading on encapsulation efficiency and loading capacity. Data are reported as mean ± S.D. (n=3).

Main Lipid	Lipid carbon atoms:double bonds	E2 loading (% mol/mol)[1]	Encapsulation efficiency (%)	Loading capacity (μg/mg)[2]
EPhC	Mixture[3]	10	18.6 ± 0.4	5.5 ± 0.2
EPhC		5	37.1 ± 2.5	5.3 ± 0.4
EPhC		1	56.0 ± 3.4	1.9 ± 0.1
DOPC	18:1	10	32.1 ± 1.2	8.9 ± 0.3
DOPC		5	51.2 ± 3.6	7.3 ± 0.5
DOPC		1	68.6 ± 2.7	1.9 ± 0.1
DPPC	16:0	10	8.2 ± 0.5	2.5 ± 0.1
DPPC		5	15.1 ± 1.0	2.2 ± 0.1
DPPC		1	63.4 ± 5.1	2.0 ± 0.2

[1]E2 loading was calculated based on the molar ratio of the main lipid (% mol/mol)
[2] Loading capacity of E2 is based on total nanoparticulate weight
[3]Mixure was composed of 34% 16:0, 2% 16:1, 11% 18:0, 32% 18:1, 18% 18:2, and 3% 20:4

In terms of selecting an appropriate formulation for E2 delivery, it was clear that DOPC supported the highest encapsulation efficiency and loading capacity of all

lipids tested. The EE of DOPC liposomes was highest at an initial loading of 1% mol/mol, a value of 68.6 ± 2.7%. However, the E2 loading capacity of the liposomes also sheds light onto the formulation structure, and informs the ultimate selection. Although, EE is traditionally utilized to determine the effectiveness of a given nanoparticulate drug delivery vehicle, in the context of lipophilic drug loading into the phospholipid bilayer of liposomes, the loading capability may be more relevant to selecting a final formulation. In this light, results from Table 7.1 indicate that the highest loading capacity with the least amount of E2 loss can be achieved in the formulation composed of DOPC, with an initial E2 loading of 5% mol/mol. Therefore, to decrease the ultimate concentration of liposomes to be administered and maximize the dosing potential, further experimentation was conducted utilizing DOPC as the primary lipid in the formulation, with an initial E2 loading of 5% mol/mol.

Table 7.2 presents the physiochemical characteristics of neutral, anionic, and cationic liposomes. DDAB, a cationic lipid was utilized to confer a positive charge, whereas DMPG was used to confer a negative charge. Results showed that the mean particle size and polydispersity index were not affected by the inclusion of a charge moiety, which is expected for liposomes produced by extrusion. Furthermore, the polydispersity index was under 0.2 for all formulations tested, indicating a narrow size distribution. The zeta potential reflected the inclusion of the appropriate

charging moiety. Liposomes lacking a charging moiety showed poor stability in solution, as demonstrated a zeta potential of -0.46 ± 2.93 mV. The liposome charge, however, did not have a significant influence on the encapsulation efficiency ($p>0.05$). However, the loading capacity was significantly larger for cationic liposomes made with DDAB, compared to anionic and un-charged liposomes ($p<0.05$). This could be attributed to the interaction and improved accommodation of E2 upon the inclusion of DDAB within the lipid bilayer and the electrostatic interactions between negatively charged E2 and the positively charged bilayer [368].

Liposomes were examined under cryo-TEM. As seen in Figure 7.1, visual size estimates were consistent with results obtained from dynamic light scattering measurements. Micrographs also demonstrate that produced liposomes were spherical in shape, bound by a single bilayer membrane and consistent with the sizes presented in Table 7.2 and measured using DLS.

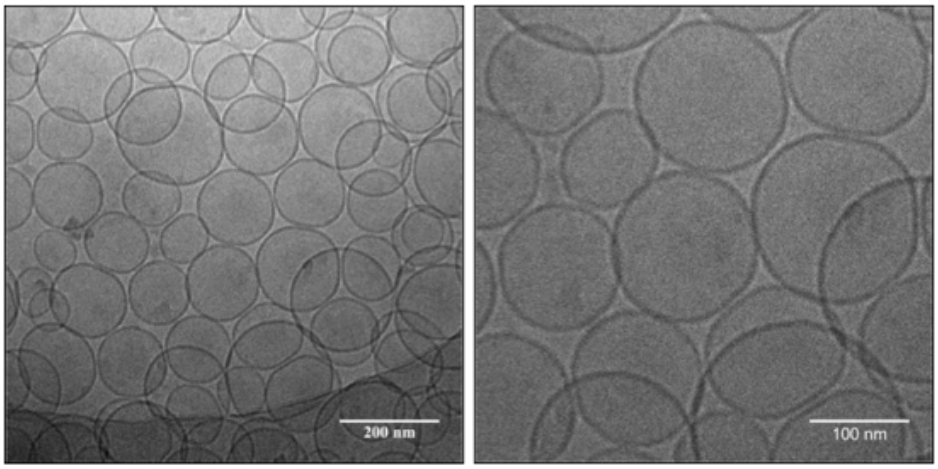

Figure 7.1 - Representative cryo-TEM micrographs of DOPC liposomes, showing unilammelar liposomes formed by thin film hydration and extrusion through 200 nm stacked membranes. Bar represents (a) 200 nm and (b) 100 nm.

Table 7.2 - Physiochemical characteristics of E2-loaded DOPC liposomes. Data are reported as mean ± S.D. (n=3).

Liposome Preparation	Mean particle size (nm)	Zeta-potential (mV)	Polydispersity index	Encapsulation efficiency (%)	Loading capacity (μg/mg)[1]	Mass Yield (%)
DOPC	217 ± 6.43	-0.46 ± 2.93	0.124 ± 0.038	41.7 ± 4.2	6.0 ± 0.6	65.3 ± 7.2
DOPC: DDAB	199 ± 6.22	26.72 ± 4.06	0.136 ± 0.006	51.2 ± 3.6	7.3 ± 0.5	81.3 ± 7.6
DOPC: DMPG	207 ± 2.05	-28.00 ± 4.61	0.113 ± 0.002	42.8 ± 2.9	5.3 ± 0.3	81.7 ± 5.8

[1]Loading capacity of E2 is based on total nanoparticulate weight

7.4.2 E2-Loaded Liposome Release Kinetics

The release kinetics of E2 from the liposomes were investigated using a dialysis membrane system. Figure 7.2 reveals the *in vitro* release kinetics from neutral, DMPG, and DDAB liposomes. An important aspect of release studies is maintaining appropriate sink conditions. It is for this reason that PBS (pH 7.4) in ethanol (60:40) was selected as the receptor phase. All liposome formulations showed a high initial drug release rate for the first 24 h, followed by a more sustained release over the following 24 h. This initial release may be due to E2 located at the outer edge of the phospholipid bilayers. Results indicated that the 50% retention time for E2 loaded liposomes was roughly 6 h for all formulations tested and little difference was observed in release with regards to the charged moieties

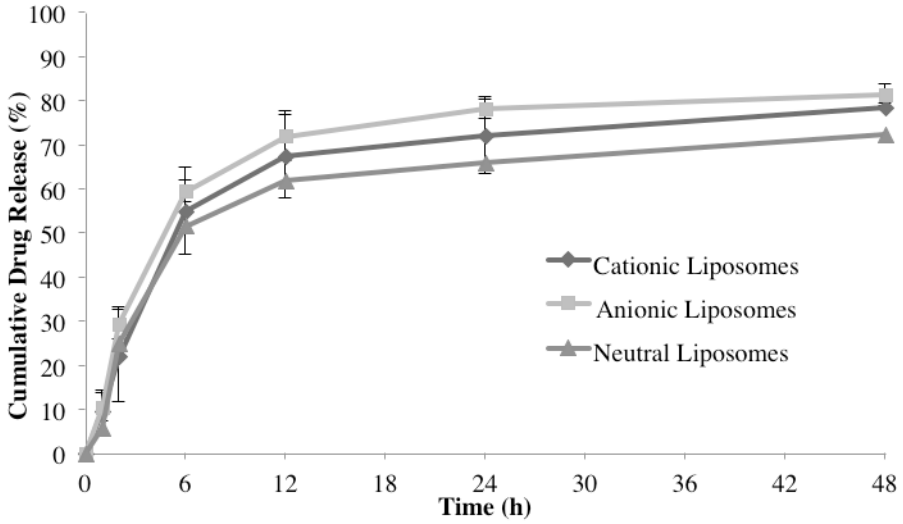

Figure 7.2 - Release rate of E2 from various liposome formulations. Results showed little contribution from the charge on drug release into solution. Each data point represents the mean and error bars represent the S.D. (n=3).

7.4.3 HCAE Cell Uptake with Liposomes

First, the MTT assay was utilized to determine the effects of liposome charge and concentration on the cellular viability of endothelial cells after 48 h. Results presented in Figure 7.3a show that the viability of HCAE cells was almost unchanged by contact with neutral liposomes, cationic liposomes made with DDAB, or anionic liposomes made with DMPG within the range of concentrations tested. These results confirmed the low cytotoxicity of the proposed liposomal delivery system. No statistically significant difference in cellular viability was observed between liposome type and concentration ($p>0.05$), except in an expanded concentration range shown in Figure 7.3b. A negative effect on cellular viability was observed at a high concentration of 100,000 nM ($p<0.05$).

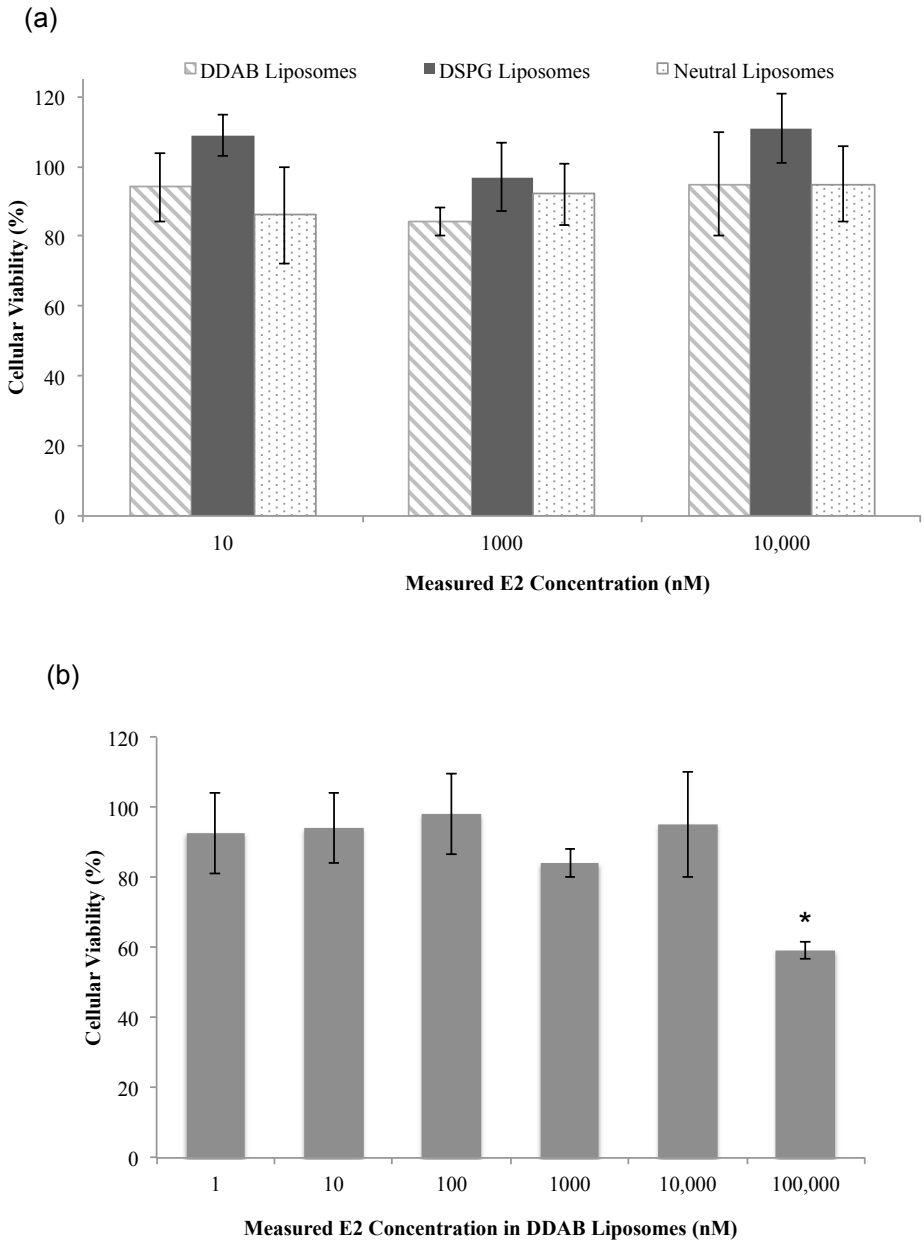

Figure 7.3 – (a) Effect of E2-loaded liposome formulations on the cytotoxicity of HCAE cells at various concentrations. (b) Expanded effects of DDAB E2-liposomes concentrations on cytotoxicity, no significant cytotoxicity effects under E2 concentrations of 100,000 nM. Data are expressed as mean ± S.D. (n=3). (*) Indicates $p < 0.05$.

To exert their therapeutic effects, liposomes must be appropriately be taken up by target cells. Intracellular delivery can occur by endocytosis, diffusion, phospholipid exchange, or fusion [149, 369]. Indeed, the degree of internalization is greatly dependent on the physical characteristics of the liposomes. In particular, the size, surface chemistry, and charge can alter liposome-cell interactions and adhesion properties. It was thusly important to assess the capability of cells to interact with E2-liposomes. Since E2 has been shown to affect endothelial cells [370], uptake was investigated using HCAE cells after 2 and 24 h using fluorescence spectroscopy. Results from Fig. 4a show that there was a significant increase in cellular uptake in liposomes formulated with DDAB, compared to those formed with DMPG or those lacking a charged component, at both time points studied. It was therefore established that liposomes carrying an overall positive charge improved cellular uptake, likely due to the electrostatic attraction with the negative charge of the cells. The effect of liposome concentration on the extent of cellular uptake was studied using low (10 μg/mL) and high (100 μg/mL) concentrations of DDAB liposomes. DDAB liposome uptake was shown to be statistically insignificant between the concentrations investigated after 2 h, which is a reflection of the endocytotic capacity of the cells. However, liposome uptake increased significantly after 24 h in cells incubated with the high concentration of liposomes, indicating a time-dependent endocytotic capacity.

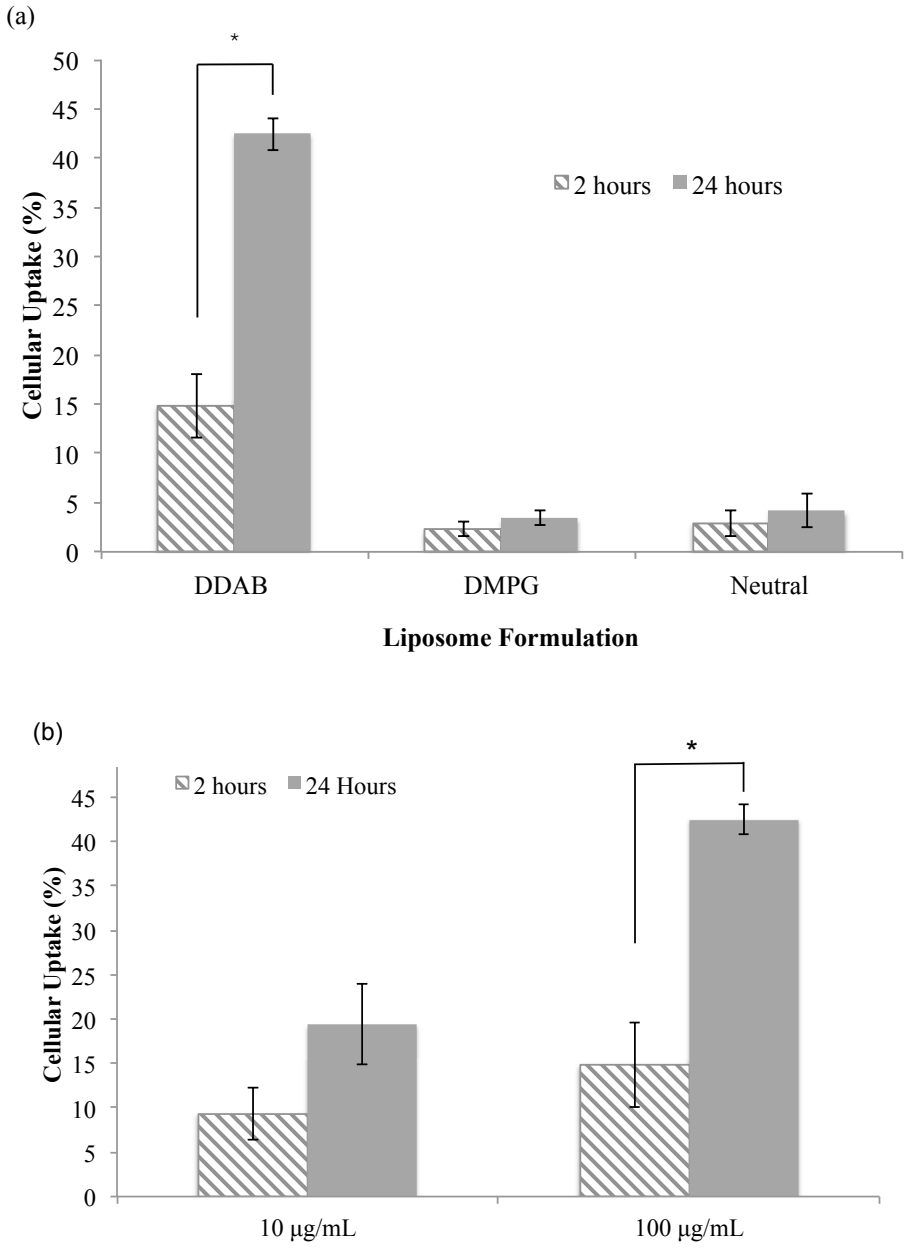

Figure 7.4 – (a) Effect of liposome formulation on HCAE cell uptake after 2 and 24 h as determined by fluorescence spectroscopy. DDAB liposomes showed significantly higher levels of uptake at both time points. (b) Effect of time and concentration on the cellular uptake of DDAB liposomes. Data are expressed as mean ± S.D. (n=3). (*) Indicates $p < 0.05$.

Confocal micrographs in Figure 7.5 show HCAE cells treated with fluorescent liposomes labeled with Texas Red® DHPE. A high degree of red fluorescence intensity can be observed around the periphery of the nucleus and demonstrates the cellular uptake capacities of HCAE cells with respect to the proposed liposomal delivery system, which could be exploited for therapeutic purposes in future studies.

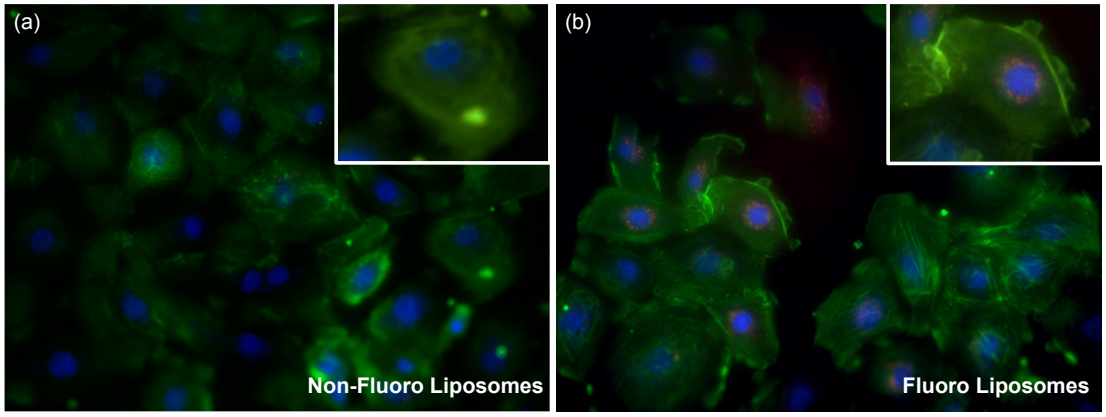

Figure 7.5 – Confocal microscopy images of HCAE cells treated with (a) non-fluorescent liposomes and (b) fluorescent liposomes; all cells were incubated with liposomes for 24 h at 37˚C. Red is the fluorescence of liposomes labeled with Texas Red ® 1,2-dihexadecanoyl-*sn*-glycero-3-phosphoethanolamine, green and blue represent the fluorescence of the cytoskeleton (phalloidin) and nucleus stain (DAPI), respectively. Liposomes appear to localize around the nucleus of the cells. Magnification of 20X.

The systemic or oral delivery of estradiol is the conventional approach for contraceptive or hormone therapy, however, given recent evidence documenting the effects of E2 on the cardiovascular system [371, 372] and endothelial cells in particular [13, 84, 373], there is a need to reduce unwanted side effects of

administration, while maximizing the potential for CVD treatment. Earlier studies examining the encapsulation of various isoforms of estradiol have been documented, including liposomal ethinylestradiol for contraception [374] and osteoporosis [375], estradiol benzoate for restenosis [363]. However, the bottom-up development of a liposome-based delivery with the aim of delivery to the endothelium had yet to be fully realized. Thus, in our experiments, we sought to develop and characterize a nanoliposome-based delivery vehicle by examining the effects of the main lipid, charge, and initial E2 loading on E2 encapsulation efficiency, loading, release kinetics, cytotoxicity, and cellular uptake in the context of human coronary artery endothelial cells, which had not previously been investigated. Based on the results presented, in particular high loading efficiency and cellular uptake, we believe that the final E2-loaded liposome formulation composed of DOPC and DDAB could be used in the future studies concerning the effects of E2 and endothelial inflammation.

7.5 Conclusions

In the present study, the incorporation of a hydrophobic molecule, E2, into the bilayer of liposomes was evaluated with the aim of developing a cellular delivery vehicle. Liposomes were selected as the ideal vehicle for delivery based on their versatility and ability to efficiently encapsulate hydrophobic molecules. Of the main lipids tested, DOPC demonstrated the greatest ability to accommodate E2 based on both the encapsulation efficiency (51.2 ± 3.6 %) and loading capacity (7.3 ± 0.5

μg/mg). The influence of charged components was also investigated based on the size, zeta potential, E2 encapsulation efficiency, and loading capacity. Based on multiple compositional parameters, it was determined that liposomes formulated with cationic DDAB would preferable compared to those formed with DMPG or without a charged component. Specifically, DDAB liposomes improved E2 loading capacity, and, through electrostatic interactions, demonstrated significantly improved cellular uptake properties in HCAE cells. It is hoped that this delivery vehicle will reduce side effects associated with excessive local concentrations of E2 and provide a means of delivery to the cardiovascular system for therapeutic applications. Furthermore, the proposed system offers the possibility of dual drug delivery and/or may incorporate imaging agents to produce therapeutic and diagnostics vehicles, which will be investigated in future studies.

7.6 Acknowledgments

The authors would like to thank Line Mongeon and Jeannie Mui for their assistance with TEM. As well as Dr. Jamal Daoud, Dr. Isabelle Cloutier, Sandra Gilligan, Julie Lebel, and Kim Tardif for their invaluable help and insights. Special thanks to Dr. Tohid Fatanat Didar and Samira Taherkhani who provided assistance with the confocal imaging and fluorescent liposome fabrication. The research was supported by the Natural Sciences and Engineering Research Council of Canada and K Bowey gratefully acknowledges NSERC for the PGS-2 scholarship.

Chapter 8: Nanolipsome-Delivered 17β-Estradiol Effectively Protects Endothelial Cells Against Inflammation: A Potential for Anti-Atherogenic Therapy

In order to meet the third objective of this thesis, which was to investigate the capacity of the E2 liposome-based delivery vehicle developed in Chapter 7 to affect inflammation, an investigation into application of such a system was undertaken. Briefly, the liposomal vector detailed in Chapter 7 consisting of DOPC, cholesterol, DDAB, and 5% initial E2 loading was tested for it's ability to attenuate an inflammatory response incited in human coronary artery endothelial (HCAE) cells. More specifically, liposomes were tested for their ability to attenuate the expression of VCAM-1 and the secretion of cytokines IL-8 and TNF-α after upregulation via C-reactive protein (CRP). Results demonstrated that liposomes were capable of conferring similar anti-inflammatory properties as water-soluble E2 in terms of attenuating VCAM-1 expression. E2-loaded liposomes were also shown to successfully modulate the secretion of inflammatory cytokines, IL-8 and TNF-α.

The results of this study are presented in following proceeding entitled "Nanolipsome-Delivered 17β-Estradiol Effectively Protects Endothelial Cells Against Inflammation: A Potential for Anti-Atherogenic Therapy", which will be presented at the *International Conference and Exhibition on Advanced and Nanomaterials* in August 2014.

Nanolipsome-Delivered 17β-Estradiol Effectively Protects Endothelial Cells Against Inflammation: A Potential for Anti-Atherogenic Therapy

Kristen Bowey[1], Jean-François Tanguay[2], Maryam Tabrizian[1,3,*]

[1]Department of Biomedical Engineering, McGill University, Montréal, Quebec, Canada

[2]Montréal Heart Institute, Department of Medicine, Université de Montréal, Montréal, Québec, Canada

[3]Faculty of Dentistry, McGill University, Montréal, Québec, Canada

*Corresponding author: maryam.tabrizian@mcgill.ca

Keywords: Nanoparticles, liposomes, drug delivery, cardiovascular disease

8.1 Abstract

The female sex hormone 17β-estradiol (E2) has been shown to decrease vascular inflammation by reducing the expression and section of inflammatory molecules. However, conventional pharmaceutical treatments of hydrophobic active agents, such as E2, cannot be administered locally due to toxicity effects, poor retention, and cellular uptake at sites of delivery. We report the application of a nano-sized liposomal E2 delivery vehicle (~200 nm in diameter) with the aforementioned properties and investigate its application as an anti-inflammatory agent *in vitro*. Human coronary artery endothelial cells were activated with the proinflammtatory agent C-reactive protein (CRP), and tested for effects on the expression of vascular cell adhesion molecule-1 (VCAM-1), the secretion of IL-8 and TNF-α. Immuoblotting and ELISA analysis showed that liposomes could successfully attenuate the inflammatory response after CRP activation and may ultimately be suited for the delivery of E2 for prevention of atherosclerotic plaque development.

8.2 Introduction

Atherosclerosis is a chronic inflammatory disease characterized by lipid plaque accumulation in arterial blood vessels, which lead to luminal reduction [46]. Over time, this condition can restrict vital blood flow causing chronic conditions, such as angina, as well as acute coronary events, such as myocardial infarction. Much of the work on the treatment and prevention of atherosclerosis has focused on

addressing hyperlipidemia and lipid plaque accumulation, however recent evidence has highlighted the prominent role of inflammation in the initiation and development of atherosclerosis [8, 10, 376]. Accordingly, the application of anti-inflammatory treatments at the early stages of plaque formation might help to mitigate the progression of the disease.

Epidemiological has shown that premenopausal woman experience significantly less incidents of adverse coronary events compared to men of the same age, and postmenopausal women [21]. Though a variety of factors may contribute to this finding, numerous studies have demonstrated convincing evidence for the role of estrogens [22]. Particularly, 17β-estradiol (E2) has been shown to affect a variety of cardiovascular processes, such as protect the heart against ischemia-reperfusion injury [14] and reduce restenosis after angioplasty [95]. Moreover, in the context of atherosclerosis, E2 has been shown to decrease the generation of reactive oxygen species [377], vascular inflammation [11-13], and, overall, attenuate the development of atherosclerotic disease.

Previously, we had developed a liposome delivery system for E2, which was optimized in terms of E2 loading capacity and encapsulation efficiency [136]. The liposomes, which are defined as artificial vesicles composed of an aqueous core surrounded by lipid bilayers, were composed of 1,2-dioleoyl-*sn*-glycero-3-phosphocholine (DOPC), dimethyldioctadecyl-ammonium (DDAB), and cholesterol,

with E2 loaded into the lipid component. They demonstrated no adverse toxicity effects and showed superior cellular uptake in human coronary artery endothelial (HCAE) cells. Accordingly, we hypothesized that the developed E2 delivery vehicles may confer anti-inflammatory properties to HCAE cells.

To study the inhibitory properties of liposomal E2, an inflammatory response was induced by the application of C-reactive protein (CRP). CRP is an inflammatory cytokine currently used in the clinic to evaluate levels of inflammation and, appropriately, as a risk marker for cardiovascular events [378]. While serum CRP concentrations are associated with high levels of inflammation, on a cellular level, it has also been shown to act as a proinflammatory agent [50, 251] and specifically to upregulate the expression of inflammatory cytokines ICAM-1 [50], VCAM-1 [379], as well as other inflammatory cytokines [380]. Previous work conducted by Cossette *et al.* (2013) demonstrated that CRP increased the expression of inflammatory cell adhesions molecules in HCAE cells and, furthermore, that pretreatment with E2 markedly decreased the expression of inflammatory biomarkers after the CRP challenge [13]. Accordingly, the current study aimed to investigate the effects of E2-liposome pre-treatment on CRP-induced inflammation by evaluating the level of expression of vascular cell adhesion molecule-1 (VCAM-1), and the secretion of interleukin-8 (IL-8) and tumor necrosis factor alpha (TNF-α) from HCAE cells,

which are known participants in cardiovascular inflammation. The experimental procedure is depicted schematically in Figure 8.1.

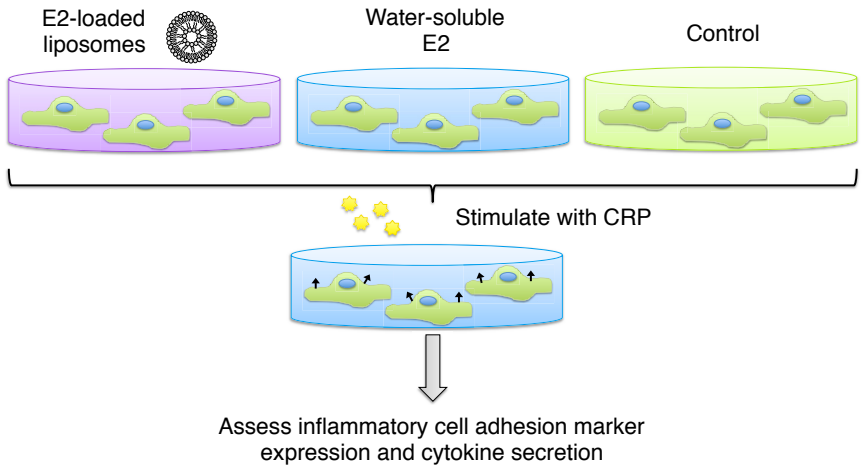

Figure 8.1 – Experimental approach to detect the effects of E2-loaded liposomes on the CRP-induced inflammatory response in HCAE cells.

8.3 Materials and Methods

8.3.1 Materials

Cholesterol, CRP, E2, water-soluble E2, methanol, and chloroform were purchased from Sigma Aldrich (St. Louis, USA). DOPC and DDAB were purchased from Avanti Polar Lipids (Alabaster, USA). Monoclonal mouse anti-VCAM-1 and anti-actin were obtained from Abcam (Cambridge, USA). Prior to contact with cells, CRP was dialyzed for 24 h using a Float-A-Lyzer® G2 device (Spectra/Por, molecular weight cut-off of 3.5-5 kDa, Spectrum Laboratories Inc. USA) to remove any preservatives, such as sodium azide.

8.3.2 Liposome Formulation

E2 multi-lamellar liposomes were prepared by the thin film hydration technique [381, 382]. Briefly, the liposomes components, DOPC, DDAB, cholesterol and E2, were weighed into a round-bottom flask and dissolved in a chloroform/methanol mixture (4:1 vol/vol). The organic solvent mixture was evaporated at 60°C under reduced pressure using a rotary evaporator (Buchi R-110 Rotavap, Switzerland). Once a thin dry film had formed on the sides of the flask, the lipid film was hydrated with 10 mL of PBS. Rehydration was carried out by rotating the flask in a water bath under normal pressure to ensure complete removal of the film. The liposome suspension was allowed to mature for 2 h at room temperature and extruded through 0.4 and 0.2 μm polycarbonate membranes to reduce their size. Unencapsulated E2 was removed by a Labscale™ tangential flow filtration system in conjunction with a Pelicon® XL polyethersulfone filter (100K) from Millipore (Billerica, USA).

8.3.3 Cell Culture

HCAE cells (Lonza, Switerland) were grown up in EGM-2MV BulletKit from Lonza, with 5% FBS and maintained in an incubator at 37°C, supplied with 5% CO_2. All serum used in these experiments was charcoal-treated FBS from Sigma Aldrich (St. Louis, USA) so as to avoid interactions from exogenous steroids present

in commercial FBS preparations. For experimentation purposes, cells were utilized at passages 4-6 and plated in 6-well plates at a density of $1.5x10^4$ cells/cm^2. Cells were allowed to reach 80-90% confluence and then starved with 0.1% FBS prior to treatment.

8.3.4 Assessment of E2 Loading Capacity and Treatment

The amount of E2 loaded into the liposomes was assessed by reverse-phase High Pressure Liquid Chromatography (HPLC) using a Flexar LC Perkin Elmer HPLC system equipped with a photodiode array detector (Waltham, USA), as previously described [136]. To assess the impact of E2-loaded liposomes on the upregulation of the inflammatory biomarker, VCAM-1, cells were treated with E2-loaded liposomes (10^{-9} M, as measured by HPLC) in 0.1% FBS starvation media. After 24 h, cells were washed 3X with PBS (pH = 7.4) and treated with CRP (25 μg/mL) for 24 h. Cells treated with water-soluble E2 (10^{-9} M) and devoid of treatment served as controls. Following the incubation, media was removed and stored at -80°C for ELISA assays. Cells were then rinsed 3X with PBS and lysed using ice-cold lysis buffer (1X Tris-buffered saline (TBS), 1% triton X-100, and Pierce™ protease and phosphatase inhibitor tablet containing aprotinin, bestatin, E-64, leupeptin, NaF, $NaVO_3$, TSPP, β-glycerophosphate, and EDTA [Fisher Scientific, Rockford, USA]). Cell lysates were centrifuged at 12,000 rpm for 5 min and supernatants were stored at -80°C for the Western blot assay.

8.3.5 Western Blot for VCAM-1 Expression

Proteins from each cell extract were separated by electrophoresis on a 4-20% SDS-PAGE gel (Bio-Rad, Hercules, USA) and transferred to a PVDF membrane at 100V for 2 h (Bio-Rad). After blocking for 1 h in 1X TBS with 1% casein, membranes were incubated overnight at 4°C with anti-actin (0.5 µg/mL) and anti-VCAM-1 (1/1000) antibodies. After washing 3X with 1X TBS-T (TBS with 1% Tween 20), the blots were incubated with Immun-Star™ goat anti-mouse horseradish peroxidase conjugate (1/20,000, Bio-Rad) for 1 h at room temperature. The membranes were then washed 6X with TBS-T and bound antibodies were detected using the Immun-Star™ WesternC™ chemiluminescent kit (Bio-Rad) and imaged using an Intas Science Imaging instrument (Göttingen, Germany).

8.3.6 ELISA Assay for IL-8 and TNF-α

Inflammatory cytokine secretion of IL-8 and TNF-α in cell culture supernatants was assessed after treatment with E2-loaded liposomes and activation by CRP. Supernatants were collected by centrifugation and cytokine excretion was measured with commercially available ELISA kits (Human IL-8 ELISA Kit II from BD OptEIA™; Human TNF alpha ELISA from Thermo Scientific) according to the manufacturer's instructions.

8.3.7 Statistical Analysis

All data are presented as mean ± S.D. Student's *t*-test test was used to assess the significance of differences between two groups. Probability values were considered significant at $p<0.05$.

8.4 Results and Discussion

8.4.1 E2-Loaded Liposomes Reduce CRP-Challenged VCAM-1 Upregulation

It has been established that incubation with CRP induces VCAM-1 gene upregulation [379] and expression [13] in vascular endothelial cells. After 24 h of treatment with CRP, HCAE cells showed a significant increase in VCAM-1 expression (Figure 8.2). To investigate the effects of E2-loaded liposomes on the expression of VCAM-1, HCAE cells were treated with E2-loaded liposomes and then incubated with CRP for 24 h, respectively. As shown in Figure 8.2, treatment with E2-loaded liposomes suppressed the expression of VCAM-1 in cells compared to untreated cells. No significant difference compared to cells pre-treated with water-soluble E2 were detected, indicating that E2-loaded liposomes can confer similar effects to E2 in terms of effects on VCAM-1 expression.

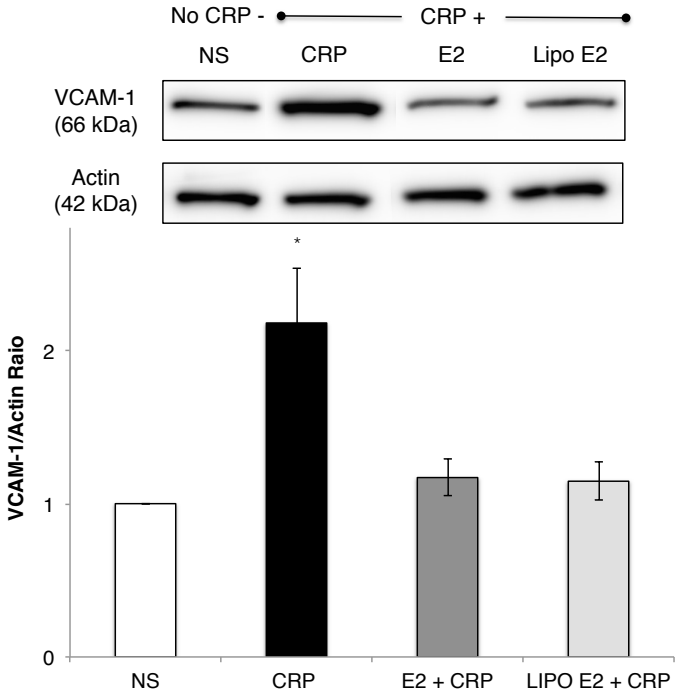

Figure 8.2 –VCAM-1 protein expression in HCAE cells after pretreatment with E2 or E2-loaded liposomes and CRP challenge determined by Western blot analysis. Controls show that the application of CRP significantly increased the expression of VCAM-1 compared to (*) non-stimulated cells (NS). E2-loaded liposomes and E2 attenuated the expression of VCAM-1 in CRP-treated cells.

8.4.2 E2-Loaded Liposomes Reduce CRP-Induced IL-8 Cytokine Secretion

IL-8 is an important mediator of cardiovascular inflammation and atherogenesis [383], accordingly, the effect of E2-loaded liposomes on the response of IL-8 in activated HCAE cells was investigated. As shown in Figure 8.3, similar to VCAM-1, CRP was shown to produce a more than two-fold increase in IL-8 production ($p<0.05$) compared to non-stimulated cells. E2-loaded liposomes

pretreatment inhibited the release of IL-8 by roughly 60%, compared to the excretion induced by CRP in untreated cells. This effect was comparable to IL-8 inhibition observed from soluble E2.

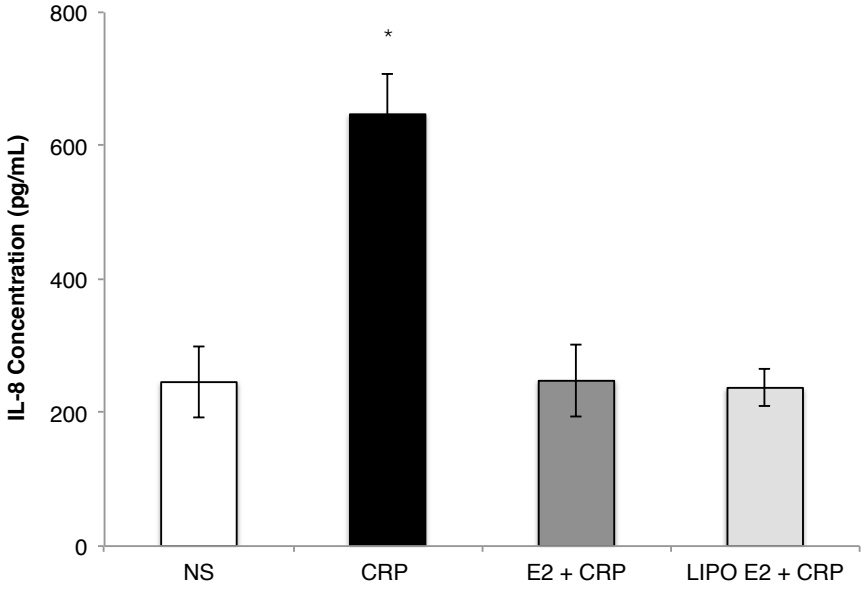

Figure 8.3 – IL-8 secretion from HCAE cells after pretreatment with E2 or E2-loaded liposomes and CRP challenge determined by ELISA. Controls show that the application of CRP significantly increased the secretion of IL-8 compared to (*) non-stimulated (NS) cells. Both E2-loaded liposomes and E2 attenuated the response from CRP-treated cells. (*) Indicates statistical significant difference ($p<0.05$) of E2-loaded liposomes and water soluble E2 compared to control samples.

8.4.3 E2-Loaded Liposomes Reduces CRP-Challenged TNF-α Secretion

To understand the capacity of E2-loaded liposomes to reduce or block the secretion of TNF-α, ELISA was used to evaluate the concentrations present in cell supernatants subjected to various treatments. As expected, Figure 8.4 shows that

CRP significantly induced the secretion of TNF-α compared to non-stimulated cells, since TNF-α is a potent mediator of inflammation [384] and contributes to cardiovascular disease [385]. Pretreatment with E2 liposomes significantly attenuated the release of TNF-α compared to untreated cells (Figure 8.4), by roughly 68% ($p<0.05$). Moreover, E2-loaded liposomes demonstrated slightly increased inhibition compared to E2 alone (68% versus 55%), indicating that the E2-loaded liposomes may confer alternate benefits in terms of reducing certain aspects of the inflammatory response induced by CRP.

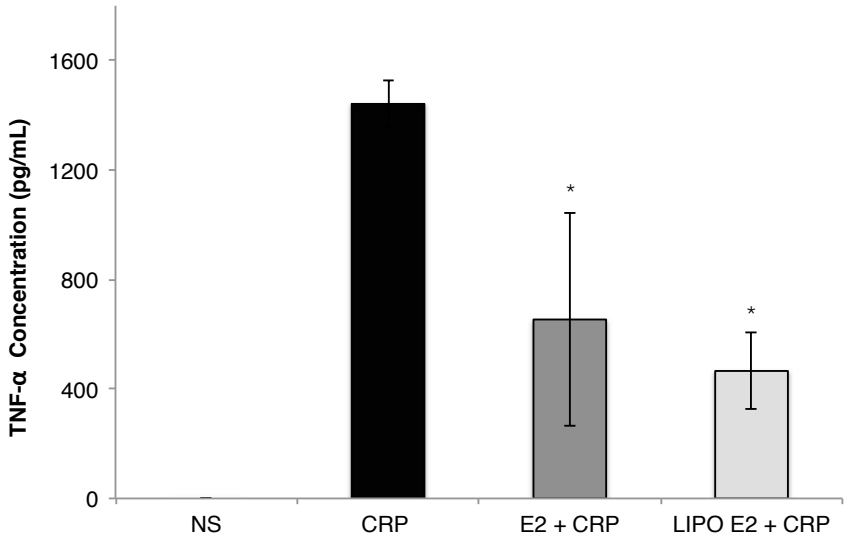

Figure 8.4 – TNF-α secretion from HCAE cells after pretreatment with E2 or E2-loaded liposomes and CRP challenge. Controls show that the application of CRP significantly increased the secretion of TNF-α compared to non-stimulated (NS) cells. Both E2-loaded liposomes and E2 significantly attenuated the release of TNF-α from CRP-treated cells (*; $p<0.05$).

8.4.4 Discussion

The initiation of atherosclerotic plaque is closely tied to local inflammation of the endothelium. An ideal approach to mitigating lipid plaque accumulation in the vasculature would be to address the inflammatory components of the disease that catalyze atherogenesis. Specifically, reducing the expression of cellular adhesion molecules on endothelial cells has been shown to significantly decrease monocyte adhesion and lipid accumulation [386]. As well, the inhibition of inflammatory cytokine secretion has been shown to reduce local inflammation and may also impede atherogenesis [387]. Therefore, attenuating the expression of cellular adhesion molecules and chemokine secretion has proposed as a viable means of therapy to decrease atherosclerotic plaque development [388, 389].

CRP is pentameric protein, found in the blood plasma and synthesized in the liver. It is widely used in the clinic as an inflammatory biomarker to assess risk of vascular events [390], however it has also been shown to play a role in atheroprogression [391] and incite a local inflammation response [50, 392]. Previous studies have shown that estrogen directly affects local inflammatory responses that contribute to the progression of atherosclerosis [11, 31], and, in particular, block the action of the inflammatory response induced by CRP [13]. However, no research has studied the application of a nanoparticulate vehicle specifically designed to deliver E2 to endothelial cells on inflammation.

Since the therapeutic dose of E2 should be strictly regulated to avoid undesirable side effects [393, 394], and conventional pharmaceutical treatments often require high dosages due to non-specific distributions and poor retention at sites of delivery, encapsulation into liposomes has been proposed as a means to address these concerns. Therefore, the design, development, and study of the therapeutic delivery of E2 by nanoparticulate delivery vehicles is a crucial step towards clinical application as a means to reduce cardiovascular inflammation.

This study demonstrated for the first time that E2-loaded liposomes could confer anti-inflammatory properties to endothelial cells in terms of VCAM-1 expression, IL-8 and TNF-α secretion. The down-regulation of VCAM-1 conferred by E2-loaded liposomes could have a substantial impact on the progression of atherosclerosis, as endothelial cells that express inflammatory adhesion molecules recruit monocytes to the area. Once monocytes are recruited to areas of activation, they can differentiate into macrophages and endocytose oxidized low-density lipoprotein to become fat-laden foam cells that serve as the basis for atherosclerotic plaque [57]. Similarly E2-loaded liposomes effects on IL-8, which is a potent chemotropic factor that recruits monocytes to areas of dysfunction, can reduce the inflammatory response [395]. While decreasing the CRP-induced response of TNF-α, a pleotropic chemokine that is a key player in the immune response, may also serve to attenuate the development of atherosclerotic lesions [384, 385]. Further studies

could be aimed at decorating the E2-loaded liposomes with different forms of phosphatidylcholine, a high affinity ligand for CD36. CD36 (macrophage scavenger receptor) is a potential target receptor that is highly expressed on lipid-laden macrophages in human atherosclerotic aortas [396, 397]. By intercalating CD36 ligands throughout E2-loaded liposomes, these nanoparticles could potentially provide site-directed therapy and reduction of atherosclerotic plaque progression.

8.5 Conclusions

This study showed that loading E2 into a liposome delivery vehicle was capable of reducing the expression of VCAM-1, as well as the response of IL-8 and TNF-α to CRP-activation *in vitro*. Liposomes demonstrated effects similar to those of free E2 in terms of downregulating VCAM-1 expression, TNF-α and IL-8 secretion. Although further studies should be conducted to investigate the delivery of E2-loaded liposomes to activated endothelial cells *in vivo*, overall results presented indicate that E2-liposomes may be a viable alternative to preventing the inflammatory response and thereby reducing the progression of atherosclerosis.

8.6 Acknowledgements

We gratefully acknowledge Dr. Hana Antonicka, Mr. Neil Webb, Mr. Timothy John, and Ms. Kim Tardif for technical assistance and very helpful discussion with the Western blot component of this study. This work was supported

by the National Science and Research Council of Canada Discovery grant and Vanier scholarship.

Chapter 9: Microwave-Assisted Surface-Enhanced Raman Scatting Nanoprobes for Vascular Disease Biomarker Detection and Mapping

One of the main issues in diagnosing and treating early onset atherosclerosis is accurately detecting the distribution upregulation of inflammatory biomarkers in the vasculature. Therefore, as a secondary objective of this work, our aim was to develop a surface-enhanced Raman scattering (SERS) nanoprobe with the capability to detect and localize VCAM-1 expression in an endothelial cell model. As such, we engineered a novel SERS nanoprobe composed of a 50 nm gold core, 4-mercaptobenzoic acid (4-MBA) Raman reporter, poly(allylamine hydrochloride) (PAH) protective coating, and anti-VCAM-1 targeting monoclonal antibody. We demonstrate, for the first time, the application of microwave technology to produce functionally stable SERS nanoprobes, capable of straightforward bioconjugation. Furthermore, we demonstrated the successful application of this probe to both detect and localize the upregulation of VCAM-1 in HCAE cells.

The results of this study are presented in following manuscript entitled "Microwave-Assisted Synthesis of Surface-Enhanced Raman Scattering Nanoprobes for Cellular Sensing", which is under consideration for publication by the journal *Surface and Colloids B: Biointerfaces* as of May 2014. The table of content graphic, which accompanied this article is presented in Figure 9.1

.

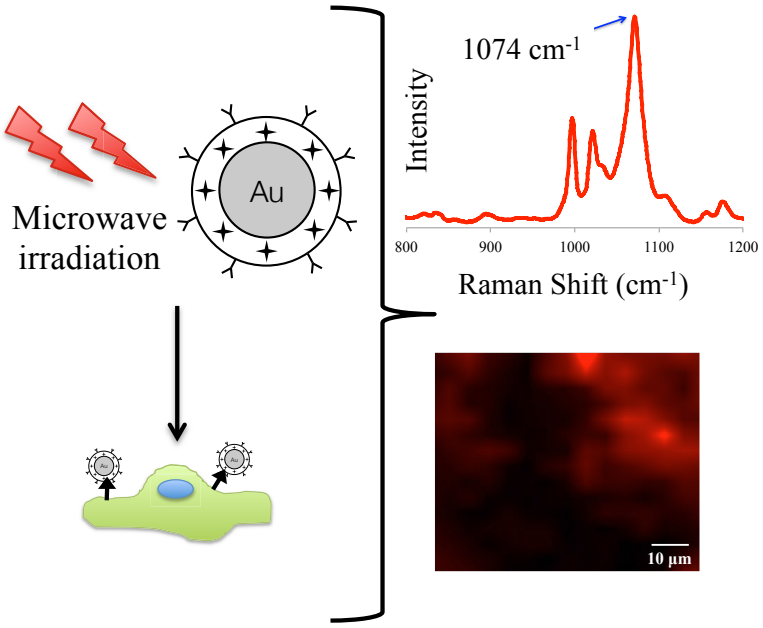

Figure 9.1 – Graphical depiction of the study conducted in Chapter 9. Surface-enhanced Raman scattering nanoprobes were constructed via microwave irradiation to detect and localize cardiovascular biomarkers *in vitro*.

Microwave-Assisted Synthesis of Surface-Enhanced Raman Scattering Nanoprobes for Cellular Sensing

Kristen Bowey[1], Jean-François Tanguay[2],

Marinella G. Sandros[3,*], Maryam Tabrizian[1,4,*]

[1]Department of Biomedical Engineering, McGill University, Montréal, Quebec, Canada

[2]Montréal Heart Institute, Department of Medicine, Université de Montréal, Montréal, Québec, Canada

[3]Department of Nanoscience, Joint School of Nanoscience and Nanoengineering University of North Carolina at Greensboro, Greensboro, NC, USA, 27401

[4]Faculty of Dentistry, McGill University, Montréal, Québec, Canada

*Corresponding author: m_sandro@uncg.edu, maryam.tabrizian@mcgill.ca

Keywords: Surface-enhanced Raman scattering, plasmonic nanoparticles, biomarker detection, cardiovascular disease, human coronary artery endothelial cells

9.1 Abstract

The fabrication of 4-mercaptobenzoic acid (4-MBA) antibody-functionalized gold nanoparticles via microwave technology for surface-enhanced Raman scattering (SERS)-based cellular nanosensing is reported. Nanoprobes were characterized by UV-vis absorbance, Raman scattering properties, and observed by TEM imaging. Results showed that microwave irradiation rapidly yielded nanoprobes with significant Raman scattering intensity and suitable stability to support antibody conjugation in under 10 min. Functionalized nanoprobes demonstrated the ability to map the expression of vascular adhesion molecule-1 (VCAM-1) in human coronary artery endothelial (HCAE) cells, indicating that microwave fabrication presents a viable and rapid approach to SERS nanoprobe construction. The successful application of SERS nanoprobes to localize biomarker expression *in vitro* may ultimately be used for early diagnostic and preventative functions in medicine.

9.2 Introduction

Surface-enhanced Raman scattering (SERS) detection using functionalized tags is emerging as a valuable analytical tool in the field of cellular biosensing owing to enhanced signal intensities, up to 10^{13}-10^{14} fold [398]. This dramatic signal enhancement is dominated by localized surface plasmon resonance (LSPR) [276, 277]. SERS has been applied to label cells [399], detect various analytes, including proteins [400] and biomarkers [401], as well as monitor subtle cellular fluctuations,

such as the effect of pH [402] and distinguishing between cell type [403, 404]. When combined with confocal microscopy, SERS-based detection yields rich spectral characterization data and spatial resolution of biomolecules or targets of interest down to the single cell level [405].

Advantages of SERS compared to conventional detection and optical imaging techniques, such as fluorescence or enzyme-linked immunosorbant assays, include lack of photobleaching, narrow spectral bandwidths, the capability to simultaneously provide structural information and spatial resolution, as well as perform multiplex analysis [318]. SERS signal enhancement occurs when molecules are adsorbed or in close proximity to surface-roughened noble metallic nanostructures. For indirect sensing, this phenomenon can be exploited by fabricating SERS nanoprobes on the order of 20-300 nm that support LSPR. Typically, these probes are composed of gold, silver, copper or a combination thereof with common modifications such as: studding with Raman reporters and attaching antibodies or aptamers to enhance target selectivity [287]. For target biorecognition, the chemical and physical stability of SERS probes is heavily affected by the percent surface coverage of reporter molecules [406] and coating with a protective shell (e.g. polymer) [41]. Typical Raman reporters include nitrogen- and sulfur-containing cationic dyes, or thiol small molecules. For biological applications, thiol modified-probes are best for chemisorption, since they are active in the NIR region and produce significant

scattering signals due to the formation of self-assembled monolayers (SAMs) on the surface of nanosubstrates [287]. However, inherent instabilities and aggregation associated with the formation of SAMs can require rigorous optimization and deter successful application *in vitro* [303]. Herein, these challenges have been addressed by investigating the feasibility of microwave technology as a means to facilitate chemisorption of the thiol small molecule to metallic nanostructures. Microwave heating can serve to increase molecular rotations and speed up transfer between molecules resulting in a significant reduction in reaction time for diverse applications [407]. Recently, Grell *et al*. (2013) demonstrated that the formation of SAMs on thin gold films using selective microwave heating was comparable to the formation of SAMs at room temperature, albeit at a significantly reduced time frame [408]. Therefore, we hypothesized that microwave technology could be used to rapidly fabricate SERS nanoprobes suitable for biomolecule functionalization, with applications as biological nanosensors. Although other groups have employed microwave technology to fabricate SERS substrates [409, 410], this work establishes for the first time, application towards Raman reporter SAM construction and demonstrated application for biomarker detection.

Recent evidence has highlighted the role of the immune system in the initiation of atherosclerosis [8, 30], a cardiovascular disease (CVD) characterized by a build-up of plaque in arteries. Consequently, various inflammatory adhesion

molecules and cytokines have been investigated as a means to detect and localize plaque during early stages of evolution [155, 224, 411]. Of particular interest is vascular cell adhesion molecule-1 (VCAM-1), which is upregulated upon activation of endothelial cells [412]. Accordingly, a robust technique to detect and localize VCAM-1 on endothelial cells could provide a practical means for early diagnosis and treatment of atherosclerosis.

In the present work, the preparation SERS nanoprobes consisting of 50 nm citrate-capped gold nanoparticles (Au-NPs) coated with the Raman reporter, 4-mercaptobenzoic acid (4-MBA), via microwave irradiation is described. For biorecognition and mapping of VCAM-1 in human coronary artery endothelial (HCAE) cells, probes were functionalized with anti-VCAM-1, as depicted schematically in Figure 9.2A. To provide a surface for bioconjugation, a protective layer of the cationic polymer, poly(allylamine hydrochloride) (PAH), was coated on the surface of the nanoprobes. Resultant amine modified nanoprobes were activated with glutaraldehyde to bind anti-VCAM-1. The optical absorbance, SERS activity, and structural properties were examined to characterize the nanoprobes. Control data from nanoprobes prepared via a conventional SAM formation technique is included to validate the microwave radiation technique. Finally, engineered SERS nanoprobes were tested for their ability to detect and map the VCAM-1 expression in HCAE cells using confocal Raman spectroscopy, represented in Figure 9.2B.

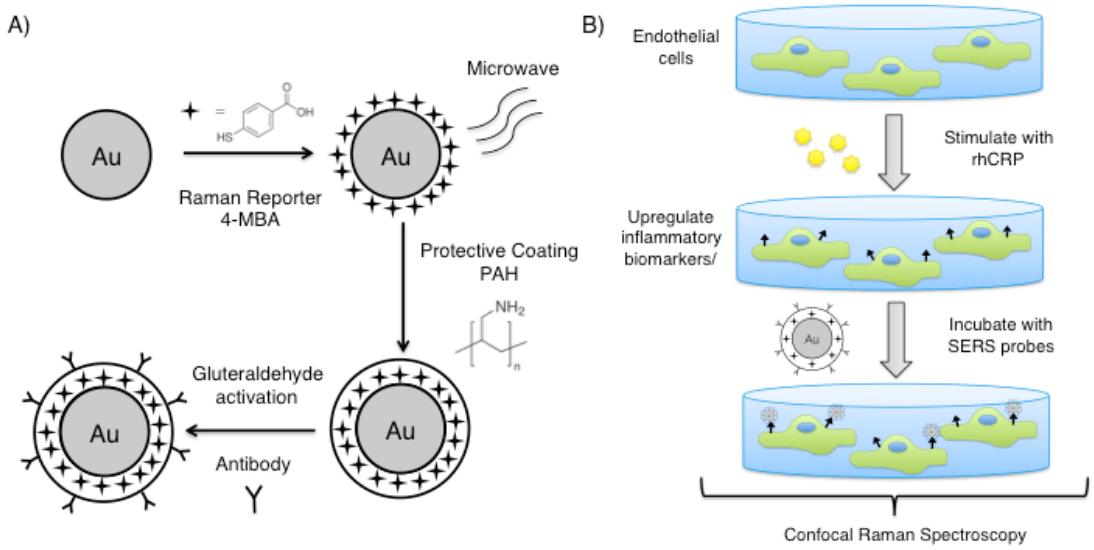

Figure 9.2 – (A) Fabrication of antibody-conjugated SERS nanoprobes via microwave irradiation. (B) Experimental approach to detect inflammatory biomarkers in HCAE cells using SERS nanoprobe technology.

9.3 Materials and Methods

9.3.1 Materials

Citrate-stabilized gold nanoparticles (Au-NPs, 3.51×10^{10} particles/mL), 4-mercaptobenzoic acid (4-MBA), 25% gluteraldehyde solution, and poly(allylamine hydrochloride) (PAH, MW 15 kDa) were purchased from Sigma Aldrich (St. Louis, USA). Recombinant human C-reactive protein (CRP), anti-VCAM-1 and mouse IgG-1 antibodies were purchased from Fisher Scientific (Rockford, USA). Ultra pure water (UPW) from a Millipore filtration system was used for all experiments. All other chemicals were analytical grade.

9.3.2 Preparation of Antibody-Conjugated SERS Nanoprobes

Au-NPs at room temperature were mixed with 50 mM of 4-MBA under vigorous stirring and reacted in an open vessel under microwave irradiation with a power of 50 W (2.45 GHz) and temperature of 50°C for 10 min (Discover, CEM Corporation). Excess 4-MBA was removed by washing for 3 rounds of centrifugation at 3000 rpm for 20 min. Next, the SERS-active probes were added drop-wise to a 1 mg/mL solution of PAH and reacted for 3 h. Excess PAH was removed by repeated rounds of centrifugation (3000 rpm, 15 min). To functionalize antibodies onto the surface of the probe, the particles were activated using the glutaraldehyde spacer method. After washing, SERS nanoprobes were rehydrated with a 5% glutaraldehyde solution in borate buffer (pH 9.2) and incubated under gentle rotation for 1 h. Afterwards, anti-VCAM-1 monoclonal antibodies were added to the activated SERS nanoprobe suspension and reacted for 2 h at room temperature. For negative controls, the same procedure was used to prepare SERS NPs conjugated to non-specific murine IgG-1 antibodies. Conventional 4-MBA adsorption was carried out by dropping a solution of 4-MBA into a suspension of Au-NPs, under vigorous stirring. The reaction was carried out overnight at room temperature, since shorter time periods were not sufficient to produce significant Raman scattering signals. Thereafter, particles were washed, as described above for the microwave technique. Ultrapure water (UPW) from a Millipore filtration system was used for all reactions

and washing steps, expect for the glutaraldehyde activation, which was carried out in borate buffer (pH 9.2).

9.3.3 SERS Nanoprobe Characterization

Ultraviolet-visible (UV-vis) absorption spectra of aqueous nanoparticle suspensions were measured by a Cary Eclipse Fluorescence spectrophotometer (Varian, Palo Alto, USA) with quartz cuvettes of 1 cm path length. Visualization of the shape and surface structure of nanoprobes was carried out by transmission electron microscopy (TEM). Briefly, 10 μL of nanoparticle suspension was dropped onto a carbon-coated copper grid. The sample was then air-dried overnight. Imaging was performed with a Carl Zeiss Libra 120 Plus TEM Microscope operating at an accelerating voltage of 120 kV. Mean particle size and size distribution was determined by Nanosight measurents, which utilizes nanoparticle tracking analysis technology (NanoSight, North Carolina, USA). The zeta potential (ζ-potential) of colloidal solutions was measured using a ZEN3600 Zetasizer Nano-ZX (Malvern Instruments, Worcestershire, United Kingdom).

9.3.4 Cell Culture and Labeling with SERS Nanoprobes

HCAE cells used in cell culture experiments were grown in tissue culture flasks, maintained in 5% CO_2 at 37°C. The culture medium was prepared using an EGM-2 BulletKit containing Endothelial Basal Medium-2, 10% FBS, and EGM-2

SingleQuots comprised of appropriate growth factors, cytokines and supplements to support cell growth (Lonza, Basel, Switzerland). Cells to be used for experimentation were released with 0.25% trypsin/0.1% EDTA (Gibco, Invitrogen) and seeded at a concentration of $1x10^4$ cells/cm^2 onto glass coverslips, which were placed in culture dishes. Cells were allowed to reach ~ 80% confluence prior to treatment.

9.3.5 Analysis of VCAM-1 Expression by SERS

Prior to experimentation, sodium azide was removed from CRP preparations by dialysis using a Float-A-Lyzer® G2 device (Spectra/Por, molecular weight cutoff of 3.5-5 kDa, Spectrum Laboratories Inc. USA). As a secondary purification step, contaminating lipopolysacharrides were removed using a Detoxigel column according to the manufacturer's instructions (Fisher Scientific). To upregulate the expression of the inflammatory biomarker, VCAM-1, by SERS, HCAE cells were treated with 25 μg/mL CRP. After 24 h of incubation, media was removed and cells were fixed with 3.7% paraformaldehyde. After washing, cells were blocked using 1% BSA for 20 min, then incubated with freshly prepared SERS nanoprobes (0.003 pM) for 4 h at room temperature. Finally, cells were washed and examined under the Raman microscope. The following controls were used: non-specific IgG-1 SERS probes to assess non-specific binding and cells incubated without SERS tags to assess background cell scattering.

9.3.6 SERS Microspectroscopy

An XploRA Raman confocal microscope system (JY Horiba, Edison, NJ) was used for all surface enhanced Raman scattering measurements. Spectra were collected on an inverted microscope with an ULWD 50X (0.55 NA) objective to focus the 785 nm laser with a power of 3mW onto the sample. Rayleigh scattering was removed using a holographic notch filter. Spatial resolution was obtained using 100- and 200 μm confocal pinholes. A Peltier-cooled CCD camera was used as detector. Peak frequencies were calibrated with silicon at 520 cm^{-1} prior to each use. Data was analyzed using LabSpec NGS. The integration time was 10 s for all SERS measurements.

9.4 Results and Discussion

9.4.1 SERS Nanoprobe Synthesis

Microwave technology is of interest to the field of synthetic and colloidal chemistry since dielectric heating can significantly decrease reaction time and improve system reproducibility [413]. In fact, reactions typically requiring several hours can be reduced to a few minutes with the application of microwave heating [414]. Accordingly, since microwave technology increases molecular rotation and speeds up material transfer, we therefore sought to investigate whether microwave irradiation could be used in the synthesis of stable SERS nanoprobes intended for

biosensing applications.

Studies on the optical properties of the nanoprobes demonstrated that the plasmon resonance absorption of 50 nm citrate-capped gold nanoparticles (Figure 9.3A, curve a) shifted slightly from 535 to 536 nm after formation of 4-MBA SAMs by microwave irradiation (Figure 9.3A, curve b). This small shift likely corresponds to changes in the dielectric medium surrounding the gold nanoparticle surface. Analysis of the SERS spectra of 4-MBA coated nanoparticles (Figure 9.3B, curve b) shows that the dominant Raman band of 4-MBA, at around 1074 cm^{-1}, is also present after only 10 min of microwave irradiation compared to uncoated citrate-capped gold nanoparticles, which do not show any SERS activity (Figure 9.3B, curve a) [325]. Typically, the reaction between gold nanoparticles and 4-MBA can take anywhere from 3 to 24 h [42, 325, 415], however a microwave irradiation time of 10 min was shown to be sufficient to yield probes with suitable Raman scattering intensities for detection. Control probes fabricated conventionally by overnight incubation showed no significant changes in optical absorbance (Figure 9.3A, curve c), or in Raman scattering data (Figure 9.3B, curve c). Furthermore, no morphological changes were observed by transmission electron microscopy (TEM) between nanoprobes fabricated by microwave (Figure 9.4A) and conventional adsorption (Figure 9.4B), demonstrating that the probes do not undergo any damaging effects after microwave irradiation.

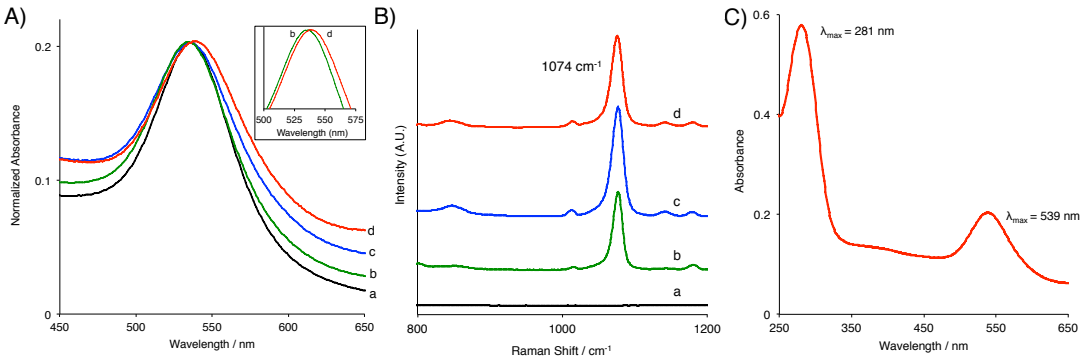

Figure 9.3 - (A) Visible absorbance of (a) citrate-capped Au-NPs, Au-NPs encoded with 4-MBA by (b) microwave and (c) conventional techniques, (d) anti-VCAM-1 studded SERS probes. (B) SERS spectra of (a) citrate-capped Au-NPs, nanoparticles coated with 4-MBA by (b) microwave and (c) conventional methods, (d) anti-VCAM-1 conjugated nanoprobes. (C) Expanded visible absorbance spectrum of anti-VCAM-1-conjugated SERS nanoprobes (λ_{max}= 281 nm, 539 nm).

To test the biomarker targeting properties of the SERS nanoparticles, probes were conjugated with anti-VCAM-1, since VCAM-1 expression is a marker for the early onset of atherosclerotic plaque formation [416]. Following PAH coating and antibody functionalization by glutaraldehyde activation, nanotags prepared by microwave radiation exhibited a further redshift of ~3 nm to 539 nm in optical absorbance (Figure 9.3A, curve d). This is likely due to the presence of the antibody on the nanoprobe surface, which causes an increase in the local refractive index of the medium [417]. The extinction spectrum of anti-VCAM-1 biofunctionalized SERS labels also showed an absorption peak at 281 nm, representing the presence of the antibody after activation and conjugation (Figure 9.4C). The characteristic peak

of 4-MBA at 1074 cm^{-1} was likewise maintained after biofunctionaliztion (Figure 9.3B, curve d), while TEM imaging of the final probes demonstrated the presence of a PAH/anti-VCAM-1 shell (Figure 9.4C). The mean particle size and ζ-potential of the particles recorded after the adsorption of 4-MBA via microwave irradiation and bioconjugation of the SERS nanoprobes are presented in Table 9.1. Results showed an increase in mean diameter of the particles after each step of the synthesis. The ζ-potential of the particles was recorded to be >10-20 mV, the absolute value of which indicates adequate particle disparity and stability of the system [311]. Taken together, these results demonstrate the successful coupling of antibody to SERS active gold nanoparticles synthesized via microwave radiation, with reproducible SERS spectra and no loss of the characteristic 4-MBA Raman peak.

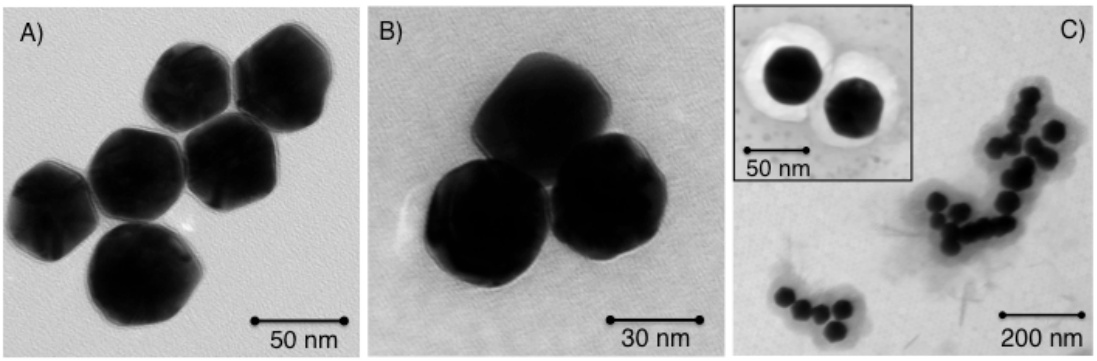

Figure 9.4 - TEM of 4-MBA coated nanoprobes prepared by (A) microwave irradiation, (B) conventional adsorption, (C) anti-VCAM-1-conjugated SERS nanoprobes prepared by microwave.

Table 9.1 - Results of particle size and ζ-potential analysis of SERS nanoprobes fabricated by microwave irradiation. Data represent average ± standard deviation (n=3).

Sample	Size (nm)	ζ-Potential (mV)	pH
Citrate-capped Au NPs	47 ± 33	-34 ± 2	7.8
4-MBA Au NPs	64 ± 43	-42 ± 6	7.8
Anti-VCAM-1/ PAH/4-MBA Au NPs	119 ± 36	-39 ± 6	9.2

9.4.2 Detection and Localization of VCAM-1 Expression in Human Coronary Artery Endothelial Cells

To demonstrate the functionality of developed SERS tags, antibody-functionalized SERS biosensors were employed to carry out detection of VCAM-1 in HCAE cells after CRP challenge. Recently, the authors have shown that CRP increases the inflammatory response in HCAE cells and specifically upregulates the expression of VCAM-1 [13]. Accordingly, cells were treated with CRP for 24 h to upregulate VCAM-1 expression, then fixed, blocked with 1% BSA, and incubated with anti-VCAM-1 SERS nanoprobes, as depicted schematically in Figure 9.2B. SERS spectra from HCAE cells incubated with anti-VCAM-1 bioconjugated probes are shown in Figure 9.5A. Spectra from three different intracellular locations,

represented in the corresponding light micrograph (Figure 9.5B), show the characteristic 4-MBA SERS peak at 1074 cm^{-1} indicating cellular binding of the nanoprobes after incubation and washing. Raman spectra were also measured on cells incubated with IgG-1-conjugated SERS nanoprobes as a non-specific control, as well as cells devoid of nanoprobes to assess background scattering. Relative to the anti-VCAM-1 bioconjugated probes, no signal was observed at 1074 cm^{-1} for cells incubated with IgG-1-conjugated SERS probes (Figure 9.7A, supplementary information), nor for cells lacking nanoprobes (Figure 9.8A, supplementary information), which were similarly collected from distinctive points on the cell (Figure 9.7B and 9.8B, supplementary information).

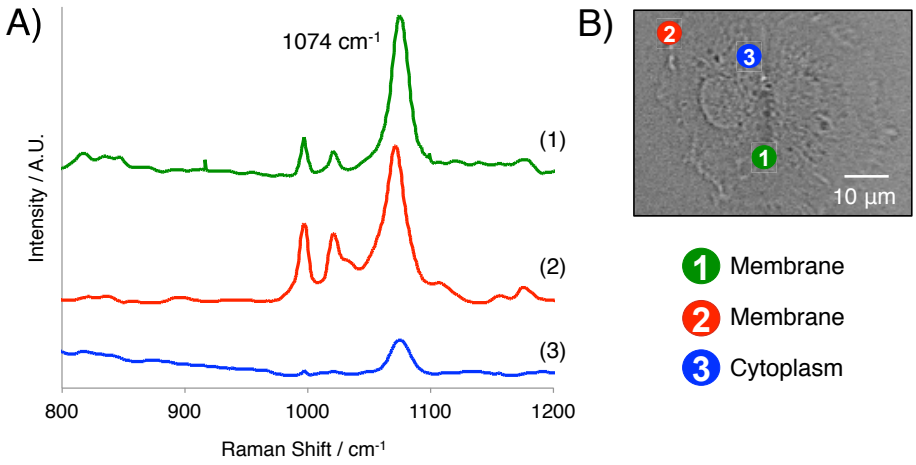

Figure 9.5 - (A) Representative SERS spectra of intracellular regions of HCAE cells incubated with anti-VCAM-1 SERS nanoprobes. (B) Light micrograph of HCAE cells incubated with anti-VCAM-1 SERS nanoprobes.

SERS maps at 1074 cm^{-1}, which is the most intense peak of 4-MBA, were then measured to assess the expression and distribution of VCAM-1. Figure 9.6A shows a SERS map of anti-VCAM-1 nanoprobes on HCAE cells. In tandem with the light micrograph and overlay (Figure 9.6B and C), the outer membrane of the cells appeared to be labeled with a dense population of nanotags as compared to probes functionalized with IgG-1 (Figure 9.9, supplementary information) and control cells devoid of nanoprobes (Figure 9.10, supplementary information), which showed limited non-specific adsorption and low levels of background scattering. These observations suggest that microwave-assisted SERS nanoprobes can successfully be applied to localize and detect VCAM-1 expression *in vitro*.

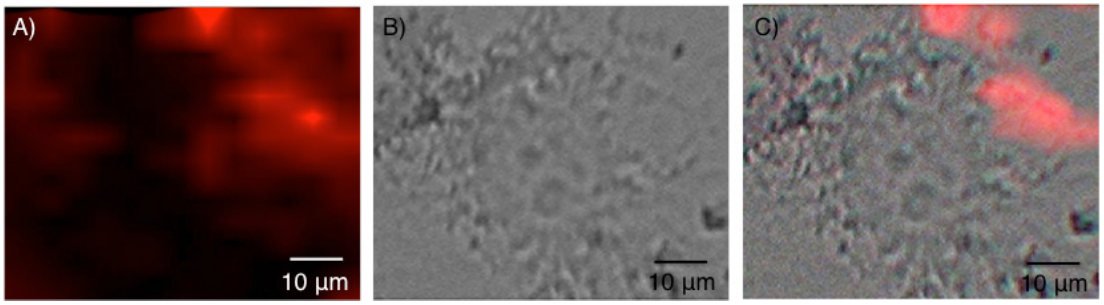

Figure 9.6 - (A) SERS map measured at 1074 cm^{-1} showing the cellular distribution of anti-VCAM-1 SERS nanoprobes. Corresponding (B) light micrograph and (C) overlay image.

A precise analytical technique for sensing and localizing the distribution of inflammatory cell adhesion markers, such as VCAM-1, is critical to diagnosis atherosclerosis and detect plaque in the early stages of formation [155]. Ideally, this

technique would be non-invasive, non-destructive, and provide both highly specific target identification, as well as localization information. Although traditional methods of biomolecule detection, such as fluorescence and quantum dots, can yield distribution information, surface-enhanced Raman scattering offers this dual advantage of both localization and accurate target identification. Furthermore, the quick and non-destructive nature of Raman spectroscopy makes it ideally suited for work in cells, with great potential for translation to *in vivo* models [418]. Despite these advantages, the complexity, time intensive, and sensitive nature of SERS nanoprobe construction can be a deterrent to more widespread use. Therefore, an alternative method to produce Raman-active nanoprobes using microwave technology is presented. Microwave technology serves to decrease reaction time for SAM construction, while yielding nanoprobes with suitable signal intensity and stability for functionalization. Compared to traditional heating, which relies on energy migration from the outside of the vessel (slow and non-specific transfer), during microwave heating the energy transfer occurs in fractions of a second (with each cycle of electromagnetic energy). This allows for a large amount of energy to be directly applied in a very efficient manner, resulting in rapid molecular rotations and therefore significantly reduces the time required for functionalization [407].

Overall, results presented in this paper indicated that microwave irradiation can be used to successfully fabricate SERS probes with appropriate stability and

functional capabilities for antibody conjugation. The approach is versatile since it could be applied to fabricate SERS probes bearing various Raman reporter molecules, which is especially important in multiplex analysis [332]. Furthermore, microwave technology could be applied to prepare targeted SERS nanoprobes for a variety of applications, in addition to CVD biomolecule detection demonstrated in this work. For example, to trace intracellular drug delivery, distinguish cancerous cells, or measure cell viability. Future investigations will explore the microwave-assisted fabrication of probes for simultaneous multiplexing of cardiovascular disease biomarkers, which has the potential to significantly improve the prognosis of atherosclerosis and inflammatory-based diseases.

9.5 Conclusions

The synthesis, characterization, and *in vitro* application of a SERS-based nanoprobe fabricated via microwave technology for the analytical nanosensing of atherosclerotic biomarkers was presented in this paper. Nanoprobes were shown to exhibit strong SERS scattering signals after coating with Raman reporter, 4-MBA, via microwave, and were subsequently capable of straightforward functionalization with a protective polymer and target antibody. Using these microwave-assisted nanoprobes with surface-enhanced Raman spectroscopy, the detection and localization of cellular adhesion molecules in HCAE cell was demonstrated. Overall, results indicated that microwave technology can be a viable option to rapidly

fabricate SERS nanoprobes for biomarker detection. This approach has potential for use as a simple and rapid fabrication technique in the burgeoning field of SERS-based nanosensing and immunoassays.

9.6 Acknowledgments

We gratefully acknowledge Stephen Vance and Effat Zeidan for helpful discussions and technical assistance. This work was supported by the National Science and Research Council of Canada, Fonds Quebécois de la Recherche sur la Nature et Technologies, and earlier.org.

9.7 Supplementary Information

9.7.1 SERS Spectra of Intracellular Regions on a HCAE Control Cells

SERS spectra were measured from cells incubated with IgG-1-conjugated SERS nanoprobes as non-specific control, in addition to cells incubated without nanoprobes to assess non-specific background. Relatively no signal was observed at 1074 cm^{-1} for cells incubated with IgG-1-conjugated SERS probes (Figure 9.7), nor for cells devoid of nanoprobes (Figure 9.8).

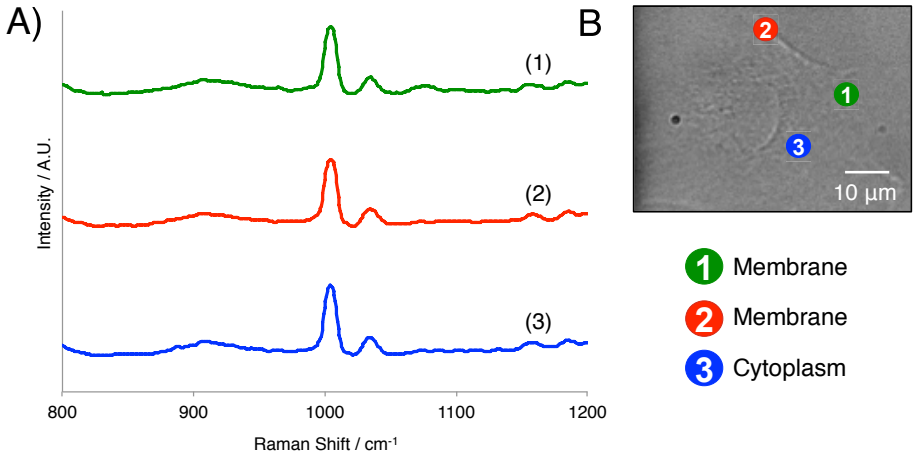

Figure 9.7 - (A) Representative SERS spectra of intracellular regions on a HCAE cell incubated with IgG-1 nanoprobes and (B) corresponding light micrograph.

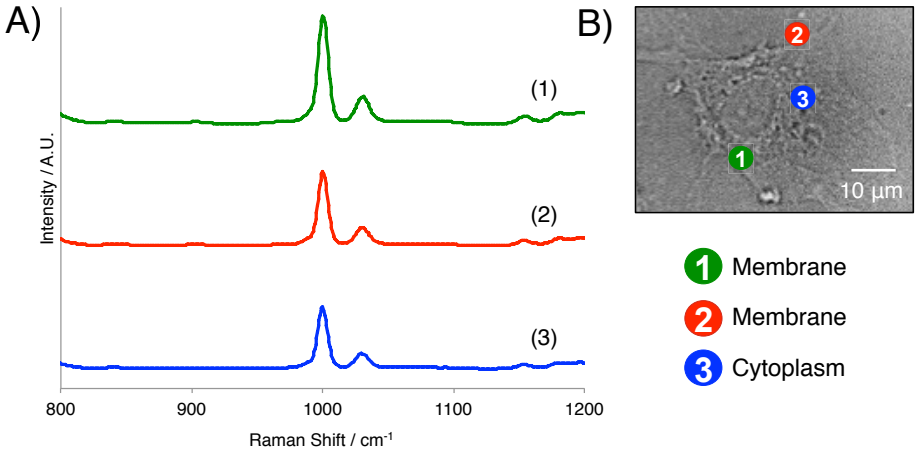

Figure 9.8 - (A) Representative SERS spectra of intracellular regions on a HCAE cell devoid of nanoprobes and (B) corresponding light micrograph.

9.7.2 SERS Maps of HCAE Control Cells

SERS maps of HCAE cells treated with CRP and incubated with IgG-1 functionalized probes or devoid of nanoprobes are presented in Figure 9.9 and Fig. 9.10, respectively. No background signal was observed at 1074 cm^{-1} for cells lacking nanoprobes and a marked decrease was observed for cells incubated with IgG-1.

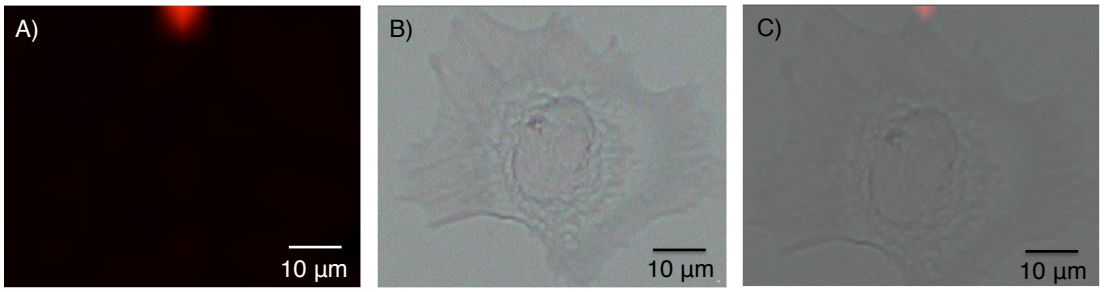

Figure 9.9 - HCAE cells incubated with IgG-1 SERS nanoprobes. (A) SERS map measured at 1074 cm^{-1}. (B) Light micrograph. (C) Overlay of SERS map and light micrograph.

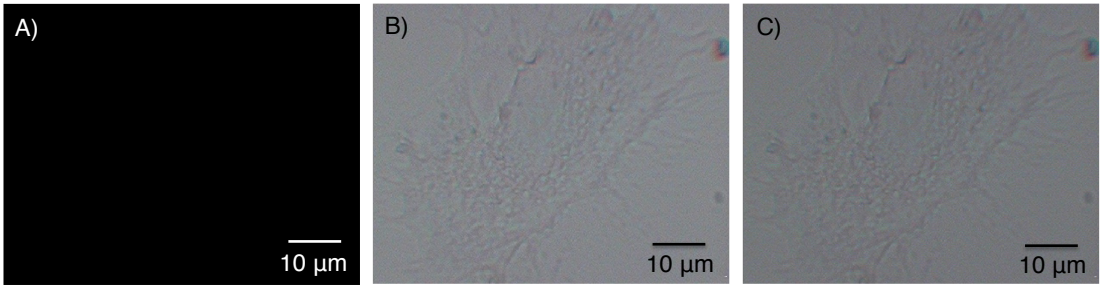

Figure 9.10 - HCAE cells without nanoprobes. (A) SERS map measured at 1074 cm^{-1}. (B) Light micrograph. (C) Overlay of SERS map and light micrograph.

Chapter 10: Conclusions and Perspectives

The overall aim of this thesis was to develop a nanoparticulate drug delivery system with the ultimate goal of treating the inflammatory component of early onset atherosclerosis. To this end, a liposome-based delivery system for the sex steroid, 17β-estradiol (E2), composed of 1,2-dioleoyl-*sn*-glycero-3-phosphocholine (DOPC), cholesterol, and a cationic charging agent, dimethyldioctadecyl-ammonium (DDAB) was optimized and evaluated in an a vascular cell model. The secondary objective was to investigate an approach to detect and localize early-onset inflammation via surface-enhanced Raman scattering (SERS). The imaging component of the project was achieved by the development of a novel Raman scattering nanoprobe composed of a gold core, 4-mercaptobenzoic acid (4-MBA) Raman reporter, and poly(allyamine hydrochloride) (PAH) protective coating. Functionalization with target monoclonal antibodies enabled *in vitro* detection and localization of VCAM-1 in HCAE cells. Herein, we review the sub-objectives of this dissertation (Chapter 3) and include a brief summary of the results.

10.1 Summary of Objectives and Achievements

10.1.1 Development and Physiochemical Characterization of a Liposomal Delivery System for 17β-Estradiol

Although liposome-based vehicles are widely used in the pharmaceutical field for the delivery of hydrophilic drugs, the knowledge and study of hydrophobic

drugs loaded into the phospholipid bilayer for cellular delivery is less well known. In particular, the study of loading efficiencies and cellular delivery of hydrophobic drugs is still an unmet goal in the development of such drug delivery systems. This work introduces the development and characterization of nanoliposomes for delivery of the hydrophobic E2, with the ultimate aim of treating the inflammatory-based component of atherosclerosis. A selection of lipids and charge inducers were used to prepare liposomes by thin film hydration in conjugation with tangential flow filtration for vector purification. DOPC-based liposomes were found to improve E2 encapsulation efficiency and loading capacity compared to those composed of egg phosphatidylcholine (EPhC) and 1,2-dipalmitoyl-*sn*-glycero-3-phosphocholine (DSPC). Ultimately, an encapsulation efficiency of 51.2 ± 3.6% and loading capacity of 7.3 ± 0.5 μg/mg were achieved for DOPC liposomes loading with a 5% molar loading of E2 (Chapter 7).

10.1.2 In Vitro Assessment of Liposomal-E2 Nanoparticles in Human Coronary Artery Endothelial Cells

To meet the second objective of this project, we demonstrated the application of our delivery system by studying the cellular uptake and cytotoxicity in a human coronary artery endothelial cell model, which is relevant to the future investigation of the effect of E2 on vascular-based diseases. The optimized DOPC liposomes were tested for their release kinetics over 48 h, as well their cytotoxicity and cellular

uptake properties in HCAE cells. The effect of liposomal charge was investigated by comparing neutral liposomes to those formulated with the cationic charging agent dimethyldioctadecyl-ammonium (DDAB) or the anionic charging agent 1,2-ditetradecanoyl-*sn*-glycero-3-phospho-(1'rac-glycerol) (DMPG). Results showed that charge had no significant influence on *in vitro* release over 48 h, however cellular uptake of positively charged liposomes increased significantly compared to neutral and anionic liposomes of the same composition. We show for the first time the effects of liposomes composition on cellular uptake for hydrophobic drug delivery, as well as distribution within the cell after uptake in HCAE cells (Chapter 7).

10.1.3 Investigation of E2-Loaded Liposomes to Attenuate CRP-Activated Inflammation in Human Coronary Artery Endothelial Cells

E2-loaded liposomes were studied for their ability to attenuate the inflammatory response incited by CRP in HCAE cells. Results from the Western blot immunoassay demonstrated that pre-treatment with E2-loaded liposomes successfully down-regulated the expression of VCAM-1 in CRP-activated HCAE cells. Similar responses were observed for the secretion of inflammatory cytokines, IL-8 and TNF-α, which were shown to decrease in significantly liposome-treated cells. We demonstrate for the first time that E2 encapsulated into nanoliposomes can successfully attenuate the inflammatory response *in vitro*. Overall, these studies

indicate that the developed liposome vector may be a promising approach to deliver E2 for inflammation-based cardiovascular diseases (Chapter 8).

10.1.4 Development of Surface-Enhanced Raman Scattering Nanoprobes Via Microwave Technology

Surface-enhanced Raman scattering (SERS) nanoprobes were successfully fabricated by microwave technology and characterized by optical absorbance, Raman scattering spectrum, transmission electron microscopy, size, and zeta potential. Results showed that gold nanoparticles coated with a self-adsorbed monolayer (SAM) of 4-MBA by microwave technology yielded a stable system capable of straightforward functionalization in under 10 min. Biofunctionalization of the target antibody, anti-VCAM-1, via glutaraldehyde activation was achieved on microwave-synthesized nanoprobes coated with PAH. We demonstrate and report for the first time, the successful application of microwave technology for SERS nanoprobe fabrication (Chapter 9).

10.1.5 Detection of Inflammatory Activation by Surface-Enhanced Raman Spectroscopy

To meet the final objective of this thesis, the SERS nanoprobes developed to meet Objective #4 were applied to detect the upregulation of VCAM-1 expression in HCAE cells. Indeed, we showed that anti-VCAM-1 SERS nanoprobes specifically bound to cells, which had been treated with CRP. The Raman signal peak,

characteristic of 4-MBA, at 1074 cm^{-1} was detected and confocal Raman mapping of VCAM-1 expression and distribution was demonstrated (Chapter 9).

10.1.6 Original Contributions

The novelty of this thesis lies in both the development and application of nanotechnology-based approaches to treat and diagnose the inflammation component of early-onset atherosclerosis. The liposome-based delivery vehicle is the first of its kind optimized specifically for the transport of E2 into human coronary artery endothelial cells. Other novel aspects of the liposome-based work are highlighted below:

- Optimized loading (encapsulation efficiency and loading capacity) of E2 into liposomes
- Applied tangential flow filtration for separation of unencapsulated E2 drug
- Demonstrated significant increase in uptake of cationic E2-liposomes in HCAE cells compared to neutral/anionic liposomes
- First to show liposome distribution within HCAE cells
- Demonstrated anti-inflammatory properties of E2-liposomes *in vitro*

The SERS-based nanoprobe fabrication and application are also original contributions of this project. The detection of the expression of VCAM-1 in an

endothelial cell model was demonstrated for the first time. Further novel aspects of this project include:

- Fabricated SERS nanoprobes by microwave technology
- Established a simple and effective bioconjugation technique after microwave irradiation
- Demonstrated SERS nanoprobe application for detection & mapping of VCAM-1 expression *in vitro*

10.2 Discussion and Future Work

Although the objectives set forth at the beginning of this thesis were successfully met, some improvements and future work could improve the ultimate application and success of the proposed systems for diagnosing and treating the inflammatory-based components of atherosclerosis. Accordingly, future directions and possible limitations to this approach are discussed in the following sections.

10.2.1 Questions Remaining in Regards to the Liposome Delivery Vehicle

It is clear from the review presented in Chapter 5 that liposomes have and will continue to successfully be applied to treat and diagnose cardiovascular disease. Within this context, we feel that the vector developed and characterized in Chapter 7 and 8 has the potential to be used in clinical applications for the treatment of vascular inflammation. However, prior to this undertaking, further investigations, which are outlined below, should be considered.

First of all, although the liposomes showed the ability to control the delivery of E2 over a 48 h timeline, it would be valuable to investigate various features that could be employed to attenuate this release or control it over a longer time period. Changing the degree of release could be employed to consequently affect the anti-inflammatory effects observed *in vitro*. Suggestions include altering the ratios of drug, lipid, and/or the cationic charging agent DDAB, which could alter the electrostatic interactions and, accordingly, the release rate. The application of polymer coats on the surface, could also serve to control the release rate of E2 from the liposomes, as shown by Haider *et al.* (2007) [419]. In conjunction, an in-depth study of the release kinetics and specifically the application a mathematical model, such as the Higuchi equation, could serve to inform the mechanism of drug release from the liposomal matrix.

A more in depth study of the effects of liposomal-E2 on vascular inflammation should also be conducted in order to expand our knowledge on the anti-inflammatory properties of the proposed system. Specifically, an experiment quantifying other biomarkers, such as ICAM-1, CRP, and IL-6, should be undertaken to achieve a more detailed understanding of effects on inflammation. Although we demonstrate that attenuation of VCAM-1 expression, Il-8 and TNF-α excretion by E2-loaded liposomes is comparable to water-soluble E2, the controlled delivery of E2, as well as perhaps the ultimate localization of the drug within the cell, may

ultimately impact effects on inflammation. That is, due to dissimilar timings and expression of such biomarkers, the extension of this study would provide a more complete picture of the effect of liposomal E2 on vascular cells. As well, given the multi-faceted effects of E2 on the cardiovascular system outlined in Chapter 4, it would be relevant to expand the study to properties other than the regulation of inflammatory biomarkers. For instance, the effects of liposomal E2 on nitric oxide [107]/nitric oxide synthase [420] production, reactive oxygen species formation [113] and antioxidant properties [377], as well as smooth muscle cell proliferation [85] could also be investigated within the framework of the attenuation of inflammation and atheroma development in general.

Next, although we demonstrate the successful incorporation of E2 within liposomal vectors, in order to be used as a pharmaceutical grade product the question of long-term stability should be addressed. In particular, it would be of interest to investigate the effects of lyophilization on liposomal samples and to test the physiochemical properties (e.g. size and zeta potential) and E2 loading before and after rehydration. The applicability of such a formulation in the clinical is conditional on its ability to be easily transported and stored, thus this study should be undertaken prior even to *in vivo* application.

Potential limitations of the current system, particularly in regards to translation into *in vivo* or clinical trials, is the lack of specific targeting to areas of the

inflamed vasculature. Given the successes of immunoliposome formulations in particular for treating and diagnosing CVD outlined in Chapter 5, it would be suggested to investigate the effects of actively targeting our system to sites of inflammation. This concept is expanded further in Section 10.2.3.

10.2.2 Questions Remaining in Regards to the SERS Imaging Agent

The application of SERS to detect and localize inflammatory biomarkers *in vitro* was successfully demonstrated in HCAE cells, however the question of whether the system can be used to quantify of the upregulation of such biomarkers remains. The next step in this aspect would be to develop a technique to quantify the expression of biomarkers, as demonstrated in a paper by Amendola *et al.* (2011), who successfully correlated the concentration of SERS nanoprobes with Raman signal intensity to quantify uptake by macrophages [421]. This would significantly improve and expand the range of applications for our SERS nanoprobe-based imaging. It could allow for the determination of inflammatory biomarker expression in response to various stimuli, for example the application of our liposomal-E2 delivery vectors.

Similar to the issue of liposomal stability detailed in Section 10.2.1, it would also be suggested to study the long-term stability of SERS probes. In particular, the question of whether SERS probes undergo significant aggregation or loss of Raman signal should be addressed.

Another question that remains to be investigated is whether the SERS-based imaging technique is comparable to traditional detection methods, such as Western blot, fluorescence, and/or ELISA approaches. The applicability of the SERS nanoparticle imaging technique developed in this thesis would accordingly benefit from a rigorous and direct comparison to the detection of cellular adhesion biomarker expression via such techniques would be recommended to demonstrate relevance within the field of biomarker detection.

It is certain that the study and application of multicomponent nanoparticle-based delivery and diagnostic systems necessitate similarly complex characterization approaches. Although conventional techniques, such as dynamic light scattering, zeta potential and UV-vis, were used to characterize the developed systems in this thesis, the application of these systems *in vitro* was the ultimate test of their utility. Assumptions made throughout this thesis work, such as liposomal stability in cellular environments and functionality of the majority of SERS nanoprobes, could also be explored in future studies. Such results would aide to confirm whether the majority of the delivered particles are being utilized by cellular systems.

10.2.3 Future Work

This dissertation sets forth the foundations for the application of nanoparticle-based vectors, specifically liposomes and SERS nanoprobes, for the diagnosis and

treatment of early onset of atherosclerosis. Future directions for the application and continuation of this project are proposed herein.

Delivery efficiency to cells could be altered if liposomes were specifically targeted to cell adhesion molecules (CAMs), such as VCAM-1 or CD36. Indeed, the success of such formulation might be significantly improved, particularly in the context of translation to *in vivo* models, where specific targeting agents can significantly improve localization and retention at sites of interest in the highly dynamic vascular system. The addition of a targeting moiety to a CAM, such as VCAM-1 [168, 257], ICAM-1 [422], as well as E- or P-selectin, or CD36, which are expressed at early stages of plaque evolution, is proposed. E- or P-selectins, in particular, afford low basal expression, which can serve to reduce 'background targeting' and improve delivery [423]. The addition of such a targeting moiety could serve to improve the affinity of our system for the endothelium, as depicted in Figure 10.1, which is particularly relevant for translation to *in vivo* models and eventual clinical translation [422].

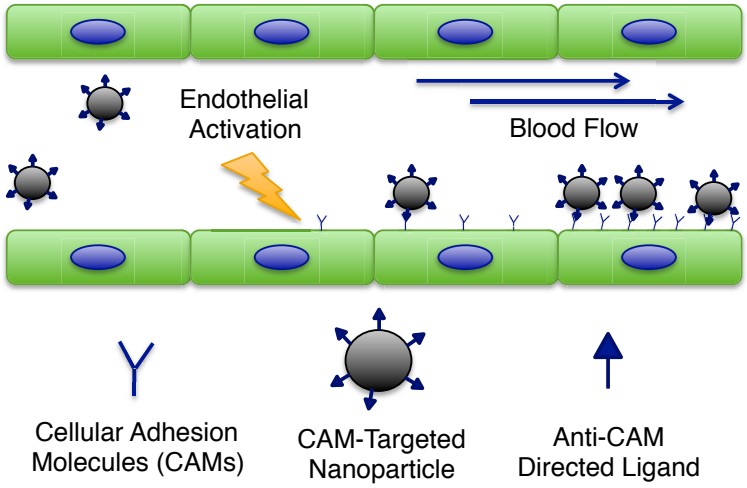

Figure 10.1 – Delivery of nanoparticles targeted towards cellular adhesion molecules (CAMs) to the vasculature.

Given the inherent suitability of SERS for multiplexing applications, it would be interesting to explore the detection of multiple inflammatory biomarkers, to further validate our system. Precise and simultaneous quantification of biomarker expression could be used to rigorously characterize the effects of active agents and, specifically, the administration of E2-loaded liposomes on vascular cells. The multiplexing capability of such a system would give it a marked advantage over conventional methods such as quantum dot imaging and fluorescence, while also providing the precise expression information supplied by Western blot and ELISA approaches.

Certainly, the ultimate goal and culmination of this project would be to incorporate the two systems developed in this dissertation into a theranostic device,

which could be used to simultaneously detect, target, and treat the inflammatory-based components of atherosclerosis. Such an optically traceable drug delivery nanocarrier could improve our understanding of the interaction between delivery vehicles and cells, as well as improve delivery efficiency and facilitate the current drive towards personalized medicine, since both diagnostic and therapeutic goals could be addressed in a single system. Figure 10.2 depicts two proposed systems in which the E2-loaded liposomes and SERS nanoprobes are amalgamated into a single theranostic device. Figure 10.2a illustrates a system in which SERS nanoparticles encoded with a Raman reporter such as 4-MBA are encapsulated within a liposome loaded with E2. Figure 10.2b shows an alternative system in which the SERS nanoprobes are attached or conjugated to the surface of the liposomes. Both proposed vectors could be employed to simultaneously deliver a therapeutic payload of E2 to cells as well as facilitate biomarker detection and imaging. In fact, a comparison of the two systems could also be pursued in future studies to advance this line of esearch.

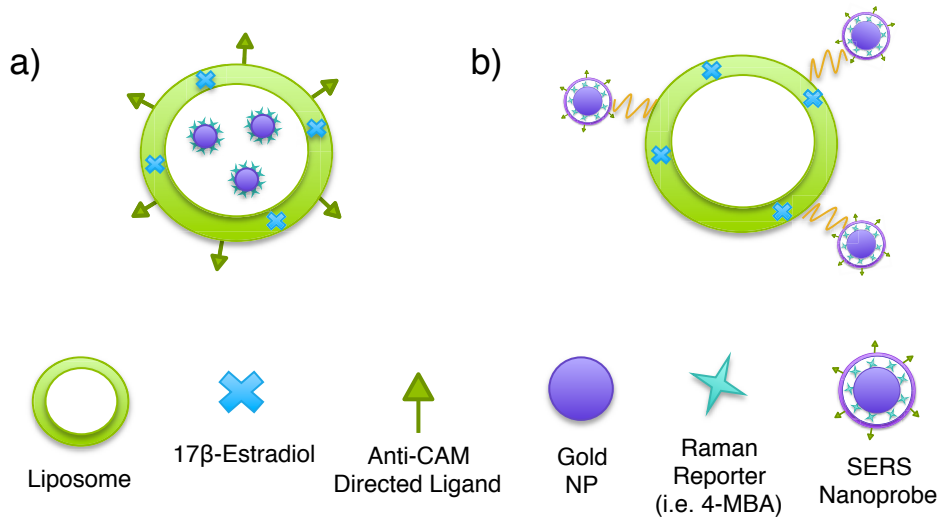

Figure 10.2 - Schematic depicting theranostic vehicles proposed based on the work conducted in this thesis.

Although significant work must be undertaken in order to apply the nanomaterial-based systems developed throughout thesis to *in vivo* or clinical applications, it is clear that the results presented represent a significant step in the goal of treating and diagnosing the early onset of atherosclerosis, and perhaps, one day, preventing pathogenesis of the disease altogether.

Appendix A: Biomedical Applications of Hybrid Organic and Inorganic Nanomaterials

The following chapter was prepared for the textbook "The Biomedical Engineering Handbook, Fourth Edition" edited by Joseph D. Bronzino and Donald R. Peterson, which is set to be published in October 2014 by CRC Press. The book chapter highlights the fabrication and usage of organic and inorganic nanoparticles in biomedicine-based applications. The chapter offers perspectives on employing hybrid nanomaterials for applications such as bone tissue engineering, theranostic drug delivery vehicles, and cellular imaging.

Biomedical Applications of Hybrid Organic and Inorganic Nanomaterials

Kristen Bowey[1], Maryam Tabrizian[1,2,*]

[1]Department of Biomedical Engineering, McGill University, Montréal, Quebec, Canada

[2]Faculty of Dentistry, McGill University, Montréal, Québec, Canada

*Corresponding author: maryam.tabrizian@mcgill.ca

Keywords: hybrid materials, nanocomposite scaffolds, tissues engineering, superparamagnetic iron oxide nanoparticles, cerasomes, liposomes, bioactive glass, nano-hydroxyapatite

A.1 Abstract

This chapter reviews recent developments and applications of hybrid nanomaterials, made of both organic and inorganic elements, to the field of medicine. These complexes offer novel properties and treatment solutions to treat diseases, such as cancer, diabetes, and bone disorders. Specifically, nanoparticulate systems, designed for therapeutic delivery and/or cellular imaging, are explored with a focus on liposomes functionalized with ceramic materials and magnetic particles coated with polymers. Nanocomposite scaffold materials for tissue engineering are also examined. In particular, biomimetic scaffolds embedded with nano-hydroxyapatite and scaffolds reinforced with bioactive glass for bone regeneration are detailed. The aim is to provide the reader with an introduction to the field of hybrid nanomaterials and examine their function in disease treatment and diagnosis.

A.2 Introduction

The application of nanotechnology to the field of medicine has engendered many novel molecular-scale devices and technologies for disease prevention, diagnosis, monitoring, and treatment [424, 425]. Indeed, recent interest and growth in the area of nanotechnology has been associated with a marked increase in the number of nanotechnology journals [426], patent applications [427], as well as governmental research funding [428]. Nanomedicine is expected to continue to revolutionize the practice of medicine by ameliorating old therapies and technologies, and by providing entirely new ones [429, 430].

Hybrid nanomaterials are composed of discrete organic and inorganic components and have at least one physical dimension in the nanometer range [431]. The combination of organic and inorganic materials is commonly found in nature, from seashells to our own amorphous skeletons, but has recently been applied to nanomedical applications [432, 433]. Biomedical hybrid systems unite properties from both elements with the aim of improving existing tools and technologies, whilst potentially presenting new properties and novel capabilities.

Although there are many forms and variations of hybrid nanomaterials used in diverse biomedical applications, this chapter will focus particularly on two of the following areas (1) multifaceted nanoparticles for imaging and drug delivery and (2) hybrid nanocomposite scaffolds for tissue engineering. Figure A.1 schematically depicts the topics covered in this chapter.

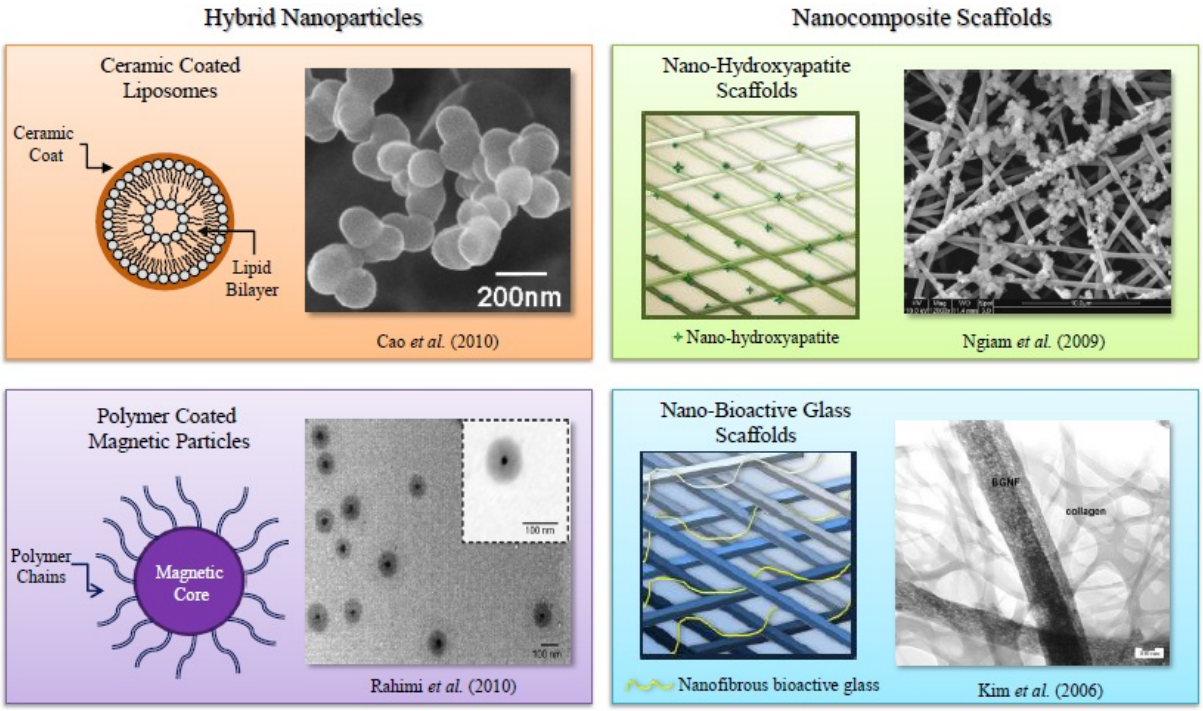

Figure A.1 - Schematic diagram of hybrid materials covered in this chapter. Micrographs reprinted from Cao *et al.* [434], Rahmini *et al.* [435], Ngiam *et al.* [436] and Kim *et al.* [437].

A.3 Hybrid Nanoparticles for Therapeutic and Diagnostic Applications

Nanoparticles (NPs) can be used to encapsulate therapeutic agents, including drugs [438], vaccine adjuvants [439], and plasmid DNA [440], to improve biocompatibility, control release kinetics, and aid to avoid clearance by the reticuloendothelial system (RES). Numerous materials have been investigated to construct delivery vehicles, most notably synthetic [441, 442] and natural polymers [443, 444], lipids [445, 446], and inorganic materials, such as silica [447, 448]. Other

types of luminescent, semiconductor, and magnetic NPs are used as contrast agents in imaging applications to study cellular interactions and biological processes [449], track cells [450], or characterize diseased tissue [451]. Example particulate imaging systems include superparamagnetic iron oxide nanoparticles (SPIONs) [452] and quantum dots (QDs) composed of cadmium, selenium, zinc, sulfur, and/or tellurium [453].

Combining the abovementioned organic and inorganic components may generate multifunctional NPs with the ability to deliver active agents and image tissues. Hybrid systems can also present other capabilities, such as increase stability over single component devices, alter physiochemical properties, and change transfection or delivery efficiencies [454]. The following paragraphs detail a selection of nanoparticulate hybrids that feature liposomes and magnetic particles for therapeutic delivery, imaging or a combination of applications. It should be noted that a large portion of hybrid nanoparticulate research is also dedicated to modifying inorganic QDs by encapsulation into liposomes [455, 456], polymers [457, 458], or decorating with ligands [459, 460]. The reader is directed to other review papers that have already extensively covered this topic [453, 461-464].

A.3.1 Ceramic-Coated Liposomes

Liposomes have been explored as cellular models [465], imaging agents [466], and delivery vehicles for both drugs [467] and genetic material [468]. However, liposomes can be unstable *in vivo,* where circulatory proteins mark particles for clearance by the RES [434]. In an attempt to improve *in vivo* stability, researchers have coated liposomal surfaces with materials such as poly(ethylene glycol) (PEG) [469, 470], antibodies [471], as well as modified the surface with ultra-thin layers of ceramic moieties to form hybrid 'cerasomes' [472, 473].

Cerasomes are typically formed by self-assembly and sol-gel reactions [474] where a silica- or ceramic layer is covalently attached to the lipid bilayer (see Figure A.2). Functionalization can often improve mechanical stability compared to conventional liposomes or silica NPs, as the rigidity of the inorganic layer is balanced by the lipid fluidity [475, 476]. In addition, ceramic moieties decrease aggregation related to vesicular fusion [474] and may also modulate release kinetics [434], thereby improving therapeutic delivery efficiency. Table A.1 contains recent papers detailing the formation of cerasomes for biomedical applications.

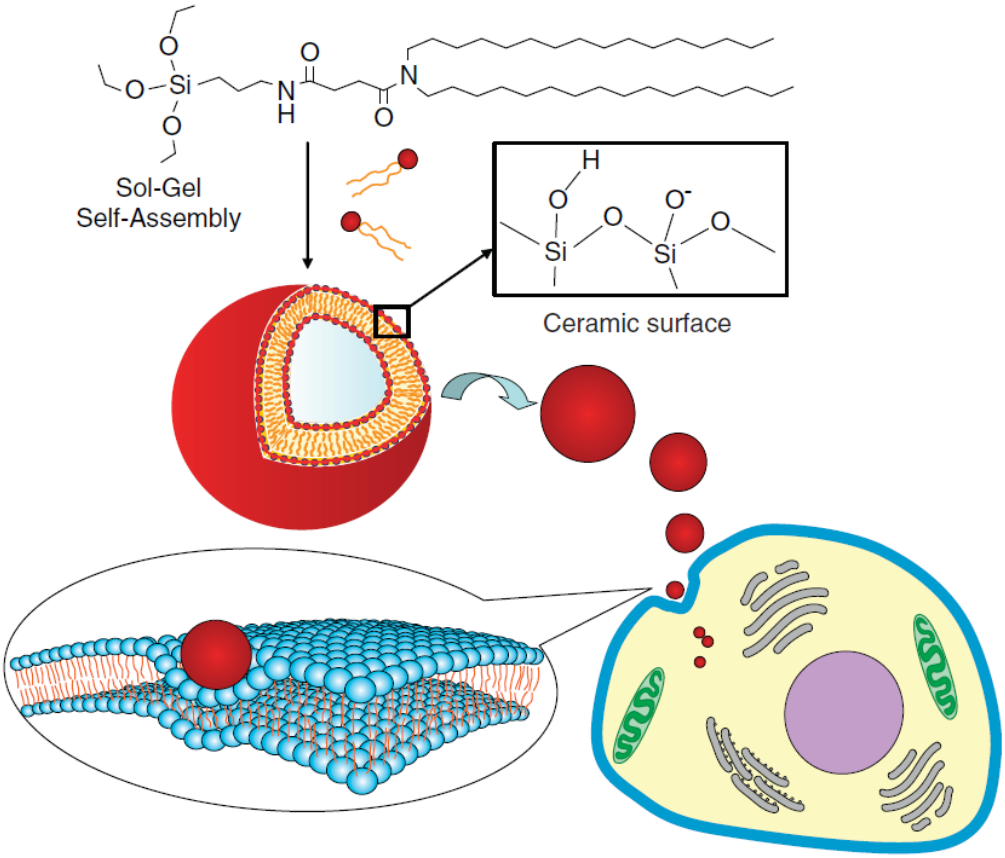

Figure A.2 - Cerasomes and their interaction with cells.
Reprinted from [477].

Table A.1 - Selected summary of recent ceramic-coated liposome systems.

Surface Material	Biomedical Application	Key Results	Ref.
Organoalkoxysilane	Drug delivery system	Uptake of cerasomes reported to be by clathrin-mediated endocytosis, improved biocompatibility compared to silica NPs	[477]
Organoalkoxysilane	Paclitaxel delivery	Cerasomes demonstrated better stability and encapsulation efficiency compared to liposomes, modulated paclitaxel kinetics	[434]
Tetra ethyl orthosilicate	Oral insulin delivery	Silica-liposomes reduced glucose levels in rats for a sustained time period	[478]
3-Isocyanatopropyl-triethoxysilane	Encapsulate QDs	Cerasomes improved aqueous dispersion and photostability compared to conventional QDs	[479]
Colloidal silica, Ludox®	Oral insulin delivery	High encapsulation efficiency (70%), exhibited controlled insulin release *in vitro* and enzymatic protection	[480]

NP = nanoparticle**; QD** = quantum dot.

Cerasomes have been used as delivery vehicles for genes [474, 481] and drugs, such as insulin [478, 480] and paclitaxel [434]. Cao *et al.* reported that paclitaxel-loaded cerasomes exhibited enhanced stability, encapsulation efficiency and *in vitro* release profiles compared to standard liposomes [434]. Though the research is still in its relative infancy, Li *et al.* also demonstrated the ability to load QDs into cerasomes and improve their photostability [479]. This development may initiate the fabrication of multifunctional, theranostic cerasomes, capable of both imaging and therapeutic delivery. Overall, the union of liposome and inorganic

coating presents unique features that are difficult to attain in single-component systems. It is clear that properties such as stability, loading properties and biocompatibility *in vivo*, make cerasomes attractive vectors for therapeutic delivery. However, further toxicological and *in vivo* experiments must be conducted before functional translation to a clinical setting.

A.3.2 Polymer Functionalized Magnetic Nanoparticles

Inorganic magnetic nanoparticles (MNPs) have been employed as drug and gene delivery vectors [482], and imaging agents [450] in several clinical applications [452]. By applying external magnetic fields, these particles can target specific areas of the body [483] and/or be heated to kill cancerous tissues, which are vulnerable to localized changes in temperature [484, 485]. MNPs are frequently designed together with an organic component to improve particulate stability and biocompatibility *in vivo*, in addition to helping prevent aggregation [486, 487]. They can be encapsulated in polymeric particles or assorted moieties may be grafted directly onto the surface [488]. Particles have been functionalized with both synthetic and natural polymers, including alginate [489], PEG [483], polyethylemeimine [486], polyvinyl alcohol [490], and methylacrylic acid [491]. Chao *et al.* developed a hybrid magnetic system by modifying gold particles with PEG and loading with doxorubicin [489]. Resultant complexes were biocompatible and drug concentrations were significantly higher in the liver of rats upon application of an external magnetic field.

SPIONs are a class of magnetic particles that are often coupled with a polymer delivery system to target a specific site in the body, though they can also serve as contrast agents for magnetic resonance imaging [452]. Biodegradable hybrid SPION complexes typically consist of a magnetite, maghemite or hematite core, surrounded by a polymer coat and may also include targeting ligands, specifically selected to increase cellular internalization (see Figure A.3). A comprehensive list of SPION coatings can be found in a review by Mahmoudi *et al.* [492]. Hybrid SPIONs have been designed to treat and target a multitude of diseases, including brain tumors [486], vascular dysfunctions [493] and atherosclerotic plaques [494]. Table A.2 provides a selection of recent papers detailing polymer functionalized magnetic particles. Key results indicate that coupling MNPs with polymers reduces aggregation compared to bare particles and can also impart multiple functionalities.

Table A.2 - Selected summary of recent polymer-coated magnetic nanoparticle systems.

Nanoparticle Core	Surface Coat	Biomedical Application	Key Results	Ref.
Iron oxide	Starch or gum arabic, poly-ethyleneimine	Magnetic drug/gene carriers to brain tumors	Low cytotoxicity, ability to penetrate cells, NPs administered by intra-carotid route were entrapped by tumors following application of magnetic field	[486]

Iron (III) and (II) chloride	Vinyltrimethoxy-silane, poly(N-isopropyl--acrylamide-acrylamide allylamine)	Doxorubicin delivery	Coated NPs exhibited lower toxicity compared to un-coated particles, temperature sensitivity, released bioactive doxorubicin	[435]
Iron (III) and (II) chloride	Oleic acid, poly(ethylene glycol)	Doxorubicin delivery and MRI contrast agent	PEG reduced aggregation, particles demonstrated long circulation time *in vivo* and ability to image by MRI	[487]
Iron (III) and (II) chloride	Polyethylenoxide triblock copolymers	Ocular magnetic drug delivery	Coating prevented aggregation, PEO tail lengths above 2 kDa were biocompatible	[495]
Magnetite/ gold hybrid	Poly(N-isopropyl acrylamide-co-acrylamide)-block-poly(ε-caprolactone)	Hyperthermia and optical imaging	Exhibited thermosensitivity, ability to be used as contrast agent for optical imaging	[484]
SPION	Poly (ethylene oxide)-trimellitic anhydride chloride-folate	Doxorubicin delivery, MRI imaging	NPs inhibited liver tumor growth in rabbits, functional as MRI contrast agent	[496]
SPION	Polyethylene glycol moiety, poly-ethyleneimine	Gene delivery	Able to protect pDNA, magnetotransfection capabilities, high transgene expression, no cytotoxicity	[497]

NP = nanoparticle; **PEG** = poly(ethylene glycol); **PEO =** polyethylenoxide; **MRI** = magnetic resonance imaging; **pDNA** = plasmid DNA.

Hybrid polymer-coated MNPs have the potential to change the way we diagnose and treat various disorders. Not only do polymeric coats offer protection and a reservoir for therapeutic agents, they may also decrease aggregation and improve longevity in the circulatory system. MNPs also impart the ability to

accumulate in a given location, which can increase cellular internalization or endocytosis by target cells, a condition generally required to produce a therapeutic effect. Overall, the unique pairing of organic polymers and inorganic magnetic particles properties can facilitate simultaneous site-specific therapy and imaging, which would not be possible in traditional single-component systems.

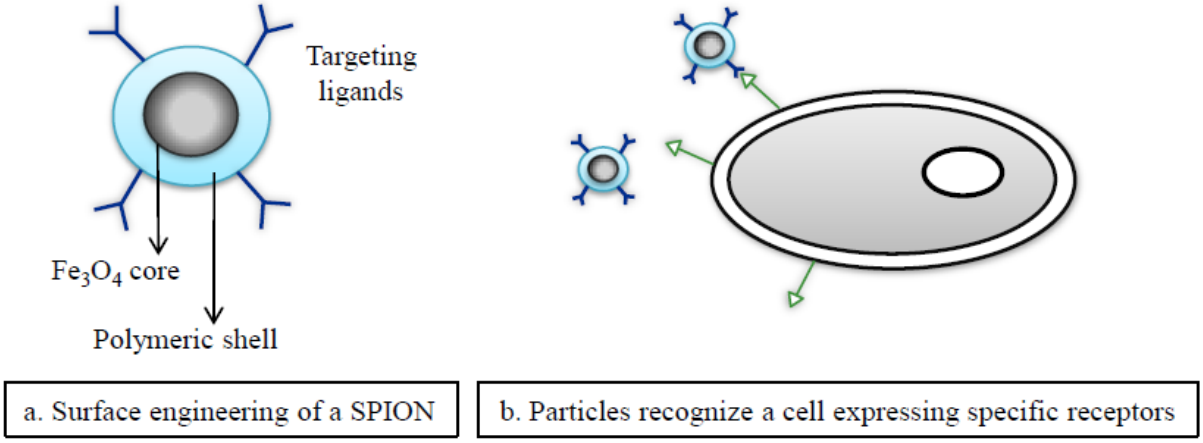

Figure A.3 - Illustration of functionalized SPIONS and cellular interaction. Adapted from [452].

A.3.3 Summary

Given the range of research and development of hybrid NPs, the above discussion is only intended to detail a subset of systems and serve as a general introduction to the field. Most evident are the enhanced properties exhibited by hybrid NPs compared to single component devices and the capacity to combine multiple functionalities into one system. This means that patients will be subjected to

fewer therapies, which may also be required less often and at lower doses. Further investigation into organic-inorganic NPs will certainly carry on, as the search for suitable *in vivo* therapeutic delivery and imaging agents continues. Indeed, researchers have already begun combining hybrid systems, such as encapsulating both iron oxides and QDs into polymeric NPs [498] or QDs into cerasomes [479] . These developments may be the future of hybrid NPs intended for use in biomedicine.

A.4 Hybrid Nanocomposite Scaffolds for Tissue Engineering

Tissue engineering is a multidisciplinary field that requires the integration of chemical and mechanical engineering, materials science, chemistry, and medical knowledge, with the aim of promoting cellular attachment, regeneration, and differentiation [499]. Research into the fabrication and application of biomaterials, such as porous 3D scaffolds, has yielded promising results, though focus has generally been at the cellular level. Recently, attention has shifted to the nano-scale, where intricate processes involved in cell signaling and differentiation can be better understood and developed [433, 500, 501].

Within the field of tissue engineering, nanocomposite matrices are typically composed of inorganic fillers, nanofibers or NPs that are integrated into polymeric matrices [433]. Hybrid organic-inorganic scaffolds may offer better structural support [502] and more closely mimic native tissue environments compared to single

component systems [503]. Indeed, combining organic and inorganic materials can also improve cellular proliferation and adhesion [504] or alter biodegradation kinetics [505]. As a result, various hybrid scaffolds have been studied, from poly(ε-caprolactone) and bioactive silica nanofibers [506] to ceric oxide NPs embedded in a poly(lactide-co-gycolide) matrix [507]. Given the range of types and variations of hybrid scaffolds, two notable inorganic fillers, nanohydroxyapatite (nHA) and bioactive glass, have been selected for particular focus, and will be discussed further in the following sections.

A.4.1 Nanohydroxyapatite Composite Scaffolds

Bone is a naturally occurring hybrid material, primarily composed of nHA and a collagenous matrix [508]. To repair bone defects after injury or disease, researchers have attempted to create biodegradable scaffolds, which can be used to introduce cells to damaged tissue or implanted to promote growth and guide remodeling. The focus is primarily on mimicking the natural extracellular matrix of bone by varying ratios of hydroxyapatite and polymers such as chitosan [509], polyamide [510], poly(L-lactide) [511] and poly(lactide-co-glycolide) [512], poly(caprolactone) [513] and, collagen [514]. Table A.3 includes a summary of recent papers detailing polymeric scaffolds embedded with nHA.

Kong *et al.* reported the fabrication of a chitosan scaffold, embedded with nHA, which successfully increased the bioactivity of preosteoblasts *in vitro*,

improved mineralization, and biocompatibility [515]. Despite promising results, nanocomposite scaffolds are typically created by physical mixing, which makes it difficult to homogeneously combine polymer and hydroxyapatite phases [516]. To overcome this problem, Koo *et al.* proposed functionalized nHA, which can covalently bind poly(L-lactide) scaffolds, resulting in a more uniform composite [511]. In addition to mineralized bone repair, nHA has also been incorporated in polymeric scaffolds to promote cartilage remodeling [512]. Based on these results and those detailed in Table A.3, it is clear that the incorporation of nHA in scaffolds for bone regeneration is a step towards developing functional materials that can improve cellular growth and proliferation in damaged tissues. However, research into the long-term effects of implantation and biodegradation is still required, in addition to improving scaffold formation technologies and the incorporation of nHA.

Table A.3 - Selected summary of recent nHA-polymer composite scaffolds.

Scaffold Matrix	Biomedical Application	Key Results	Ref.
Polyvinyl alcohol nanofibers, collagen	Bone regeneration	PVA/Col/nHA showed similar structure to bone, addition of nHA increased tensile strength and elastic modulus of scaffolds compared to pure PVA and PVA/collagen	[517]
Collagen	Bone regeneration	Incorporation of nHA increased Young's modulus dose dependently, collagen/nHA scaffolds exhibited no significant differences in cellular viability tests for biocompatibility	[514]

Poly(L-lactic acid), collagen	Bone regeneration	PLLA/col/nHA scaffolds seeded with BMP-2 transfected mesenchymal stem cells accelerated bone formation in the radius of rabbits	[518]
Poly(L-lactic acid)	Bone regeneration	Surface immobilized nHA enhanced bone tissue growth *in vivo* compared to pure PLLA and scaffold prepared by bulk-phase mixing PLLA and nHA	[511]
Chitosan	Bone regeneration	*In situ* deposited nHA was similar to bone, attachment and growth of human bone mesenchymal cells increased compared to CS, good biocompatibility	[509]
Polyamide	Repair of mandibular defects	PA/nHA scaffolds seeded with mesenchymal stem cells that were transduced with BMP-7 accelerated bone formation in mandible of rabbits	[510]
Poly(DL-lactide-co-glycolide)	Mineralization by preosteoblasts for bone regeneration	*In vitro* preosteoblasts secreted more mineral on apatite-coated PLGA/nHA scaffolds and uncoated PLGA/nHA compared to pure PLGA	[519]
Poly(lactide-co-glycolide)	Cartilage tissue engineering	Better viability and proliferation of mesenchymal stem cells on PLGA/nHA scaffolds compared to pure PLGA, better *in vivo* osteochondral repair	[512]

PVA = Polyvinyl alcohol; **Col** = collagen; **nHA** = nano-hydroxyapatite; **BMP** = bone morphogenetic protein; **PLLA** = Poly(L-lactic acid); **CS** = chitosan; **PA** = polyamide; **PLGA** = poly(DL-lactide-co-glycolide).

A.4.2 Bioactive Glass Nanocomposite Scaffolds

Bioactive glass is typically composed of silica and varying amounts of calcium, phosphorous, and sodium [520]. It has been used in several biomedical applications, including solid implants and composite scaffolds, owing to unique interactions with the biological milieu and favorable mechanical properties [521]. Lately, bioactive glass NPs and nanofibers have been incorporated into polymeric

matrices to form composite scaffolds for tissue engineering [522, 523]. These scaffolds are predominantly used in bone regeneration applications, where structurally sound scaffolds are required to support a patient's load [524]. Table A.4 provides a review of recent papers reporting the use of bioactive glass nanocomposite scaffolds in tissue engineering.

Incorporation of bioactive glass NPs into polymeric scaffolds has been detailed by several groups [525-527]. NPs, produced by sol-gel methods, provide stability to organic matrices and may also promote osteoconductivity, which is essential to bone reformation [528]. Hong *et al.* showed that bioactive glass NPs improved the mechanical properties of their scaffolds, by studying the compressive modulus and strength [525]. However, porosity decreased significantly once bioactive glass reached 30% of the composite content by weight, which highlights the importance of characterizing and adequately optimizing each individual device.

Table A.4 - Selected summary of recent bioactive glass nanocomposite scaffolds.

Scaffold Matrix	Organic Fillers	Biomedical Application	Key Results	Ref.
Chitosan, gelatin	BGNPs	Alveolar bone regeneration	Protein adsorption and biomineralization increased with addition of BGNPs, improved degradation and swelling properties	[526]
Chitosan	BGNPs	Bone regeneration	CS/BGNPs were bioactive, cytocompatible, promoted cell attachment and spreading, exhibited slower degradation in buffer compared to pure CS	[522]
Poly(ε-caprolactone)	Bioactive glass nanofibers and BGNPs	Bone regeneration	Nanofibers showed better biocompatibility, *in vitro* osteoblast activity and *in vivo* bone forming properties compared to BCNPs	[529]
Poly(lactic acid)	Bioactive glass nanofibers	Bone regeneration	Nanofibers improved *in vitro* apatite formation, osteoblasts showed good adhesion and proliferation on scaffold	[523]
Calcium phosphate	BGNPs + Poly(ε-caprolactone)	Bone regeneration	CaP/BGNPs/PCL showed improved bioactivity, ability to differentiate human bone-derived cells	[530]

NP = nanoparticle; **BGNP** = bioactive glass nanoparticle; **CS** = chitosan; **CaP** = Calcium phosphate; **PCL** = poly(ε-caprolactone).

Fibrous bioactive glass can be created by laser spinning [531] or electrospinning [532], yielding fibers with diameters as small as a few hundred nanometers in magnitude. The mixture of nanofibrous bioglass and polymeric matrices closely mimics the extracellular matrix of bone compared to single component systems. Kim *et al.* incorporated bioactive glass nanofibers into collagen

[437] and poly(lactic acid) matrices [533]. In both studies, it was determined that hybrid nanocomposites increased the activity of human osteoblasts *in vitro* compared to polymer alone. Furthermore, Jo *et al.* reported that nanofibrous bioactive glass in poly(ε-caprolactone) scaffolds was superior to the powdered form, in terms of both bioactivity and strength [529]. In light of these results, it is evident that the integration of bioactive glass, in either nanoparticulate or fibrous form, into an organic matrix imparts superior mechanical properties and bioactivity *in vitro*. Nevertheless, additional *in vivo* studies are essential to validate these findings and further clinical research in this promising area.

A.4.3 Summary

The application of nanotechnology and hybrid blends to scaffolds has yielded some promising devices and technologies, a subsection of which are detailed above. By combining organic and inorganic elements, scaffolds are increasingly similar in composition to many native extracellular matrices. These advancements move us closer to reaching the ultimate goal of mimicking native tissues in an attempt to promote cellular growth and regeneration after damages caused by injury or disease. Further developments in the field of hybrid scaffolds include the combination of both nanoparticles and nanofibers, which has just begun to be reported in recent literature [534, 535]. Indeed, the combination of nanofibrous and nanocomposite hybrid

scaffolds may be the best option to engineer hard tissues in particular, since they most closely mimic the native environment.

A.5 Conclusions

This chapter has been intended to provide an introduction to the field of hybrid systems for nanomedicine, with a particular focus on composite nanoparticles and scaffolds reinforced with inorganic material fillers. It is clear that the combination of organic and inorganic materials in nano-ranged systems improves a number of physiochemical properties, whilst also providing the opportunity to develop multifunctional systems. Incorporation of a magnetic component into polymeric nanospheres, for instance, can be used to direct particles to a specific location and deliver their payload. Indeed, a new generation of multifunctional nanoparticulate systems, with treatment, diagnostic, and imaging capabilities may only be properly realized with the application of hybrid nanomaterials.

Appendix B: High Performance Liquid Chromatography Method Validation for 17β-Estradiol Quantification

In order to determine the amount of 17β-estradiol (E2) present in liposome formulations and in the medium following release studies, a high performance liquid chromatography (HPLC) method validation was conducted. The instrument properties and conditions of measurement are outlined in Table B.1, while Figure B.1 shows a representative standard curve for E2 with a linearity over 0.500 – 100 μg/mL.

Table B.1 - High performance liquid chromatography measurement properties

Parameter	Value
Column	Brownlee Spheri-5, 220x4.6mm, 5μm
Mobile Phase	70:30 Acetonitrile:Water (v/v)
Flow Rate	1 mL/min
UV Detection	281 nm
Temperature	25°C
Injection Volume	50 μL

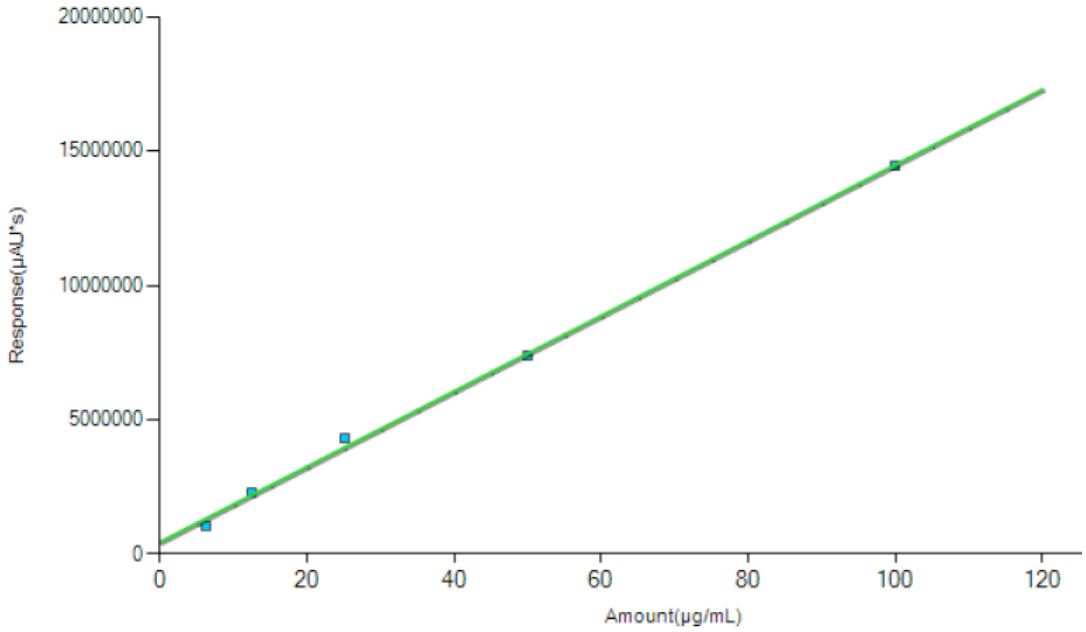

Figure B.1 – Standard curve for E2 fitted by Chromera software (Version 3.3, Perkin Elmer). Linearity was assessed to be 0.9979 over 0.5 -100 µg/mL.

Figure B.2 shows representative chromatographs for an E2 standard and E2 released from a liposomal matrix. The amount of E2 was calculated by determining the area under the curve and fitting it to the standard using the Chromera software package by Perkin Elmer.

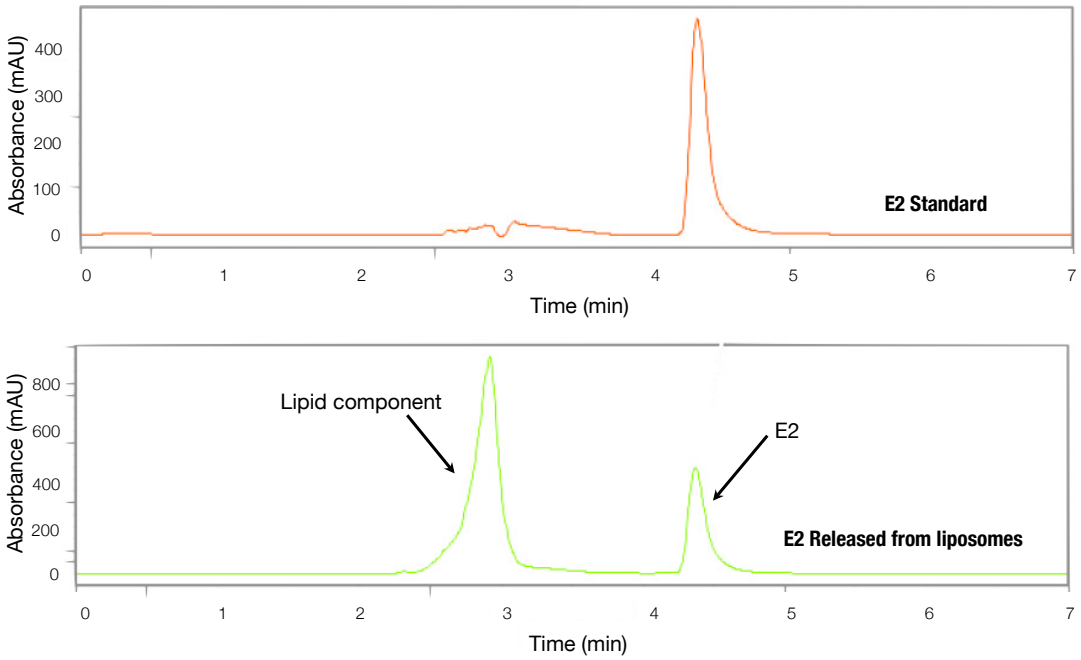

Figure B.2 – Chromatograph for E2 as represented in the Chromera software (Version 3.3, Perkin Elmer). E2 retention time in the column is ~4.4 min.

Appendix C: List of Manuscripts Accepted and Submitted for Publication, Book Chapters, Patents, Selected Conference Proceedings and Awards

Manuscripts Submitted and Accepted

1. **Bowey K**, Tanguay JF, Sandros M, Tabrizian M. *Microwave-assisted surface-enhanced Raman scattering nanoprobes for vascular disease biomarker detection and mapping.* (Submitted to Colloids and Surface B: Biointerfaces, May 2014)

2. Bowey K, Tanguay JF, Tabrizian M. *Nanolipsome-Delivered 17β-Estradiol Effectively Protects Endothelial Cells Against Inflammation: A Potential for Anti-Atherogenic Therapy.* **(**Submitted to Proceedings for the International Conference and Exhibition on Advanced and Nanomaterials, August 2014)

2. **Bowey K**, Tanguay JF, Tabrizian M. (2013) 1,*2-Dioleoyl-sn-glycero-3-phosphocholine–based liposomal nanoparticles as an effective delivery platform for 17β-estradiol*. European Journal of Pharmaceutics and Biopharmaceutics. (Accepted and available online at: http://www.sciencedirect.com/science/article/pii/S0939641113003329)

3. Fatanat Didar TF, **Bowey K**, Guillermina A, Tabrizian M. (2013) *A miniaturized platform for rapid, label-free and simultaneous separation, patterning and in vitro culture of primary and rare cells*. Advanced Healthcare Materials**.** (Accepted and available online at: http://onlinelibrary.wiley.com/doi/10.1002/adhm.201300099/abstract)

4. **Bowey K**, Tanguay JF, Tabrizian M. (2012) *Liposome technology for cardiovascular disease treatment and diagnosis.* Expert Opinion on Drug Delivery. 9 (2): 249 – 265.

Book Chapters

5. **Bowey K**, Tabrizian M. (2012) *Biomedical applications of hybrid organic and inorganic nanomaterials*. Invited chapter. The Biomedical Engineering Handbook, Fourth Edition. (In press**)**

Patents

6. Fatanat Didar T, **Bowey K**, Tabrizian M. *Platform for separation, patterning, and in vitro culture of cells.* Provisional patent, ROI 12082.

Master's Publications

7. **Bowey K**, Swift B, Flynn LE, Neufeld RJ. (2012) *Characterization of biologically active insulin-loaded alginate microparticles by spray drying.* Drug Development and Industrial Pharmacy.

8. **Bowey K**, Neufeld R. (2010) *Systemic and mucosal delivery of drugs within polymeric microparticles produced by spray drying – Review Article.* Biodrugs. 24 (6): 359 – 377.

Conferences

1. **Bowey K**, Tanguay JF, Sandros M. and Tabrizian M. (2013) *Surface-enhanced Raman scattering of antibody functionalized gold nanoparticles for the detection of cardiovascular biomarkers in vitro.* NanoManufacturing Conference. Greensboro, USA (Poster).

2. **Bowey K**, Tanguay JF, and Tabrizian M. (2012*) Characterization and Optimization of Nanoliposomes to Deliver 17β-Estradiol.* Society for Biomaterials Annual Meeting and Exposition. New Orleans, USA (Poster).

3. **Bowey K**, Tanguay JF, and Tabrizian M. (2011) *Characterization of Polyelectrolyte-Coated Liposomes for Delivery of 17β-Estradiol.* Society for Biomaterials Annual Meeting and Exposition. Orlando, USA (Poster).

Awards

1. NSERC PGSD3 Scholarship, 2010-2013 (21,000$/year)
2. FQRNT International Scholarship, 2013 (15,000$)
3. BME Research Day Student Poster Award, 2012 (100$)
4. Queen's Graduate Scholarship, 2007-2009 (1500$/year)
5. Zurbrigg Memorial Graduate Scholarship, 2007 (5000$)
6. Senator Frank Carrel Upper Year Scholarship, 2006-07 (1500$)

References

1. *Mortality, Summary List of Causes* 2011, Statistics Canada.
2. Braunwald, E., et al., eds. *Braunwald's Heart Disease: A Textbook of Cardiovascular Medicine*. 8 ed. Vol. 1 and 2. 2008, Sauders Elsevier: Philadelphia.
3. Wouters, K., et al., *Understanding hyperlipidemia and atherosclerosis: lessons from genetically modified apoe and ldlr mice.* Clin Chem Lab Med, 2005. **43**(5): p. 470-9.
4. Tian, J., et al., *Effect of statin therapy on the progression of coronary atherosclerosis.* BMC Cardiovasc Disord, 2012. **12**: p. 70.
5. Nissen, S.E., et al., *Effect of very high-intensity statin therapy on regression of coronary atherosclerosis: the ASTEROID trial.* JAMA, 2006. **295**(13): p. 1556-65.
6. Dzau, V.J., *Mechanism of protective effects of ACE inhibition on coronary artery disease.* Eur Heart J, 1998. **19 Suppl J**: p. J2-6.
7. Bradley, H.A., et al., *How strong is the evidence for use of beta-blockers as first-line therapy for hypertension? Systematic review and meta-analysis.* J Hypertens, 2006. **24**(11): p. 2131-41.
8. Libby, P., et al., *Inflammation in atherosclerosis: transition from theory to practice.* Circ J, 2010. **74**(2): p. 213-20.
9. Libby, P., et al., *Inflammation in atherosclerosis: from pathophysiology to practice.* J Am Coll Cardiol, 2009. **54**(23): p. 2129-38.
10. Hansson, G.K. and J. Nilsson, *Introduction: atherosclerosis as inflammation: a controversial concept becomes accepted.* J Intern Med, 2008. **263**(5): p. 462-3.
11. Chakrabarti, S., O. Lekontseva, and S.T. Davidge, *Estrogen is a modulator of vascular inflammation.* IUBMB Life, 2008. **60**(6): p. 376-82.
12. Novella, S., et al., *Effects of estrogen on vascular inflammation: a matter of timing.* Arterioscler Thromb Vasc Biol, 2012. **32**(8): p. 2035-42.
13. Cossette, E., et al., *Estradiol inhibits vascular endothelial cells pro-inflammatory activation induced by C-reactive protein.* Mol Cell Biochem, 2013. **373**(1-2): p. 137-47.
14. Beer, S., et al., *High-dose 17beta-estradiol treatment prevents development of heart failure post-myocardial infarction in the rat.* Basic Res Cardiol, 2007. **102**(1): p. 9-18.
15. Chandrasekar, B. and J.F. Tanguay, *Local delivery of 17-beta-estradiol decreases neointimal hyperplasia after coronary angioplasty in a porcine model.* J Am Coll Cardiol, 2000. **36**(6): p. 1972-8.
16. Chang, L.C., et al., *Optimization of rate-controlled 17beta-estradiol nanoparticles for cerebral ischemia therapy.* J Biomed Nanotechnol, 2013. **9**(10): p. 1724-35.
17. Tomoda, K., et al., *Enhanced transdermal permeability of estradiol using combination of PLGA nanoparticles system and iontophoresis.* Colloids Surf B Biointerfaces, 2012. **97**: p. 84-9.
18. Ma, J., et al., *The study of core-shell molecularly imprinted polymers of 17beta-estradiol on the surface of silica nanoparticles.* Biosens Bioelectron, 2011. **26**(5): p. 2791-5.
19. Du, B., et al., *Preparation, characterization and in vivo evaluation of 2-methoxyestradiol-loaded liposomes.* Int J Pharm, 2010. **384**(1-2): p. 140-7.
20. Haeri, A., et al., *PEGylated estradiol benzoate liposomes as a potential local vascular delivery system for treatment of restenosis.* J Microencapsul, 2012. **29**(1): p. 83-94.

21. Antonicelli, R., et al., *Prevention of cardiovascular events in early menopause: A possible role for hormone replacement therapy.* International Journal of Cardiology, 2008. **130**(2): p. 140-146.
22. Babiker, F.A., et al., *Estrogenic hormone action in the heart: regulatory network and function.* Cardiovascular Research, 2002. **53**(3): p. 709-719.
23. Liu, H., A. Pedram, and J.K. Kim, *Oestrogen prevents cardiomyocyte apoptosis by suppressing p38 alpha-mediated activation of p53 and by down-regulating p53 inhibition on p38 beta.* Cardiovascular Research, 2011. **89**(1): p. 119-128.
24. Kolodgie, F.D., et al., *Estradiol attenuates directed migration of vascular smooth muscle cells in vitro.* Am J Pathol, 1996. **148**(3): p. 969-76.
25. Deshpande, D., D.R. Janero, and M. Amiji, *Engineering of an omega-3 polyunsaturated fatty acid-containing nanoemulsion system for combination C6-ceramide and 17beta-estradiol delivery and bioactivity in human vascular endothelial and smooth muscle cells.* Nanomedicine, 2013.
26. Wang, L.L., et al., *Estradiol pretreatment attenuated nicotine-induced endothelial cell apoptosis via estradiol functional membrane receptor.* Int Immunopharmacol, 2011. **11**(6): p. 675-82.
27. Guo, Z.Y., et al., *RNAi targeting ryanodine receptor 2 protects rat cardiomyocytes from injury caused by simulated ischemia-reperfusion.* Biomedicine & Pharmacotherapy, 2010. **64**(3): p. 184-190.
28. Miller, A.P., et al., *Estrogen modulates inflammatory mediator expression and neutrophil chemotaxis in injured arteries.* Circulation, 2004. **110**(12): p. 1664-9.
29. Mestas, J. and K. Ley, *Monocyte-endothelial cell interactions in the development of atherosclerosis.* Trends Cardiovasc Med, 2008. **18**(6): p. 228-32.
30. Moore, K.J. and I. Tabas, *Macrophages in the pathogenesis of atherosclerosis.* Cell, 2011. **145**(3): p. 341-55.
31. Huo, H.L., et al., *Effect of 17-beta-Estradiol on Hypoxia-reoxygenation-induced NF-kappa B Activity, ICAM-1 and VCAM-1 Expression in Cardiac Myocytes.* Chemical Journal of Chinese Universities-Chinese, 2010. **31**(4): p. 746-750.
32. Chotirmall, S.H., et al., *17Beta-estradiol inhibits IL-8 in cystic fibrosis by up-regulating secretory leucoprotease inhibitor.* Am J Respir Crit Care Med, 2010. **182**(1): p. 62-72.
33. Ferreri, N.R., *Estrogen-TNF interactions and vascular inflammation.* Am J Physiol Heart Circ Physiol, 2007. **292**(6): p. H2566-9.
34. Kaminskas, L.M., et al., *A comparison of changes to doxorubicin pharmacokinetics, antitumor activity, and toxicity mediated by PEGylated dendrimer and PEGylated liposome drug delivery systems.* Nanomedicine : nanotechnology, biology, and medicine, 2011.
35. Maciel, N.R., et al., *Reduced cardiovascular alterations of tartar emetic administered in long-circulating liposomes in rats.* Toxicol Lett, 2010. **199**(3): p. 234-8.
36. Takahama, H., et al., *Prolonged Targeting of Ischemic/Reperfused Myocardium by Liposomal Adenosine Augments Cardioprotection in Rats.* Journal of the American College of Cardiology, 2009. **53**(8): p. 709-717.

37. Mittal, G., et al., *Estradiol loaded PLGA nanoparticles for oral administration: effect of polymer molecular weight and copolymer composition on release behavior in vitro and in vivo.* J Control Release, 2007. **119**(1): p. 77-85.
38. Kiss, T., et al., *Evaluation of the cytotoxicity of beta-cyclodextrin derivatives: evidence for the role of cholesterol extraction.* Eur J Pharm Sci, 2010. **40**(4): p. 376-80.
39. Klein, K., et al., *Label-free live-cell imaging with confocal Raman microscopy.* Biophys J, 2012. **102**(2): p. 360-8.
40. Zong, S., et al., *Surface enhanced Raman scattering traceable and glutathione responsive nanocarrier for the intracellular drug delivery.* Anal Chem, 2013. **85**(4): p. 2223-30.
41. Qian, X.M., et al., *In vivo tumor targeting and spectroscopic detection with surface-enhanced Raman nanoparticle tags.* Nature Biotechnology, 2008. **26**(1): p. 83-90.
42. Xu, S.P., et al., *Immunoassay using probe-labelling immunogold nanoparticles with silver staining enhancement via surface-enhanced Raman scattering.* Analyst, 2004. **129**(1): p. 63-68.
43. Ochsenkuhn, M.A., et al., *Nanoshells for surface-enhanced Raman spectroscopy in eukaryotic cells: cellular response and sensor development.* ACS Nano, 2009. **3**(11): p. 3613-21.
44. Jain, S., et al., *Polyelectrolyte stabilized multilayered liposomes for oral delivery of paclitaxel.* Biomaterials, 2012. **33**(28): p. 6758-6768.
45. Toh, B.H., et al., *Atherosclerosis* in *The Autoimmune Diseases*, N. Rose and I. Mackay, Editors. 2005, Elsevier.
46. Lusis, A.J., *Atherosclerosis.* Nature, 2000. **407**(6801): p. 233-41.
47. Sherer, Y. and Y. Shoenfeld, *Mechanisms of disease: atherosclerosis in autoimmune diseases.* Nat Clin Pract Rheumatol, 2006. **2**(2): p. 99-106.
48. Glass, C.K. and J.L. Witztum, *Atherosclerosis. the road ahead.* Cell, 2001. **104**(4): p. 503-16.
49. Ridker, P.M., M.J. Stampfer, and N. Rifai, *Novel risk factors for systemic atherosclerosis: a comparison of C-reactive protein, fibrinogen, homocysteine, lipoprotein(a), and standard cholesterol screening as predictors of peripheral arterial disease.* JAMA, 2001. **285**(19): p. 2481-5.
50. Montecucco, F., et al., *C-reactive protein (CRP) induces chemokine secretion via CD11b/ICAM-1 interaction in human adherent monocytes.* Journal of Leukocyte Biology, 2008. **84**(4): p. 1109-1119.
51. Libby, P., P.M. Ridker, and G.K. Hansson, *Progress and challenges in translating the biology of atherosclerosis.* Nature, 2011. **473**(7347): p. 317-25.
52. Weber, C. and H. Noels, *Atherosclerosis: current pathogenesis and therapeutic options.* Nat Med, 2011. **17**(11): p. 1410-22.
53. Lewis, S.J., *Prevention and treatment of atherosclerosis: a practitioner's guide for 2008.* Am J Med, 2009. **122**(1 Suppl): p. S38-50.
54. Kovarnik, T., et al., *Virtual histology evaluation of atherosclerosis regression during atorvastatin and ezetimibe administration: HEAVEN study.* Circ J, 2012. **76**(1): p. 176-83.

55. Mason, C.M. and A.L. Doneen, *Niacin-a critical component to the management of atherosclerosis: contemporary management of dyslipidemia to prevent, reduce, or reverse atherosclerotic cardiovascular disease.* J Cardiovasc Nurs, 2012. **27**(4): p. 303-16.
56. Inaba, T., et al., *Cholesterol reduction and atherosclerosis inhibition by bezafibrate in low-density lipoprotein receptor knockout mice.* Hypertens Res, 2008. **31**(5): p. 999-1005.
57. Insull, W., Jr., *The pathology of atherosclerosis: plaque development and plaque responses to medical treatment.* Am J Med, 2009. **122**(1 Suppl): p. S3-S14.
58. Rudd, P., *Review: beta-blockers are less effective than other antihypertensive drugs for reducing risk for stroke in primary hypertension.* ACP J Club, 2006. **144**(3): p. 67.
59. Sun, Y.P., et al., *Comparative effects of ACE inhibitors and an angiotensin receptor blocker on atherosclerosis and vascular function.* J Cardiovasc Pharmacol Ther, 2001. **6**(2): p. 175-81.
60. Riccioni, G., *The effect of antihypertensive drugs on carotid intima media thickness: an up-to-date review.* Curr Med Chem, 2009. **16**(8): p. 988-96.
61. Bhatt, D.L., et al., *Clopidogrel and aspirin versus aspirin alone for the prevention of atherothrombotic events.* N Engl J Med, 2006. **354**(16): p. 1706-17.
62. Hansson, G.K., A.K. Robertson, and C. Soderberg-Naucler, *Inflammation and atherosclerosis.* Annu Rev Pathol, 2006. **1**: p. 297-329.
63. Habets, K.L., et al., *Vaccination using oxidized low-density lipoprotein-pulsed dendritic cells reduces atherosclerosis in LDL receptor-deficient mice.* Cardiovasc Res, 2010. **85**(3): p. 622-30.
64. Binder, C.J., et al., *Pneumococcal vaccination decreases atherosclerotic lesion formation: molecular mimicry between Streptococcus pneumoniae and oxidized LDL.* Nat Med, 2003. **9**(6): p. 736-43.
65. Nicoletti, A., et al., *Induction of neonatal tolerance to oxidized lipoprotein reduces atherosclerosis in ApoE knockout mice.* Mol Med, 2000. **6**(4): p. 283-90.
66. van Puijvelde, G.H., et al., *Induction of oral tolerance to oxidized low-density lipoprotein ameliorates atherosclerosis.* Circulation, 2006. **114**(18): p. 1968-76.
67. Charo, I.F. and R. Taub, *Anti-inflammatory therapeutics for the treatment of atherosclerosis.* Nat Rev Drug Discov, 2011. **10**(5): p. 365-76.
68. Elhage, R., et al., *17 beta-estradiol prevents fatty streak formation in apolipoprotein E-deficient mice.* Arteriosclerosis Thrombosis and Vascular Biology, 1997. **17**(11): p. 2679-2684.
69. Lee, J.H., et al., *Cilostazol reduces atherosclerosis by inhibition of superoxide and tumor necrosis factor-alpha formation in low-density lipoprotein receptor-null mice fed high cholesterol.* J Pharmacol Exp Ther, 2005. **313**(2): p. 502-9.
70. Yoshida, M., *Potential role of statins in inflammation and atherosclerosis.* J Atheroscler Thromb, 2003. **10**(3): p. 140-4.
71. Gardin, J.M., et al., *Relationship of cardiovascular risk factors to echocardiographic left ventricular mass in healthy young black and white adult men and women. The*

CARDIA study. Coronary Artery Risk Development in Young Adults. Circulation, 1995. **92**(3): p. 380-7.
72. Rose, V.L., *American Heart Association releases scientific statement on cardiovascular disease in women.* Am Fam Physician, 1998. **57**(11): p. 2873-6.
73. Chen, Y., et al., *Endogenous hormones and coronary heart disease in postmenopausal women.* Atherosclerosis, 2011. **216**(2): p. 414-9.
74. Dubey, R.K. and E.K. Jackson, *Genome and hormones: Gender differences in physiology - Invited review: Cardiovascular protective effects of 17 beta-estradiol metabolites.* Journal of Applied Physiology, 2001. **91**(4): p. 1868-1883.
75. Hamelin, B.A., et al., *Influence of the menstrual cycle on the timing of acute coronary events in premenopausal women.* Am J Med, 2003. **114**(7): p. 599-602.
76. Grodstein, F., et al., *A prospective, observational study of postmenopausal hormone therapy and primary prevention of cardiovascular disease.* Ann Intern Med, 2000. **133**(12): p. 933-41.
77. Cao, J., et al., *Estrogen induces cardioprotection in male C57BL/6J mice after acute myocardial infarction via decreased activity of matrix metalloproteinase-9 and increased Akt-Bcl-2 anti-apoptotic signaling.* Int J Mol Med, 2011. **28**(2): p. 231-7.
78. Wang, M., et al., *17-beta-Estradiol decreases p38 MAPK-mediated myocardial inflammation and dysfunction following acute ischemia.* J Mol Cell Cardiol, 2006. **40**(2): p. 205-12.
79. Strehlow, K., et al., *Estrogen increases bone marrow-derived endothelial progenitor cell production and diminishes neointima formation.* Circulation, 2003. **107**(24): p. 3059-65.
80. Watanabe, T., et al., *Inhibitory effect of low-dose estrogen on neointimal formation after balloon injury of rat carotid artery.* Eur J Pharmacol, 2004. **502**(3): p. 265-70.
81. Lemieux, C., I. Cloutier, and J.F. Tanguay, *Estrogen-induced gene expression in bone marrow c-kit+ stem cells and stromal cells: identification of specific biological processes involved in the functional organization of the stem cell niche.* Stem Cells Dev, 2008. **17**(6): p. 1153-63.
82. Barrett-Connor, E., *Hormones and heart disease in women: the timing hypothesis.* Am J Epidemiol, 2007. **166**(5): p. 506-10.
83. Knowlton, A.A. and A.R. Lee, *Estrogen and the cardiovascular system.* Pharmacol Ther, 2012. **135**(1): p. 54-70.
84. Novella, S., et al., *Estradiol, acting through estrogen receptor alpha, restores dimethylarginine dimethylaminohydrolase activity and nitric oxide production in oxLDL-treated human arterial endothelial cells.* Mol Cell Endocrinol, 2013. **365**(1): p. 11-6.
85. Zhao, J., et al., *Estrogen receptor-mediated regulation of microRNA inhibits proliferation of vascular smooth muscle cells.* Arterioscler Thromb Vasc Biol, 2013. **33**(2): p. 257-65.
86. Mendelsohn, M.E., *Genomic and nongenomic effects of estrogen in the vasculature.* Am J Cardiol, 2002. **90**(1A): p. 3F-6F.
87. Lokuge, S., et al., *The rapid effects of estrogen: a mini-review.* Behav Pharmacol, 2010. **21**(5-6): p. 465-72.

88. Patten, R.D., et al., *17beta-estradiol reduces cardiomyocyte apoptosis in vivo and in vitro via activation of phospho-inositide-3 kinase/Akt signaling.* Circ Res, 2004. **95**(7): p. 692-9.
89. Meyer, M.R., E.R. Prossnitz, and M. Barton, *The G protein-coupled estrogen receptor GPER/GPR30 as a regulator of cardiovascular function.* Vascular Pharmacology, 2011. **55**(1-3): p. 17-25.
90. Meoli, L., et al., *GPR30: New insights in cardiovascular and metabolic diseases.* Hypertension, 2007. **50**(4): p. 814-814.
91. Chakrabarti, S. and S.T. Davidge, *G-protein coupled receptor 30 (GPR30): a novel regulator of endothelial inflammation.* PLoS One, 2012. **7**(12): p. e52357.
92. Wu, Q., et al., *Non-nuclear estrogen receptor signaling in the endothelium.* J Biol Chem, 2011. **286**(17): p. 14737-43.
93. Mendelsohn, M.E., *Protective effects of estrogen on the cardiovascular system.* Am J Cardiol, 2002. **89**(12A): p. 12E-17E; discussion 17E-18E.
94. Selzman, C.H., et al., *The biology of estrogen-mediated repair of cardiovascular injury (vol 65, pg 868, 1998).* Annals of Thoracic Surgery, 1998. **66**(1): p. 310-310.
95. Chandrasekar, B., et al., *Local delivery of 17beta-estradiol improves reendothelialization and decreases inflammation after coronary stenting in a porcine model.* Thromb Haemost, 2005. **94**(5): p. 1042-7.
96. Fu, X., et al., *17beta-Estradiol attenuates atherosclerosis development: the possible role of hydrogen sulfide.* Int J Cardiol, 2013. **167**(3): p. 1061-3.
97. Hamada, H., et al., *Estrogen receptors alpha and beta mediate contribution of bone marrow-derived endothelial progenitor cells to functional recovery after myocardial infarction.* Circulation, 2006. **114**(21): p. 2261-70.
98. Barrett-Connor, E., *Hormones and heart disease in women: where are we in 2005?* Curr Atheroscler Rep, 2006. **8**(2): p. 85-7.
99. Shearman, A.M., et al., *Association between estrogen receptor alpha gene variation and cardiovascular disease.* JAMA, 2003. **290**(17): p. 2263-70.
100. Lamon-Fava, S., et al., *Effect of hormone replacement therapy on plasma lipoprotein levels and coronary atherosclerosis progression in postmenopausal women according to type 2 diabetes mellitus status.* Metabolism, 2010. **59**(12): p. 1794-800.
101. Samsioe, G., et al., *Changes in lipid and lipoprotein profile in postmenopausal women receiving low-dose combinations of 17beta-estradiol and norethisterone acetate.* Menopause, 2002. **9**(5): p. 335-42.
102. Mendelsohn, M.E. and R.H. Karas, *The protective effects of estrogen on the cardiovascular system.* N Engl J Med, 1999. **340**(23): p. 1801-11.
103. Simoncini, T., et al., *Genomic and non-genomic effects of estrogens on endothelial cells.* Steroids, 2004. **69**(8-9): p. 537-42.
104. Ruiz-Sanz, J.I., et al., *17beta-estradiol affects in vivo the low density lipoprotein composition, particle size, and oxidizability.* Free Radic Biol Med, 2001. **31**(3): p. 391-7.
105. Anderson, S.E., et al., *Acute effects of 17beta-estradiol on myocardial pH, Na+, and Ca2+ and ischemia-reperfusion injury.* Am J Physiol Cell Physiol, 2005. **288**(1): p. C57-64.

106. Iwakura, A., et al., *Estrogen-mediated, endothelial nitric oxide synthase-dependent mobilization of bone marrow-derived endothelial progenitor cells contributes to reendothelialization after arterial injury.* Circulation, 2003. **108**(25): p. 3115-21.
107. Lindsey, S.H., L. Liu, and M.C. Chappell, *Vasodilation by GPER in mesenteric arteries involves both endothelial nitric oxide and smooth muscle cAMP signaling.* Steroids, 2013.
108. Freudenberger, T., et al., *Estradiol inhibits hyaluronic acid synthase 1 expression in human vascular smooth muscle cells.* Basic Res Cardiol, 2011. **106**(6): p. 1099-109.
109. Darblade, B., et al., *Estradiol alters nitric oxide production in the mouse aorta through the alpha-, but not beta-, estrogen receptor.* Circ Res, 2002. **90**(4): p. 413-9.
110. Simoncini, T., E. Rabkin, and J.K. Liao, *Molecular basis of cell membrane estrogen receptor interaction with phosphatidylinositol 3-kinase in endothelial cells.* Arterioscler Thromb Vasc Biol, 2003. **23**(2): p. 198-203.
111. Elhage, R., et al., *Involvement of interleukin-6 in atherosclerosis but not in the prevention of fatty streak formation by 17beta-estradiol in apolipoprotein E-deficient mice.* Atherosclerosis, 2001. **156**(2): p. 315-20.
112. Uzui, H., S.K. Sinha, and T.B. Rajavashisth, *17 beta-Estradiol Inhibits Oxidized Low-Density Lipoprotein-Induced Increase in Matrix Metalloproteinase-9 Expression in Human Macrophages.* Journal of Investigative Medicine, 2011. **59**(7): p. 1104-1108.
113. Kim, J.K., et al., *Estrogen prevents cardiomyocyte apoptosis through inhibition of reactive oxygen species and differential regulation of p38 kinase isoforms.* J Biol Chem, 2006. **281**(10): p. 6760-7.
114. Borras, C., et al., *17 beta-oestradiol up-regulates longevity-related, antioxidant enzyme expression via the ERK1 and ERK2([MAPK])/NF kappa B cascade.* Aging Cell, 2005. **4**(3): p. 113-118.
115. Xu, Y., et al., *Estrogen improves cardiac recovery after ischemia/reperfusion by decreasing tumor necrosis factor-alpha.* Cardiovascular Research, 2006. **69**(4): p. 836-44.
116. Gourdy, P., et al., *Transforming growth factor activity is a key determinant for the effect of estradiol on fatty streak deposit in hypercholesterolemic mice.* Arterioscler Thromb Vasc Biol, 2007. **27**(10): p. 2214-21.
117. Oviedo, P.J., et al., *Estradiol induces endothelial cell migration and proliferation through estrogen receptor-enhanced RhoA/ROCK pathway.* Mol Cell Endocrinol, 2011. **335**(2): p. 96-103.
118. Han, G., et al., *Nongenomic, endothelium-independent effects of estrogen on human coronary smooth muscle are mediated by type I (neuronal) NOS and PI3-kinase-Akt signaling.* Am J Physiol Heart Circ Physiol, 2007. **293**(1): p. H314-21.
119. Tanguay, J.F., *Vascular healing after stenting: the role of 17-beta-estradiol in improving re-endothelialization and reducing restenosis.* Can J Cardiol, 2005. **21**(12): p. 1025-30.
120. Resanovic, I., et al., *Anti-atherogenic effects of 17beta-estradiol.* Horm Metab Res, 2013. **45**(10): p. 701-8.

121. Murphy, E. and C. Steenbergen, *Cardioprotection in females: a role for nitric oxide and altered gene expression.* Heart Failure Reviews, 2007. **12**(3-4): p. 293-300.
122. Chambliss, K.L., et al., *Estrogen receptor alpha and endothelial nitric oxide synthase are organized into a functional signaling module in caveolae.* Circ Res, 2000. **87**(11): p. E44-52.
123. Tziros, C. and J.E. Freedman, *The many antithrombotic actions of nitric oxide.* Current Drug Targets, 2006. **7**(10): p. 1243-1251.
124. Bian, K., M.F. Doursout, and F. Murad, *Vascular System: Role of Nitric Oxide in Cardiovascular Diseases.* Journal of Clinical Hypertension, 2008. **10**(4): p. 304-310.
125. Channon, K.M., H. Qian, and S.E. George, *Nitric oxide synthase in atherosclerosis and vascular injury: insights from experimental gene therapy.* Arterioscler Thromb Vasc Biol, 2000. **20**(8): p. 1873-81.
126. Mendelsohn, M.E., *Estrogen actions in the cardiovascular system.* Climacteric, 2009. **12**: p. 18-21.
127. Ruifrok, W.P., et al., *Estradiol-induced, endothelial progenitor cell-mediated neovascularization in male mice with hind-limb ischemia.* Vasc Med, 2009. **14**(1): p. 29-36.
128. Suwannaprapha, P., et al., *Improvement of function and morphology of tumor necrosis factor-alpha treated endothelial cells with 17-beta estradiol: a preliminary study for a feasible simple model for atherosclerosis.* Circ J, 2005. **69**(6): p. 730-8.
129. Yin, H., L. Chao, and J.L. Chao, *Nitric oxide mediates cardiac protection of tissue kallikrein by reducing inflammation and ventricular remodeling after myocardial ischemia/reperfusion.* Life Sciences, 2008. **82**(3-4): p. 156-165.
130. Abbas, A.M. and A.Z. Elsamanoudy, *Effects of 17 beta-estradiol and antioxidant administration on oxidative stress and insulin resistance in ovariectomized rats.* Canadian Journal of Physiology and Pharmacology, 2011. **89**(7): p. 497-504.
131. Patel, R.P., et al., *Cell signaling by reactive nitrogen and oxygen species in atherosclerosis.* Free Radic Biol Med, 2000. **28**(12): p. 1780-94.
132. Lee, M.Y., et al., *Estradiol-17 beta protects against hypoxia-induced hepatocyte injury through ER-mediated upregulation of Bcl-2 as well as ER-independent antioxidant effects.* Cell Research, 2008. **18**(4): p. 491-499.
133. Villablanca, A.C., et al., *17beta-estradiol prevents early-stage atherosclerosis in estrogen receptor-alpha deficient female mice.* J Cardiovasc Transl Res, 2009. **2**(3): p. 289-99.
134. Haas, E., et al., *Differential effects of 17beta-estradiol on function and expression of estrogen receptor alpha, estrogen receptor beta, and GPR30 in arteries and veins of patients with atherosclerosis.* Hypertension, 2007. **49**(6): p. 1358-63.
135. Billon-Gales, A., et al., *Endothelial estrogen receptor-alpha plays a crucial role in the atheroprotective action of 17beta-estradiol in low-density lipoprotein receptor-deficient mice.* Circulation, 2009. **120**(25): p. 2567-76.
136. Bowey, K., J.F. Tanguay, and M. Tabrizian, *2-Dioleoyl-sn-glycero-3-phosphocholine-based nanoliposomes as an effective delivery platform for 17beta-estradiol.* Eur J Pharm Biopharm, 2013.

137. Nippe, S. and S. General, *Combination of injectable ethinyl estradiol and drospirenone drug-delivery systems and characterization of their in vitro release.* Eur J Pharm Sci, 2012. **47**(4): p. 790-800.
138. Dasaratha Dhanaraju, M., et al., *Preparation and characterization of injectable microspheres of contraceptive hormones.* Int J Pharm, 2003. **268**(1-2): p. 23-9.
139. Mittal, G., et al., *Development and evaluation of polymer nanoparticles for oral delivery of estradiol to rat brain in a model of Alzheimer's pathology.* J Control Release, 2011. **150**(2): p. 220-8.
140. Tang, X., X.M. Wang, and N. Chi, *Preparation of estradiol chitosan nanoparticles for improving nasal absorption and brain targeting.* European Journal of Pharmaceutics and Biopharmaceutics, 2008. **70**(3): p. 735-740.
141. Das, M., et al., *Intranuclear Drug Delivery and Effective in Vivo Cancer Therapy via Estradiol-PEG-Appended Multiwalled Carbon Nanotubes.* Mol Pharm, 2013.
142. Abizaid, A., et al., *First human experience with the 17-beta-estradiol-eluting stent - The Estrogen And Stents To Eliminate Restenosis (EASTER) Trial.* Journal of the American College of Cardiology, 2004. **43**(6): p. 1118-1121.
143. Seegers, J.C., et al., *The cytotoxic effects of estradiol-17 beta, catecholestradiols and methoxyestradiols on dividing MCF-7 and HeLa cells.* J Steroid Biochem, 1989. **32**(6): p. 797-809.
144. Knight, C.G., ed. *Liposomes: From Physical Structure to Theraputic Applications*. Research Monographs in Cell and Tissue Physiology, ed. J.T. Dingle and J.L. Gordon. Vol. 7. 1981, Elsevier North-Holland: Amsterdam. 497.
145. New, R.R., ed. *Liposomes: A Practical Approash*. The Practical Approach Series, ed. D. Rickwood and B.D. Hames. IRL Press at Oxford University Press: New York. 301.
146. Afergan, E., et al., *Liposomal Simvastatin Attenuates Neointimal Hyperplasia in Rats.* Aaps Journal, 2010. **12**(2): p. 181-187.
147. Ma, K., et al., *Development of a successive targeting liposome with multi-ligand for efficient targeting gene delivery.* Journal of Gene Medicine, 2011. **13**(5): p. 290-301.
148. Okamura, Y., et al., *Visualization of liposomes carrying fibrinogen gamma-chain dodecapeptide accumulated to sites of vascular injury using computed tomography.* Nanomedicine : nanotechnology, biology, and medicine, 2010. **6**(2): p. 391-6.
149. Torchilin, V.P., *Recent advances with liposomes as pharmaceutical carriers.* Nature Reviews Drug Discovery, 2005. **4**(2): p. 145-160.
150. Woodle, M.C., *Controlling liposome blood clearance by surface-grafted polymers.* Advanced Drug Delivery Reviews, 1998. **32**(1-2): p. 139-152.
151. Malam, Y., M. Loizidou, and A.M. Seifalian, *Liposomes and nanoparticles: nanosized vehicles for drug delivery in cancer.* Trends in Pharmacological Sciences, 2009. **30**(11): p. 592-9.
152. McCarthy, J.R., *Multifunctional agents for concurrent imaging and therapy in cardiovascular disease.* Adv Drug Deliv Rev, 2010. **62**(11): p. 1023-30.
153. Juliano, R.L. and D. Stamp, *Effect of Particle-Size and Charge on Clearance Rates of Liposomes and Liposome Encapsulated Drugs.* Biochemical and Biophysical Research Communications, 1975. **63**(3): p. 651-658.

154. Caride, V.J. and B.L. Zaret, *Liposome Accumulation in Regions of Experimental Myocardial-Infarction.* Science, 1977. **198**(4318): p. 735-738.
155. Kaufmann, B.A., et al., *Molecular imaging of inflammation in atherosclerosis with targeted ultrasound detection of vascular cell adhesion molecule-1.* Circulation, 2007. **116**(3): p. 276-84.
156. Palmer, T.N., et al., *The Mechanism of Liposome Accumulation in Infarction.* Biochimica Et Biophysica Acta, 1984. **797**(3): p. 363-368.
157. Khaw, B.A., et al., *Plug and Seal - Prevention of Hypoxic Cardiocyte Death by Sealing Membrane Lesions with Antimyosin-Liposomes.* Nature Medicine, 1995. **1**(11): p. 1195-1198.
158. Torchilin, V.P., et al., *Poly(ethylene glycol)-coated anti-cardiac myosin immunoliposomes: Factors influencing targeted accumulation in the infarcted myocardium.* Biochimica Et Biophysica Acta-Biomembranes, 1996. **1279**(1): p. 75-83.
159. Monkkonen, J., et al., *The Effects of Liposome Surface-Charge and Size on the Intracellular Delivery of Clodronate and Gallium in-Vitro.* International Journal of Pharmaceutics, 1994. **107**(3): p. 189-197.
160. Monkkonen, J., et al., *Studies on Liposome Formulations for Intraarticular Delivery of Clodronate.* Journal of Controlled Release, 1995. **35**(2-3): p. 145-154.
161. Bally, M.B., et al., *Influence of poly(ethylene glycol) grafting density and polymer length on liposomes: Relating plasma circulation lifetimes to protein binding.* Biochimica Et Biophysica Acta-Biomembranes, 2007. **1768**(6): p. 1367-1377.
162. Immordino, M.L., F. Dosio, and L. Cattel, *Stealth liposomes: review of the basic science, rationale, and clinical applications, existing and potential.* Int J Nanomedicine, 2006. **1**(3): p. 297-315.
163. Lestini, B.J., et al., *Surface modification of liposomes for selective cell targeting in cardiovascular drug delivery.* J Control Release, 2002. **78**(1-3): p. 235-47.
164. Gregoriadis, G. and E.D. Neerunjun, *Homing of Liposomes to Target-Cells.* Biochemical and Biophysical Research Communications, 1975. **65**(2): p. 537-544.
165. Gao, J., et al., *The promotion of siRNA delivery to breast cancer overexpressing epidermal growth factor receptor through anti-EGFR antibody conjugation by immunoliposomes.* Biomaterials, 2011. **32**(13): p. 3459-3470.
166. Scott, R.C., et al., *Targeting VEGF-encapsulated immunoliposomes to MI heart improves vascularity and cardiac function.* Faseb Journal, 2009. **23**(10): p. 3361-7.
167. Verma, D.D., et al., *ATP-loaded immunoliposomes specific for cardiac myosin provide improved protection of the mechanical functions of myocardium from global ischemia in an isolated rat heart model.* Journal of Drug Targeting, 2006. **14**(5): p. 273-280.
168. Lim, S.J., et al., *Preparation and in vitro evaluation of anti-VCAM-1-Fab''-conjugated liposomes for the targeted delivery of the poorly water-soluble drug celecoxib.* Journal of Microencapsulation, 2011. **28**(3): p. 220-227.
169. Conyers, J.L., et al., *Antibody-Labeled Liposomes for CT Imaging of Atherosclerotic Plaques In Vitro Investigation of an Anti-ICAM Antibody-Labeled Liposome*

Containing Iohexol for Molecular Imaging of Atherosclerotic Plaques via Computed Tomography. Texas Heart Institute Journal, 2009. **36**(5): p. 393-403.
170. Gunawan, R.C. and D.T. Auguste, *The role of antibody synergy and membrane fluidity in the vascular targeting of immunoliposomes.* Biomaterials, 2010. **31**(5): p. 900-7.
171. Auguste, D.T. and R.C. Gunawan, *Immunoliposomes That Target Endothelium In Vitro Are Dependent on Lipid Raft Formation.* Molecular Pharmaceutics, 2010. **7**(5): p. 1569-1575.
172. Hamilton, A.J., et al., *Intravascular ultrasound molecular Imaging of atheroma components in vivo.* Journal of the American College of Cardiology, 2004. **43**(3): p. 453-460.
173. Hamilton, A., et al., *Left ventricular thrombus enhancement after intravenous injection of echogenic immunoliposomes - Studies in a new experimental model.* Circulation, 2002. **105**(23): p. 2772-2778.
174. Elbayoumi, T.A. and V.P. Torchilin, *Liposomes for targeted delivery of antithrombotic drugs.* Expert Opinion on Drug Delivery, 2008. **5**(11): p. 1185-1198.
175. Homem de Bittencourt, P.I., Jr., et al., *LipoCardium: endothelium-directed cyclopentenone prostaglandin-based liposome formulation that completely reverses atherosclerotic lesions.* Atherosclerosis, 2007. **193**(2): p. 245-58.
176. Torchilin, V.P., et al., *Preservation of Antimyosin Antibody-Activity after Covalent Coupling to Liposomes.* Biochemical and Biophysical Research Communications, 1979. **89**(4): p. 1114-1119.
177. Khaw, B.A., et al., *Cytoskeleton-specific immunoliposomes: sealing of hypoxic cells and intracellular delivery of DNA.* International Journal of Pharmaceutics, 1998. **162**(1-2): p. 71-76.
178. Khaw, B.A., J. DaSilva, and W.C. Hartner, *Cytoskeletal-antigen specific immunoliposome-targeted in vivo preservation of myocardial viability.* Journal of Controlled Release, 2007. **120**(1-2): p. 35-40.
179. Scott, R.C., et al., *Aiming for the heart: targeted delivery of drugs to diseased cardiac tissue.* Expert Opinion on Drug Delivery, 2008. **5**(4): p. 459-470.
180. Doggrell, S.A., *Statins in the 21st century: end of the simple story?* Expert Opinion on Investigational Drugs, 2001. **10**(9): p. 1755-1766.
181. Assmus, B., et al., *HMG-CoA reductase inhibitors reduce senescence and increase proliferation of endothelial progenitor cells via regulation of cell cycle regulatory genes.* Circ Res, 2003. **92**(9): p. 1049-55.
182. Nusca, A., R. Melfi, and G. Di Sciascio, *Percutaneous coronary interventions and statins therapy.* Ther Adv Cardiovasc Dis, 2008. **2**(2): p. 101-7.
183. Aso, S., et al., *Effective uptake of N-acetylglucosamine-conjugated liposomes by cardiomyocytes in vitro.* J Control Release, 2007. **122**(2): p. 189-98.
184. Csempesz, F., A. Sule, and I. Puskas, *Induced surface activity of supramolecular cyclodextrin-statin complexes: Relevance in drug delivery.* Colloids and Surfaces a-Physicochemical and Engineering Aspects, 2010. **354**(1-3): p. 308-313.

185. Verma, D.D., et al., *ATP-loaded liposomes effectively protect the myocardium in rabbits with an acute experimental myocardial infarction.* Pharm Res, 2005. **22**(12): p. 2115-20.
186. Haber, E., et al., *Route of administration-dependent anti-inflammatory effect of liposomal alendronate.* Journal of Controlled Release, 2010. **148**(2): p. 226-233.
187. Huang, S.L., et al., *Nitric oxide-loaded echogenic liposomes for nitric oxide delivery and inhibition of intimal hyperplasia.* J Am Coll Cardiol, 2009. **54**(7): p. 652-9.
188. Laing, S.T., et al., *Ultrasound-Enhanced Thrombolytic Effect of Tissue Plasminogen Activator-Loaded Echogenic Liposomes in an In Vivo Rabbit Aorta Thrombus Model.* Arterioscler Thromb Vasc Biol, 2011.
189. Leach, J.K., et al., *Accelerated thrombolysis in a rabbit model of carotid artery thrombosis with liposome-encapsulated and microencapsulated streptokinase.* Thromb Haemost, 2003. **90**(1): p. 64-70.
190. Joner, M., et al., *Site-Specific Targeting of Nanoparticle Prednisolone Reduces In-Stent Restenosis in a Rabbit Model of Established Atheroma.* Arteriosclerosis Thrombosis and Vascular Biology, 2008. **28**(11): p. 1960-U113.
191. Levchenko, T.S., et al., *ATP-loaded liposomes for targeted treatment in models of myocardial ischemia.* Methods Mol Biol, 2010. **605**: p. 361-75.
192. Hartner, W.C., et al., *ATP-loaded liposomes for treatment of myocardial ischemia.* Wiley Interdisciplinary Reviews-Nanomedicine and Nanobiotechnology, 2009. **1**(5): p. 530-539.
193. Xu, G.X., et al., *Adenosine-Triphosphate Liposomes - Encapsulation and Distribution Studies.* Pharmaceutical Research, 1990. **7**(5): p. 553-557.
194. Liang, W., et al., *ATP-containing immunoliposomes specific for cardiac myosin.* Curr Drug Deliv, 2004. **1**(1): p. 1-7.
195. Verma, D.D., et al., *ATP-loaded liposomes effectively protect mechanical functions of the myocardium from global ischemia in an isolated rat heart model.* J Control Release, 2005. **108**(2-3): p. 460-71.
196. Watts, N., *Bisphosphonates, statins, osteoporosis, and atherosclerosis.* South Med J, 2002. **95**(6): p. 578-82.
197. Moreau, M.F., et al., *Comparative effects of five bisphosphonates on apoptosis of macrophage cells in vitro.* Biochemical Pharmacology, 2007. **73**(5): p. 718-23.
198. Yu, B., et al., *Zoledronate inhibits the proliferation, adhesion and migration of vascular smooth muscle cells.* European Journal of Pharmacology, 2009. **602**(1): p. 124-131.
199. Shi, W.H., et al., *Zoledronate Inhibits Intimal Hyperplasia in Balloon-injured Rat Carotid Artery.* European Journal of Vascular and Endovascular Surgery, 2011. **41**(2): p. 288-293.
200. Damrauer, S.M., et al., *A20 inhibits post-angioplasty restenosis by blocking macrophage trafficking and decreasing adventitial neovascularization.* Atherosclerosis, 2010. **211**(2): p. 404-408.
201. Danenberg, H.D., et al., *Macrophage depletion by clodronate-containing liposomes reduces neointimal formation after balloon injury in rats and rabbits.* Circulation, 2002. **106**(5): p. 599-605.

202. Ylitalo, R., J. Monkkonen, and S. Yla-Herttuala, *Effects of liposome-encapsulated bisphosphonates on acetylated LDL metabolism, lipid accumulation and viability of phagocyting cells.* Life Sciences, 1997. **62**(5): p. 413-422.
203. Danenberg, H.D., et al., *Liposomal alendronate inhibits systemic innate immunity and reduces in-stent neointimal hyperplasia in rabbits.* Circulation, 2003. **108**(22): p. 2798-2804.
204. Epstein, H., et al., *Preparation of Alendronate Liposomes for Enhanced Stability and Bioactivity: In Vitro and In Vivo Characterization.* Aaps Journal, 2008. **10**(4): p. 505-515.
205. *Biorest Liposomal Alendronate With Stenting sTudy (BLAST)*. ClinicalTrials.gov 2010]; Available from: http://clinicaltrials.gov/ct2/show/NCT00739466.
206. Theoharis, S., M. Manunta, and P.H. Tan, *Gene delivery to vascular endothelium using chemical vectors: implications for cardiovascular gene therapy.* Expert Opin Biol Ther, 2007. **7**(5): p. 627-43.
207. Baker, A.H., *Designing gene delivery vectors for cardiovascular gene therapy.* Prog Biophys Mol Biol, 2004. **84**(2-3): p. 279-99.
208. Lavu, M., S. Gundewar, and D.J. Lefer, *Gene therapy for ischemic heart disease.* J Mol Cell Cardiol, 2011. **50**(5): p. 742-50.
209. Khurana, R., et al., *Vascular endothelial growth factor gene transfer inhibits neointimal macrophage accumulation in hypercholesterolemic rabbits.* Arteriosclerosis Thrombosis and Vascular Biology, 2004. **24**(6): p. 1074-1080.
210. Abegunewardene, N., et al., *Local Transient Myocardial Liposomal Gene Transfer of Inducible Nitric Oxide Synthase Does Not Aggravate Myocardial Function and Fibrosis and Leads to Moderate Neovascularization in Chronic Myocardial Ischemia in Pigs.* Microcirculation, 2010. **17**(1): p. 69-78.
211. Hedman, M., et al., *Safety and feasibility of catheter-based local intracoronary vascular endothelial growth factor gene transfer in the prevention of postangioplasty and in-stent restenosis and in the treatment of chronic myocardial ischemia - Phase II results of the Kuopio Angiogenesis Trial (KAT).* Circulation, 2003. **107**(21): p. 2677-2683.
212. von der Leyen, H.E., et al., *A Prospective, Single-Blind, Multicenter, Dose Escalation Study of Intracoronary iNOS Lipoplex (CAR-MP583) Gene Therapy for the Prevention of Restenosis in Patients with de novo or Restenotic Coronary Artery Lesion (REGENT I Extension).* Hum Gene Ther, 2011.
213. Hinkel, R., T. Trenkwalder, and C. Kupatt, *Gene therapy for ischemic heart disease.* Expert Opin Biol Ther, 2011. **11**(6): p. 723-37.
214. McEwan, J.R., et al., *Application to vascular adventitia of a nonviral vector for TIMP-1 gene therapy to prevent intimal hyperplasia.* Human Gene Therapy, 2006. **17**(7): p. 717-727.
215. Pfosser, A., et al., *Liposomal Hsp90 cDNA induces neovascularization via nitric oxide in chronic ischemia.* Cardiovascular Research, 2005. **65**(3): p. 728-736.
216. Pelisek, J., et al., *Vascular endothelial growth factor response in porcine coronary and peripheral arteries using nonsurgical occlusion model, local delivery, and*

liposome-mediated gene transfer. Endothelium-Journal of Endothelial Cell Research, 2003. **10**(4-5): p. 247-255.
217. Kaneda, Y., Y. Saeki, and R. Morishita, *Gene therapy using HVJ-liposomes: the best of both worlds?* Molecular Medicine Today, 1999. **5**(7): p. 298-303.
218. Ellison, K.E., et al., *Fusigenic liposome-mediated DNA transfer into cardiac myocytes.* J Mol Cell Cardiol, 1996. **28**(7): p. 1385-99.
219. Yin, X.H., et al., *Tissue factor pathway inhibitor gene delivery using HVJ-AVE liposomes markedly reduces restenosis in atherosclerotic arteries.* Cardiovascular Research, 2002. **56**(3): p. 454-463.
220. Yin, X., et al., *HVJ-AVE liposome-mediated Tissue Factor Pathway Inhibitor (TFPI) gene transfer with recombinant TFPI (rTFPI) irrigation attenuates restenosis in atherosclerotic arteries.* Int J Cardiol, 2009. **135**(2): p. 245-8.
221. Sakurai, H., et al., *Innate immune response induced by gene delivery vectors.* International Journal of Pharmaceutics, 2008. **354**(1-2): p. 9-15.
222. Leuschner, F. and M. Nahrendorf, *Molecular imaging of coronary atherosclerosis and myocardial infarction: considerations for the bench and perspectives for the clinic.* Circulation Research, 2011. **108**(5): p. 593-606.
223. Lipinski, M.J., et al., *MRI to detect atherosclerosis with gadolinium-containing immunomicelles targeting the macrophage scavenger receptor.* Magnetic resonance in medicine : official journal of the Society of Magnetic Resonance in Medicine / Society of Magnetic Resonance in Medicine, 2006. **56**(3): p. 601-10.
224. Lipinski, M.J., et al., *Macrophage-specific lipid-based nanoparticles improve cardiac magnetic resonance detection and characterization of human atherosclerosis.* JACC Cardiovasc Imaging, 2009. **2**(5): p. 637-47.
225. Eraso, L.H., et al., *Emerging diagnostic and therapeutic molecular imaging applications in vascular disease.* Vascular Medicine, 2011. **16**(2): p. 145-156.
226. Meaney, J.F.M. and M. Goyen, *Recent advances in contrast-enhanced magnetic resonance angiography.* European Radiology, 2007. **17**: p. B2-B6.
227. Kaul, S. and J.R. Lindner, *Visualizing coronary atherosclerosis in vivo: Thinking big, imaging small.* Journal of the American College of Cardiology, 2004. **43**(3): p. 461-463.
228. Ayyagari, A.L., et al., *Long-circulating liposomal contrast agents for magnetic resonance imaging.* Magnetic Resonance in Medicine, 2006. **55**(5): p. 1023-1029.
229. Annapragada, A.V., et al., *High-resolution vascular imaging of the rat spine using liposomal blood pool MR agent.* American Journal of Neuroradiology, 2007. **28**(1): p. 48-53.
230. Maiseyeu, A., et al., *Gadolinium-containing phosphatidylserine liposomes for molecular imaging of atherosclerosis.* Journal of Lipid Research, 2009. **50**(11): p. 2157-2163.
231. Allen, C., et al., *In vivo performance of a liposomal vascular contrast agent for CT and MR-based image guidance applications.* Pharmaceutical Research, 2007. **24**(6): p. 1193-1201.

232. Kluza, E., et al., *Synergistic Targeting of alpha(v)beta(3) Integrin and Galectin-1 with Heteromultivalent Paramagnetic Liposomes for Combined MR Imaging and Treatment of Angiogenesis.* Nano Letters, 2010. **10**(1): p. 52-58.
233. Lanza, G.M. and S.A. Wickline, *Targeted ultrasonic contrast agents for molecular imaging and therapy.* Progress in Cardiovascular Diseases, 2001. **44**(1): p. 13-31.
234. Smith, D.A., et al., *Destruction thresholds of echogenic liposomes with clinical diagnostic ultrasound.* Ultrasound in Medicine and Biology, 2007. **33**(5): p. 797-809.
235. Huang, S.L., et al., *Improving ultrasound reflectivity and stability of echogenic liposomal dispersions for use as targeted ultrasound contrast agents.* Journal of Pharmaceutical Sciences, 2001. **90**(12): p. 1917-1926.
236. Demos, S.M., et al., *In vivo targeting of acoustically reflective liposomes for intravascular and transvascular ultrasonic enhancement.* J Am Coll Cardiol, 1999. **33**(3): p. 867-75.
237. Hagisawa, K., et al., *Enhancement of ultrasonic thrombus imaging using novel liposomal bubbles targeting activated platelet glycoprotein IIb/IIIa complex-in vitro and in vivo study.* Int J Cardiol, 2010.
238. Herbst, S.M., et al., *Delivery of Stem Cells to Porcine Arterial Wall with Echogenic Liposomes Conjugated to Antibodies against CD34 and Intercellular Adhesion Molecule-1.* Molecular Pharmaceutics, 2010. **7**(1): p. 3-11.
239. Yang, C.S., L.A. Tai, and Y.C. Wang, *Heat-activated sustaining nitric oxide release from zwitterionic diazeniumdiolate loaded in thermo-sensitive liposomes.* Nitric Oxide-Biology and Chemistry, 2010. **23**(1): p. 60-64.
240. Laing, S.T., et al., *Ultrasound-mediated delivery of echogenic immunoliposomes to porcine vascular smooth muscle cells in vivo.* Journal of Liposome Research, 2010. **20**(2): p. 160-7.
241. Schroeder, A., J. Kost, and Y. Barenholz, *Ultrasound, liposomes, and drug delivery: principles for using ultrasound to control the release of drugs from liposomes.* Chem Phys Lipids, 2009. **162**(1-2): p. 1-16.
242. Buchanan, K.D., et al., *Encapsulation of NF-kappaB decoy oligonucleotides within echogenic liposomes and ultrasound-triggered release.* J Control Release, 2010. **141**(2): p. 193-8.
243. Newman, C.M., et al., *Ultrasound gene therapy: On the road from concept to reality.* Echocardiography-a Journal of Cardiovascular Ultrasound and Allied Techniques, 2001. **18**(4): p. 339-347.
244. Szebeni, J., et al., *Activation of complement by therapeutic liposomes and other lipid excipient-based therapeutic products: Prediction and prevention.* Advanced Drug Delivery Reviews, 2011. **63**(12): p. 1020-1030.
245. Laye, C., D.J. McClements, and J. Weiss, *Formation of biopolymer-coated liposomes by electrostatic deposition of chitosan.* Journal of Food Science, 2008. **73**(5): p. N7-N15.
246. Scarioti, G.D., et al., *Nanocapsule of cationic liposomes obtained using "in situ" acrylic acid polymerization: Stability, surface charge and biocompatibility.* Colloids and Surfaces B-Biointerfaces, 2011. **87**(2): p. 267-272.

247. Preat, V., F. Danhier, and O. Feron, *To exploit the tumor microenvironment: Passive and active tumor targeting of nanocarriers for anti-cancer drug delivery.* Journal of Controlled Release, 2010. **148**(2): p. 135-146.
248. Libby, P., P.M. Ridker, and A. Maseri, *Inflammation and atherosclerosis.* Circulation, 2002. **105**(9): p. 1135-43.
249. Libby, P., *Vascular biology of atherosclerosis: overview and state of the art.* Am J Cardiol, 2003. **91**(3A): p. 3A-6A.
250. Wild, D.G., ed. *Immunoassay Handbook - Theory and Applications of Ligand Binding, ELISA and Related Techniques* 4th Edition ed. 2013, Elsiver: http://app.knovel.com/hotlink/toc/id:kpIHTALBE2/immunoassay-handbook.
251. Liang, Y.J., et al., *C-reactive protein activates the nuclear factor-kappaB pathway and induces vascular cell adhesion molecule-1 expression through CD32 in human umbilical vein endothelial cells and aortic endothelial cells.* J Mol Cell Cardiol, 2006. **40**(3): p. 412-20.
252. Leico Technologies, I. *General Western Blot Protocol*. 2014 [cited 2014.
253. Hayworth, D. *Overview of ELISA*. 2014 January 12, 2013.
254. Odell, I.D. and D. Cook, *Immunofluorescence techniques.* J Invest Dermatol, 2013. **133**(1): p. e4.
255. Zhang, J., et al., *Regulation of endothelial cell adhesion molecule expression by mast cells, macrophages, and neutrophils.* PLoS One, 2011. **6**(1): p. e14525.
256. Rautou, P.E., et al., *Microparticles from human atherosclerotic plaques promote endothelial ICAM-1-dependent monocyte adhesion and transendothelial migration.* Circ Res, 2011. **108**(3): p. 335-43.
257. Chen, Y., et al., *Characterization of VCAM-1-binding peptide-functionalized quantum dots for molecular imaging of inflamed endothelium.* PLoS One, 2013. **8**(12): p. e83805.
258. Kitayama, Y. and T. Takeuchi, *Localized Surface Plasmon Resonance Nanosensing of C-Reactive Protein with Poly(2-methacryloyloxyethyl phosphorylcholine)-Grafted Gold Nanoparticles Prepared by Surface-Initiated Atom Transfer Radical Polymerization.* Anal Chem, 2014.
259. Riezzo, I., et al., *Confocal Laser Scanning Microscope, Raman Microscopy and Western Blotting to Evaluate Inflammatory Response After Myocardial Infarction.* Curr Vasc Pharmacol, 2013.
260. Matthaus, C., et al., *Chapter 10: Infrared and Raman microscopy in cell biology.* Methods Cell Biol, 2008. **89**: p. 275-308.
261. Draux, F., et al., *Raman spectral imaging of single living cancer cells: a preliminary study.* Analyst, 2009. **134**(3): p. 542-8.
262. Notingher, L., et al., *Multivariate analysis of Raman spectra for in vitro non-invasive studies of living cells.* Journal of Molecular Structure, 2005. **744**: p. 179-185.
263. Scientific, H. *Introduction to Raman Spectroscopy* 2014 2014].
264. Milewski, R.J., et al., *Automated processing of label-free Raman microscope images of macrophage cells with standardized regression for high-throughput analysis.* Immunome Res, 2010. **6**: p. 11.

265. Fleischmann, M., P.J. Hendra, and Mcquilla, *Raman spectra of pyridine adsorbed at a silver electrode.* Chem Phys Lett, 1974. **26**: p. 163-166.
266. Lee, S.J., A.R. Morrill, and M. Moskovits, *Hot spots in silver nanowire bundles for surface-enhanced Raman spectroscopy.* J Am Chem Soc, 2006. **128**(7): p. 2200-1.
267. Negri, P., et al., *Ultrasensitive surface-enhanced Raman scattering flow detector using hydrodynamic focusing.* Anal Chem, 2013. **85**(21): p. 10159-66.
268. Schutz, M., et al., *Hydrophilically stabilized gold nanostars as SERS labels for tissue imaging of the tumor suppressor p63 by immuno-SERS microscopy.* Chem Commun (Camb), 2011. **47**(14): p. 4216-8.
269. Yin, W.Z., et al., *Application of surface-enhanced Raman in skin cancer by plasma.* Laser Physics, 2012. **22**(5): p. 996-1001.
270. Yuan, H.K., et al., *Spectral characterization and intracellular detection of Surface-Enhanced Raman Scattering (SERS)-encoded plasmonic gold nanostars.* Journal of Raman Spectroscopy, 2013. **44**(2): p. 234-239.
271. Tian, L., N. Gandra, and S. Singamaneni, *Monitoring controlled release of payload from gold nanocages using surface enhanced Raman scattering.* ACS Nano, 2013. **7**(5): p. 4252-60.
272. Jung, S., et al., *Theragnostic pH-sensitive gold nanoparticles for the selective surface enhanced Raman scattering and photothermal cancer therapy.* Anal Chem, 2013. **85**(16): p. 7674-81.
273. Le Ru, E.C., et al., *Surface Enhanced Raman Scattering Enhancement Factors: A Comprehensive Study.* The Journal of Physical Chemistry 2007. **111**(37): p. 13794-13803.
274. McGuinness, C.D., et al., *Single molecule level detection of allophycocyanin by surface enhanced resonance Raman scattering.* Analyst, 2007. **132**(7): p. 633-4.
275. Li, L., et al., *Single molecule SERS and detection of biomolecules with a single gold nanoparticle on a mirror junction.* Analyst, 2013. **138**(16): p. 4574-8.
276. Le Ru, E.C. and P.G. Etchegoin, *Principles of Surface-Enhanced Raman Spectroscopy and Related Plasmonic Effects*. 2009, Amsterdam: Elsevier.
277. Le Ru, E.C. and P.G. Etchegoin, *Basic Electromagnetic Theory of SERS, in Surface-Enhanced Raman Spectroscopy: Analytical, Biophysical and Life Science Applications*, ed. S. Schlucker. 2011, Weinheim, Germany: Wiley-VCH.
278. Hering, K., et al., *SERS: a versatile tool in chemical and biochemical diagnostics.* Anal Bioanal Chem, 2008. **390**(1): p. 113-24.
279. Fan, M., G.F. Andrade, and A.G. Brolo, *A review on the fabrication of substrates for surface enhanced Raman spectroscopy and their applications in analytical chemistry.* Anal Chim Acta, 2011. **693**(1-2): p. 7-25.
280. Grubisha, D.S., et al., *Femtomolar detection of prostate-specific antigen: an immunoassay based on surface-enhanced Raman scattering and immunogold labels.* Anal Chem, 2003. **75**(21): p. 5936-43.
281. Papadopoulou, E. and S.E. Bell, *Label-free detection of nanomolar unmodified single- and double-stranded DNA by using surface-enhanced Raman spectroscopy on Ag and Au colloids.* Chemistry, 2012. **18**(17): p. 5394-400.

282. Dougan, J.A. and K. Faulds, *Surface enhanced Raman scattering for multiplexed detection.* Analyst, 2012. **137**(3): p. 545-54.
283. Wang, Y., L.J. Tang, and J.H. Jiang, *Surface-enhanced Raman spectroscopy-based, homogeneous, multiplexed immunoassay with antibody-fragments-decorated gold nanoparticles.* Anal Chem, 2013. **85**(19): p. 9213-20.
284. Wang, Y., B. Yan, and L. Chen, *SERS tags: novel optical nanoprobes for bioanalysis.* Chem Rev, 2013. **113**(3): p. 1391-428.
285. Vitol, E.A., et al., *Nanoprobes for intracellular and single cell surface-enhanced Raman spectroscopy (SERS).* Journal of Raman Spectroscopy, 2012. **43**(7): p. 817-827.
286. Kneipp, J., et al., *Novel optical nanosensors for probing and imaging live cells.* Nanomedicine, 2010. **6**(2): p. 214-26.
287. Schlucker, S., *SERS microscopy: nanoparticle probes and biomedical applications.* Chemphyschem, 2009. **10**(9-10): p. 1344-54.
288. McQueenie, R., et al., *Detection of Inflammation in Vivo by Surface-Enhanced Raman Scattering Provides Higher Sensitivity Than Conventional Fluorescence Imaging.* Analytical Chemistry, 2012. **84**(14): p. 5968-5975.
289. Mao, Z., et al., *Predictive value of the surface-enhanced resonance Raman scattering-based MTT assay: a rapid and ultrasensitive method for cell viability in situ.* Anal Chem, 2013. **85**(15): p. 7361-8.
290. Jiang, X., et al., *Surface-Enhanced Raman Scattering-Based Sensing In Vitro: Facile and Label-Free Detection of Apoptotic Cells at the Single-Cell Level.* Anal Chem, 2013.
291. Zhang, Y., et al., *Molecular imaging with SERS-active nanoparticles.* Small, 2011. **7**(23): p. 3261-9.
292. Park, H., et al., *SERS imaging of HER2-overexpressed MCF7 cells using antibody-conjugated gold nanorods.* Phys Chem Chem Phys, 2009. **11**(34): p. 7444-9.
293. Potara, M., et al., *Chitosan-coated triangular silver nanoparticles as a novel class of biocompatible, highly sensitive plasmonic platforms for intracellular SERS sensing and imaging.* Nanoscale, 2013. **5**(13): p. 6013-22.
294. Wang, Y. and T. Asefa, *Poly(allylamine)-stabilized colloidal copper nanoparticles: synthesis, morphology, and their surface-enhanced Raman scattering properties.* Langmuir, 2010. **26**(10): p. 7469-74.
295. Liu, X., et al., *Liposome-mediated enhancement of the sensitivity in immunoassay based on surface-enhanced Raman scattering at gold nanosphere array substrate.* Talanta, 2008. **75**(3): p. 797-803.
296. Maiti, K.K., et al., *Development of biocompatible SERS nanotag with increased stability by chemisorption of reporter molecule for in vivo cancer detection.* Biosens Bioelectron, 2010. **26**(2): p. 398-403.
297. Ji, X.H., et al., *Immunoassay using the probe-labeled Au/Ag core-shell nanoparticles based on surface-enhanced Raman scattering.* Colloids and Surfaces a-Physicochemical and Engineering Aspects, 2005. **257-58**: p. 171-175.

298. Freitag, I., et al., *Preparation and characterization of multicore SERS labels by controlled aggregation of gold nanoparticles.* Vibrational Spectroscopy, 2012. **60**: p. 79-84.
299. Boca, S., et al., *Flower-shaped gold nanoparticles: synthesis, characterization and their application as SERS-active tags inside living cells.* Nanotechnology, 2011. **22**(5): p. 055702.
300. Yang, J., et al., *Surface-enhanced Raman spectroscopy based quantitative bioassay on aptamer-functionalized nanopillars using large-area Raman mapping.* ACS Nano, 2013. **7**(6): p. 5350-9.
301. Craig, G.A., P.J. Allen, and M.D. Mason, *Synthesis, characterization, and functionalization of gold nanoparticles for cancer imaging.* Methods Mol Biol, 2010. **624**: p. 177-93.
302. Krpetic, Z., et al., *Importance of nanoparticle size in colorimetric and SERS-based multimodal trace detection of Ni(II) ions with functional gold nanoparticles.* Small, 2012. **8**(5): p. 707-14.
303. Joseph, V., et al., *SERS enhancement of gold nanospheres of defined size.* Journal of Raman Spectroscopy, 2011. **42**(9): p. 1736-1742.
304. Guo, X., et al., *Silver-gold core-shell nanoparticles containing methylene blue as SERS labels for probing and imaging of live cells.* Microchimica Acta, 2012. **178**(1-2): p. 229-236.
305. Liu, M., et al., *Intracellular surface-enhanced Raman scattering probe based on gold nanorods functionalized with mercaptohexadecanoic acid with reduced cytotoxicity.* Biotechnology and Applied Biochemistry, 2012. **59**(5): p. 381-387.
306. Li, Q., et al., *High surface-enhanced Raman scattering performance of individual gold nanoflowers and their application in live cell imaging.* Small, 2013. **9**(6): p. 927-32.
307. Fales, A.M., H. Yuan, and T. Vo-Dinh, *Silica-Coated Gold Nanostars for Combined Surface-Enhanced Raman Scattering (SERS) Detection and Singlet-Oxygen Generation: A Potential Nanoplatform for Theranostics.* Langmuir, 2011. **27**(19): p. 12186-12190.
308. Kneipp, K., et al., *Ultrasensitive chemical analysis by Raman spectroscopy.* Chem Rev, 1999. **99**(10): p. 2957-76.
309. Hinterwirth, H., W. Lindner, and M. Lammerhofer, *Bioconjugation of trypsin onto gold nanoparticles: effect of surface chemistry on bioactivity.* Anal Chim Acta, 2012. **733**: p. 90-7.
310. Chen, J.W., et al., *Immunoassay using surface-enhanced Raman scattering based on aggregation of reporter-labeled immunogold nanoparticles.* Anal Bioanal Chem, 2008. **392**(1-2): p. 187-93.
311. Porter, M.D., et al., *SERS as a bioassay platform: fundamentals, design, and applications.* Chem Soc Rev, 2008. **37**(5): p. 1001-11.
312. Hu, J., et al., *Sub-attomolar HIV-1 DNA detection using surface-enhanced Raman spectroscopy.* Analyst, 2010. **135**(5): p. 1084-9.
313. Rodriguez-Lorenzo, L., et al., *Zeptomol detection through controlled ultrasensitive surface-enhanced Raman scattering.* J Am Chem Soc, 2009. **131**(13): p. 4616-8.

314. Li, M., et al., *Three-dimensional hierarchical plasmonic nano-architecture enhanced surface-enhanced Raman scattering immunosensor for cancer biomarker detection in blood plasma.* ACS Nano, 2013. **7**(6): p. 4967-76.
315. Noble, J., et al., *Optical scattering artifacts observed in the development of multiplexed surface enhanced Raman spectroscopy nanotag immunoassays.* Anal Chem, 2012. **84**(19): p. 8246-52.
316. Lee, M., et al., *Highly reproducible immunoassay of cancer markers on a gold-patterned microarray chip using surface-enhanced Raman scattering imaging.* Biosens Bioelectron, 2011. **26**(5): p. 2135-41.
317. Chon, H., et al., *Simultaneous immunoassay for the detection of two lung cancer markers using functionalized SERS nanoprobes.* Chemical Communications, 2011. **47**(46): p. 12515-12517.
318. Lee, S., et al., *Rapid and sensitive phenotypic marker detection on breast cancer cells using surface-enhanced Raman scattering (SERS) imaging.* Biosens Bioelectron, 2014. **51**: p. 238-43.
319. Nithipatikom, K., et al., *Characterization and application of Raman labels for confocal Raman microspectroscopic detection of cellular proteins in single cells.* Anal Biochem, 2003. **322**(2): p. 198-207.
320. Ock, K., et al., *Real-time monitoring of glutathione-triggered thiopurine anticancer drug release in live cells investigated by surface-enhanced Raman scattering.* Anal Chem, 2012. **84**(5): p. 2172-8.
321. Balint, S., et al., *Monitoring of local pH in photodynamic therapy-treated live cancer cells using surface-enhanced Raman scattering probes.* Journal of Raman Spectroscopy, 2011. **42**(6): p. 1215-1221.
322. Sathuluri, R.R., et al., *Gold nanoparticle-based surface-enhanced Raman scattering for noninvasive molecular probing of embryonic stem cell differentiation.* PLoS One, 2011. **6**(8): p. e22802.
323. Yang, J., et al., *Tracking multiplex drugs and their dynamics in living cells using the label-free surface-enhanced Raman scattering technique.* Mol Pharm, 2012. **9**(4): p. 842-9.
324. Wang, Y., L. Chen, and P. Liu, *Biocompatible triplex Ag@SiO2@mTiO2 core-shell nanoparticles for simultaneous fluorescence-SERS bimodal imaging and drug delivery.* Chemistry, 2012. **18**(19): p. 5935-43.
325. Yang, J., et al., *Distinguishing breast cancer cells using surface-enhanced Raman scattering.* Anal Bioanal Chem, 2012. **402**(3): p. 1093-100.
326. Lee, S., et al., *Fabrication of SERS-fluorescence dual modal nanoprobes and application to multiplex cancer cell imaging.* Nanoscale, 2012. **4**(1): p. 124-129.
327. Ko, J., et al., *SERS-based immunoassay of tumor marker VEGF using DNA aptamers and silica-encapsulated hollow gold nanospheres.* Phys Chem Chem Phys, 2012.
328. Maiti, K.K., et al., *Multiplex cancer cell detection by SERS nanotags with cyanine and triphenylmethine Raman reporters.* Chem Commun (Camb), 2011. **47**(12): p. 3514-6.

329. Matschulat, A., D. Drescher, and J. Kneipp, *Surface-enhanced Raman scattering hybrid nanoprobe multiplexing and imaging in biological systems.* ACS Nano, 2010. **4**(6): p. 3259-69.
330. Zavaleta, C.L., et al., *Multiplexed imaging of surface enhanced Raman scattering nanotags in living mice using noninvasive Raman spectroscopy.* Proc Natl Acad Sci U S A, 2009. **106**(32): p. 13511-6.
331. Bantz, K.C., et al., *Recent progress in SERS biosensing.* Physical Chemistry Chemical Physics, 2011. **13**(24): p. 11551-11567.
332. Maiti, K.K., et al., *Multiplex targeted in vivo cancer detection using sensitive near-infrared SERS nanotags.* Nano Today, 2012. **7**(2): p. 85-93.
333. Gregoriadis, G., *Drug entrapment in liposomes.* FEBS Lett, 1973. **36**(3): p. 292-6.
334. Bangham, A.D. and R.W. Horne, *Negative Staining of Phospholipids and Their Structural Modification by Surface-Active Agents as Observed in the Electron Microscope.* J Mol Biol, 1964. **8**: p. 660-8.
335. Horne, R.W., A.D. Bangham, and V.P. Whittaker, *Negatively Stained Lipoprotein Membranes.* Nature, 1963. **200**: p. 1340.
336. Lopes, R.M., et al., *Formulation of oryzalin (ORZ) liposomes: in vitro studies and in vivo fate.* Eur J Pharm Biopharm, 2012. **82**(2): p. 281-90.
337. Murata, M., et al., *Pulmonary delivery of elcatonin using surface-modified liposomes to improve systemic absorption: Polyvinyl alcohol with a hydrophobic anchor and chitosan oligosaccharide as effective surface modifiers.* European Journal of Pharmaceutics and Biopharmaceutics, 2012. **80**(2): p. 340-346.
338. Wang, J.P. and G.H. Huang, *Preparation of itraconazole-loaded liposomes coated by carboxymethyl chitosan and its pharmacokinetics and tissue distribution.* Drug Delivery, 2011. **18**(8): p. 631-638.
339. Soininen, S.K., et al., *Targeted delivery via avidin fusion protein: intracellular fate of biotinylated doxorubicin derivative and cellular uptake kinetics and biodistribution of biotinylated liposomes.* Eur J Pharm Sci, 2012. **47**(5): p. 848-56.
340. Kontogiannopoulos, K.N., et al., *Shikonin-loaded liposomes as a new drug delivery system: Physicochemical characterization and in vitro cytotoxicity.* European Journal of Lipid Science and Technology, 2011. **113**(9): p. 1113-1123.
341. Al-Jamal, W.T. and K. Kostarelos, *Liposomes: From a Clinically Established Drug Delivery System to a Nanoparticle Platform for Theranostic Nanomedicine.* Accounts of Chemical Research, 2011. **44**(10): p. 1094-1104.
342. Mattheolabakis, G., et al., *Sterically stabilized liposomes incorporating the novel anticancer agent phospho-ibuprofen (MDC-917): preparation, characterization, and in vitro/in vivo evaluation.* Pharm Res, 2012. **29**(6): p. 1435-43.
343. Rahman, Y.E., et al., *Liposomes containing 3H-actinomycin D. differential tissue distribution by varying the mode of drug incorporation.* Eur J Cancer, 1975. **11**(12): p. 883-9.
344. Gregoriadis, G., Leathwoo.Pd, and B.E. Ryman, *Enzyme Entrapment in Liposomes.* Febs Letters, 1971. **14**(2): p. 95-&.

345. Yun, X., et al., *Nanoparticles for targeted delivery of antioxidant enzymes to the brain after cerebral ischemia and reperfusion injury.* J Cereb Blood Flow Metab, 2013. **33**(4): p. 583-92.
346. Kowapradit, J., et al., *Methylated N-(4-N,N-dimethylaminobenzyl) chitosan coated liposomes for oral protein drug delivery.* Eur J Pharm Sci, 2012. **47**(2): p. 359-66.
347. Gregoriadis, G. and B.E. Ryman, *Fate of Protein-Containing Liposomes Injected into Rats - Approach to Treatment of Storage Diseases.* European Journal of Biochemistry, 1972. **24**(3): p. 485-&.
348. Yang, S.Y., et al., *Comprehensive study of cationic liposomes composed of DC-Chol and cholesterol with different mole ratios for gene transfection.* Colloids Surf B Biointerfaces, 2013. **101**: p. 6-13.
349. Fraley, R., et al., *Introduction of Liposome-Encapsulated Sv40 DNA into Cells.* Journal of Biological Chemistry, 1980. **255**(21): p. 431-435.
350. Mitchell, N., et al., *Incorporation of paramagnetic, fluorescent and PET/SPECT contrast agents into liposomes for multimodal imaging.* Biomaterials, 2013. **34**(4): p. 1179-92.
351. Magin, R.L., et al., *Liposome delivery of NMR contrast agents for improved tissue imaging.* Magn Reson Med, 1986. **3**(3): p. 440-7.
352. Channarong, S., et al., *Development and Evaluation of Chitosan-Coated Liposomes for Oral DNA Vaccine: The Improvement of Peyer's Patch Targeting Using a Polyplex-Loaded Liposomes.* AAPS PharmSciTech, 2011. **12**(1): p. 192-200.
353. Michalek, S.M., et al., *Liposomes as oral adjuvants.* Curr Top Microbiol Immunol, 1989. **146**: p. 51-8.
354. Xu, Q.G., Y. Tanaka, and J.T. Czernuszka, *Encapsulation and release of a hydrophobic drug from hydroxyapatite coated liposomes.* Biomaterials, 2007. **28**(16): p. 2687-2694.
355. El Maghraby, G.M.M., A.C. Williams, and B.W. Barry, *Drug interaction and location in liposomes: correlation with polar surface areas.* International Journal of Pharmaceutics, 2005. **292**(1-2): p. 179-185.
356. Lemieux, C., I. Cloutier, and J.F. Tanguay, *Menstrual cycle influences endothelial progenitor cell regulation: a link to gender differences in vascular protection?* Int J Cardiol, 2009. **136**(2): p. 200-10.
357. Stice, J.P., et al., *17beta-Estradiol, aging, inflammation, and the stress response in the female heart.* Endocrinology, 2011. **152**(4): p. 1589-98.
358. Ortmann, J., et al., *Estrogen receptor-alpha but not -beta or GPER inhibits high glucose-induced human VSMC proliferation: potential role of ROS and ERK.* J Clin Endocrinol Metab, 2011. **96**(1): p. 220-8.
359. Geraldes, P., et al., *Local delivery of 17-beta-estradiol modulates collagen content in coronary porcine arteries after PTCA and stent implantation.* J Vasc Res, 2008. **45**(6): p. 503-11.
360. Machado, S.R., et al., *Preparation and characterization of D, L-PLA loaded 17-beta-Estradiol valerate by emulsion/evaporation methods.* J Microencapsul, 2008: p. 1-11.

361. Cerne, J.Z., et al., *Estrogen metabolism genotypes, use of long-term hormone replacement therapy and risk of postmenopausal breast cancer.* Oncol Rep, 2011. **26**(2): p. 479-85.
362. Reddy, B.S. and R. Banerjee, *17 beta-estradiol-associated stealth-liposomal delivery of anticancer gene to breast cancer cells.* Angewandte Chemie-International Edition, 2005. **44**(41): p. 6723-6727.
363. Haeri, A., et al., *PEGylated estradiol benzoate liposomes as a potential local vascular delivery system for treatment of restenosis.* J Microencapsul, 2011.
364. Parveen, S., R. Misra, and S.K. Sahoo, *Nanoparticles: a boon to drug delivery, therapeutics, diagnostics and imaging.* Nanomedicine, 2012. **8**(2): p. 147-66.
365. Machado, S.R.P., et al., *Preparation and characterization of D, L-PLA loaded 17-beta-Estradiol valerate by emulsion/evaporation methods.* Journal of Microencapsulation, 2009. **26**(3): p. 202-213.
366. Muthu, M.S., et al., *Vitamin E TPGS coated liposomes enhanced cellular uptake and cytotoxicity of docetaxel in brain cancer cells.* Int J Pharm, 2011. **421**(2): p. 332-40.
367. Biruss, B., R. Dietl, and C. Valenta, *The influence of selected steroid hormones on the physicochemical behaviour of DPPC liposomes.* Chemistry and Physics of Lipids, 2007. **148**(2): p. 84-90.
368. Parrish, D., et al., *Experimental charge density study of estrogens: 17beta-estradiol.urea.* J Phys Chem B, 2006. **110**(51): p. 26442-7.
369. Zhang, L., et al., *Physical characterization and cellular uptake of propylene glycol liposomes in vitro.* Drug Development and Industrial Pharmacy, 2012. **38**(3): p. 365-371.
370. Favre, J., et al., *Endothelial estrogen receptor {alpha} plays an essential role in the coronary and myocardial protective effects of estradiol in ischemia/reperfusion.* Arterioscler Thromb Vasc Biol, 2010. **30**(12): p. 2562-7.
371. Erwin, G.S., et al., *Estradiol-treated mesenchymal stem cells improve myocardial recovery after ischemia.* J Surg Res, 2009. **152**(2): p. 319-24.
372. Donaldson, C., et al., *Estrogen Attenuates Left Ventricular and Cardiomyocyte Hypertrophy by an Estrogen Receptor-Dependent Pathway That Increases Calcineurin Degradation.* Circulation Research, 2009. **104**(2): p. 265-U275.
373. Thor, D., et al., *The effect of 17 beta-estradiol on intracellular calcium homeostasis in human endothelial cells.* Eur J Pharmacol, 2010. **630**(1-3): p. 92-9.
374. Garg, M., et al., *Ethinylestradiol-loaded ultraflexible liposomes: pharmacokinetics and pharmacodynamics.* Journal of Pharmacy and Pharmacology, 2006. **58**(4): p. 459-68.
375. Lu, T.L., et al., *Ethinylestradiol liposome preparation and its effects on ovariectomized rats' osteoporosis.* Drug Delivery, 2011. **18**(7): p. 468-477.
376. Bjorkbacka, H., G.N. Fredrikson, and J. Nilsson, *Emerging biomarkers and intervention targets for immune-modulation of atherosclerosis - a review of the experimental evidence.* Atherosclerosis, 2013. **227**(1): p. 9-17.
377. Priyanka, H.P., et al., *Estrogen modulates in vitro T cell responses in a concentration- and receptor-dependent manner: effects on intracellular molecular targets and antioxidant enzymes.* Mol Immunol, 2013. **56**(4): p. 328-39.

378. Devaraj, S., U. Singh, and I. Jialal, *The evolving role of C-reactive protein in atherothrombosis.* Clin Chem, 2009. **55**(2): p. 229-38.
379. Kawanami, D., et al., *C-reactive protein induces VCAM-1 gene expression through NF-kappaB activation in vascular endothelial cells.* Atherosclerosis, 2006. **185**(1): p. 39-46.
380. Kibayashi, E., et al., *Inhibitory effect of pitavastatin (NK-104) on the C-reactive-protein-induced interleukin-8 production in human aortic endothelial cells.* Clin Sci (Lond), 2005. **108**(6): p. 515-21.
381. Elzainy, A.A., et al., *Hydroxyzine- and cetirizine-loaded liposomes: effect of duration of thin film hydration, freeze-thawing, and changing buffer pH on encapsulation and stability.* Drug Dev Ind Pharm, 2005. **31**(3): p. 281-91.
382. Ghanbarzadeh, S., H. Valizadeh, and P. Zakeri-Milani, *Application of response surface methodology in development of sirolimus liposomes prepared by thin film hydration technique.* Bioimpacts, 2013. **3**(2): p. 75-81.
383. Apostolakis, S., et al., *Interleukin 8 and cardiovascular disease.* Cardiovasc Res, 2009. **84**(3): p. 353-60.
384. Bradley, J.R., *TNF-mediated inflammatory disease.* J Pathol, 2008. **214**(2): p. 149-60.
385. Kleinbongard, P., R. Schulz, and G. Heusch, *TNF alpha in myocardial ischemia/reperfusion, remodeling and heart failure.* Heart Failure Reviews, 2011. **16**(1): p. 49-69.
386. Huo, Y. and K. Ley, *Adhesion molecules and atherogenesis.* Acta Physiol Scand, 2001. **173**(1): p. 35-43.
387. Hartman, J. and W.H. Frishman, *Inflammation and atherosclerosis: a review of the role of interleukin-6 in the development of atherosclerosis and the potential for targeted drug therapy.* Cardiol Rev, 2014. **22**(3): p. 147-51.
388. Lutters, B.C., et al., *Blocking endothelial adhesion molecules: a potential therapeutic strategy to combat atherogenesis.* Curr Opin Lipidol, 2004. **15**(5): p. 545-52.
389. Hope, S.A. and I.T. Meredith, *Cellular adhesion molecules and cardiovascular disease. Part I. Their expression and role in atherogenesis.* Intern Med J, 2003. **33**(8): p. 380-6.
390. Ridker, P.M. and J.D. Silvertown, *Inflammation, C-reactive protein, and atherothrombosis.* J Periodontol, 2008. **79**(8 Suppl): p. 1544-51.
391. Grad, E. and H.D. Danenberg, *C-reactive protein and atherothrombosis: Cause or effect?* Blood Rev, 2013. **27**(1): p. 23-9.
392. Pasceri, V., J.T. Willerson, and E.T. Yeh, *Direct proinflammatory effect of C-reactive protein on human endothelial cells.* Circulation, 2000. **102**(18): p. 2165-8.
393. Shifren, J.L., et al., *A comparison of the short-term effects of oral conjugated equine estrogens versus transdermal estradiol on C-reactive protein, other serum markers of inflammation, and other hepatic proteins in naturally menopausal women.* J Clin Endocrinol Metab, 2008. **93**(5): p. 1702-10.

394. Wakatsuki, A., Y. Okatani, and T. Fukaya, *Effect of transdermal estradiol and oral conjugated equine estrogen on C-reactive protein in retinoid-placebo trial in healthy women.* Circulation, 2003. **107**(18): p. e127-8; author reply e127-8.
395. Boisvert, W.A., L.K. Curtiss, and R.A. Terkeltaub, *Interleukin-8 and its receptor CXCR2 in atherosclerosis.* Immunol Res, 2000. **21**(2-3): p. 129-37.
396. Uno, K. and S.J. Nicholls, *Biomarkers of inflammation and oxidative stress in atherosclerosis.* Biomark Med, 2010. **4**(3): p. 361-73.
397. Ouimet, T., et al., *Molecular and cellular targets of the MRI contrast agent P947 for atherosclerosis imaging.* Mol Pharm, 2012. **9**(4): p. 850-61.
398. Nie, S. and S.R. Emory, *Probing Single Molecules and Single Nanoparticles by Surface-Enhanced Raman Scattering.* Science, 1997. **275**(5303): p. 1102-6.
399. Song, J.B., J.J. Zhou, and H.W. Duan, *Self-Assembled Plasmonic Vesicles of SERS-Encoded Amphiphilic Gold Nanoparticles for Cancer Cell Targeting and Traceable Intracellular Drug Delivery.* Journal of the American Chemical Society, 2012. **134**(32): p. 13458-13469.
400. Dinish, U.S., et al., *Highly sensitive SERS detection of cancer proteins in low sample volume using hollow core photonic crystal fiber.* Biosens Bioelectron, 2012. **33**(1): p. 293-8.
401. Kim, I., et al., *SERS-based multiple biomarker detection using a gold-patterned microarray chip.* Journal of Molecular Structure, 2012. **1023**: p. 197-203.
402. Laurence, T., et al., *Application of SERS nanoparticles to intracellular pH measurements.* Biophysical Journal, 2005. **88**(1): p. 553A-553A.
403. Pascut, F.C., et al., *Non-invasive label-free monitoring the cardiac differentiation of human embryonic stem cells in-vitro by Raman spectroscopy.* Biochim Biophys Acta, 2013.
404. Huefner, A., et al., *Intracellular SERS nanoprobes for distinction of different neuronal cell types.* Nano Lett, 2013. **13**(6): p. 2463-70.
405. Nolan, J.P., et al., *Single cell analysis using surface enhanced Raman scattering (SERS) tags.* Methods, 2012. **57**(3): p. 272-279.
406. Kustner, B., et al., *SERS Labels for Red Laser Excitation: Silica-Encapsulated SAMs on Tunable Gold/Silver Nanoshells.* Angewandte Chemie-International Edition, 2009. **48**(11): p. 1950-1953.
407. Galema, S.A., *Microwave chemistry.* Chemical Society Reviews, 1997. **26**(3): p. 233-238.
408. Grell, T.A., et al., *Microwave-accelerated surface modification of plasmonic gold thin films with self-assembled monolayers of alkanethiols.* Langmuir, 2013. **29**(43): p. 13209-16.
409. Yuen, C., W. Zheng, and Z.W. Huang, *Low-level detection of anti-cancer drug in blood plasma using microwave-treated gold-polystyrene beads as surface-enhanced Raman scattering substrates.* Biosens Bioelectron, 2010. **26**(2): p. 580-584.
410. Xia, L., et al., *Microwave-assisted synthesis of sensitive silver substrate for surface-enhanced Raman scattering spectroscopy.* J Chem Phys, 2008. **129**(13): p. 134703.
411. Revkin, J.H., et al., *Biomarkers in the prevention and treatment of atherosclerosis: need, validation, and future.* Pharmacol Rev, 2007. **59**(1): p. 40-53.

412. Libby, P., M. DiCarli, and R. Weissleder, *The vascular biology of atherosclerosis and imaging targets.* J Nucl Med, 2010. **51 Suppl 1**: p. 33S-37S.
413. Bilecka, I. and M. Niederberger, *Microwave chemistry for inorganic nanomaterials synthesis.* Nanoscale, 2010. **2**(8): p. 1358-74.
414. Ahnfeldt, T., et al., *High-throughput and time-resolved energy-dispersive X-ray diffraction (EDXRD) study of the formation of CAU-1-(OH)2: microwave and conventional heating.* Chemistry, 2011. **17**(23): p. 6462-8.
415. Wu, Z., et al., *A "turn-off" SERS-based detection platform for ultrasensitive detection of thrombin based on enzymatic assays.* Biosens Bioelectron, 2013. **44**: p. 10-5.
416. Nahrendorf, M., et al., *Noninvasive vascular cell adhesion molecule-1 imaging identifies inflammatory activation of cells in atherosclerosis.* Circulation, 2006. **114**(14): p. 1504-11.
417. Wang, C. and J. Irudayaraj, *Gold Nanorod Probes for the Detection of Multiple Pathogens.* Small, 2008. **4**(12): p. 2204-2208.
418. Kang, H., et al., *Near-Infrared SERS Nanoprobes with Plasmonic Au/Ag Hollow-Shell Assemblies for In Vivo Multiplex Detection.* Advanced Functional Materials, 2013. **23**(30): p. 3719-3727.
419. Haidar, Z.S., R.C. Hamdy, and M. Tabrizian, *Protein release kinetics for core-shell hybrid nanoparticles based on the layer-by-layer assembly of alginate and chitosan on liposomes.* Biomaterials, 2008. **29**(9): p. 1207-15.
420. Tofovic, S.P., et al., *Estradiol metabolites attenuate renal and cardiovascular injury induced by chronic nitric oxide synthase inhibition.* Journal of Cardiovascular Pharmacology, 2005. **46**(1): p. 25-35.
421. Amendola, V., et al., *SERS labels for quantitative assays: application to the quantification of gold nanoparticles uptaken by macrophage cells.* Analytical Methods, 2011. **3**(4): p. 849-856.
422. Cabot, P.J., et al., *Targeting of ICAM-1-directed immunoliposomes specifically to activated endothelial cells with low cellular uptake: use of an optimized procedure for the coupling of low concentrations of antibody to liposomes.* Journal of Liposome Research, 2011. **21**(2): p. 95-105.
423. Chacko, A.M., et al., *Targeted Nanocarriers for Imaging and Therapy of Vascular Inflammation.* Curr Opin Colloid Interface Sci, 2011. **16**(3): p. 215-227.
424. Jain, K.K., *Nanomedicine: application of nanobiotechnology in medical practice.* Med Princ Pract, 2008. **17**(2): p. 89-101.
425. Riehemann, K., et al., *Nanomedicine-Challenge and Perspectives.* Angewandte Chemie-International Edition, 2009. **48**(5): p. 872-897.
426. Grieneisen, M.L., *The proliferation of nano journals.* Nature Nanotechnology, 2010. **5**(12): p. 825-825.
427. Dang, Y., et al., *Trends in worldwide nanotechnology patent applications: 1991 to 2008.* Journal of Nanoparticle Research, 2010. **12**(3): p. 687-706.
428. *National Nanotechnology Initiative*. 2011 [cited 2011; Available from: http://www.nano.gov/.

429. Caruthers, S.D., S.A. Wickline, and G.M. Lanza, *Nanotechnological applications in medicine.* Curr Opin Biotechnol, 2007. **18**(1): p. 26-30.
430. Vizirianakis, I.S., *Nanomedicine and personalized medicine toward the application of pharmacotyping in clinical practice to improve drug-delivery outcomes.* Nanomedicine, 2011. **7**(1): p. 11-7.
431. Sanchez, C., et al., *Applications of advanced hybrid organic-inorganic nanomaterials: from laboratory to market.* Chemical Society Reviews, 2011. **40**(2): p. 696-753.
432. Aili, D. and M.M. Stevens, *Bioresponsive peptide-inorganic hybrid nanomaterials.* Chemical Society Reviews, 2010. **39**(9): p. 3358-70.
433. Armentano, I., et al., *Biodegradable polymer matrix nanocomposites for tissue engineering: A review.* Polymer Degradation and Stability, 2010. **95**(11): p. 2126-2146.
434. Cao, Z., et al., *Stabilized liposomal nanohybrid cerasomes for drug delivery applications.* Chemical Communications, 2010. **46**(29): p. 5265-5267.
435. Rahimi, M., et al., *In vitro evaluation of novel polymer-coated magnetic nanoparticles for controlled drug delivery.* Nanomedicine, 2010. **6**(5): p. 672-80.
436. Ngiam, M., et al., *The fabrication of nano-hydroxyapatite on PLGA and PLGA/collagen nanofibrous composite scaffolds and their effects in osteoblastic behavior for bone tissue engineering.* Bone, 2009. **45**(1): p. 4-16.
437. Kim, H.W., J.H. Song, and H.E. Kim, *Bioactive glass nanofiber-collagen nanocomposite as a novel bone regeneration matrix.* Journal of Biomedical Materials Research Part A, 2006. **79**(3): p. 698-705.
438. Zhang, C., et al., *Folate-mediated poly(3-hydroxybutyrate-co-3-hydroxyoctanoate) nanoparticles for targeting drug delivery.* European Journal of Pharmaceutics and Biopharmaceutics, 2010. **76**(1): p. 10-16.
439. Li, X.Y., et al., *Preparation of N-trimethyl chitosan-protein nanoparticles intended for vaccine delivery.* J Nanosci Nanotechnol, 2010. **10**(8): p. 4850-8.
440. Zhang, C., et al., *Inhibitory efficacy of hypoxia-inducible factor 1 alpha short hairpin RNA plasmid DNA-loaded poly (D, L-lactide-co-glycolide) nanoparticles on choroidal neovascularization in a laser-induced rat model.* Gene Therapy, 2010. **17**(3): p. 338-351.
441. Manchanda, R., et al., *Preparation and characterization of a polymeric (PLGA) nanoparticulate drug delivery system with simultaneous incorporation of chemotherapeutic and thermo-optical agents.* Colloids and Surfaces B-Biointerfaces, 2010. **75**(1): p. 260-267.
442. Gou, M., et al., *Polymeric matrix for drug delivery: honokiol-loaded PCL-PEG-PCL nanoparticles in PEG-PCL-PEG thermosensitive hydrogel.* Journal of Biomedical Materials Research Part A, 2010. **93**(1): p. 219-26.
443. Millotti, G., et al., *The use of chitosan-6-mercaptonicotinic acid nanoparticles for oral peptide drug delivery.* Drug Deliv, 2010.
444. Sarmento, B., et al., *Alginate/chitosan nanoparticles are effective for oral insulin delivery.* Pharm Res, 2007. **24**(12): p. 2198-206.

445. Zhao, L., et al., *Preparation and the in-vivo evaluation of paclitaxel liposomes for lung targeting delivery in dogs.* Journal of Pharmacy and Pharmacology, 2011. **63**(1): p. 80-6.
446. Gaur, P.K., et al., *Targeted drug delivery of Rifampicin to the lungs: formulation, characterization, and stability studies of preformed aerosolized liposome and in situ formed aerosolized liposome.* Drug Dev Ind Pharm, 2010. **36**(6): p. 638-46.
447. Shah, D.A., et al., *Regulation of stem cell signaling by nanoparticle-mediated intracellular protein delivery.* Biomaterials, 2011.
448. Lu, J., et al., *Biocompatibility, biodistribution, and drug-delivery efficiency of mesoporous silica nanoparticles for cancer therapy in animals.* Small, 2010. **6**(16): p. 1794-805.
449. Nguyen, B.T., et al., *Immobilization of iron oxide magnetic nanoparticles for enhancement of vessel wall magnetic resonance imaging--an ex vivo feasibility study.* Bioconjug Chem, 2010. **21**(8): p. 1408-12.
450. Meng, X., et al., *Magnetic CoPt nanoparticles as MRI contrast agent for transplanted neural stem cells detection.* Nanoscale, 2011.
451. Yang, K., et al., *Quantum dot-based visual in vivo imaging for oral squamous cell carcinoma in mice.* Oral Oncol, 2010. **46**(12): p. 864-8.
452. Lin, M.M., et al., *Development of superparamagnetic iron oxide nanoparticles (SPIONS) for translation to clinical applications.* IEEE Trans Nanobioscience, 2008. **7**(4): p. 298-305.
453. Wang, Y. and L. Chen, *Quantum dots, lighting up the research and development of nanomedicine.* Nanomedicine, 2011.
454. Zhang, Y.F., et al., *O-Carboxymethyl-chitosan/organosilica hybrid nanoparticles as non-viral vectors for gene delivery.* Materials Science & Engineering C-Materials for Biological Applications, 2009. **29**(6): p. 2045-2049.
455. Yang, C., et al., *Folate receptor-targeted quantum dot liposomes as fluorescence probes.* Journal of Drug Targeting, 2009. **17**(7): p. 502-511.
456. Sigot, V., D.J. Arndt-Jovin, and T.M. Jovin, *Targeted Cellular Delivery of Quantum Dots Loaded on and in Biotinylated Liposomes.* Bioconjugate Chemistry, 2010. **21**(8): p. 1465-1472.
457. Kim, J.S., et al., *In vivo NIR imaging with CdTe/CdSe quantum dots entrapped in PLGA nanospheres.* J Colloid Interface Sci, 2011. **353**(2): p. 363-71.
458. Gao, X.H., et al., *In vivo cancer targeting and imaging with semiconductor quantum dots.* Nature Biotechnology, 2004. **22**(8): p. 969-976.
459. Prinzen, L., et al., *Optical and magnetic resonance imaging of cell death and platelet activation using annexin A5-functionalized quantum dots.* Nano Letters, 2007. **7**(1): p. 93-100.
460. Tekle, C., et al., *Cellular trafficking of quantum dot-ligand bioconjugates and their induction of changes in normal routing of unconjugated ligands.* Nano Letters, 2008. **8**(7): p. 1858-65.
461. Byers, R.J. and E.R. Hitchman, *Quantum dots brighten biological imaging.* Prog Histochem Cytochem, 2011. **45**(4): p. 201-37.

462. Liu, T., et al., *The fluorescence bioassay platforms on quantum dots nanoparticles.* J Fluoresc, 2005. **15**(5): p. 729-33.
463. Tavares, A.J., et al., *Quantum dots as contrast agents for in vivo tumor imaging: progress and issues.* Anal Bioanal Chem, 2011. **399**(7): p. 2331-42.
464. Zrazhevskiy, P., M. Sena, and X.H. Gao, *Designing multifunctional quantum dots for bioimaging, detection, and drug delivery.* Chemical Society Reviews, 2010. **39**(11): p. 4326-4354.
465. Tran, C., et al., *Liposomes as cellular membrane model for the prediction of both UV-filter capacity and photoprotective effect of lipophilic molecules.* Journal of Investigative Dermatology, 2001. **117**(2): p. 502-502.
466. Prassl, R., et al., *Targeted Sterically Stabilized Liposomes for Diagnostic Imaging of Atherosclerotic Plaques.* Atherosclerosis Supplements, 2010. **11**(2): p. 19-19.
467. Chen, H.L., et al., *Lactoferrin-modified procationic liposomes as a novel drug carrier for brain delivery.* European Journal of Pharmaceutical Sciences, 2010. **40**(2): p. 94-102.
468. He, Z.Y., et al., *Development of glycyrrhetinic acid-modified stealth cationic liposomes for gene delivery.* International Journal of Pharmaceutics, 2010. **397**(1-2): p. 147-154.
469. Xu, H., et al., *Effects of cleavable PEG-cholesterol derivatives on the accelerated blood clearance of PEGylated liposomes.* Biomaterials, 2010. **31**(17): p. 4757-4763.
470. Abu Lila, A.S., et al., *Sequential administration with oxaliplatin-containing PEG-coated cationic liposomes promotes a significant delivery of subsequent dose into murine solid tumor.* Journal of Controlled Release, 2010. **142**(2): p. 167-173.
471. Gosk, S., et al., *VCAM-1 directed immunoliposomes selectively target tumor vasculature in vivo.* Biochim Biophys Acta, 2008. **1778**(4): p. 854-63.
472. Katagiri, K., K. Ariga, and J. Kikuchi, *Preparation of organic-inorganic hybrid vesicle "cerasome" derived from artificial lipid with alkoxysilyl head.* Chemistry Letters, 1999(7): p. 661-662.
473. Ariga, K., K. Katagiri, and J. Kikuchi, *Preparation condition of a novel organic-inorganic hybrid vesicle "Cerasome".* Kobunshi Ronbunshu, 2000. **57**(4): p. 251-253.
474. Sasaki, Y., et al., *Cerasome as an infusible and cell-friendly gene carrier: synthesis of cerasome-forming lipids and transfection using cerasome.* Nature Protocols, 2006. **1**(3): p. 1227-34.
475. Hashizume, M., et al., *Stable vesicular nanoparticle 'Cerasome' as an organic-inorganic hybrid formed with organoalkoxysilane lipids having a hydrogen-bonding unit.* Thin Solid Films, 2003. **438**: p. 20-26.
476. Katagiri, K., et al., *Preparation and characterization of a novel organic-inorganic nanohybrid "cerasome" formed with a liposomal membrane and silicate surface.* Chemistry, 2007. **13**(18): p. 5272-81.
477. Ma, Y., et al., *Liposomal architecture boosts biocompatibility of nanohybrid cerasomes.* Nanotoxicology, 2011.
478. Dwivedi, N., et al., *Silica-Coated Liposomes for Insulin Delivery.* Journal of Nanomaterials, 2010: p. -.

479. Li, S.Z., et al., *Encapsulation of Quantum Dots Inside Liposomal Hybrid Cerasome Using a One-Pot Procedure.* Journal of Dispersion Science and Technology, 2010. **31**(12): p. 1727-1731.
480. Mohanraj, V.J., T.J. Barnes, and C.A. Prestidge, *Silica nanoparticle coated liposomes: a new type of hybrid nanocapsule for proteins.* Int J Pharm, 2010. **392**(1-2): p. 285-93.
481. Matsui, K., et al., *Cerasome as an infusible, cell-friendly, and serum-compatible transfection agent in a viral size.* Journal of the American Chemical Society, 2006. **128**(10): p. 3114-5.
482. McBain, S.C., H.H. Yiu, and J. Dobson, *Magnetic nanoparticles for gene and drug delivery.* Int J Nanomedicine, 2008. **3**(2): p. 169-80.
483. Chao, X., et al., *PEG-modified GoldMag nanoparticles (PGMNs) combined with the magnetic field for local drug delivery.* Journal of Drug Targeting, 2010.
484. Kim, D.H., et al., *Synthesis of Hybrid Gold/Iron Oxide Nanoparticles in Block Copolymer Micelles for Imaging, Drug Delivery, and Magnetic Hyperthermia.* Ieee Transactions on Magnetics, 2009. **45**(10): p. 4821-4824.
485. Dennis, C.L., et al., *The influence of magnetic and physiological behaviour on the effectiveness of iron oxide nanoparticles for hyperthermia.* Journal of Physics D-Applied Physics, 2008. **41**(13): p. -.
486. Chertok, B., A.E. David, and V.C. Yang, *Polyethyleneimine-modified iron oxide nanoparticles for brain tumor drug delivery using magnetic targeting and intra-carotid administration.* Biomaterials, 2010. **31**(24): p. 6317-24.
487. Yallapu, M.M., et al., *PEG-functionalized magnetic nanoparticles for drug delivery and magnetic resonance imaging applications.* Pharm Res, 2010. **27**(11): p. 2283-95.
488. Sun, L., et al., *A biocompatible approach to surface modification: Biodegradable polymer functionalized super-paramagnetic iron oxide nanoparticles.* Materials Science & Engineering C-Materials for Biological Applications, 2010. **30**(4): p. 583-589.
489. Guo, R., et al., *Dual-Functional Alginic Acid Hybrid Nanospheres for Cell Imaging and Drug Delivery.* Small, 2009. **5**(6): p. 709-717.
490. Petri-Fink, A. and H. Hofmann, *Superparamagnetic iron oxide nanoparticles (SPIONs): from synthesis to in vivo studies--a summary of the synthesis, characterization, in vitro, and in vivo investigations of SPIONs with particular focus on surface and colloidal properties.* IEEE Trans Nanobioscience, 2007. **6**(4): p. 289-97.
491. Hong, J., et al., *Facile synthesis of polymer-enveloped ultrasmall superparamagnetic iron oxide for magnetic resonance imaging.* Nanotechnology, 2007. **18**(13): p. -.
492. Mahmoudi, M., et al., *Superparamagnetic iron oxide nanoparticles (SPIONs): Development, surface modification and applications in chemotherapy.* Adv Drug Deliv Rev, 2010.
493. Namgung, R., et al., *Hybrid superparamagnetic iron oxide-branched polyethylenimine magnetoplexes for gene delivery.* Human Gene Therapy, 2010. **21**(10): p. 1488-1488.

494. Smith, B.R., et al., *Localization to atherosclerotic plaque and biodistribution of biochemically derivatized superparamagnetic iron oxide nanoparticles (SPIONs) contrast particles for magnetic resonance imaging (MRI).* Biomed Microdevices, 2007. **9**(5): p. 719-27.
495. Hafeli, U.O., et al., *Cell uptake and in vitro toxicity of magnetic nanoparticles suitable for drug delivery.* Mol Pharm, 2009. **6**(5): p. 1417-28.
496. Maeng, J.H., et al., *Multifunctional doxorubicin loaded superparamagnetic iron oxide nanoparticles for chemotherapy and magnetic resonance imaging in liver cancer.* Biomaterials, 2010. **31**(18): p. 4995-5006.
497. Namgung, R., et al., *Hybrid superparamagnetic iron oxide nanoparticle-branched polyethylenimine magnetoplexes for gene transfection of vascular endothelial cells.* Biomaterials, 2010. **31**(14): p. 4204-13.
498. Tan, Y.F., et al., *Multimodal tumor imaging by iron oxides and quantum dots formulated in poly (lactic acid)-d-alpha-tocopheryl polyethylene glycol 1000 succinate nanoparticles.* Biomaterials, 2011. **32**(11): p. 2969-78.
499. Langer, R. and J.P. Vacanti, *Tissue Engineering.* Science, 1993. **260**(5110): p. 920-926.
500. Dvir, T., et al., *Nanotechnological strategies for engineering complex tissues.* Nature Nanotechnology, 2011. **6**(1): p. 13-22.
501. Wan, A.C.A. and J.Y. Ying, *Nanomaterials for in situ cell delivery and tissue regeneration.* Advanced Drug Delivery Reviews, 2010. **62**(7-8): p. 731-740.
502. Cao, Y., et al., *Triple-helix scaffolds of grafted collagen reinforced by Al2O3-ZrO2 nanoparticles.* Advanced Materials, 2006. **18**(14): p. 1838-+.
503. Wei, G. and P.X. Ma, *Structure and properties of nano-hydroxyapatite/polymer composite scaffolds for bone tissue engineering.* Biomaterials, 2004. **25**(19): p. 4749-57.
504. Hong, Z.K., et al., *Nano-composite of poly(L-lactide) and surface grafted hydroxyapatite: Mechanical properties and biocompatibility.* Biomaterials, 2005. **26**(32): p. 6296-6304.
505. Wang, X.J., G.J. Song, and T. Lou, *Fabrication and characterization of nano-composite scaffold of PLLA/silane modified hydroxyapatite.* Medical Engineering & Physics, 2010. **32**(4): p. 391-397.
506. Shin, K.H., et al., *Direct coating of bioactive sol-gel derived silica on poly(epsilon-caprolactone) nanofibrous scaffold using co-electrospinning.* Materials Letters, 2010. **64**(13): p. 1539-1542.
507. Mandoli, C., et al., *Stem Cell Aligned Growth Induced by CeO2 Nanoparticles in PLGA Scaffolds with Improved Bioactivity for Regenerative Medicine.* Advanced Functional Materials, 2010. **20**(10): p. 1617-1624.
508. Porter, J.R., T.T. Ruckh, and K.C. Popat, *Bone Tissue Engineering: A Review in Bone Biomimetics and Drug Delivery Strategies.* Biotechnology Progress, 2009. **25**(6): p. 1539-1560.
509. Chen, J., et al., *Characterization and biocompatibility of nanohybrid scaffold prepared via in situ crystallization of hydroxyapatite in chitosan matrix.* Colloids Surf B Biointerfaces, 2010. **81**(2): p. 640-7.

510. Li, J.H., et al., *Enhancement of bone formation by BMP-7 transduced MSCs on biomimetic nano-hydroxyapatite/polyamide composite scaffolds in repair of mandibular defects.* Journal of Biomedical Materials Research Part A, 2010. **95A**(4): p. 973-981.
511. Koo, A.N., et al., *Enhanced bone regeneration by porous poly(L-lactide) scaffolds with surface-immobilized nano-hydroxyapatite.* Macromolecular Research, 2010. **18**(10): p. 1030-1036.
512. Xue, D.T., et al., *Osteochondral repair using porous poly(lactide-co-glycolide)/nano-hydroxyapatite hybrid scaffolds with undifferentiated mesenchymal stem cells in a rat model.* Journal of Biomedical Materials Research Part A, 2010. **94A**(1): p. 259-270.
513. Heo, S.J., et al., *In Vitro and Animal Study of Novel Nano-Hydroxyapatite/Poly(epsilon-Caprolactone) Composite Scaffolds Fabricated by Layer Manufacturing Process.* Tissue Engineering Part A, 2009. **15**(5): p. 977-989.
514. Cunniffe, G.M., et al., *Development and characterisation of a collagen nano-hydroxyapatite composite scaffold for bone tissue engineering.* Journal of Materials Science-Materials in Medicine, 2010. **21**(8): p. 2293-2298.
515. Kong, L.J., et al., *A study on the bioactivity of chitosan/nano-hydroxyapatite composite scaffolds for bone tissue engineering.* European Polymer Journal, 2006. **42**(12): p. 3171-3179.
516. Kim, H.W., *Biomedical nanocomposites of hydroxyapatite/polycaprolactone obtained by surfactant mediation.* Journal of Biomedical Materials Research Part A, 2007. **83A**(1): p. 169-177.
517. Asran, A.S., S. Henning, and G.H. Michler, *Polyvinyl alcohol-collagen-hydroxyapatite biocomposite nanofibrous scaffold: Mimicking the key features of natural bone at the nanoscale level.* Polymer, 2010. **51**(4): p. 868-876.
518. Dong, J.L., et al., *Bone Regeneration with BMP-2 Gene-modified Mesenchymal Stem Cells Seeded on Nano-hydroxyapatite/Collagen/Poly(L-Lactic Acid) Scaffolds.* Journal of Bioactive and Compatible Polymers, 2010. **25**(6): p. 547-566.
519. Choi, S.W., et al., *In Vitro Mineralization by Preosteoblasts in Poly(DL-lactide-co-glycolide) Inverse Opal Scaffolds Reinforced with Hydroxyapatite Nanoparticles.* Langmuir, 2010. **26**(14): p. 12126-12131.
520. Boccaccini, A.R., et al., *Polymer/bioactive glass nanocomposites for biomedical applications: A review.* Composites Science and Technology, 2010. **70**(13): p. 1764-1776.
521. Hoppe, A., N.S. Guldal, and A.R. Boccaccini, *A review of the biological response to ionic dissolution products from bioactive glasses and glass-ceramics.* Biomaterials, 2011. **32**(11): p. 2757-74.
522. Peter, M., et al., *Nanocomposite scaffolds of bioactive glass ceramic nanoparticles disseminated chitosan matrix for tissue engineering applications.* Carbohydrate Polymers, 2010. **79**(2): p. 284-289.
523. Noh, K.T., et al., *Composite nanofiber of bioactive glass nanofiller incorporated poly(lactic acid) for bone regeneration.* Materials Letters, 2010. **64**(7): p. 802-805.

524. Rezwan, K., et al., *Biodegradable and bioactive porous polymer/inorganic composite scaffolds for bone tissue engineering.* Biomaterials, 2006. **27**(18): p. 3413-31.
525. Hong, Z., R.L. Reis, and J.F. Mano, *Preparation and in vitro characterization of scaffolds of poly(L-lactic acid) containing bioactive glass ceramic nanoparticles.* Acta Biomaterialia, 2008. **4**(5): p. 1297-306.
526. Peter, M., et al., *Novel biodegradable chitosan-gelatin/nano-bioactive glass ceramic composite scaffolds for alveolar bone tissue engineering.* Chemical Engineering Journal, 2010. **158**(2): p. 353-361.
527. Hajiali, H., et al., *Preparation of a novel biodegradable nanocomposite scaffold based on poly (3-hydroxybutyrate)/bioglass nanoparticles for bone tissue engineering.* Journal of Materials Science-Materials in Medicine, 2010. **21**(7): p. 2125-2132.
528. Furusawa, T. and K. Mizunuma, *Osteoconductive properties and efficacy of resorbable bioactive glass as a bone-grafting material.* Implant Dent, 1997. **6**(2): p. 93-101.
529. Jo, J.H., et al., *In vitro/in vivo biocompatibility and mechanical properties of bioactive glass nanofiber and poly(epsilon-caprolactone) composite materials.* J Biomed Mater Res B Appl Biomater, 2009. **91**(1): p. 213-20.
530. Roohani-Esfahani, S.I., et al., *Effects of bioactive glass nanoparticles on the mechanical and biological behavior of composite coated scaffolds.* Acta Biomaterialia, 2011. **7**(3): p. 1307-18.
531. Quintero, F., et al., *Laser Spinning of Bioactive Glass Nanofibers.* Advanced Functional Materials, 2009. **19**(19): p. 3084-3090.
532. Kim, H.W., H.E. Kim, and J.C. Knowles, *Production and potential of bioactive glass nanofibers as a next-generation biomaterial.* Advanced Functional Materials, 2006. **16**(12): p. 1529-1535.
533. Kim, H.W., H.H. Lee, and G.S. Chun, *Bioactivity and osteoblast responses of novel biomedical nanocomposites of bioactive glass nanofiber filled poly(lactic acid).* Journal of Biomedical Materials Research Part A, 2008. **85A**(3): p. 651-663.
534. Teo, W.E., et al., *Fabrication and characterization of hierarchically organized nanoparticle-reinforced nanofibrous composite scaffolds.* Acta Biomaterialia, 2011. **7**(1): p. 193-202.
535. Kannarkat, J.T., et al., *Embedding of magnetic nanoparticles in polycaprolactone nanofiber scaffolds to facilitate bone healing and regeneration.* Journal of Applied Physics, 2010. **107**(9): p. -.